

RADIOLOGY AND ONCOLOGY

vol.49 no.1

march 2015



NOVA SMER DO PODALJŠANJA CELOKUPNEGA PREŽIVETJA



Prva in edina samostojna kemoterapija, ki v primerjavi z ostalimi možnostmi zdravljenja z enim zdravilom, pri bolnicah s predhodno že večkratno zdravljenim metastatskim rakom dojke, dokazano značilno podaljša celokupno preživetje.^{1,2}



- **Halaven** (eribulin): ne-taksanski zaviralec dinamike mikrotubulov, prvo zdravilo iz nove skupine kemoterapevtikov, imenovanih *halihondrini*.
- Zdravilo HALAVEN je indicirano za zdravljenje bolnic z lokalno napredovalim ali metastatskim rakom dojke, ki je napredoval po vsaj enem režimu kemoterapije za napredovalno bolezen. Predhodna zdravljenja morajo vključevati antraciklin in taksan, bodisi kot adjuvantno zdravljenje ali za zdravljenje metastatskega raka dojke, razen če to zdravljenje za bolnice ni bilo primerno.¹
- Priporočeni odmerek 1,23 mg/m², intravensko, v obliki 2- do 5-minutne infuzije, 1. in 8. dan vsakega 21-dnevnega cikla.
- Ena 2 ml viala vsebuje 0,88 mg eribulina.
- Rastopina, pripravljena za uporabo, redčenje ni potrebno.

SKRAJŠAN POVZETEK GLAVNIH ZNAČILNOSTI ZDRAVILA

HALAVEN 0,44 mg/ml raztopina za injiciranje (eribulin)
TERAPEVTSKE INDIKACIJE: Zdravljenje lokalno napredovalga ali metastatskega raka dojke, ki je napredoval po vsaj enem režimu kemoterapije za napredovalno bolezen vključno z antraciklinom in taksanom (adjuvantno zdravljenje ali zdravljenje metastatskega raka dojke), razen če to ni bilo primerno. **ODMERJANJE IN NAČIN UPORABE:** Halaven se daje v enotah, specializiranih za dajanje citotoksične kemoterapije, in le pod nadzorom usposobljenega zdravnika z izkušnjami v uporabi citotoksičnih zdravil. **Odmerjanje:** Priporočeni odmerek eribulina v obliki raztopine je 1,23 mg/m² i.v. v obliki 2- do 5-minutne infuzije 1. in 8. dan vsakega 21-dnevnega cikla. Bolnikom je lahko slabo ali bruhanje. Treba je razmisлити o antiemetični profilaksi, vključno s kortikosteroidi. **Preložitev odmerka med zdravljenjem:** Dajanje Halavena je treba preložiti, če se pojavi kaj od naslednjih: absolutno število nevtrofilcev (ANC) < 1 x 10⁹/l, trombociti < 75 x 10⁹/l ali nehematološki neželeni učinki 3. ali 4. stopnje. **Zmanjšanje odmerka med zdravljenjem:** Za priporočila za zmanjšanje odmerka ob pojavu hematoloških ali nehematoloških neželenih učinkov glejte celoten povzetek glavnih značilnosti zdravila. **Okvara jeter zaradi zasevkov:** Priporočeni odmerek pri blagi okvari jeter (stopnje A po Child-Pughu) je 0,97 mg/m² v obliki 2- do 5-minutne i.v. infuzije 1. in 8. dan 21-dnevnega cikla. Pri hudi okvari jeter (stopnje B po Child-Pughu) je 0,62 mg/m² v obliki 2- do 5-minutne i.v. infuzije 1. in 8. dan 21-dnevnega cikla. Pri hudi okvari jeter (stopnje C po Child-Pughu) se pričakuje, da je treba dati še manjši odmerek eribulina. **Okvara jeter zaradi ciroze:** Zgornje odmerke se lahko uporabi za blago do zmerno okvaro, vendar se priporoča skrbno nadziranje, saj bo odmerek morda treba ponovno prilagoditi. **Okvara ledvic:** Pri hudi okvari ledvic (očistek kreatinina < 40 ml/min) morda treba odmerek zmanjšati. Priporočila za skrbno nadziranje vrnite. **Način uporabe:** Odmerek se lahko razredi z do 100 ml 0,9 % raztopine natrijevega klorida (9 mg/ml) za injiciranje. Ne sme se ga redčiti v 5 % infuzijski raztopini glukoze. Pred dajanjem glejte navodila glede redčenja zdravila v celotnem povzetku glavnih značilnosti zdravila ter se prepričajte, da obstaja dober periferni venski dostop ali prehodna centralna linija. Ni znakov, da bi eribulin povzročal mehurje ali dražlj. V primeru ekstravazacije mora biti zdravljenje simptomatsko. **KONTRAINDIKACIJE:** Preobčutljivost na zdravilno učinkovino ali katerokoli pomožno snov. Dojenje. **POSEBNA OPOZORILA IN PREVIDNOSTNI UKREPI:** Mielosupresija je odvisna od odmerka in se kaže kot nevropatija. Pred vsakim odmerkom eribulina je treba opraviti pregled celotne krvne slike. Zdravljenje z eribulinom se lahko uvede le pri bolnikih z vrednostmi ANC $\geq 1,5 \times 10^9/l$ in s trombociti > 100 x 10⁹/l. Bolnike, pri katerih se pojavijo febrilna nevropatija, huda nevropatija ali trombotična, je treba zdravit v skladu s priporočili v celotnem povzetku glavnih značilnosti zdravila. Hudo nevropatijo se lahko zdravi z uporabo G-CSF ali enakovrednim zdravilom v skladu s smernicami. Bolnike je treba skrbno nadzirati za znake periferne motorične in senzorične nevropatije. Pri razvoju hude periferne nevrotoksičnosti je treba odmerek prestaviti ali zmanjšati. Če začnemo zdravljenje pri bolnikih s kongestivnim srčnim popuščanjem, z bradibradijami ali sočasno z zdravili, za katera je znano, da podaljšujejo interval QT, vključno z antiaritmiki razreda la in III, in z

elektrolitskimi motnjami, je priporočljivo spremljanje EKG. Pred začetkom zdravljenja s Halavenom je treba popraviti hipokallemijo in hipomagnezijo in te elektrolite je treba občasno kontrolirati med zdravljenjem. Eribulina ne smemo dajati bolnikom s prirojenim sindromom dolgega intervala QT. To zdravilo vsebuje majhne količine etanola (alkohola), manj kot 100 mg na odmerek. Eribulin je pri podganah embriotoksičen, fetotoksičen in teratogen. Halavena se ne sme uporabljati med nosečnostjo, razen kadar je to nujno potrebno. Ženske v rodni dobi naj ne zanosi v času, ko same ali njihov moški partner dobivajo Halaven, in naj med zdravljenjem in še do 3 mesece po njem uporabljajo učinkovito kontracepcijo. Moški naj se pred zdravljenjem posvetujejo o shranjevanju sperme zaradi možnosti nepopravljive neplodnosti. **INTERAKCIJE:** Eribulin se izloča do 70 % prek žolča. Sočasna uporaba učinkovin, ki zavirajo jetrne transportne beljakovine, kot so beljakovine za prenos organskih anionov in beljakovine, odporne na številna zdravila, z eribulinom se ne priporoča (npr. ciklosporin, ritonavir, sakvinavir, lopinavir in nekateri drugi zaviralci proteaze, efavirenz, emtricitabin, verapamil, klaritromicin, kinin, kinidin, dipiramid itd.). Sočasno zdravljenje z indukcijami učinkovinami, kot so rifampicin, karbamazepin, fenitoin, šentjanževka, lahko povzroči znižanje koncentracij eribulina v plazmi, zato je ob sočasni uporabi indaktorjev potrebna previdnost. Eribulin je blag inhibitor encima CYP3A4. Priporočila je previdnost in spremljanje glede neželenih učinkov pri sočasni uporabi snovi, ki imajo ozko terapevtsko okno in se odstranjujejo iz telesa predvsem preko CYP3A4 (npr. alfentanil, ciklosporin, ergotamin, fentanil, pimožid, kinidin, sirolimus, takrolimus). **NEŽELENI UČINKI:** Povzetek varnostnega profila Neželeni učinek, o katerem najpogosteje poročajo v zvezi s Halavenom, je supresija kostnega mozga, ki se kaže kot nevropatija, levkopenija, anemija, trombocitopenija s pridruženimi okužbami. Poročali so tudi o novem začetku ali poslabšanju že obstoječe periferne nevropatije. Med neželenimi učinki, o katerih poročajo, je toksičnost za prebavila, ki se kaže kot anoreksija, navzea, bruhanje, driska, zaprtost in stomatitis. Med drugimi neželenimi učinki so utrujenost, alopecija, zvečani jetrni encimi, sepsa in mišičnoskeletni bolečinski sindrom. **Seznam neželenih učinkov:** *Zelo pogosti* ($\geq 1/10$): nevropatija (57,0 %) (3/4. stopnje: 49,7 %), levkopenija (29,3 %) (3/4. stopnje: 17,3 %), anemija (20,6 %) (3/4. stopnje: 2,0 %), zmanjšani apetit (21,9 %) (3/4. stopnje: 0,7 %), periferne nevropatije (35,6 %) (3/4. stopnje: 7,6 %), glavobol (17,2 %) (3/4. stopnje: 0,8 %), dispneja (13,9 %) (3/4. stopnje: 3,1 %), kašelj (13,6 %) (3/4. stopnje: 0,6 %), navzea (33,8 %) (3/4. stopnje: 1,1 %), zaprtost (19,6 %) (3/4. stopnje: 0,6 %), driska (17,9 %) (3/4. stopnje: 0,8 %), bruhanje (17,6 %) (3/4. stopnje: 0,9 %), alopecija, artralgijska in mialgijska (19,4 %) (3/4. stopnje: 1,1 %), bolečina v hrbtu (13,0 %) (3/4. stopnje: 1,5 %), bolečina v udih (10,0 %) (3/4. stopnje: 0,7 %), utrujenost/astenija (47,9 %) (3/4. stopnje: 7,8 %), pireksija (20,4 %) (3/4. stopnje: 0,6 %), zmanjšanje telesne mase (11,3 %) (3/4. stopnje: 0,3 %). *Pogosti* ($\geq 1/100$ do < 1/10): okužba sečil (8 %) (3/4. stopnje: 0,5 %), pljučnica (1,2 %) (3/4. stopnje: 0,8 %), ustna kandidiaza, ustni herpes, okužba zgornjih dihal, nazofarngitis, rinitis, limfopenija (4,9 %) (3/4. stopnje: 1,4 %), febrilna nevropatija (4,7 %) (3/4. stopnje: 4,5 %), trombotična (4,3 %) (3/4. stopnje: 0,7 %), hipokallemija (6,1 %) (3/4. stopnje:

1,7 %), hipomagnezija (2,9 %) (3/4. stopnje: 0,2 %), dehidracija (2,8 %) (3/4. stopnje: 0,5 %), hiperglikemija, hipofosfatemija, nespečnost, depresija, disgezija, omotičnost (7,9 %) (3/4. stopnje: 0,5 %), hipoestezija, letargija, nevrotoksičnost, obilnejše solzenje (6,0 %) (3/4. stopnje: 0,1 %), konjunktivitis, vrtoglavica, tahikardija, vročinski valovi, orofaringealna bolečina, epistaksa, rinoreja, bolečina v trebuhu, stomatitis (9,3 %) (3/4. stopnje: 0,8 %), suha usta, dispneja (5,9 %) (3/4. stopnje: 0,2 %), gastroezofagealna refluksna bolezen, razjede v ustih, distenzija trebuha, zvišanje alanin-aminotransferaze (7,6 %) (3/4. stopnje: 2,1 %), zvišanje aspartat-aminotransferaze (7,4 %) (3/4. stopnje: 1,5 %), zvišanje gama-glutamiltansferaze (1,8 %) (3/4. stopnje: 0,9 %), hiperbilirubinemija (1,5 %) (3/4. stopnje: 0,3 %), izpuščaji, pruritus (3,9 %) (3/4. stopnje: 0,1 %), boleznin nohtov, nočno potenje, suha koža, eritem, hiperhidroza, bolečina v kosteh (9,6 %) (3/4. stopnje: 1,7 %), mišični spazmi (5,1 %) (3/4. stopnje: 0,1 %), mišično-skeletna bolečina in mišično-skeletna bolečina v prsih, mišična oslabelost, disurija, vnetje sluznice (8,3 %) (3/4. stopnje: 1,1 %), periferni edem, bolečina, mrzlica, bolečina v prsih, gripi podobna bolezen. *Občasni* ($\geq 1/1.000$ do < 1/100): sepsa (0,5 %) (3/4. stopnje: 0,2 %), nevropenična sepsa (0,1 %) (3/4. stopnje: 0,1 %), herpes zoster, tinitus, globoka venska tromboza, pljučna embolija, hepatotoksičnost (1,0 %) (3/4. stopnje: 0,6 %), palmarno-plantarna eritrodisezija, hematurnija, proteinurija, odpoved ledvic. *Redki* ($\geq 1/10.000$ do < 1/1.000): diseminirana intravaskularna koagulacija, intersticijska pljučna bolezen, pankreatitis, angioedem. Za popoln opis neželenih učinkov glejte celoten povzetek glavnih značilnosti zdravila. Vrsta ovjnine in vsebina: viala z 2 ml raztopine. **Režim izdaje:** H Imetnik dovoljenja za promet: Eisai Europe Ltd, European Knowledge Centre, Mosquito Way, Hatfield, Hertfordshire, AL10 9SN, Velika Britanija HAL-270614, julij 2014

Pred predpisovanjem in uporabo zdravila prosimo preberite celoten povzetek glavnih značilnosti zdravila!

Viri: (1) Povzetek glavnih značilnosti zdravila Halaven, junij 2014; (2) Cortes J et al. *Lancet* 2011; 377: 914–23.

 **PharmaSwiss**
Choose More Life

Odgovoren za trženje v Sloveniji:
PharmaSwiss d.o.o., Brodišče 32, 1236 Trzin
telefon: +386 1 236 47 00, faks: +386 1 283 38 10

HAL-0714-01, julij 2014



Publisher

Association of Radiology and Oncology

Affiliated with

Slovenian Medical Association – Slovenian Association of Radiology, Nuclear Medicine Society,
Slovenian Society for Radiotherapy and Oncology, and Slovenian Cancer Society
Croatian Medical Association – Croatian Society of Radiology
Societas Radiologorum Hungarorum
Friuli-Venezia Giulia regional groups of S.I.R.M.
Italian Society of Medical Radiology

Aims and scope

Radiology and Oncology is a journal devoted to publication of original contributions in diagnostic and interventional radiology, computerized tomography, ultrasound, magnetic resonance, nuclear medicine, radiotherapy, clinical and experimental oncology, radiobiology, radiophysics and radiation protection.

Editor-in-Chief

Gregor Serša, Institute of Oncology Ljubljana,
Department of Experimental Oncology, Ljubljana,
Slovenia

Executive Editor

Viljem Kovač, Institute of Oncology Ljubljana,
Department of Radiation Oncology, Ljubljana, Slovenia

Editorial Board

Sotirios Bisdas, University Clinic Tübingen,
Department of Neuroradiology, Tübingen, Germany

Karl H. Bohuslavizki, Facharzt für
Nuklearmedizin, Hamburg, Germany

Serena Bonin, University of Trieste, Department of
Medical Sciences, Trieste, Italy

Boris Brkljačić, University Hospital "Dubrava",
Department of Diagnostic and Interventional
Radiology, Zagreb, Croatia

Luca Campana, Veneto Institute of Oncology
(IOV-IRCCS), Padova, Italy

Christian Dittrich, Kaiser Franz Josef - Spital,
Vienna, Austria

Metka Filipič, National Institute of Biology,
Department of Genetic Toxicology and Cancer Biology,
Ljubljana, Slovenia

Maria Gódehy, National Institute of Oncology,
Budapest, Hungary

Janko Kos, University of Ljubljana, Faculty of
Pharmacy, Ljubljana, Slovenia

Robert Jeraj, University of Wisconsin, Carbone
Cancer Center, Madison, Wisconsin, USA

Advisory Committee

Tullio Girdali, University of Trieste, Faculty of
Medicine and Psychology, Trieste, Italy

Vassil Hadjidekov, Medical University,
Department of Diagnostic Imaging, Sofia, Bulgaria

Deputy Editors

Andrej Cör, University of Primorska, Faculty of
Health Science, Izola, Slovenia

Maja Čemažar, Institute of Oncology Ljubljana,
Department of Experimental Oncology, Ljubljana,
Slovenia

Igor Kocijančič, University Medical Centre
Ljubljana, Institute of Radiology, Ljubljana, Slovenia

Karmen Stanič, Institute of Oncology Ljubljana,
Department of Radiation Oncology, Ljubljana, Slovenia

Primož Strojjan, Institute of Oncology Ljubljana,
Department of Radiation Oncology, Ljubljana, Slovenia

Tamara Lah Turnšek, National Institute of
Biology, Ljubljana, Slovenia

Damijan Miklavčič, University of Ljubljana,
Faculty of Electrical Engineering, Ljubljana, Slovenia

Luka Milas, UT M. D. Anderson Cancer Center,
Houston, USA

Damir Miletić, Clinical Hospital Centre Rijeka,
Department of Radiology, Rijeka, Croatia

Håkan Nyström, Skandionkliniken,
Uppsala, Sweden

Maja Osmak, Ruder Bošković Institute,
Department of Molecular Biology, Zagreb, Croatia

Dušan Pavčnik, Dotter Interventional Institute,
Oregon Health Science University, Oregon,
Portland, USA

Geoffrey J. Pilkington, University of
Portsmouth, School of Pharmacy and Biomedical
Sciences, Portsmouth, UK

Ervin B. Podgoršak, McGill University,
Montreal, Canada

Matthew Podgorsak, Roswell Park Cancer
Institute, Departments of Biophysics and Radiation
Medicine, Buffalo, NY, USA

Marko Hočevar, Institute of Oncology Ljubljana,
Department of Surgical Oncology, Ljubljana, Slovenia

Miklós Kásler, National Institute of Oncology,
Budapest, Hungary

Csaba Polgar, National Institute of Oncology,
Budapest, Hungary

Dirk Rades, University of Lubeck, Department of
Radiation Oncology, Lubeck, Germany

Mirjana Rajer, Institute of Oncology Ljubljana,
Department of Radiation Oncology, Ljubljana, Slovenia

Luis Souhami, McGill University, Montreal,
Canada

Borut Štabuc, University Medical Centre Ljubljana,
Department of Gastroenterology, Ljubljana, Slovenia

Katarina Šurlan Popovič, University Medical
Center Ljubljana, Clinical Institute of Radiology,
Ljubljana, Slovenia

Justin Teissié, CNRS, IPBS, Toulouse, France

Gillian M. Tozer, University of Sheffield,
Academic Unit of Surgical Oncology, Royal
Hallamshire Hospital, Sheffield, UK

Andrea Veronesi, Centro di Riferimento
Oncologico - Aviano, Division of Medical Oncology,
Aviano, Italy

Branko Zakotnik, Institute of Oncology Ljubljana,
Department of Medical Oncology, Ljubljana, Slovenia

Stojan Plesničar, Institute of Oncology Ljubljana,
Department of Radiation Oncology, Ljubljana, Slovenia

Tomaž Benulič, Institute of Oncology Ljubljana,
Department of Radiation Oncology, Ljubljana, Slovenia

Editorial office

Radiology and Oncology

Zaloška cesta 2

P. O. Box 2217

SI-1000 Ljubljana

Slovenia

Phone: +386 1 5879 369

Phone/Fax: +386 1 5879 434

E-mail: gsera@onko-i.si

Copyright © Radiology and Oncology. All rights reserved.

Reader for English

Vida Kološa

Secretary

Mira Klemenčič

Zvezdana Vukmirović

Design

Monika Fink-Serša, Samo Rován, Ivana Ljubanović

Layout

Matjaž Lužar

Printed by

Tiskarna Ozimek, Slovenia

Published quarterly in 400 copies

Beneficiary name: DRUŠTVO RADIOLOGIJE IN ONKOLOGIJE

Zaloška cesta 2

1000 Ljubljana

Slovenia

Beneficiary bank account number: SI56 02010-0090006751

IBAN: SI56 0201 0009 0006 751

Our bank name: Nova Ljubljanska banka, d.d.,

Ljubljana, Trg republike 2,

1520 Ljubljana; Slovenia

SWIFT: LJBASIX

Subscription fee for institutions EUR 100, individuals EUR 50

The publication of this journal is subsidized by the Slovenian Research Agency.

Indexed and abstracted by:

- *Celdes*
- *Chemical Abstracts Service (CAS)*
- *Chemical Abstracts Service (CAS) - SciFinder*
- *CNKI Scholar (China National Knowledge Infrastructure)*
- *CNPIEC*
- *DOAJ*
- *EBSCO - Biomedical Reference Collection*
- *EBSCO - Cinahl*
- *EBSCO - TOC Premier*
- *EBSCO Discovery Service*
- *Elsevier - EMBASE*
- *Elsevier - SCOPUS*
- *Google Scholar*
- *J-Gate*
- *JournalTOCs*
- *Naviga (Softweco)*
- *Primo Central (ExLibris)*
- *ProQuest - Advanced Technologies Database with Aerospace*
- *ProQuest - Health & Medical Complete*
- *ProQuest - Illustrata: Health Sciences*
- *ProQuest - Illustrata: Technology*
- *ProQuest - Medical Library*
- *ProQuest - Nursing & Allied Health Source*
- *ProQuest - Pharma Collection*
- *ProQuest - Public Health*
- *ProQuest - Science Journals*
- *ProQuest - SciTech Journals*
- *ProQuest - Technology Journals*
- *PubMed*
- *PubsHub*
- *ReadCube*
- *SCImago (SJR)*
- *Summon (Serials Solutions/ProQuest)*
- *TDOne (TDNet)*
- *Thomson Reuters - Journal Citation Reports/Science Edition*
- *Thomson Reuters - Science Citation Index Expanded*
- *Ulrich's Periodicals Directory/ulrichsweb*
- *WorldCat (OCLC)*

This journal is printed on acid-free paper

On the web: ISSN 1581-3207

<http://www.degruyter.com/view/j/raon>

<http://www.radioloncol.com>

Our efforts to continuous growth of Radiology and Oncology

Dear authors, readers, members of Editorial Board. The year 2014 was quite successful for our journal. We believe that we have had a continuous growth that we want to ensure also in the forthcoming 2015. In 2014 our Impact factor increased to 1.667, and we expect further increase this year.

In 2014 we have had steady increase in the published articles, and noticeable increase in quotations of our journal, also in some distinguished journals. The internationality of our journal is visible also through the diversity of the countries that the authors originate from. We are especially pleased that we published the manuscripts from some renowned institutions from the USA and that we have authors publishing in Radiology and Oncology from almost all European countries, Japan, China and other parts of the world.

The De Gruyter, publisher of electronic edition of Radiology and Oncology, has strived and succeeded in enlisting Radiology and Oncology into a long list of databases. However, our goal is to join the best, so we are planning to apply for the MEDLINE. That would enable us to post in PubMed also papers that are ahead of print. This, in our belief, would be a big step forward in early dissemination of the accepted papers for publication in Radiology and Oncology.

The term of the members of Editorial Board has expired, so we have asked some new, distinguished experts from various fields of radiology and oncology to join us. We thank them for accepting this task, which will support our efforts for the high quality of Radiology and Oncology in coming years.

So far Radiology and Oncology has been enlisted only in category of *oncology* in Web of Science. However, starting from 2015 it will be also in the category of *radiology and nuclear medicine*. This might also increase the visibility of the published papers in a more specific field of radiology and nuclear medicine.

The publication of our journal is a massive endeavor and requires also substantial funds. Since we are independent journal, with increasing costs of publishing Radiology and Oncology, we were forced to increase the publication fee of the papers to 700 EUR + VAT. We are sure that this will not influence the submission rate to our journal.

In the end, we would like to thank the authors, Editors, Editorial board and specially the reviewers for their efforts, and ask them to continue supporting our journal.

With best regards,

Prof. Gregor Serša, Ph.D.
Editor in Chief

Assoc. Prof. Viljem Kovač, M.D., Ph.D.
Executive Editor

Online Manuscript Submission

Now you can submit your manuscript to Radiology and Oncology online at editorial manager.

All correspondence, peer review, revisions and editing can be done through your account on the website.

- Go to www.radioloncol.com
- Register and create an account.
- Log in and submit manuscript in 5 easy steps.

If you have expertise and are interested in reviewing manuscripts within your specialty area, please let us know by sending E-mail to gsera@onko-i.si

Submit manuscripts to the Radiology and Oncology on

www.radioloncol.com

RADIOLOGY and ONCOLOGY, Zaloska 2, P.O.Box 2217, SI-1000 Ljubljana, Slovenia, T/F: +386 1 5879 434, E: gsera@onko-i.si



RADIOLOGY and ONCOLOGY

[HOME](#) [ABOUT](#) [LOG IN](#) [REGISTER](#) [SEARCH](#) [CURRENT](#) [ARCHIVES](#) [FOR AUTHORS](#)

Home > [Log In](#)

Log In

Username
Password
 Remember my username and password

[Not a user? Register with this site](#)
[Forgot your password?](#)

RADIOLOGY AND ONCOLOGY, Association of Radiology and Oncology.

Zaloska 2, P.O.Box 2217, SI-1000 Ljubljana, Slovenia, T/F: +386 1 5879 434, Open access on the web: ISSN 1518-3207, [Verzila Open](#)

OPEN JOURNAL SYSTEMS

[Journal Info](#)

USER

Username
Password
 Remember me

JOURNAL CONTENT

Search
All

Browse

- [By Issue](#)
- [By Author](#)
- [By Title](#)
- [Other Journals](#)

FONT SIZE

INFORMATION

- [For Readers](#)
- [For Authors](#)
- [For Subscribers](#)

contents

review

- 1 **The role of PET-CT in radiotherapy planning of solid tumours**
Stasa Jelercic, Mirjana Rajer

radiology

- 10 **Clinical value of whole-body magnetic resonance imaging in health screening of general adult population**
David Laszlo Tarnoki, Adam Domonkos Tarnoki, Antje Richter, Kinga Karlinger, Viktor Berczi, Dirk Pickuth
- 17 **Dynamic contrast-enhanced computed tomography to assess early activity of cetuximab in squamous cell carcinoma of the head and neck**
Sandra Schmitz, Denis Rommel, Nicolas Michoux, Renaud Lhommel, François-Xavier Hanin, Thierry Duprez, Jean-Pasca Machiels

nuclear medicine

- 26 **Appearance of Hürthle cell carcinoma soon after surgical extirpation of Hürthle cell adenoma and follicular adenoma of the thyroid gland**
Nevena Ristevska, Sinisa Stojanoski, Daniela Pop Gjorceva

experimental oncology

- 32 **Adjuvant TNF- α therapy to electrochemotherapy with intravenous cisplatin in murine sarcoma exerts synergistic antitumor effectiveness**
Maja Cemazar, Vesna Todorovic, Janez Scancar, Ursa Lamprecht, Monika Stimac, Urska Kamensek, Simona Kranjc, Andrej Coer, Gregor Sersa
- 41 **Mild hyperthermia influence on Herceptin[®] properties**
Jean-Michel Escoffre, Roel Deckers, Noboru Sasaki, Clemens Bos, Chrit Moonen

clinical oncology

- 50 **EGFR-expression in primary urinary bladder cancer and corresponding metastases and the relation to HER2-expression. On the possibility to target these receptors with radionuclides**
Jörgen Carlsson, Kenneth Wester, Manuel De La Torre, Per-Uno Malmström, Truls Gårdmark

- 59 **Higher levels of total pepsin and bile acids in the saliva as a possible risk factor for early laryngeal cancer**
Maja Sereg-Bahar, Ales Jerin, Irena Hocevar-Boltezar
- 65 **Hypodontia phenotype in patients with epithelial ovarian cancer**
Anita Fekonja, Andrej Cretnik, Danijel Zerdoner, Iztok Takac
- 71 **Consolidation electrochemotherapy with bleomycin in metastatic melanoma during treatment with dabrafenib**
Sara Valpione, Luca G. Campana, Jacopo Pigozzo, Vanna Chiarion-Sileni
- 75 **Treatment of tongue cavernous haemangioma with direct puncture and sclerotization with ethanol**
Tomaz Seruga, Jernej Lucev, Marko Jevsek
- 80 **Bevacizumab and irinotecan in recurrent malignant glioma, a single institution experience**
Tanja Mesti, Maja Ebert Moltara, Marko Boc, Martina Rebersek, Janja Ocvirk
- 86 **A new instrument for estimating the survival of patients with metastatic epidural spinal cord compression from esophageal cancer**
Dirk Rades, Stefan Huttenlocher, Amira Bajrovic, Johann H Karstens, Tobias Bartscht
- 91 **Dosimetric comparison for volumetric modulated arc therapy and intensity-modulated radiotherapy on the left-sided chest wall and internal mammary nodes irradiation in treating post-mastectomy breast cancer**
Qian Zhang, Xiao Li Yu, Wei Gang Hu, Jia Yi Chen, Jia Zhou Wang, Jin Song Ye, Xiao Mao Guo

radiophysics

- 99 **Estimated collective effective dose to the population from radiological examinations in Slovenia**
Dejan Zontar, Urban Zdesar, Dimitrij Kuhelj, Dean Pekarovic, Damijan Skrk

slovenian abstracts

The role of PET-CT in radiotherapy planning of solid tumours

Stasa Jelercic and Mirjana Rajer

Department of Radiotherapy, Institute of Oncology Ljubljana, Ljubljana, Slovenia

Radiol Oncol 2015; 49(1): 1-9.

Received 1 April 2013

Accepted 5 May 2013

Correspondence to: Mirjana Rajer, M.D., Ph.D., Department of Radiotherapy, Institute of Oncology, Zaloška 2, 1000 Ljubljana.
Phone: +386 1 5879 617; Fax: +386 1 5879 400; E-mail: mrajer@onko-i.si

Disclosure: No potential conflicts of interest were disclosed.

Background. PET-CT is becoming more and more important in various aspects of oncology. Until recently it was used mainly as part of diagnostic procedures and for evaluation of treatment results. With development of personalized radiotherapy, volumetric and radiobiological characteristics of individual tumour have become integrated in the multistep radiotherapy (RT) planning process. Standard anatomical imaging used to select and delineate RT target volumes can be enriched by the information on tumour biology gained by PET-CT. In this review we explore the current and possible future role of PET-CT in radiotherapy treatment planning. After general explanation, we assess its role in radiotherapy of those solid tumours for which PET-CT is being used most.

Conclusions. In the nearby future PET-CT will be an integral part of the most radiotherapy treatment planning procedures in an every-day clinical practice. Apart from a clear role in radiation planning of lung cancer, with forthcoming clinical trials, we will get more evidence of the optimal use of PET-CT in radiotherapy planning of other solid tumours.

Key words: positron emission therapy; radiotherapy; radiotherapy planning; tumour biology

Introduction

Cancer treatment has undergone major progress in the past decades. Many previously untreatable malignancies are now-days being successfully cured mostly by the combination of various treatment modalities. Radiotherapy (RT) is almost always part of them. When prescribing radical radiotherapy to the patients we need to achieve two goals; the target volume of the tissue irradiated to high-dose must encompass the entire tumour and any microscopic extensions of disease and the dose to the normal tissues should be kept as low as possible to avoid major acute and late complications. To arrive at these goals we have to combine technical improvements and clinical experiences.¹

The most important technical improvements consist of integration of computed tomography (CT) imaging into treatment planning and introduction of computer controlled multileaf collimator system. They enable development of more efficient techniques for dose delivery, such as

3-dimensional conformal radiotherapy (3D-CRT), intensity-modulated radiotherapy (IMRT) and volumetric arc radiotherapy (VMAT).^{1,2} Combined with innovative in-room image-guidance systems they increase precision and accuracy of radiation delivery.³

For target delineation we need accurate tumour assessment. Until recently, morphologic (anatomical) imaging with CT and/or MRI scans, was the only information available in the treatment planning process.^{1,4,5} This type of imaging is unable to describe all tumour characteristics. The progress in nuclear medicine has brought an additional perspective to define the extent and characteristics of the tumour. A new concept of 'biologic imaging' has been coined, which provides metabolic, functional, physiological, genotyping and fenotyping information.²

Namely, alongside with the innovations in medical physics and nuclear medicine imaging, there has been a major leap in the understanding of tumour biology. It is now recognized that cancer is not a ho-

mogeneous ensemble of cancer cells with similar attributes, but that consists of subvolumes with very different radiobiological properties such as hypoxic areas that are known to be highly radio-resistant, regions with uncontrolled cellular proliferation.³

The role of PET in tumour assessment and RT treatment planning

The integration of [18F]-fluorodeoxyglucose-positron emission tomography with computed tomography imaging (18FDG-PET-CT) has become an essential part in the evaluation of various types of malignancies.^{2,6} Its role has been widely accepted and confirmed in the staging process, the evaluation of response to treatment and detection of tumour recurrence.⁷⁻¹¹ However, the role of PET-CT has been proposed and studied in some other settings, especially in the planning of radiation delivery.^{5,7,12,13}

Positron Emission Tomography (PET) scanning has become a paradigm for molecular imaging.⁶ By administering different radiolabeled substances to the patients, we can identify biological characteristics of their tumours non-invasively.¹ Examples include the uptake of radiolabeled misonidazole as a surrogate for some forms of hypoxia, thymidine for cell proliferation, acetate and choline for lipid metabolism, methionine for amino acid uptake and the most used and studied [18F]-fluorodeoxyglucose (FDG).¹⁴ It is well known that many malignancies have higher metabolism and consequently uptake FDG more than surrounding normal tissues. This allows FDG-PET to image them.¹ Today more than 95% of the molecular imaging procedures in oncology make use of FDG.¹⁵

In radiotherapy planning, biologic imaging is particularly useful when the patient has poorly defined target volumes, (*e.g.* brain tumour or lung cancer), or when the intent of RT is to deliver higher than standard doses of radiotherapy (called dose escalation) to the tumour in order to kill as many tumour cells as possible and damage as few as possible normal tissue cells (*e.g.* head and neck cancer, lung carcinoma, prostate carcinoma).¹⁶ This type of RT planning needs accurate definition of the metabolically active tumour volume and its differentiation from surrounding tissue.

In the International Atomic Energy Agency report 2006-2007 experts concluded that RT based on PET-CT can be more accurate compared to RT based on standard CT in these cases:¹

- Imaging of lesions not apparent on CT or MRI, such as unsuspected lymph nodes or distant metastases
- Prevention of irradiation of tissues that don't contain tumour cells, such as atelectasis in the case of lung carcinoma
- When chemotherapy is added to RT, response to it can be assessed better with PET-CT, than with CT alone
- Development of "response adapted therapy" in which changes to target volumes could potentially be made during a treatment course.

Additionally, PET-CT is being studied as a replacement of conventional imaging techniques, especially in IMRT planning, which allows the delivery of non-uniform radiation intensity and non-homogeneous dose distribution inside the target volume.¹⁷⁻¹⁹ Imaging of biologically diverse tumour sub-volumes could potentially allow administration of different radiation doses to different tumour regions based on suspected tumour burden or radiosensitivity of the region of interest.¹⁷ For this focal dose escalation (inside the target) with the intent to improve the local control the terms 'dose painting' (2D) or 'dose sculpting' (3D) have been coined.⁶

In conformal 3D radiotherapy planning different volumes (anatomical units) need to be defined in order to deliver RT: gross tumour volume (GTV) includes macroscopically visible tumour and involved lymph nodes; clinical target volume (CTV) is derived from GTV by adding margins to it and includes all subclinical disease; and planning target organ (PTV) which is derived from variations in the size/position of CTV (physiological processes, tumour reduction or swelling) and the patient (weight loss, physiological processes, movements, daily set-up or technical errors).¹⁷ With development of biologically orientated RT, beside the search for a reliable delineation of the whole malignant lesion, the definition of biologically tumour subvolumes (BTV) is becoming another point of interest.¹⁶ The idea is that by selectively boosting radio-resistant areas while decreasing the dose to more susceptible zones, local tumour control rates could increase without increased side effects.²¹

When PET or PET-CT is used for RT planning, precise protocols should be followed and consistently applied.²² Main uncertainty in applying these protocols in every day clinical practice is tumour contouring based on PET (PET-CT). Up to now PET-based tumour contouring was mainly affected

by the (investigator's) choice of threshold. There have been some attempts to standardize lesion delineation (GTV) in FDG-PET-derived images: from arbitrary appointed threshold value as a percentage of the maximum uptake (e.g. 40%, 50%), threshold depending on the background signal, to defined absolute standardized uptake value (SUV) (e.g. 2 ± 0.4), and, the most commonly used, the visual interpretation of the PET scan.²³⁻²⁵ Nestle *et al.* compared different techniques of tumour contour definition by FDG-PET that lead to substantially different volumes, especially in patients with inhomogeneous tumors.²⁶ Furthermore, Yu *et al.* tried to determine the cut-off value of SUV by matching the pathologic gross tumour volume from whole-mount serial section of stage I non-small cell lung cancer (NSCLC) to PET-based GTV.²⁷ In this prospective study, the most appropriate threshold for tumour contour was a 3.0 absolute SUV or 31% of maximal SUV. In contrast, Devic *et al.* questioned use of various automatic delineation methods for several reasons: poor resolution of functional imaging, tumour motion, and distinct pathologic subtypes.²⁸ In exchange, authors considered a possible option of biologic targeting defined by anatomical modalities (CT and MRI) and multiple biological tracers to determine tumour subvolumes with different biological characteristic and different radiation dose to obtain better tumour control.

For more accurate results, innovations in image quality and reconstruction are required in order to determine the most proficient delineation technique.

The following sections provide a review of the clinical application of PET-CT in radiation treatment planning of some common cancers.

Lung cancer

When available PET-CT should be used to select patients with NSCLC for treatment with radical RT.¹ Several studies have shown that inclusion of PET-CT in the staging process of locally advanced NSCLC patients alters the planned treatment in up to 30% of cases by making them ineligible for radical RT, because of distant metastasis or extensive intrathoracic disease detected by PET-CT.²⁹⁻³¹ Gregory *et al.* reported in a prospective study that for patients with NSCLC treated with radical intent, PET-CT-based staging was significantly more powerfully correlated with overall survival than conventional imaging-based staging, across all staging and within cohorts of patients given any particular form of therapy.³⁰

In comparison to conventional imaging with CT or PET alone, integrated PET-CT can distinguish malignant lesions from benign lesions with an accuracy of 82% with varying sensitivity and specificity values (from 79% to 96% and from 40% to 83%, respectively).³² For mediastinal node stage, the benefit of PET-CT lies especially in very high negative predictive value over 90% with the sensitivity, specificity, positive predictive value and accuracy of 73%, 80%, 78% and 87%, respectively.³³

Evaluation of the neoadjuvant chemo-radiotherapy response before potential surgery is another possible implication of functional imaging.³⁴⁻³⁶ The survival of patients with persistent FDG uptake after radiotherapy or surgery is significantly worse than those without residual activity.³⁷ A recent study published by Usmanij *et al.* revealed that the degree of early metabolic change already after the second week of chemo-radiotherapy can predict the response to treatment.³⁸

Main limitation of FDG-PET as re-assessment tool is that it is not as good as in primary staging of mediastinal lymph nodes (sensitivity and specificity for detection being 63% and 85%, respectively). Currently it is not recommended as the only diagnostic tool in therapeutic decisions when restaging patients after induction therapy in stage III NSCLC.³⁴

Aerts *et al.* disclosed that areas with residual FDG uptake after high dose (chemo)-radiotherapy largely overlapped with the areas of high FDG uptake locations before treatment.³⁹ However, future trials should provide the basis to test if FDG uptake reflects 'radioresistance', by boosting high FDG uptake areas. Moreover, more specific tracer as 18F-fluoromisonidazole may be useful for dose-painting within the tumour as well.⁴⁰

PET-CT in the planning of lung tumour radiotherapy

Of all the common cancers, lung cancer has been most intensively studied by integrating dual imaging into the radiation treatment management of patients.^{1,41} There are two main reasons to use PET-CT in definitions of the volume needed to be irradiated:

- PET-CT significantly changes lymph node staging in the thorax, usually by showing more positive lymph nodes than CT
- In cases with atelectasis, PET-CT helps to define the border between tumour and atelectasis, allowing a smaller volume of lung to be treated.

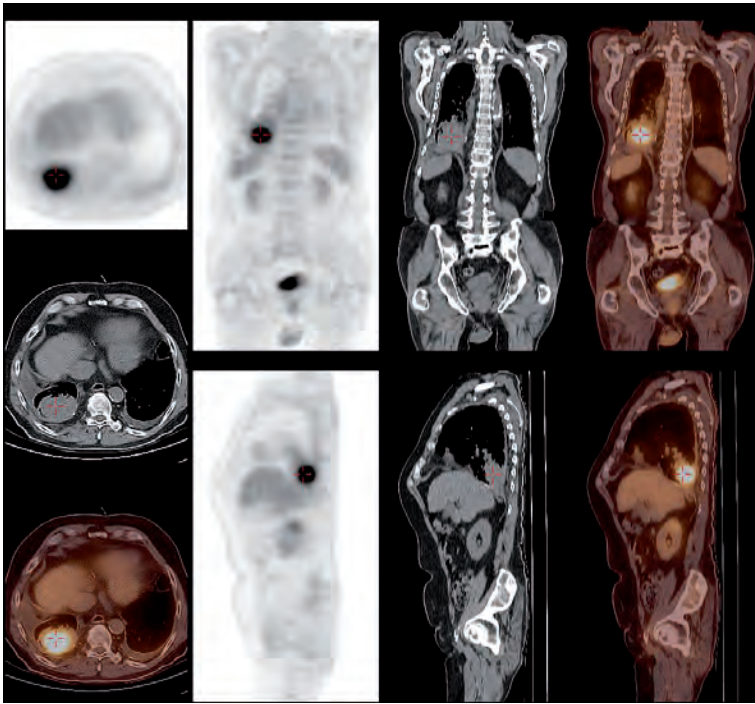


FIGURE 1. Differences in lung tumour and atelectasis seen on PET-CT.

Differences between tumour and atelectasis on PET-CT image are shown in Figure 1.

Nestle *et al.* have reviewed the results of 18 trials involving 661 patients with lung cancer that compared delineated target volumes, GTV, CTV and PTV using CT alone with the target volumes delineated using additional FDG-PET.⁴¹ Although the method of comparison was very different between trials, all of them came to the same conclusion that addition of FDG-PET would add essential information to CT result with significant consequences on GTV, CTV and PTV delineation. The main reasons for size modification lied in the better diagnosis of lymph node involvement and distinguishing tumour from atelectasis.⁴² Another important aspect of integrated PET-CT imaging in radiation planning was reduced interobserver delineation variability in respect to CT planning alone. The largest reduction was seen in the atelectasis region.^{43,44}

Head and neck cancer

Use of PET-CT can influence the treatment strategy of head and neck cancer patients in various ways. The greatest impact usually results from changes of nodal status before therapy, detection of distant metastasis and/or treatment evaluation.^{4,45-47}

In patients with high risk factors for higher nodal stage or distant metastases present (poor differentiation of primary tumour, advanced T stage (T3/T4), advanced N stage (N>2), tumours arising in hypopharynx and larynx, tumours with nodes in lower neck levels (IV/IVb))⁴⁸, the addition of pre-treatment PET imaging should be routinely used to avoid their over-treatment.⁴⁹ Combined PET-CT showed the highest sensitivity in detecting distant metastases in comparison to only FDG-PET and CT imaging (63% *vs.* 53% and 37%).⁵⁰

PET may also be of help in searching for the index tumour in patients presented with lymph node metastases of squamous cell carcinoma from unknown primary to the neck.⁵¹ Although detection rate of primary tumour ranges from 24%-44% as reviewed by Strojan *et al.*⁵², PET-CT should be performed when no primary lesion is suggested after thorough physical examination, indirect laryngoscopy and CT/MRI (Figure 2).⁵¹

The assessment of residual disease in the neck by PET-CT after chemoradiotherapy has become a standard for recognizing patients, who may avoid unnecessary neck dissection.⁵³ When evaluation is performed 3 months after the end of chemoradiation, PET-CT exhibit very high negative predictive value (97-100%, as reviewed by Hamoir *et al.*)⁵³, and metabolic complete response is predictive for disease-free and overall survival.⁵⁴

PET-CT in the planning of head and neck tumour radiotherapy

Recent studies have mainly focused on the feasibility of integrating FDG-PET with radiotherapy planning CT with the goal of enhancing tumour localization for IMRT, so the tumour coverage and normal tissue sparing can be optimized.⁵⁵ This is an important issue when very high doses of 70 Gy or more are being administered to lesions close to radiosensitive vital structures (*e.g.* brainstem or optic chiasm).¹ Schwartz *et al.* examined 20 head and neck cancer patients and studied the potential impact of PET-CT imaging on more tailored IMRT plans, with the exclusion of prophylactic irradiation of PET-negative regions.⁵⁵ Their PET-CT-based IMRT planning did not suffer a geographical nodal miss when correlated with pathological examination, and dose escalation up to 75 Gy was feasible in a selected group of patients without exceeding limiting doses of critical organs.

Several published studies on head and neck cancer patients that compared RT volumes on PET images with standard CT-based planning volumes,

observed significant differences in target delineation depending on the imaging technique.¹ Daisne *et al.* compared GTVs delineated at CT, MRI and PET-CT images with resected tumour specimen.⁵⁶ Although none of these imaging modalities was 100% accurate, the GTVs delineated at FDG-PET-CT were by far the closest to the reference volume from the surgical specimens. Burri *et al.* tried to correlate the SUV to pathologic specimen size and found that fixed threshold of 40% of maximum SUV would offer the best compromise between accuracy and the risk of underestimating tumour extent.⁴⁷

Several investigators analyzed the correlation between pre-therapeutic SUV and disease outcome and were reviewed by Inokuchi *et al.*⁵⁷ They disclosed that not only primary tumour SUVmax, but also SUVmax of cervical lymph nodes is a prognostic factor for local control, disease-free and overall survival.⁵⁷ Greven *et al.* reported that the changes in primary tumour SUV during and soon after completed treatment were also highly predictive of tumour recurrence compared to CT imaging alone.⁵⁸ They concluded that adaptive therapy planning based on PET-CT may be needed in order to improve the results of the radiation therapy.

As already said, FDG uptake correlates with outcome in head and neck cancer patients and most of loco-regional recurrences occur within FDG-avid areas⁵⁹, which would represent a reasonable target for focal dose escalation.^{23,24,58-60} The concept of dose painting of tumour subvolumes has been evaluated with two different methods: as dose painting by biologic image-defined contours²⁴, and as dose painting by numbers, *i.e.* prescribing dose to points in the target depending of biologic signal intensity.⁶¹ The latter has been demonstrated to allow higher intratumour doses at similar rates of toxicity. In the study of Duprez *et al.*, the median dose was escalated either to 80.9 Gy to the high-dose CTV or to 85.9 Gy to the GTV.⁶¹ None of the patients in the study required a treatment break and no Grade 4 acute toxicity was observed. However, which biologic characteristics of tumour and which biologic tracers are most relevant for dose painting are to be found out.

Two other promising PET tracers are 18F-fluoromisonidazole (FMISO) and 18F-fluoroazomycin arabinoside (FAZA), which provide quantitative measurements of tissue hypoxia, one of the main factors affecting treatment resistance in head and neck cancer.⁶² Rajendran *et al.* performed pretreatment FMISO-PET on 73 head and neck cancer patients and found that both

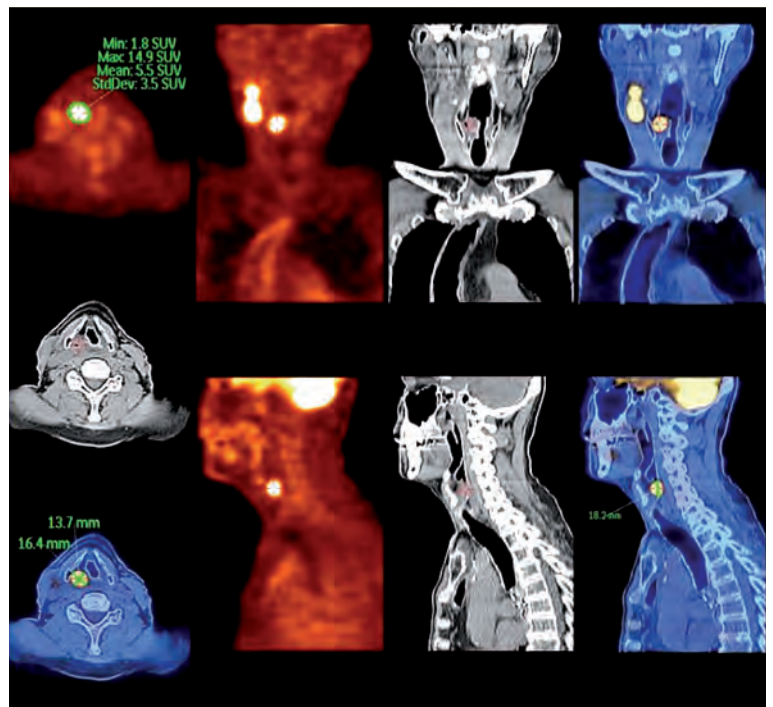


FIGURE 2. PET-CT images of 51-year old male with metastatic squamous cell carcinoma of unknown origin in cervical lymph nodes. The origin was found by PET-CT and later confirmed by a biopsy.

the degree of hypoxia and the size of hypoxic volume measured by FMISO-PET were independent predictive factors of survival.⁶³ Mortensen *et al.* found similar prognostic value of FAZA PET-CT imaging, demonstrating a significant difference in disease free survival rate in patients with non hypoxic tumours and patients with hypoxic tumours (93% and 60%, respectively, median follow up 19 months).⁶⁴

Despite the progress in anatomical and functional imaging in defining tumour borders, meticulous, peer reviewed clinical examination cannot be replaced by any of the imaging techniques when determining mucosal extent of primary tumour.⁶⁵ Future large clinical trials are warranted to evaluate the exact position of PET-CT in the radiotherapy treatment of head and neck cancer patients.

Oesophageal cancer

FDG-PET-CT can provide incremental staging information compared to combined CT and endoscopic ultrasonography in up to 40% of patients and can change management in one third of patients with oesophageal carcinoma.⁶⁶ In a systematic review by Muijs *et al.*, authors found a sig-

nificant improvement of the sensitivity (93%), accuracy (92%) and negative predictive value (98%) in the assessment of locoregional lymph nodes by integrated imaging, compared to the use of CT or PET alone.⁶⁷

There is no doubt that addition of FDG-PET in radiotherapy planning has a significant impact on target volume delineation (in 20–94% of patients), resulting in either reduction or increase in target volumes based on CT images as it is reviewed by Muijs *et al.*⁶⁷ Trials on patients undergoing resection or endoscopic ultrasound (EUS), which is the gold standard for clinical T-staging, report that PET-based tumour length correlate well with tumour length assessed by pathologic exam or EUS. However, this does not automatically mean correct allocation of malignant tissue *in vivo*, since the FDG uptake in pathologic areas on one side can be compensated on the other side by inflammation.⁶⁷

Some prospective studies^{68,69} reported about positive contribution of PET-based tumour delineation, which prevented geographic miss by identifying unsuspected malignant involvement in 30–60% of patients. However, given the poorer sensitivity of FDG-PET for primary tumour, the irradiated volume should not be reduced based on a negative FDG-PET finding in a region with suspect malignant involvement on other diagnostic investigations.⁷⁰

Another method to utilize FDG-PET in RT treatment planning is to reduce inter- and intra-observer variability. Toya *et al.* showed significantly increased concordance rate in GTV definition (*i.e.* ratio of the intersection of the GTVs to their union) in inter- and intraobserver comparison, when incorporating FDG-PET-CT images in comparison to CT images of cervical oesophageal carcinoma.⁷¹ In contrast, Scheuers *et al.* found no significant effect of the additional use of FDG-PET on the interobserver variability.⁶⁹ Several automatic (or semi-automatic) contouring methods using various thresholds have been tested, but until now have not yielded satisfactory results.⁶⁷

Omloo *et al.* evaluated the potential prognostic value of FDG uptake in oesophageal cancer patients.⁷² Most of 31 reviewed studies showed that pretreatment FDG uptake and postneoadjuvant treatment FDG uptake, as absolute values, are predictors for survival in univariate analysis. An early decrease in FDG uptake during neoadjuvant therapy is also predictive for pathologic response and survival in most studies. However, for more reliable results, a standardized protocol for FDG-PET acquisition and reconstruction is warranted.

Cervical cancer

T2 weighted MRI is currently the gold standard for primary tumour staging, especially in determining tumour extension in the parametria (reported accuracy of MRI is 80 to 90% compared to 60 to 69% for CT.^{73,74} In nodal staging PET-CT has been proven as an effective imaging technique in patients with locally advanced cervical carcinoma (*i.e.* FIGO stage is \geq IB2), with significantly better sensitivity and specificity in comparison to other morphological imaging (PET-CT sensitivity ranging from 77% to 96% for pelvic lymph nodes (PELN) and 50% to 100% for para-aortic lymph nodes (PALN), specificity from 55% to 75% for PELN and 83% to 95% for PALN, as reviewed by Magne *et al.*⁷⁵ In spite a high negative predictive value of 92% for PALN involvement⁷⁶, many authors still recommend a PALN dissection prior to beginning of chemoradiation, in order to avoid a possible miss of 8% of positive PALN patients.⁷⁴

Although the presence of metastatic lymph nodes in the PELN and PALN regions does not alter the clinical stage of disease, it alters radiation treatment strategy (either by extending irradiated volume to the common iliac or para-aortic areas or by escalating irradiated dose to the involved lymph nodes).⁷⁴ Moreover, Kidd *et al.* showed that the presence and extent (*i.e.* the most distant level of involved lymph nodes) of PET positive nodal metastases correlate well with recurrence-free and disease-free survival.⁷⁷

Esthappan *et al.* attempted to develop a treatment plan to deliver an escalated irradiation dose to involved nodal regions without harming adjacent organ at risk.⁷⁸ By the means of PET-CT-guided IMRT they delivered 50.4 Gy to the entire para-aortic region and 59.4 Gy to the positive para-aortic lymph nodes with acceptable irradiating dose to adjacent organs at risk. In their subsequent study, authors provided description of image acquisition, definitions of target volumes based on PET-CT and the doses prescribed to these different target volumes.⁷⁹ Kidd *et al.* prospectively compared toxicity and clinical outcomes of cervical cancer patients treated with PET-CT-guided IMRT and conventional radiation therapy, treated to the same prescription dose. The late bowel and bladder toxicity (of Grade 3 or more) were present in only 6% in IMRT group compared to 17% in non-IMRT group. The IMRT group also showed (unexpectedly) better overall and disease specific survival and a trend towards better recurrence free survival.⁸⁰

Several studies demonstrated that post-treatment metabolic response immediately after RT and 3 months after RT are predictive of patient outcome.^{81,82} Schwartz *et al.* proposed the implementation of routine post-treatment PET-CT, which could affect the approach and timing of salvage therapy of patients with cervical cancer recurrence and would also provide long-term prognostic information only 3 months after completion of therapy.⁸² Yoon *et al.* found that even earlier assessment (after receiving 54–60 Gy) of metabolic response of PELN in patients with initial PELN metastases correlates to disease free survival rate and could be a useful milestone for selecting patients who need more intense treatment.⁸¹

Conclusions

Recent advances in PET-CT can broaden the radiation oncologist's knowledge on the extent of the disease, in order to avoid missing the tumour, with consequent reduction of local control probability, and, on the other hand, avoiding the unjustified irradiation of healthy tissue. Furthermore, the correct definition of the disease stage is mandatory for selection of the most appropriate therapeutic strategy. Another important information for the radiation oncologist relates to biological characteristics of treated tumour, which could affect the response to radiotherapy and are of paramount importance for personalized and biologically oriented radiotherapy. The consensus of using PET-CT information for automated target volume delineation has not been reached yet and is awaiting further validation. PET-CT can answer many questions regarding correct disease staging and its biologic characteristics, but its exact role in every-day RT treatment planning is expected to be defined in future clinical trials.

Acknowledgement

Authors would like to thank doctors Ivana Žagar and Barbara Vidergar-Kralj for the pictures provided.

References

- MacManus M, Nestle U, Rosenzweig KE, Carrio I, Messa C, Belohlavek O, et al. Use of PET and PET/CT for radiation therapy planning: IAEA expert report 2006–2007. *Radiother Oncol* 2009; **91**: 85–94.
- The modern technology of radiation oncology, Volumes 1 & 2. Van Dyk J, editor. Madison: Medical Physics Publishing Corporation; 2005.
- Thorwarth D, Geets X, Pausco M. Physical radiotherapy treatment planning based on functional PET/CT data. *Radiother Oncol* 2010; **96**: 317–24.
- Vernon MR, Maheshwari M, Schultz CJ, Michel MA, Wong SJ, Campbell BH, et al. Clinical outcomes of patients receiving integrated PET/CT-guided radiotherapy for head and neck carcinoma. *Int J Radiat Oncol Biol Phys* 2008; **70**: 678–84.
- Petric P, Hudej R, Rogelj P, Blas M, Segedin B, Logar HBZ, et al. Comparison of 3D MRI with high sampling efficiency and 2D multiplanar MRI for contouring in cervix cancer brachytherapy. *Radiol Oncol* 2012; **46**: 242–51.
- Ling CC, Humm J, Larson S, Amols H, Fuks Z, Leibel S, et al. Towards multidimensional radiotherapy (MD-CRT): biological imaging and biological conformality. *Int J Radiat Oncol Biol Phys* 2000; **47**: 551–60.
- PET Professional resources and outreach source: 18F-fluorodeoxyglucose (FDG) PET and PET/CT practice guidelines in oncology. A summary of the recommendations and practice guidelines of professional groups. Available April 2013: http://www.snm.org/docs/PET_PROS/OncologyPracticeGuidelineSummary.pdf
- Fletcher JW, Djulbegovic B, Soares HP, Siegel BA, Lowe VJ, Lyman GH, et al. Recommendations on the use of 18F-FDG PET in oncology. *J Nucl Med* 2008; **49**: 480–507.
- Ben-Haim S, Ell P. 18F-FDG PET and PET/CT in the evaluation of cancer treatment response. *J Nucl Med* 2009; **50**: 88–99.
- Quartuccio N, Treglia G, Salsano M, Mattoli MV, Muoio B, Piccardo A, et al. The role of Fluorine-18-Fluorodeoxyglucose positron emission tomography in staging and restaging of patients with osteosarcoma. *Radiol Oncol* 2013; **47**: 97–102.
- Kim JS, Jeong YJ, Sohn MH, Jeong HJ, Lim ST, Kim DW, et al. Usefulness of F-18 FDG PET/CT in subcutaneous panniculitis-like T cell lymphoma: disease extent and treatment response evaluation. *Radiol Oncol* 2012; **46**: 279–83.
- Gregoire V, Haustermans K, Geets X, Roels S, Lonnew M. PET-Based treatment planning in Radiotherapy: A new standard? *J Nucl Med* 2007; **48**: 68–77.
- Giernik IF, Dizendorf E, Baumert BG, Reiner B, Burger C, Davis JB, et al. Radiation treatment planning with an integrated positron emission and computer tomography (PET/CT): A feasibility study. *Int J Radiat Oncol Biol Phys* 2003; **57**: 853–63.
- Haubner R. PET radiopharmaceuticals in radiation treatment planning – synthesis and biological characteristics. *Radiat Oncol* 2010; **96**: 280–7.
- Halldin C. How to image (tracers). State of the art and future development. [Abstract]. *Radiat Oncol* 2010; **94(Suppl 1)**: S5–6.
- Nestle U. Clinical requirements for target volume selection/ delineation. [Abstract]. *Radiother Oncol* 2010; **94(Suppl 1)**: S9.
- Bentzen SM, Gregoire V. Molecular imaging-based dose painting: a novel paradigm for radiation therapy prescription. *Semin Radiat Oncol* 2011; **21**: 101–10.
- Madani I, Duthoy W, Derie C, De Gersem W, Boterberg T, Jacobs F, et al. Positron emission tomography-guided, focal-dose escalation using intensity-modulated radiotherapy for head and neck cancer. *Int J Radiat Oncol Biol Phys* 2007; **68**: 126–35.
- Pinkawa M, Piroth M, Holy R, Klotz J, Nussen S, KrohnT, et al. Intensity-modulated radiotherapy for prostate cancer implementing molecular imaging with 18F-choline PET-CT to define a simultaneous integrated boost. [Abstract]. *Radiother Oncol* 2010; **94(Suppl 1)**: S11.
- Bethesda MD. International Commission on Radiation Units 1993. ICRU Report 50. Prescribing, recording and reporting photon beam therapy.
- Aerts HJWL, Van Baardwijk AAW, Petit SF, Offermann C, Van Loon J, Houben R, et al. Identification of residual metabolic-active areas within individual NSCLC tumours using a pre-radiotherapy 18Fluorodeoxyglucose-PET-CT scan. *Radiother Oncol* 2009; **91**: 386–92.
- Sattler B, Lee JA, Lonsdale M, Coche E. PET/CT (and CT) instrumentation, image reconstruction and data transfer for radiotherapy planning. *Radiother Oncol* 2010; **96**: 288–97.
- Mah K, Caldwell CB, Ung YC, Danjoux CE, Balogh JM, Ganguli SN, et al. The impact of 18FDG-PET on target and critical organs in CT-based treatment planning of patients with poorly defined non-small-cell lung carcinoma: a prospective study. *Int J Radiat Oncol Bio Phys* 2002; **52**: 339–50.

24. Bradley J, Thorstad WL, Mutic S. Impact of FDG-PET on radiation therapy volume delineation in non-small cell lung cancer. *Int J Radiat Oncol Biol Phys* 2003; **57**: 853-63.
25. Erdi YE, Rosenzweig K, Erdi AK, Macapinlac HA, Hu YC, Braban LE, et al. Radiotherapy treatment planning for patients with non-small cell lung cancer using positron emission tomography (PET). *Radiother Oncol* 2002; **62**: 51-60.
26. Nestle U, Kremp S, Schaefer-Schuler A, Sebastian-Welsch C, Hellwig D, Rube C, et al. Comparison of different methods for delineation of 18F-FDG PET-positive tissue for target volume definition in radiotherapy of patients with non-small cell lung cancer. *J Nucl Med* 2005; **46**: 1342-8.
27. Yu J, Li X, Xing L, Mu D, Fu Z, Sun X, et al. Comparison of tumor volumes as determined by pathologic examination and FDG-PET/CT images of non-small-cell lung cancer: a pilot study. *Int J Radiat Oncol Biol Phys* 2009; **75**: 1468-74.
28. Devic S, Tomic N, Faria S, Menard S, Lisbona R, Lehnert S. Defining radiotherapy target volumes using 18F-fluoro-deoxy-glucose positron emission tomography/computed tomography: Still a Pandora's box? *Int J Radiat Oncol Biol Phys* 2010; **78**: 1555-62.
29. Deniaud-Alexandre E, Touboul E, Lerouge D, Grahek D, Foulquier JN, Petegnief Y, et al. Impact of computed tomography and 18F-deoxyglucose coincidence detection emission tomography image fusion for optimization of conformal radiotherapy in non-small cell lung cancer. *Int J Radiat Oncol Biol Phys* 2005; **63**: 1432-41.
30. Gregory DL, Hicks RJ, Hogg A, Binns DS, Shum PL, Milner A, et al. Effect of PET/CT on management of patients with non-small cell lung cancer: results of prospective study with 5-year prospective data. *J Nucl Med* 2012; **53**: 1007-15.
31. Cuaron J, Dunphy M, Rimner A. Role of FDG-PET scans in staging, response assessment and follow-up care for non-small cell lung cancer. *Front Oncol* 2013; **2**: 1-7.
32. Hellwig D, Baum RP, Kirsch CM. FDG-PET, PET/CT and conventional nuclear medicine procedures in the evaluation of lung cancer: A systematic review. *Nuklearmedizin* 2009; **48**: 59-69.
33. De Wever W, Stroobants S, Coolen J, Verschakelen JA. Integrated PET/CT in the staging of non-small cell lung cancer: technical aspects and clinical integration. *Eur Respir J* 2009; **33**: 201-12.
34. Rebollo-Aguirre AC, Ramos-Font C, Villegas Portero R, Cook GJ, Llamas Elvira JM, Romero Tabares A. Is FDG-PET suitable for evaluation of neoadjuvant therapy in non-small cell lung cancer? Evidence with systematic review of the literature. *J Surg Oncol* 2010; **101**: 486-94.
35. Cistaro A, Quartuccio N, Mojtahedi A, Fania P, Filosso PL, Ficola U, et al. Prediction of 2 years-survival in patients with stage I and II non-small cell lung cancer utilizing 18F-FDG PET/CT SUV quantification. *Radiol Oncol* 2013; **47**: 219-23.
36. Berghmans T, Dusart M, Paesmans M, Hossein-Foucher C, Buvat I, Cataigne C, et al. Primary tumor standardised uptake value (SUVmax) measured on fluorodeoxyglucose positron emission tomography (FDG-PET) is of prognostic value for survival in non-small cell lung cancer (NSCLC): a systematic review and meta-analysis (MA) by the European Lung Cancer Working Party for the IASLC Lung Cancer Staging Project. *J Thorac Oncol* 2008; **3**: 6-12.
37. Mac Manus MP, Hicks RJ, Matthew JP, Wirth A, Rischin D, Ball DL. Metabolic (FDG-PET) response after radical radiotherapy/chemoradiotherapy for non-small cell lung cancer correlates with patterns of failure. *Lung Cancer* 2005; **49**: 95-108.
38. Usmanij EA, Geus-Oei LF, Troost EG, Peters-Bax L, van der Heijden EH, Kaanders JH, et al. 18F-FDG PET early response evaluation of locally advanced non-small cell lung cancer treated with concomitant chemoradiotherapy. *J Nucl Med* 2013; **54**: 1528-34.
39. Aerts HJWL, Van Baardwijk AAW, Petit SF, Offermann C, Van Loon J, Houben R, et al. Identification of residual metabolic-active areas within individual NSCLC tumours using a pre-radiotherapy 18F-fluorodeoxyglucose-PET-CT scan. *Radiother Oncol* 2009; **91**: 386-92.
40. Gagel B, Reinartz P, Demirel C, Kaiser HJ, Zimny M, Piroth M, et al. [18F] fluoromisonidazole and [18F] fluorodeoxyglucose positron emission tomography in response evaluation after chemo-radiotherapy of non-small-cell lung cancer: a feasibility study. *BMC Cancer* 2006; **6**: 51.
41. Nestle U, Kremp S, Grosu AL. Practical integration of 18F-FDG-PET and PET-CT in the planning of radiotherapy for non-small cell lung cancer (NSCLC): The technical basis, ICRU-target volumes, problems, perspectives. *Radiother Oncol* 2006; **81**: 209-25.
42. De Ruyscher D, Wanders S, van Haren E, Hochstenbag M, Geeraedts W, Utama I, et al. Selective mediastinal node irradiation based on FDG-PET scan data in patients with non-small cell lung cancer: a prospective clinical study. *Int J Radiat Oncol Biol Phys* 2005; **62**: 988-94.
43. Steenbakkens RJ, Duppen JC, Fitton I, Deurloo KE, Zipp LJ, Comans EF, et al. Reduction of observer variation using matched CT-PET for lung cancer delineation: a three dimensional analysis. *Int J Radiat Oncol Biol Phys* 2006; **64**: 435-48.
44. Ashamalla H, Rafla S, Parikh K, Mokhtar B, Goshwami G, Kambam S, et al. The contribution of integrated PET/CT to the evolving definition of treatment volumes in radiation treatment planning in lung cancer. *Int J Radiat Oncol Biol Phys* 2005; **63**: 1016-23.
45. Lonneux M, Hamoir M, Reyckler H, Maingon P, Duvillard C, Calais G, et al. Positron emission tomography with [18F]fluorodeoxyglucose improves staging and patient management in patients with head and neck squamous cell carcinoma: a multicenter prospective study. *J Clin Oncol* 2010; **28**: 1190-5.
46. Xu GT, Guan DJ, He ZY. 18F-FDG-PET/CT for detecting distant metastases and second primary cancers in patients with head and neck cancer: A meta-analysis. *Oral Oncol* 2011; **28**: 1190-5.
47. Burri RJ, Rangaswamy B, Kostakoglu L, Hoch B, Genden EM, Som PM, et al. Correlation of positron emission tomography standard uptake value and pathologic specimen size in cancer of the head and neck. *Int J Radiat Oncol Biol Phys* 2008; **71**: 682-8.
48. Haerle SK, Schmid DT, Ahmad N, Hany TF, Stoekli SJ. The value of (18) F-FDG PET/CT for the detection of distant metastases in high-risk patients with head and neck squamous cell carcinoma. *Oral Oncol* 2011; **47**: 653-9.
49. Ford EC, Herman J, Yorke E, Wahl RL. 18-FDG-PET/CT for Image-guided and Intensity modulated radiotherapy. *J Nucl Med* 2009; **50**: 1655-65.
50. Senft A, De Bree R, Hokstra O, Kuik DJ, Golding R, Oyen WJG, et al. Screening for distant metastases in head and neck cancer patients by chest CT or whole body FDG-PET: a prospective multicenter trial. *Radiat Oncol* 2008; **87**: 221-9.
51. De Bree R. The real additional value of FDG-PET in detecting the occult primary tumour in patients with cervical lymph node metastases of unknown primary tumour. *Eur Arch Otorhinolaryngol* 2010; **267**: 1653-5.
52. Strojanc P, Ferlito A, Medina J, Woolgar JA, Rinaldo A, Robbins KT, et al. Contemporary management of lymph node metastases from an unknown primary to the neck: I. A review of diagnostic approaches. *Head Neck* 2011; **35**: 123-32.
53. Hamoir M, Ferlito A, Schmitz S, Hanin FX, Thariat J, Weynad B, et al. The role of neck dissection in the setting of chemoradiation therapy for head and neck squamous cell carcinoma with advanced neck disease. *Oral Oncology* 2012; **48**: 203-10.
54. Conell CA, Corry J, Milner AD, Hogg A, Hicks RJ, Riscin D, et al. Clinical impact of, and prognostic stratification by, F-18 FDG PET/CT in head and neck mucosal squamous cell carcinoma. *Head Neck* 2007; **29**: 986-95.
55. Schwartz DL, Ford EC, Rajendran J, Yueh B, Coltrera MD, Virgin J, et al. FDG-PET/CT-guided intensity modulated head and neck radiotherapy: A pilot investigation. *Head Neck* 2005; **27**: 478-87.
56. Daisne JF, Duprez T, Weynad B, Lonneux M, Hamoir M, Reyckler H, et al. Tumor volume in pharyngolaryngeal squamous cell carcinoma: Comparison at CT, MR imaging, and FDG PET and validation with surgical specimen. *Radiology* 2004; **233**: 93-100.
57. Inokuchi H, Kodaira T, Tachibana H, Nakamura T, Tomita N, Nakahara R, et al. Clinical usefulness of [18F] Fluoro-2-deoxy-D-Glucose uptake in 178 head-and-neck cancer patients with nodal metastasis treated with definitive chemoradiotherapy: consideration of its prognostic value and ability to provide guidance for optimal selection of patients for planned neck dissection. *Int J Radiat Oncol Biol Phys* 2011; **79**: 747-55.
58. Greven KM, Williams D, Mattern M, West T, Kearns W, Staab D, et al. Prospective study of serial PET/CT imaging for patients with squamous cell cancer of the head and neck and the possibility of adaptive planning. [Abstract]. *Int J Radiat Oncol Biol Phys* 2009; **75**(Suppl 1): S394.

59. Soto DE, Kessler ML, Piert M, Eisbruch A. Correlation between pretreatment FDG-PET biological target volume and anatomical location of failure after radiation therapy for head and neck cancers. *Radioth Oncol* 2008; **89**: 13-8.
60. Dirix P, Vandecayeve V, De Keyzer F, Stroobants S, Hermans R, Nuyts S. Dose painting in radiotherapy for head and neck squamous cell carcinoma: Value of repeated functional imaging with ¹⁸F-FDG PET, ¹⁸F-fluoromisonidazole PET, diffusion-weighted MRI, and dynamic contrast-enhanced MRI. *J Nucl Med* 2009; **50**: 1020-7.
61. Duprez F, De Neve W, De Gersem W, Coghe M, Madani I. Adaptive dose painting by numbers for head-and-neck cancer. *Int J Radiat Oncol Biol Phys* 2011; **80**: 1045-55.
62. Brizel DM, Sibley GS, Prosnitz LR, Scher RL, Dewhirst MW. Tumor hypoxia adversely affects the prognosis of carcinoma of the head and neck. *Int J Radiat Oncol Biol Phys* 1997; **38**: 285-9.
63. Rajendran JG, Schwartz DL, O'Sullivan J, Peterson LM, Ng P, Scharnhorst J, et al. Tumor hypoxia imaging with F18 fluroromisonidazole positron emission tomography in head and neck cancer. *Clin Cancer Res* 2006; **12**: 5435-41.
64. Mortensen LS, Johansen J, Kallehague J, Primdahl H, Busk M, Lassen P, et al. FAZA PET/CT hypoxia imaging in patients with squamous cell carcinoma of head and neck treated with radiotherapy: results from the DAHANCA 24 trial. *Radiother Oncol* 2012; **105**: 14-20.
65. Rosenthal DI, Asper JA, Barker JL, Garden AS, Chao KSC, Morrison WH, et al. Importance of patient examination to clinical quality assurance in head and neck radiation oncology. *Head Neck* 2006; **28**: 967-73.
66. Barber TW, Duong CP, Leong T, Bressel M, Drummond EG, Hicks RJ. 18F-FDG PET/CT has a high impact on patient management and provides powerful prognostic stratification in the primary staging of esophageal cancer: A prospective study with mature survival data. *J Nucl Med* 2012; **53**: 864-71.
67. Muijs CT, Beukema JC, Pruim J, Mul VE, Groen H, Plukker JT, et al. A systematic review on the role of FDG-PET/CT in tumour delineation and radiotherapy planning in patients with esophageal cancer. *Radiother Oncol* 2010; **97**: 165-71.
68. Leong T, Everitt C, Yuen K. A prospective study to evaluate the impact of FDG-PET on CT-based radiotherapy treatment planning for esophageal cancer. *Radiother Oncol* 2006; **78**: 254-61.
69. Schreurs LM, Busz DM, Paardekooper GM, Beukema JC, Jager PL, Van der Jagt EJ, et al. Impact of 18-fluorodeoxyglucose positron emission tomography defined target volumes in radiation treatment planning of esophageal cancer: reduction in geographic misses with equal inter-observer variability. *Dis Esophaus* 2010; **23**: 483-510.
70. Vrieze O, Haustermans K, DeWever W, Lerut T, Van Cutsem E, Ectors N, et al. Is there a role for FDG-PET in radiotherapy planning in esophageal carcinoma? *Radioth Oncol* 2004; **73**: 269-75.
71. Toya R, Murakami R, Imuta M, Matsuyama T, Saito T, Shiraishi S, et al. Impact of Hybrid FDG-PET/CT on Gross Tumor Volume Definition of Cervical Esophageal Cancer: Improving Inter- and Intra-observer Variations. [Abstract]. *Int J Radiat Oncol Biol Phys* 2011; **81(Suppl 1)**: S324.
72. Omloo JMT, Van Heijl M, Hoekstra OS, Van Berge Henegouen MI, Van Lanschot JJB, Sloof GW. FDG-PET parameters as prognostic factor in esophageal cancer patients: a review. *Ann Surg Oncol* 2011; **18**: 3338-52.
73. Mitchel DG, Snyder B, Coakley F, Reinhold C, Thomas G, Amendola M, et al. Early invasive cervical cancer: Tumor delineation by magnetic resonance imaging, computed tomography, and clinical examination, verified by pathologic results, in the ACRIN 6651/GIG 183 Intergroup study. *J Clin Oncol* 2006; **24**: 5687-94.
74. Haie-Meder C, Mazon R, Magne N. Clinical evidence on PET-CT for radiation therapy planning in cervix and endometrial cancer. *Radiother Oncol* 2010; **96**: 351-5.
75. Magne N, Chargari C, Vicenzi L, Gillion N, Messai T, Magne J, et al. New trends in the evaluation and treatment of cervix cancer. The role of FDG-PET. *Cancer Treatm Rev* 2008; **34**: 671-81.
76. Boughanim M, Leboulleux S, Rey A, Pham CT, Zafrani Y, Duvillard P, et al. Histologic results of para-aortic lymphadenectomy in patients treated for stage Ib2/II cervical cancer with negative (18F) Fluorodeoxyglucose positron emission tomography scans in the para-aortic area. *J Clin Oncol* 2008; **26**: 2558-61.
77. Kidd EA, Siegel BA, Dehdashti F, Rader JS, Mutch DG, Powell MA, et al. Lymph node staging by positron emission tomography in cervical cancer: Realltion to prognosis. *J Clin Oncol* 2010; **28**: 2108-13.
78. Esthappan J, Mutic S, Malyapa RS, Grigsby PW, Zoberi I, Dehdashti F, et al. Treatment planning guidelines regarding the use of CT/PET-guided IMRT for cervical carcinoma with positive paraaortic lymph nodes. *Int J Radiat Oncol Biol Phys* 2004; **58**: 1289-97.
79. Esthappan J, Chaudhari S, Santanam L, Mutic S, Olsen J, MacDonald DM, et al. Prospective clinical trial of positron emission tomography/computed tomography image-guided intensity-modulated radiation therapy for cervical carcinoma with positive para-aortic lymph nodes. *Int J Radiat Oncol Biol Phys* 2008; **72**: 1134-9.
80. Kidd EA, Siegel BA, Dehdashti F, Rader JS, Mutic S, Mutch DG, et al. Clinical outcomes of definitive intensity-modulated radiation therapy with fluoro-deoxyglucose – positron emission tomography simulation in patient with locally advanced cervical carcinoma. *Int J Radiat Oncol Biol Phys* 2010; **77**: 1085-91.
81. Yoon MS, Ahn SJ, Nah BS, Chung WK, Song HC, Yoo SW, et al. Metabolic response of lymph nodes immediately after RT is related with survival outcome of patients with pelvic node-positive cervical cancer using consecutive (¹⁸F)fluorodeoxyglucose-positron emission tomography/computed tomography. *Int J Radiat Oncol Biol Phys* 2012; **84**: 491-7.
82. Schwartz JK, Siegel BA, Dehdashti F, Grigsby PW. Association of post-therapy positron emission tomography with tumor response and survival in cervical carcinoma. *JAMA* 2007; **298**: 2289-95.

Clinical value of whole-body magnetic resonance imaging in health screening of general adult population

David Laszlo Tarnoki^{1,2}, Adam Domonkos Tarnoki^{1,2}, Antje Richter¹, Kinga Karlinger², Viktor Berczi², Dirk Pickuth¹

¹ Department of Diagnostic and Interventional Radiology, Caritasklinikum Saarbrücken St. Theresia, Academic Teaching Hospital of Saarland University, Saarbrücken, Germany

² Department of Radiology and Oncotherapy, Semmelweis University School of Medicine, Budapest, Hungary

Radiol Oncol 2015; 49(1): 10-16.

Received 12 December 2013

Accepted 18 June 2014

Correspondence to: David Laszlo Tarnoki, M.D., Ph.D., Department of Radiology and Oncotherapy, Semmelweis University, Budapest, Hungary, 78/a Ulloi street, Budapest 1082, Hungary. E-mail: tarnoki4@gmail.com

Disclosure: No potential conflicts of interest were disclosed.

* David Laszlo Tarnoki and Adam Domonkos Tarnoki contributed equally to this work.

Background. Whole-body magnetic resonance imaging (WB-MRI) and angiography (WB-MRA) has become increasingly popular in population-based research. We evaluated retrospectively the frequency of potentially relevant incidental findings throughout the body.

Materials and methods. 22 highly health-conscious managers (18 men, mean age 47±9 years) underwent WB-MRI and WB-MRA between March 2012 and September 2013 on a Discovery MR750w wide bore 3 Tesla device (GE Healthcare) using T1 weighted, short tau inversion recovery (STIR) and diffusion weighted imaging (DWI) acquisitions according to a standardized protocol.

Results. A suspicious (pararectal) malignancy was detected in one patient which was confirmed by an endorectal sonography. Incidental findings were described in 20 subjects, including hydrocele (11 patients), benign bony lesion (7 patients) and non-specific lymph nodes (5 patients). Further investigations were recommended in 68% (ultrasound: 36%, computed tomography: 28%, mammography: 9%, additional MRI: 9%). WB-MRA were negative in 16 subjects. Vascular normal variations were reported in 23%, and a 40% left proximal common carotid artery stenosis were described in one subject.

Conclusions. WB-MRI and MRA lead to the detection of clinically relevant diseases and unexpected findings in a cohort of healthy adults that require further imaging or surveillance in 68%. WB-MR imaging may play a paramount role in health screening, especially in the future generation of (epi)genetic based screening of malignant and atherosclerotic disorders. Our study is the first which involved a highly selected patient group using a high field 3-T wide bore magnet system with T1, STIR, MRA and whole-body DWI acquisitions as well.

Key words: angiography; incidentaloma; atherosclerosis; high field magnet; diffusion weighted imaging

Introduction

Whole-body magnetic resonance imaging (WB-MRI) has become increasingly popular in the recent decade due to its high soft tissue spatial resolution, multiplanarity, lack of ionising radiation, low incidence of nephrotoxicity caused by contrast agents, as well as high sensitivity and specificity in the de-

tection of vascular and malignant diseases.^{1,2} Due to financial reasons and limited availability, WB-MRI enables an early diagnosis mainly in defined groups of subjects who do not show symptoms yet. The most common diseases in elderly population include malignant tumours and cardiovascular diseases.³ WB-MRI is capable of detecting a wide range of malignant diseases; such as bronchial car-

cinoma, hepatic malignancies, renal carcinoma, colonic cancer, lymphoma, and also rare malignancies such as bone or soft tissue tumours.⁴

With wider availability of WB-MRI, increased number of incidental findings of potential clinical relevance (36%) have been reported.⁵ Only a limited number of studies on screening with 1.5-T WB-MRI is available in the literature, often restricted to a single organ system.⁵ However, the prevalence of incidental findings has not yet been described on a 3-Tesla (T) wide bore device. Furthermore, no screening studies including both whole-body diffusion weighted imaging (DWI) and WB-MRA have been performed.

Our aim was to retrospectively analyze the frequencies of potentially relevant incidental findings throughout the body, especially in view of those that require further medical evaluation.

Materials and methods

We carried out a retrospective analysis of healthy adults (mainly managers, lawyers, accountants, chief executive officers, company directors) with extreme health consciousness who underwent whole-body MRI and MRA at the Institute of Diagnostic and Interventional Radiology, Caritasklinikum Saarbrücken St. Theresia, Germany between March 2012 and September 2013. Subjects were referred to WB-MRI scan by a family doctor, their company or were self referrals. The healthy adults completed a comprehensive questionnaire including their current symptoms, previous clinical findings, operations, and risk factors. MR studies were acquired on a Discovery MR750w 3 Tesla wide bore device (General Electric Healthcare, GE, Milwaukee, USA; 70 cm wide bore magnet) using T1 weighted (fast Spin Echo technique with a slice thickness of 5 mm), short tau inversion recovery (STIR), and DWI sequences according to a standardized protocol (Figure 1, 2). Depending upon the height of the patient, 6 or 7 slabs were acquired in a slab-by-slab-technique with no continuous table movement. The WB-MRI protocol was identical for all participants and included a plain WB-MRI and detailed examination of head, neck, chest, abdomen, pelvis, spine and extremities. A rolling platform with extended field of view allowed whole-body examinations with a table range of more than 200 cm, several dozen simultaneous receiver channels, and multiple plugs for attaching several RF coils concurrently enabling the individual to be covered with coils from “head to toe”. The high number of



FIGURE 1. Whole-body MRI set-up of coils (head, chest, abdomen and extremity coils) in a wide bore magnet device.



FIGURE 2. A-C Whole-body MRI acquired on a dedicated whole-body MRI system and matrix coils in asymptomatic, smoker male 46-year-old patient, coronal (A) T1, (B) STIR and (C) DWI images.



FIGURE 3. Whole-body MRA acquired on a dedicated whole-body MRI system and matrix coils with a single injection of contrast agent in an asymptomatic male 52-year-old patient, coronal reconstruction, pasted image.

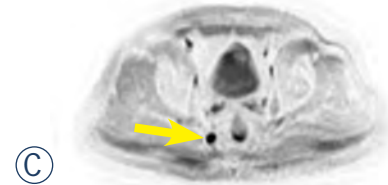


FIGURE 4. A-C Whole-body MR image of a 52-year-old male patient with history of sleep disorder, night sweats, hypercholesterinaemia and previous smoking. Note the right pararectal 16x14 mm mass (arrows) on the coronal (A) T1 (hypointense signal) and (B) STIR images (hyperintense signal); (C) diffusion weighted (DWI) axial image indicating a restricted diffusion. Inverted DWI image is similar to a PET image.

coils allowed for parallel imaging which speeded up the data acquisition.

MR angiography (using 3D technique) was performed by the administration of 0.45 ml/kg body weight gadolinium contrast agent (0.5 mmol/ml gadoterate meglumine, Dotarem, Guerbet, Roissy, France), and was automatically injected at a flow rate of 1.2 ml/s in the first and 0.6 ml/s in the second phase (Figure 3). The patient was placed in the supine position, and the phases were acquired using respiratory gating.

Findings and anatomical variants were documented in a standardized reading protocol. Picture archiving and communication system (AGFA IMPAX and KIS-RIS ORBIS, AGFA Healthcare, Mortsel, Belgium) were used for image storing. In order to ensure the best possible quality and to minimize the inter-reader variability, three readers reported the whole set of images: first-line reading was performed by a resident in radiology (2-4 years' experience), followed by two senior radiologists including the head of the department. The three readers evaluated the studies independently from each other. Then the results were discussed in consensus. Finally, opinion, diagnoses/differential diagnoses and recommendation were evaluated together. The evaluation of images were carried out retrospectively by reviewing the reports and images of the patients. Findings were classified as normal, insignificant (abnormalities without well-defined diagnostic and therapeutic consequences according to existing guidelines and best practice recommendations), potentially significant (abnormalities potentially needing further medical evaluation or follow-up), and significant (findings that require further medical evaluation and immediate referral). Statistical analysis was performed by Microsoft Excel. The investigators followed the Helsinki Declarations and the European Council Convention on Protection of Human Rights in Bio-Medicine.

Results

Subject characteristics

Twenty-two healthy adults (18 men, age 47±9 years, mean±standard deviation) who underwent whole-body MRI and MRA imaging between March 2012 and September 2013 were included in the study. The WB-MR scans were analyzed retrospectively. The mean body mass index of the subjects was 25.2 kg/m². Fourteen subjects were completely asymptomatic. Nine subjects had a history of allergy (*e.g.*, drug, animals, pollens). Nineteen subjects were never smokers, two reported a previous smoking history and one was active smoker. Subjects reported never, occasional, and regular sport activity in 5%, 10% and 85%, respectively. Four-fifth of the subjects had current symptoms, previous symptoms/surgeries.

WB-MRI findings

A suspicious (pararectal) malignancy was detected in one patient (Figure 4). Two patients had negative MR reports, whereas incidental findings were

described in 20 subjects. The findings are shown in Figure 5. Hydrocele was the most common incidental finding (11 patients; 11 of 18 men), followed by a benign bony lesion in 7 patients. Incidental findings would have needed diagnostic workup at an urologist (17 lesions), rheumatologist (15 lesions), internist (13 lesions), otorhinolaryngologist (6 lesions), pulmonologist (6 lesions), surgeon (5 lesions), gynecologist (4 lesions), and dermatologist (1 lesion). Further investigations were recommended in 68% of subjects including eight sonographies (2/3 abdominal), five chest computed tomographies (CT), one pelvic CT, two mammographies and two additional MRIs. In case of the suspicious pararectal malignancy, biopsy was recommended. The patient had an endorectal sonography which confirmed the presence of a highly suspicious mass, probably a lymph node. A rectoscopy/colonoscopy was planned, however the patient moved to another city and the further diagnostic/therapeutic workup is unknown yet.

WB-MRA findings

WB-MRA was negative in 16 subjects. Vascular normal variations (*e.g.* irregular caliber of the vertebral artery, polar renal artery, stronger posterior communicant artery) were reported in five subjects, and a non-significant stenosis was described in one subject (Figure 6). A further subject had a possible right subclavian stenosis which might be confounded by motion artifact.

Discussion

To the best of our knowledge, this is the first study to investigate the clinical value of whole-body MRI and MRA in a highly selected group of extremely health conscious general adult population on a 3-T basis using a wide bore magnet including WB-DWI acquisitions. We demonstrated a potentially malignant lesion detection rate of 4.5% in our cohort and a high number of incidental findings (91%) requiring further radiological investigations in 68% of individuals. WB-MRA demonstrated normal vascular variations in 23% of subjects and a non-significant left proximal common carotid artery stenosis in 4.5%.

The patient, who had a suspicious (pararectal) malignant lesion underwent a pelvis CT, which found a 16 x 14 mm large mass with central discrete hypodensity in the right pararectal fat tissue and a thickened mesorectal fascia. Tumor markers

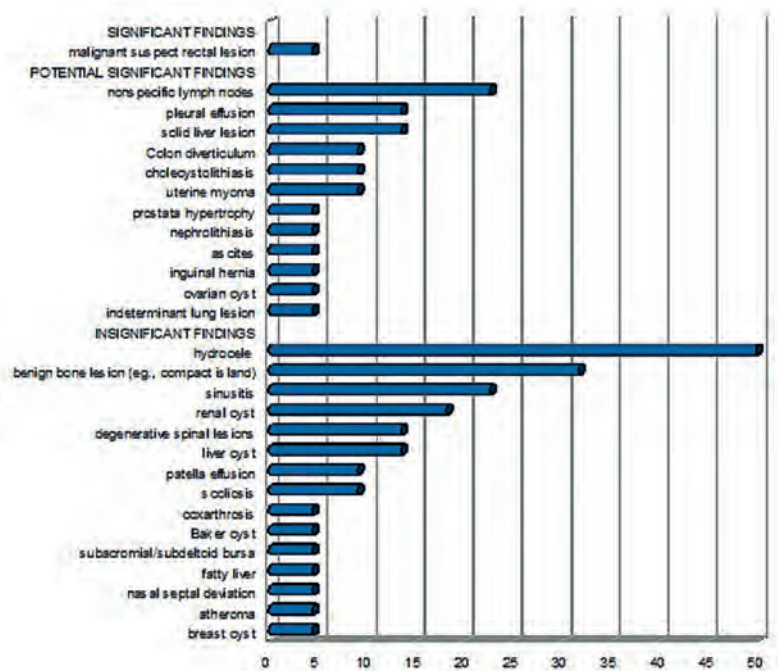


FIGURE 5. Prevalence of WB-MRI findings in all patients (%).



FIGURE 6. Coronal reconstruction of whole-body MRA in a 52-year-old male patient with history of appendectomy and previous smoking. Note the 2 mm long, approximately 40% concentric stenosis of the left common carotid artery 3 cm distal to the aortic arch (arrow). Please note the left vertebral hypoplasia, kinking of the midcervical portion of the right internal carotid artery and the coiling of the distal cervical portion of the left internal cerebral artery.

were in the normal range, and colonoscopy reported sigma polyps without dysplasia (no suspicious colon carcinoma). The patient did not show up in the follow-ups later.

Only few studies performed on a lower magnetic field (usually 1.5 T) have reported WB-MRI screening results in the past years.^{4,5} Gohde *et al.* reported lower rates of clinically significant incidental findings compared to our results in general (*e.g.* peripheral arterial stenoses in 2%, significant incidental findings 5–9%), and demonstrated only one malignancy (a renal cell carcinoma).⁶ Studies performed on ‘healthy’ employees reported only few unknown vascular pathologies, usually below 5% (*e.g.* silent myocardial infarction, cerebral infarctions, significant carotid/renal artery stenoses).^{7–9} Some population-based studies indicated similar prevalence, for example the Uppsala PIVUS study (performed in 306 70-year-old men) demonstrated significant carotid/renal artery stenoses in 1.5–1.8%, and abdominal aortic aneurysms in 2%.¹⁰ A study of 2536 healthy young men using axial brain MRI reported brain incidental findings with frequency of 0.47–1.7%.¹¹ We suspect that the higher prevalence of incidental findings in our study can be referred to the higher magnetic field and the technical novelties in MRI, such as extended body coverage, a rolling platform with extended large field of view and a high number of simultaneous signal receiver channels, and multiple plugs for attaching several RF coils concurrently – allowing “parallel imaging”.^{1,12} In our study, homogeneity of the main magnetic field B₀ of 3 T bore magnet with the largest bore diameter available on the market, higher signal to noise ratio, better image resolution, shorter acquisition time, and more patient comfort can further increase and facilitate the specificity and patient compliance in contrast to the 1.5 T MRI systems. Spatial resolution data of our MR acquisitions are shown in Table 1.

In our cohort, hydrocele was the most common incidental finding (61% of men). The cause is unknown, however, it might be a marker of physical trauma, infection, or tumor as well. There are approximately 26 million cases of hydrocele worldwide.¹³ Hydrocele is more common on the right side and it is usually bilateral in elderly patients.¹⁴

The second most common incidental finding was the benign bony lesion in 32% of the individuals, most commonly bone islands (these lesions appeared to be benign but were unspecific, maybe just inhomogeneous bone marrow). These small (majority of lesions measure from 0.1 to 2.0 cm in greatest diameter), asymptomatic lesions can

TABLE 1. Spatial resolution data of our study acquisitions

WB-T1	448 x 256	voxel	Freq. 1,12 Phase 1,95 Sl. 5
WB-STIR	384 x 224	voxel	Freq. 1,3 Phase 2,23 Sl. 5
WB-DWI	128 x 128		Freq. 3,9 Phase 3,9 Sl. 8
WB-MRA – Thorax/ Abdomen/Pelvis	288 x 192		Freq. 1,67 Phase 2,5 Sl. 2,8
WB-MRA – Upper extremity	384 x 192		Freq. 1,25 Phase 2,5 Sl. 2,4
WB-MRA – Lower extremity	320 x 192		Freq. 1,5 Phase 2,5 Sl. 1,8

WB = Whole-body; STIR = Short T1 Inversion Recovery; DWI = diffusion weighted imaging; MRA = magnetic resonance angiography, Freq.: frequency, Sl.: slice thickness in mm

be found in most parts of the skeleton with a preference for the pelvis, femur, ribs and other long bones (usually at the ends of tubular bones).¹⁵ Most of these bone islands do not require treatment after the diagnosis is established.

Due to atherosclerosis as the number one in morbidity and mortality in developed countries and its high prevalence, there is an increasing need to detect the most threatening manifestations of vascular disease well in advance.¹⁶ WB-MRA is a promising technique providing the depiction of the arterial system from “head to toe” (except the coronaries) in less than 45 minutes, visualizing macroscopic changes in the arterial system and potential organ damage (*e.g.* cerebral microangiopathy, stroke, myocardial infarction) with high accuracy of up to 95% concerning relevant stenosis.^{1,17} In our sample, WB-MRA was negative in 73%, and vascular normal variations and a non-significant stenosis were described. Our findings are comparable with studies performed in asymptomatic patients for cardiovascular diseases where the prevalence for vascular (< 3 T) MR findings were relatively low.^{4,9,10} However, in high-risk groups, screening studies have revealed many previously unknown vascular pathologies, which in part had been overseen by common clinical examinations and tests.⁴ Our most commonly reported vascular normal variation was the asymmetry of the vertebral arteries (VAs). The asymmetry of the VAs might be due to hypoplasia which is very common and can be identified on MRI, its prevalence is unknown.¹⁸ A Swiss study reported that vertebral artery hypoplasia is more common on the right side.¹⁹ Hypertension or

hyperlipidemia are hypothesized to be in the background; furthermore, vertebral artery hypoplasia may contribute to a higher risk for posterior circulation stroke.¹⁹

WB-MRI can be performed by the application of various sequences. T1-weighted images after contrast agent application can depict lesions in parenchymal organs and bone and soft tissues due to higher spatial resolution.^{1,20} STIR can visualize vertebral metastases and bone marrow infiltration with high sensitivity.²¹ Due to these benefits, these sequences were also acquired in our study in accordance with the literature. However, to the best of our knowledge, DWI has never been applied in a WB-MRI screening study. Advantage of adding a DWI sequence to this study has the depiction of areas of restricted diffusion which allows the better visualization of areas of high cellularity, *i.e.* malignancies.

The ideal screening technique must be both sensitive and specific, widely available, cost-effective, reader independent, and without harmful side effects. The diagnostic test must be standardized implying a low number of false results.¹ In addition, criteria for a screening programme (either Wilson and Jungner, or adapted WHO) should be met. MR is likely to meet these criteria especially in diseases which are ideal for screening, including colorectal cancer and cardiovascular disease, as demonstrated with examples in our study.^{1,22,23} MR angiography has also been shown to be equivalently effective in demonstrating vascular abnormalities compared to invasive techniques.^{1,24} In our study, further investigations were recommended in case of 15 subjects (68%), mainly abdominal sonographies and chest CTs. The incidental findings were mainly related to the fields of urology, rheumatology and internal medicine in almost two-thirds of the cases. The corresponding screening costs are also determined by these indirect costs related to these subsequent and follow-up tests beyond the direct costs of the screening test itself.¹

The strengths of our study include the highly selected patient group, the advantages of high field 3-T wide bore magnet system and the use of whole-body DWI acquisitions. Second, the investigated healthy adults represent a small proportion of the population at risk, and the prevalence of malignancies and cardiovascular (atherosclerotic) lesions are likely to occur in the higher-risk group with lower socioeconomic status. Therefore, these are individuals who are likely to undergo WB-MRI scans in the near future due to financial reasons, and our findings are highly relevant in this context.

However, the present study also has some limitations.

The major limitation of our study is the relatively low number of subjects, although it is comparable to other previous investigations.⁹ In addition, follow-up analysis of disclosed potentially relevant incidental findings is still incomplete.

In conclusion, our data suggest that 3 T wide bore WB-MRI, DWI and MRA of high diagnostic accuracy lead to the detection of clinically relevant diseases and many incidental findings in a cohort of healthy adults that require further imaging or surveillance in two-third of subjects. Furthermore, research involving large numbers of patients is required to determine the potential benefit or burden of communicating incidental findings to study volunteers. Our research was the first one which involved this highly selected patient group, using a high field 3 T wide bore magnet system with T1, STIR, whole-body DWI and MRA acquisitions. Our study was the first which added a DWI sequence to the WB-MRI screening protocol which might help the depiction of areas of malignancies.

Acknowledgments

BBraun Medical Ltd. provided travel support for authors ADT and DLT.

References

1. Ladd SC, Ladd ME. Perspectives for preventive screening with total body MRI. *Eur Radiol* 2007; **17**: 2889-97.
2. Fenchel M, Requardt M, Tomaschko K, Kramer U, Stauder NI, Naegele T, et al. Whole-body MR angiography using a novel 32-receiving-channel magnetic resonance (MR) system with surface coil technology: first clinical experience. *J Magn Reson Imaging* 2005; **21**: 596-603.
3. Sans S, Kesteloot H, Kromhout D. The burden of cardiovascular diseases mortality in Europe. Task Force of the European Society of Cardiology on Cardiovascular Mortality and Morbidity Statistics in Europe. *Eur Heart J* 1997; **18**: 1231-48.
4. Ladd SC. Whole-body MRI as a screening tool? *Eur J Radiol* 2009; **70**: 452-62.
5. Hegenscheid K, Seipel R, Schmidt CO, Völzke H, Kühn JP, Biffar R, et al. Potentially relevant incidental findings on research whole-body MRI in the general adult population: frequencies and management. *Eur Radiol* 2013; **23**: 816-26.
6. Gohde SC, Goyen M, Forsting M, Debatin JF. Prevention without radiation - a strategy for comprehensive early detection using magnetic resonance tomography. *Radiologe* 2002; **42**: 622-9.
7. Baumgart D, Egelhof T. Preventive whole-body screening encompassing modern imaging using magnetic resonance tomography. *Herz* 2007; **32**: 387-94.
8. Goehde SC, Hunold P, Vogt FM, Ajaj W, Goyen M, Herborn CU, et al. Full-body cardiovascular and tumor MRI for early detection of disease: feasibility and initial experience in 298 subjects. *AJR Am J Roentgenol* 2005; **184**: 598-611.

9. Kramer H, Schoenberg SO, Nikolaou K, Huber A, Struwe A, Winnik E, et al. Cardiovascular screening with parallel imaging techniques and a whole-body MR imaging. *Radiology* 2005; **236**: 300-10.
10. Hansen T, Wikström J, Johansson LO, Lind L, Ahlström H. The prevalence and quantification of atherosclerosis in an elderly population assessed by whole-body magnetic resonance angiography. *Arterioscler Thromb Vasc Biol* 2007; **27**: 649-54.
11. Weber F, Knopf H. Incidental findings in magnetic resonance imaging of the brains of healthy young men. *J Neurol Sci* 2006; **240**: 81-4.
12. Quick HH, Vogt FM, Maderwald S, Herborn CU, Bosk S, Göhde S, et al. High spatial resolution wholebody MR angiography featuring parallel imaging: initial experience. *Rofo* 2004; **176**: 163-9.
13. Michael E, Bundy DA, Grenfell BT. Re-assessing the global prevalence and distribution of lymphatic filariasis. *Parasitology* 1996; **112**: 409-28.
14. Okorie CO, Pisters LL, Liu P. Longstanding hydrocele in adult Black Africans: Is preoperative scrotal ultrasound justified? *Niger Med J* 2011; **52**: 173-6.
15. Onitsuka H. Roentgenologic aspects of bone islands. *Radiology* 1977; **123**: 607-12.
16. Diehm C, Kareem S, Lawall H. Epidemiology of peripheral arterial disease. *Vasa* 2004; **33**: 183-9.
17. Fenchel M, Scheule AM, Stauder NI, Kramer U, Tomaschko K, Nägele T, et al. Atherosclerotic disease: whole-body cardiovascular imaging with MR system with 32 receiver channels and total-body surface coil technology—initial clinical results. *Radiology* 2006; **238**: 280-91.
18. Lovrencic-Huzjan A, Demarin V, Rundek T, Vukovic V. Role of vertebral artery hypoplasia in migraine. *Cephalgia* 1998; **18**: 684-6.
19. Peterson C, Phillips L, Linden A, Hsu W. Vertebral artery hypoplasia: prevalence and reliability of identifying and grading its severity on magnetic resonance imaging scans. *J Manipulative Physiol Ther* 2010; **33**: 207-11.
20. Lauenstein TC, Goehde SC, Herborn CU, Treder W, Ruehm SG, Debatin JF, et al. Three-dimensional volumetric interpolated breath-hold MR imaging for whole-body tumor staging in less than 15 minutes: a feasibility study. *AJR Am J Roentgenol* 2002; **179**: 445-9.
21. Eustace S, Tello R, DeCarvalho V, Carey J, Wroblecka JT, Melhem ER, et al. A comparison of whole-body turboSTIR MR imaging and planar ^{99m}Tc-methylene diphosphonate scintigraphy in the examination of patients with suspected skeletal metastases. *AJR Am J Roentgenol* 1997; **169**: 1655-61.
22. Villavicencio RT, Rex DX. Colonic adenomas: prevalence and incidence rates, growth rates, and miss rates at colonoscopy. *Semin Gastrointest Dis* 2000; **11**: 185-93.
23. Chambless L, Keil U, Dobson A, Mähönen M, Kuulasmaa K, Rajakangas AM, et al. Population versus clinical view of case fatality from acute coronary heart disease—results from the WHO Monica project 1985–1990. *Circulation* 1997; **96**: 3849-59.
24. Goyen M, Quick HH, Debatin JF, Ladd ME, Barkhausen J, Herborn CU, et al. Whole body 3D MR angiography using a rolling table platform: initial clinical experience. *Radiology* 2002; **224**: 270-7.

Dynamic contrast-enhanced computed tomography to assess early activity of cetuximab in squamous cell carcinoma of the head and neck

Sandra Schmitz^{1*}, Denis Rommel^{2*}, Nicolas Michoux^{2*}, Renaud Lhommel³, François-Xavier Hanin³, Thierry Duprez², Jean-Pascal Machiels¹

¹ Department of Medical Oncology and Head and Neck Surgery, Cliniques Universitaires Saint-Luc and Institut de Recherche Clinique et Expérimentale (Pole MIRO), Université Catholique de Louvain, Brussels, Belgium

² Department of Medical Imaging and Radiology, Cliniques Universitaires Saint-Luc and Institut de Recherche Clinique et Expérimentale (Pole IMAG), Université Catholique de Louvain, Brussels, Belgium

³ Department of Nuclear Medicine, Cliniques Universitaires Saint-Luc, Université Catholique de Louvain, Brussels, Belgium

Radiol Oncol 2015; 49(1): 17-25.

Received: 6 April 2013
Accepted: 23 May 2013

Correspondence to: Sandra Schmitz M.D., Oncology Department, Cliniques Universitaires Saint-Luc, Université Catholique de Louvain, Avenue Hippocrate 10, B-1200 Brussels, Belgium. E-mail: sandra.schmitz@uclouvain.be

*These three authors contributed equally to this work.

Disclosure: No potential conflicts of interest were disclosed.

Background. Cetuximab, a monoclonal antibody targeting the Epidermal Growth Factor Receptor (EGFR), has demonstrated activity in various tumor types. Using dynamic contrast-enhanced computed tomography (DCE-CT), we investigated the early activity of cetuximab monotherapy in previously untreated patients with squamous cell carcinoma of the head and neck (SCCHN).

Methods. Treatment-naïve patients with SCCHN received cetuximab for 2 weeks before curative surgery. Treatment activity was evaluated by DCE-CT at baseline and before surgery. Tumor vascular and interstitial characteristics were evaluated using the Brix two-compartment kinetic model. Modifications of the perfusion parameters (blood flow F_p , extravascular space v_e , vascular space v_p , and transfer constant PS) were assessed between both time points. DCE data were compared to FDG-PET and histopathological examination obtained simultaneously. Plasmatic vascular markers were investigated at different time points.

Results. Fourteen patients had evaluable DCE-CT parameters at both time points. A significant increase in the extravascular extracellular space v_e accessible to the tracer was observed but no significant differences were found for the other kinetic parameters (F_p , v_p or PS). Significant correlations were found between DCE parameters and the other two modalities. Plasmatic VEGF, PDGF-BB and IL-8 decreased as early as 2 hours after cetuximab infusion.

Conclusions. Early activity of cetuximab on tumor interstitial characteristics was detected by DCE-CT. Modifications of plasmatic vascular markers are not sufficient to confirm anti-angiogenic cetuximab activity in vivo. Further investigation is warranted to determine to what extent DCE-CT parameters are modified and to evaluate whether they are able to predict treatment outcome.

Key words: cetuximab; head and neck cancer; perfusion; DCE-CT

Introduction

The Epidermal Growth Factor Receptor (EGFR) is overexpressed in up to 90% of all squamous cell

carcinomas of the head and neck (SCCHN)¹, and EGFR overexpression is linked with poor prognosis.^{2,3} The EGFR is a member of the HER tyrosine kinase receptor family composed of four different

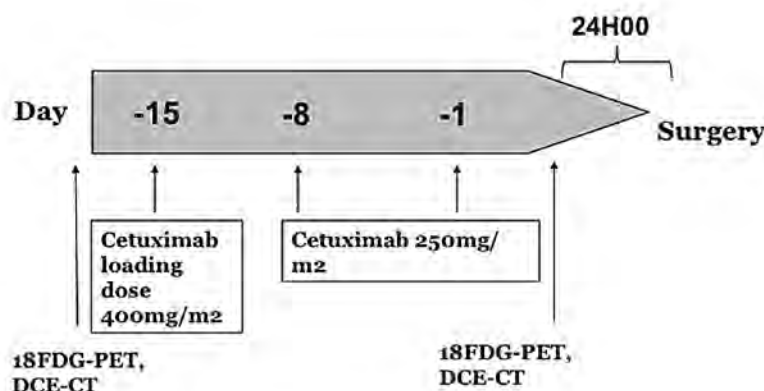


FIGURE 1. Schematic view of the study protocol.

receptors (EGFR/c-erbB-1, c-erbB-2/HER-2/neu, c-erbB-3/HER-3, and c-erbB4/HER-4), all of which are transmembrane proteins with tyrosine kinase activity.⁴ The EGFR has an extracellular domain which provides a ligand-binding site. Upon ligand fixation, EGFR homodimerization or heterodimerization with another HER receptor occurs leading to activation of the intracellular tyrosine kinase. This stimulates kinase signal transduction pathways involved in tumor proliferation, inhibition of apoptosis, angiogenesis and cell migration/invasion. Downstream signaling through the Ras/Raf/Mek/Erk pathway controls cell proliferation and cell cycle progression, while the phosphatidylinositol-3-kinase/protein kinase B (PI3K/Akt) pathway stimulates numerous antiapoptotic signals.

Cetuximab, a chimeric IgG1 monoclonal antibody (mAb) that specifically binds to the EGFR with high affinity, has been approved in combination with radiotherapy for locally advanced SCCHN and in combination with platinum based chemotherapy for recurrent and/or metastatic SCCHN.⁵⁻⁷ However the objective response rate in monotherapy remains low at between 10% and 13%.⁸ Postulated mechanisms of action of cetuximab include (i) downregulation of the EGFR and its downstream molecular signaling pathways by competing with EGFR natural ligands like EGF or TGF- α , (ii) antibody-dependent cell-mediated cytotoxicity (ADCC) through the activation of macrophages and natural killer cells, and (iii) inhibition of DNA double strand-break repair.⁹⁻¹² Furthermore decreased secretion of vascular ligands like VEGF-A, IL-8 and FGF-2 has been described by other investigators^(13,14), leading to the hypothesis that beside a direct effect on tumour cell proliferation, cetuximab could also induce anti-angiogenic effects and thereby influence in-

directly tumor progression. Other investigators showed vascular normalization associated with increased vessel density and blood flow after anti-EGFR treatment in xenograft models.^{15,16}

Dynamic Contrast-Enhanced Computed Tomography (DCE-CT) is now recognized as a useful non-invasive imaging tool to investigate vascular and interstitial tumor characteristics.¹⁷⁻¹⁹ In SCCHN, DCE-CT has been used to study blood volume, blood flow, permeability, tumor neoangiogenesis, and consecutive intratumoral arteriovenous shunts.²⁰⁻²² These observations have been confirmed in several studies²²⁻²⁵ and were correlated with intratumoral microvessel density (MVD)²⁶, and with pathological aggressiveness and angiogenic markers such as vascular endothelial growth factor.²⁷⁻²⁹ Several investigators have also used DCE-CT to try to establish predictive markers of treatment response after induction chemotherapy or radio-chemotherapy in patients with SCCHN.^{20,21,30}

We therefore implemented this technique in a pre-operative window opportunity study in SCCHN, in which cetuximab activity was investigated.³¹ Cetuximab monotherapy was administered for two weeks prior to surgery to treatment-naïve patients selected for primary surgical treatment. 2-[fluorine-18]-fluoro-2-deoxy-D-glucose positron emission tomography (¹⁸F-FDG-PET) and imaging, including DCE-CT, were performed at baseline and before surgery. It has been shown that ¹⁸F-FDG-PET and DCE-CT are complementary imaging techniques for surveillance assessment in patients with SCCHN and that their combination may improve tumor outcome prediction.³² In this paper, we report on the effect of cetuximab monotherapy to modify the vascular and interstitial characteristics of SCCHN tumors as assessed by DCE-CT.

Patients and methods

Thirty-three treatment naïve patients with operable SCCHN were enrolled into a monocentric window pre-operative study between August 2008 and February 2011.³¹ In the first part of the study (N = 12 patients), safety of the concept was evaluated by progressive reduction of the delay between the last cetuximab administration and surgery. In the expansion part of the study (N = 20 patients), all patients were treated with a loading dose of 400 mg/m² of cetuximab on day -15 before surgery followed by 250mg/m² on days -8 and -1 before

surgery (day 0) (Figure 1). Details of the eligibility criteria, ^{18}F FDG-PET responses of the whole group, biology and safety have been published.³¹ The clinical and translational parts of the study were approved by the Independent Ethics Committee and the Belgian Health Authorities and conducted in accordance with the Declaration of Helsinki (October 2000). Written informed consent was obtained for each patient. It was prospectively planned to perform translational research and patients gave their informed consent for repeated imaging.

Perfusion imaging

DCE-CT scans were performed on the 20 patients treated in the expansion part of the study at two time points: before the first cetuximab infusion and strictly two hours after the third dose. Imaging used a 16-detector row CT scanner (Philips Medical Systems, Best, the Netherlands). Acquisition parameters were: tube voltage 90 kVp; reference tube current-time product 200 mAs, temporal resolution 1 s, total scan time 120 s, number of slices 4, in-plane spatial resolution 0.68x0.68 mm, slice thickness 6 mm, image matrix size 512x512. Raw data were reconstructed by using a FBP algorithm. PET-CT fusion was used to locate the lesions on CT images.

The software Image J (processing program developed by the National Institutes of Health, <http://rsbweb.nih.gov/ij/>) was used to segment the regions of interest (ROI). An expert head and neck radiologist manually drew the ROI which included the internal carotid (for the arterial input function calculation) and the whole tumor (Figure 2).

Time intensity curves (TICs) were analyzed according to the Brix two-compartment kinetic model (Figure 2).³³ This model relies on four parameters: blood flow F_p ($\text{mL}\cdot\text{s}^{-1}\cdot\text{g}^{-1}$); fraction of extravascular extracellular space accessible to the contrast agent v_e (%); fraction of vascular space v_p (%); and the transfer constant PS ($\text{mL}\cdot\text{s}^{-1}\cdot\text{g}^{-1}$), which depends on the permeability and surface area for transendothelial exchanges of the capillary wall. An additional free parameter τ (s), to account for the contrast agent bolus arrival time in the tissues of interest, was included. As a result, the final expression of the kinetic model was:

$$C_{\text{tissue}}(t) = F_p \cdot C_{\text{plasma}}(t-\tau) \otimes R_{\text{tissue}}(t) \quad [1]$$

where $C_{\text{plasma}}(t-\tau)$ is the TIC in the feeding artery and $R_{\text{tissue}}(t)$ is the impulse response function of the tissue taken the form:

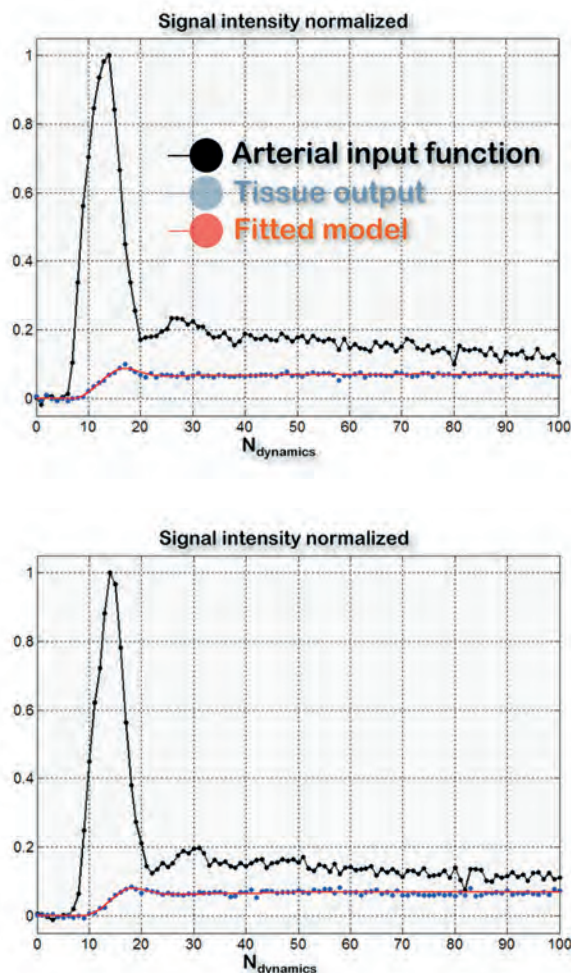


FIGURE 2. Example of time intensity curves derived from the internal carotid and tumoral lesion before (A) and during treatment with cetuximab (B) in a patient with a squamous cell carcinoma of the head and neck. The quality of the fits of TICs using the Brix two-compartment kinetic model was found to be good (estimation of the root mean squared error of the regression averaged on the 14 normalized fits: $\epsilon_{\text{pre-treatment}} = 5\%$, $\epsilon_{\text{during-treatment}} = 6\%$).

$$\begin{aligned} R_{\text{tissue}}(t) &= A \cdot e^{-\alpha t} + (1-A) \cdot e^{-\beta t} \\ v_p &= F_p / [A \cdot (\alpha - \beta) + \beta] \\ PS &= [\alpha + \beta - \alpha\beta / (A \cdot (\alpha - \beta) + \beta)] \cdot v_p \\ v_e &= PS / [\alpha\beta / (A \cdot (\alpha - \beta) + \beta)] \end{aligned} \quad [2]$$

The model was fitted to the TICs using a trust region algorithm.³⁴ Multiple start values for the free parameters were explored in an attempt to find the solution corresponding to the true global minimum of the error function. All parameters were constrained to be positive. The sum ($v_e + v_p$) was constrained to be less than 1. No upper boundary was imposed on F_p or PS. To obtain the coefficients F_p and PS in $\text{mL}\cdot\text{min}^{-1}\cdot 100\text{g}^{-1}$, the coefficients expressed in $\text{mL}\cdot\text{s}^{-1}\cdot\text{g}^{-1}$ were multiplied by 60 $\text{s}\cdot\text{min}^{-1}$ and by 100. Cetuximab-induced changes in the

pharmacokinetic parameters F_p , v_e , v_p and PS were then investigated.

18FDG-PET imaging

All patients underwent two ^{18}F FDG-PET/CT assessments on a Philips 16-slice GEMINI TF camera (Philips Healthcare, The Netherlands): a baseline PET at the time of inclusion and an evaluation ^{18}F FDG-PET aimed at estimating the residual tumor metabolic activity at the end of the cetuximab regimen (performed strictly 2 hours after the final infusion of cetuximab and one day before surgery).

As a surrogate of tumor metabolic activity, the maximal standardized FDG uptake value (SUV_{max}) was recorded at each time point within the entire tumor volume using 3D volumes of interest (VOIs) and calculated using the following formula:

$$\text{SUV}_{\text{max}} = \text{maximal pixel value} * \text{weight} / \text{corrected injected dose} * 1000 \quad [3]$$

with SUV_{max} in $\text{g}\cdot\text{mL}^{-1}$, maximal pixel value in $\text{Bq}\cdot\text{mL}^{-1}$, weight in kg, and the dose in Bq. To reflect the modification in tumor metabolism induced by the treatment between two PET studies, the parameter $\Delta\text{SUV}_{\text{max}}$ (in %) was defined using the following formula:

$$\Delta\text{SUV}_{\text{max}} = [(\text{SUV}_{\text{max}}^{\text{E-PET}} - \text{SUV}_{\text{max}}^{\text{B-PET}}) / \text{SUV}_{\text{max}}^{\text{B-PET}}] * 100 \quad [4]$$

Based on published EORTC criteria for solid tumor evaluation with PET³⁵, tumor metabolism was considered to be progressive (non responding to treatment) if $\Delta\text{SUV}_{\text{max}}$ was $> 25\%$ between the two PET studies; stable for $\Delta\text{SUV}_{\text{max}}$ between -25% and $+25\%$; partially responding for $\Delta\text{SUV}_{\text{max}} \leq -25\%$, and in complete metabolic response in case of non residual uptake. The PET-CTs were centrally reviewed by the same person.

Tumor cellularity

Residual tumor cellularity was determined on hematoxylin and eosin-stained (HE) slides including the whole tumor as previously described.³¹ Stained slides were digitized by a slide scanner (Mirax Scan; Zeiss, Jena, Germany). The surface composed of tumor cells only and the surface of the whole tumor were manually drawn by the same investigator (SS) who was blinded to the DCE-CT and ^{18}F FDG-PET results. Tumor cellularity (expressed as a %) was the surface occupied by tumor cells divid-

ed by the surface of the whole tumor that included tumor cells, inflammatory cells, normal interstitial tissue and areas with morphologic signs of therapy-induced regression such as fibrosis and scarring.

Plasma analyses

Plasma samples (3 ml) were collected at several time points: (T1) at baseline before any cetuximab infusion; (T2a) before the last dose of cetuximab (day -1 before surgery); (T2b) 2 hours after the last dose of cetuximab; (T3) before surgery after intubation; and (T4) 5 weeks after surgery.

Vascular endothelial growth factor (VEGF), fibroblast growth factor (FGF)-basic, platelet derived growth factor (PDGF)-BB and interleukin (IL)-8 plasma levels were quantified using the Bio-Rad multiplex bead immunoassay (Luminex). The assay was performed in a 96 well plate format and analysed with the Luminex200 instrument (BIO-RAD), which monitors the spectral properties of the capture beads while simultaneously measuring the quantity of associated fluorophore.

Statistical analysis

Numerical variables were expressed as mean \pm standard deviation. DCE-CT parameters, ^{18}F FDG-PET parameters, tumor cellularity and Luminex results were compared before and during treatment using the non-parametric Wilcoxon rank-sum test. A non-parametric test was chosen as the normality of the data distribution was not verified (on the basis of the D'agostino-Pearson test). Correlations between parameters were assessed based on Spearman's rank coefficient. All calculations were done with Matlab (Matlab R2011b, MathWorks, Natick, MA, USA). A p -value < 0.05 was regarded as statistically significant for all tests cited above.

Results

Study population

Twenty patients were included in the expansion part and treated with three doses of cetuximab. DCE-CT images were spatially registered with a rigid transformation in order to compensate for patient motions.³⁶ However, in four patients out of 20, displacement or deformation of the oral cavity during the perfusion sequence was too severe to be corrected. In two additional patients, dental artifacts prevented from measuring the first pass of the contrast agent in the ROI with a high signal to

TABLE 1. Quantitative imaging parameters from DCE-CT and ¹⁸F-FDG-PET before and during treatment with cetuximab in 14 patients with squamous cell carcinoma of the head and neck

Patient	F _p	v _e [*]	v _p	PS	SUV [*]	Cellularity	Tumor
	(mL.min ⁻¹ .100g ⁻¹)	(%)	(%)	(mL.min ⁻¹ .100g ⁻¹)		(%)	localization, staging
Pretreatment							
1	313.7	30.3	8.1	53.8	14.3	-	L, T2N0
2	378.6	39.2	12.0	59.7	16.8	-	OC, T2N0
3	157.2	15.4	16.0	37.7	10.6	-	OC, T2N0
4	366.5	60.5	13.7	81.9	11.4	-	OC, T1N0
5	73.9	41.8	15.3	28.6	9.9	-	OC, T1N0
6	136.1	30.9	11.1	69.2	13.4	-	OC,T4N0
7	278.0	36.4	15.5	47.3	8.8	-	L, T2N0
8	116.9	39.5	13.6	42.0	8.3	-	OC, T2N1
9	93.7	41.9	13.0	82.9	16.2	-	OC, T2N1
10	163.2	21.9	9.5	37.2	12.3	-	L, T2N0
11	72.7	29.1	9.2	38.1	7.4	-	OC, T2N0
12	286.6	49.8	5.6	40.9	28.9	-	OC, T3N0
13***	128.0	37.0	10.8	44.6	14.8	-	OC, T2N0
14	222.8	21.1	18.7	36.2	18.9	-	OC, T2N2b
m ± SD	199 ± 107	35 ± 12	12 ± 3.5	50 ± 17	14 ± 5.6	-	
Post treatment							
1	281.1	30.3	9.0	42.6	9.2	77	
2	292.6	47.9	8.5	87.4	8.4	45	
3	305.9	40.1	11.8	45.6	4.8	38	
4	357.9	66.7	14.5	75.0	4.9	34	
5	40.8	46.1	8.6	31.4	11.4	55	
6	99.1	18.0	4.5	78.3	6.8	40	
7	219.6	38.7	2.2	40.4	4.5	54	
8	411.9	53.3	3.9	60.5	4.9	49	
9	72.4	68.4	31.2	30.7	4.3	25	
10	92.3	53.5	12.8	22.8	6.7	63	
11	75.9	77.6	14.6	44.1	3.9	35	
12	184.0	47.4	8.9	33.8	3.4	22	
13***	131.2	46.1	9.9	60.7	6.0	26	
14	359.2	33.7	13.7	53.7	8.3	36	
m ± SD	209 ± 126	48 ± 16	11 ± 7.0	51 ± 20	6.3 ± 2.3	42.8± 15.5	

* Parameters with significant statistical differences between pretreatment and during treatment ($p < 0.05$)

*** PET/CT, Diffusion-weighted MR images and TICs are given in Figures 4 and 2.

F_p = blood flow; v_e = extracellular, extravascular fraction; v_p = fraction of vascular space; PS = transfer constant, L = larynx; OC = oral cavity

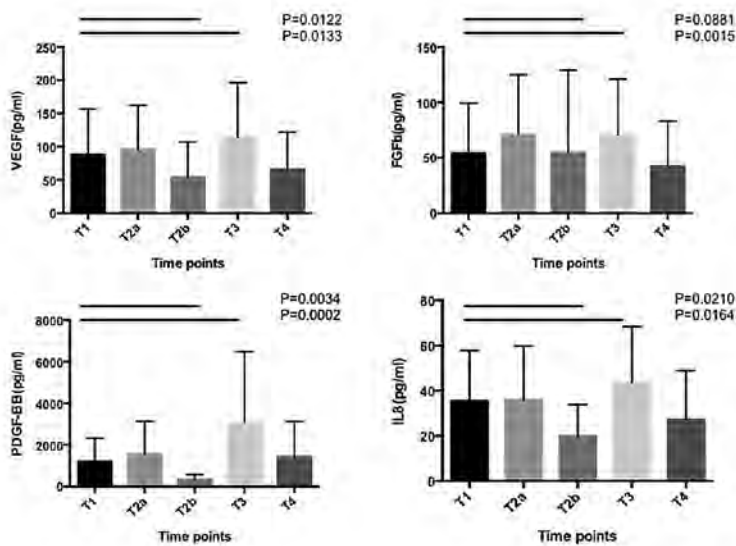


FIGURE 3. Modifications of VEGF, FGF-basic, IL-8 and PDGF-BB plasmatic levels at different time points. T1: baseline sample, T2a: after 2 doses of cetuximab and before the third dose of cetuximab; T2b: 2 hours after the third dose of cetuximab and just before ^{18}F FDG-PET (24 hours before surgery); T3: at induction of anesthesia, before incision; T4: 5 weeks after surgery. (Representation of the mean and SD for each time point, $n=14$ pts)

noise ratio. As a result, 14 patients out of the original 20 qualified at both imaging time points for a quantitative assessment of the tumoral perfusion. Eleven and three patients had SCC of the oral cavity and larynx, respectively.

Anatomic imaging

Nine out of the 14 patients had measurable lesions according to response evaluation criteria in solid tumor (RECIST) version 1.1. The largest diameter of the tumor decreased by more than 30% in only one patient. Other patients had stable disease (SD) according to RECIST criteria.

Functional imaging and tumor cellularity

Quantitative imaging parameters are summarized in Table 1. A significant difference between pretreatment and during cetuximab treatment was observed for the extravascular extracellular space v_e ($p = 0.0085$). Other kinetic parameters were not found to differ significantly (F_p : $p = 0.5416$; v_p : $p = 0.2958$; PS: $p = 0.5830$).

Among the 14 patients, all except one had a partial response (PR) according to the ^{18}F FDG-PET EORTC guidelines. Only one patient had an increase in SUV_{max} between the two ^{18}F FDG-PET scans ($\Delta\text{SUV}_{\text{max}} + 15\%$). For the other patients, $\Delta\text{SUV}_{\text{max}}$ was between -25% and -50% for 7 patients and below -50% for 6 patients.

We have previously shown that cetuximab decreased tumor cellularity in resected specimens compared to untreated patients.³¹ Analysis of tumor cellularity in HE slides of resected tumor specimens showed a median cellularity of 43% [range: 22% - 77%]. Tumor cellularity was more pronounced for the 3 larynx carcinomas [range: 54% - 77%] than in the 11 tongue carcinomas [range: 22% - 51%]. Ten out of the 14 patients (71%) had a tumor cellularity < 50%.

A significant though moderate inverse correlation between the extravascular extracellular space v_e and SUV_{max} ($\rho = -0.40$, $p = 0.03$) was observed. No other correlation was observed between DCE-CT parameters and ^{18}F FDG-PET parameters and tumor cellularity, or between the delta values of the respective parameters. A significantly strong correlation was found between cellularity and $\Delta\text{SUV}_{\text{max}}$ ($\rho = 0.84$, $p = 0.0003$) in these 14 patients.

Plasma analysis

VEGF, FGF-basic, PDGF-BB and IL-8 plasmatic levels decreased as early as 2 hours (T2b) after cetuximab perfusion. At the moment of surgery, the plasmatic levels of all these ligands were significantly upregulate (Figure 3).

Discussion

The main purpose of this study was to investigate, using DCE-CT, the ability of cetuximab monotherapy to modify a tumor's vascular and interstitial characteristics. Cetuximab is known to block EGFR-dependent intracellular downstream molecular pathways.

In our model, a significant increase in the extravascular extracellular space v_e between pretreatment and during treatment was observed. In addition to the modification of v_e , a ^{18}F FDG-PET partial response according to EORTC criteria and tumor cellularity inferior to 50% in the resected specimens were observed in 90% and 71% of the 14 reported patients, respectively.

Modifications on blood flow F_p , vascular space v_p or transendothelial exchanges PS could not be demonstrated. Since most of our patients did not experience tumor shrinkage, our results suggest that cetuximab induces modifications in tumor composition reflected by reduced metabolic tumor activity ($\Delta\text{SUV}_{\text{max}}$) and increased peritumoral space, as shown by an increase in v_e and a decrease in tumor cellularity. These modifications are con-

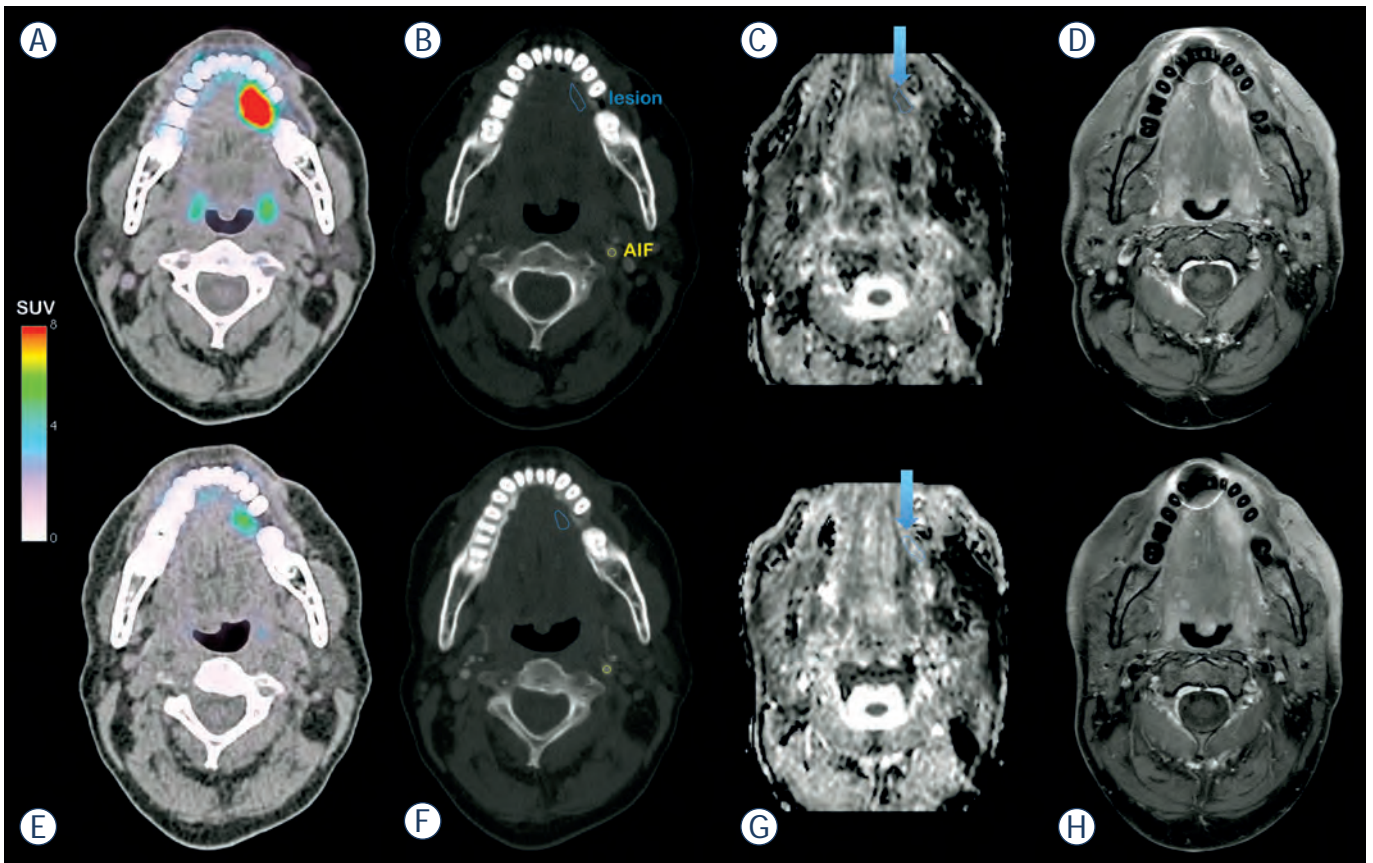


FIGURE 4. A patient with squamous cell carcinoma of the head and neck. Before cetuximab treatment: (A) PET/CT fusion imaging showing the anatomical location of FDG uptake. (B) CT imaging with the regions of interest used for kinetic analysis. (C) ADC mapping derived from DW-MRI with a measured $ADC^{\text{lesion}} = 1009 \text{ mm}^2 \cdot \text{s}^{-1} \pm 123 \text{ mm}^2 \cdot \text{s}^{-1}$. (D) Spin Echo T1-weighted MR imaging with fast suppression technique (SPIR) after gadolinium injection (lesion long axis: 2.88 cm, lesion short axis: 1.52 cm). MRI examination was performed 6 days after PET/CT. During treatment with cetuximab: (E) PET/CT fusion showing imaging of the decrease of FDG uptake. (F) CT imaging with the regions of interest used for kinetic analysis. (G) ADC mapping derived from DW-MRI with an increased $ADC^{\text{lesion}} = 1325 \text{ mm}^2 \cdot \text{s}^{-1} \pm 192 \text{ mm}^2 \cdot \text{s}^{-1}$. (H) Spin Echo T1-weighted MR imaging with fast suppression technique (SPIR) after gadolinium injection (lesion long axis: 2.72 cm, lesion short axis: 1.12 cm). MRI and CT examinations were performed the same day.

sistent with our previous report based on the apparent diffusion coefficient (ADC) parameter derived from diffusion-weighted magnetic resonance imaging (DW-MRI).³¹ Here, a measure of the mobility of water molecules in tissues, as influenced by physiological barriers (endothelium, cell membrane) and obstacles (constituents of the extracellular matrix, intracellular organelles), showed an increase in three out of four patients, from a mean $ADC^{\text{lesion}} = 1065 \text{ mm}^2 \cdot \text{s}^{-1} \pm 139 \text{ mm}^2 \cdot \text{s}^{-1}$ to a mean $ADC^{\text{lesion}} = 1226 \text{ mm}^2 \cdot \text{s}^{-1} \pm 209 \text{ mm}^2 \cdot \text{s}^{-1}$ after cetuximab.²³ An example of ¹⁸FDG-PET, DCE-CT and DW-MRI for one patient before and after treatment is illustrated in Figure 4.

Although less investigated and characterized, anti-angiogenic properties of cetuximab have also been described *in vitro*. Luwor *et al.* found a reduction of hypoxia-inducible factor 1- α (HIF-1 α) and

transcriptional inhibition of vascular endothelial growth factor (VEGF) expression in response to cetuximab treatment.³⁷ According to previous reports^{13,14,38}, we also observed decreased secretion of VEGF, FGF-2 and IL-8 supporting anti-angiogenic effects of cetuximab. These modifications occurred as early as 2 hours after cetuximab administration. However, at the moment of surgery, we noticed a significantly increase of these proteins probably induced by the operative stress.^{39,40} Furthermore, vascular normalization and normalized tumor oxygenation was observed in xenograft models treated by EGFR-TKIs.^{15,16} These data were not confirmed by the present *in vivo* study which failed to demonstrate a significant change in vascularization parameters recorded by DCE except for the v_e which could be explained by the cetuximab-induced cytoreduction, as shown by

the decreased tumour cellularity and metabolic imaging.

The main limitation of our study was the low number of patients assessed by DCE-CT. Statistical considerations to determine the number of patients to be included in this study were based on ¹⁸FDG-PET responses³¹ - the DCE-CT analyses were exploratory and hypotheses generating. However, the number of patients was sufficient to observe differences in tumor metabolism and extravascular extracellular space composition induced by the therapy but probably insufficient to detect slight modifications in tumor vascularization.

Conclusions

To our knowledge, this is the first article to study the variation of DCE-CT and ¹⁸FDG-PET parameters in patients with SCCHN treated with cetuximab monotherapy. A significant increase in the extravascular extracellular space v_e as well as a decrease in tumor metabolism by ¹⁸FDG-PET, was observed. Further investigation in larger cohorts of patients is warranted to assess the extent of change in perfusion measurements prior to and during treatment. Data from such studies could ideally translate into values that could predict treatment efficacy and provide information on the potential effects on tumor blood flow and vascular volume. Since only a minority of patients benefit from targeted therapies, identification of early imaging markers to predict treatment outcome would be of great value to the oncology community.

Acknowledgements

The authors wish to thank Aileen Eiszlele for revising and editing this manuscript.

References

- Kalyankrishna S, Grandis JR. Epidermal growth factor receptor biology in head and neck cancer. *J Clin Oncol* 2006; **24**: 2666-72.
- Ang KK, Berkey BA, Tu X, Zhang HZ, Katz R, Hammond EH, et al. Impact of epidermal growth factor receptor expression on survival and pattern of relapse in patients with advanced head and neck carcinoma. *Cancer Res* 2002; **62**: 7350-6.
- Wheeler S, Siwak DR, Chai R, LaValle C, Seethala RR, Wang L, et al. Tumor epidermal growth factor receptor and EGFR PY1068 are independent prognostic indicators for head and neck squamous cell carcinoma. *Clin Cancer Res* 2012; **18**: 2278-89.
- Schmitz S, Machiels JP. Molecular biology of squamous cell carcinoma of the head and neck : relevance and therapeutic implications. *Expert Rev Anticancer Ther* 2010; **10**: 1471-84.
- Bonner JA, Harari PM, Giral J, Azarnia N, Shin DM, Cohen RB, et al. Radiotherapy plus cetuximab for squamous-cell carcinoma of the head and neck. *N Engl J Med* 2006; **354**: 567-78.
- Bonner JA, Harari PM, Giral J, Cohen RB, Jones CU, Sur RK, et al. Radiotherapy plus cetuximab for locoregionally advanced head and neck cancer: 5-year survival data from a phase 3 randomised trial, and relation between cetuximab-induced rash and survival. *Lancet Oncol* 2010; **11**: 21-8.
- Vermorken JB, Mesia R, Rivera F, Remenar E, Kaweckki A, Rottey S, et al. Platinum-based chemotherapy plus cetuximab in head and neck cancer. *N Engl J Med* 2008; **359**: 1116-27.
- Vermorken JB, Trigo J, Hitt R, Koralewski P, Diaz-Rubio E, Rolland F, et al. Open-label, uncontrolled, multicenter phase II study to evaluate the efficacy and toxicity of cetuximab as a single agent in patients with recurrent and/or metastatic squamous cell carcinoma of the head and neck who failed to respond to platinum-based therapy. *J Clin Oncol* 2007; **25**: 2171-7.
- Li S, Schmitz KR, Jeffrey PD, Wiltzius JJ, Kussie P, Ferguson KM. Structural basis for inhibition of the epidermal growth factor receptor by cetuximab. *Cancer Cell* 2005; **7**: 301-11.
- Lopez-Albaitero A, Lee SC, Morgan S, Grandis JR, Gooding WE, Ferrone S, et al. Role of polymorphic Fc gamma receptor IIIa and EGFR expression level in cetuximab mediated, NK cell dependent in vitro cytotoxicity of head and neck squamous cell carcinoma cells. *Cancer Immunol Immunother* 2009; **58**: 1853-64.
- Huang SM, Bock JM, Harari PM. Epidermal growth factor receptor blockade with C225 modulates proliferation, apoptosis, and radiosensitivity in squamous cell carcinomas of the head and neck. *Cancer Res* 1999; **59**: 1935-40.
- Chen DJ, Nirodi CS. The epidermal growth factor receptor: a role in repair of radiation-induced DNA damage. *Clin Cancer Res* 2007; **13**: 6555-60.
- De Luca A, Carotenuto A, Rachiglio A, Gallo M, Maiello MR, Aldinucci D et al. The role of the EGFR signaling in tumor microenvironment. *J Cell Physiol* 2008; **214**: 559-67.
- Viloria-Petit A, Crombet T, Jothy S, Hicklin D, Bohlen P, Schlaeppli JM, et al. Acquired resistance to the antitumor effect of epidermal growth factor receptor-blocking antibodies in vivo: a role for altered tumor angiogenesis. *Cancer Res* 2001; **61**: 5090-101.
- Cerniglia GJ, Pore N, Tsai JH, Schultz S, Mick R, Choe R, et al. Epidermal growth factor receptor inhibition modulates the microenvironment by vascular normalization to improve chemotherapy and radiotherapy efficacy. *PLoS One* 2009; **4**: e6539.
- Qayum N, Muschel RJ, Im JH, Balathasan L, Koch CJ, Patel S, et al. Tumor vascular changes mediated by inhibition of oncogenic signaling. *Cancer Res* 2009; **69**: 6347-54.
- Miles KA. Perfusion CT for the assessment of tumour vascularity: which protocol? *Br J Radiol* 2003; **76**: S36-42.
- Veit-Haibach P, Schmid D, Strobel K, Soyka JD, Schaefer NG, Haerle SK, et al. Combined PET/CT-perfusion in patients with head and neck cancers. *Eur Radiol* 2013; **23**: 163-73.
- Rumboldt Z, Al-Okailli R, Deveikis JP. Perfusion CT for head and neck tumors: pilot study. *Am J Neuroradiol* 2005; **26**: 1178-85.
- Gandhi D, Chepeha DB, Miller T, Carlos RC, Bradford CR, Karamchandani R, et al. Correlation between initial and early follow-up CT perfusion parameters with endoscopic tumor response in patients with advanced squamous cell carcinomas of the oropharynx treated with organ -preservation therapy. *Am J Neuroradiol* 2006; **27**: 101-6.
- Zima A, Carlos R, Gandhi D, Case I, Teknos T, Mukherji SK. Can pretreatment CT perfusion predict response of advanced squamous cell carcinoma of the upper aerodigestive tract treated with induction chemotherapy? *Am J Neuroradiol* 2007; **28**: 328-34.
- de Geus-Oei LF, van Krieken JH, Aliredjo RP, Krabbe PF, Frielink C, Verhagen AF, et al. Biological correlates of FDG uptake in non-small cell lung cancer. *Lung Cancer* 2007; **55**: 79-87.
- Hirasawa S, Tsushima Y, Takei H, Hirasawa H, Taketomi-Takahashi A, Takano A, et al. Inverse correlation between tumor perfusion and glucose uptake in human head and neck tumors. *Acad Radiol* 2007; **14**: 312-8.
- Tateishi U, Nishihara H, Tsukamoto E, Morikawa T, Tamaki N, Miyasaka K. Lung tumors evaluated with FDG-PET and dynamic CT: the relationship between vascular density and glucose metabolism. *J Comput Assist Tomogr* 2002; **26**: 185-90.

25. Halligan S. Reproducibility, repeatability, correlation and measurement error. *Br J Radiol* 2002; **75**: 193-5.
26. Ash L, Teknos TN, Gandhi D, Patel S, Mukherji SK. Head and neck squamous cell carcinoma: CT perfusion can help noninvasively predict intratumoral microvessel density. *Radiology* 2009; **251**: 422-8.
27. Surlan-Popovic K, Bisdas S, Rumboldt Z, Koh TS, Strojan P. Changes in perfusion CT of advanced squamous cell carcinoma of the head and neck treated during the course of concomitant chemoradiotherapy. *Am J Neuroradiol* 2010; **31**: 570-5.
28. Maia AC Jr, Malheiros SM, da Rocha AJ, da Silva CJ, Gabbai AA, Ferraz FA, et al. MR cerebral blood volume maps correlated with vascular endothelial growth factor expression and tumor grade in nonenhancing gliomas. *Am J Neuroradiol* 2005; **26**: 777-83.
29. Kosaka N, Uematsu H, Kimura H, Ishimori Y, Kurokawa T, Matsuda T, et al. Assessment of the vascularity of uterine leiomyomas using double-echo dynamic perfusion-weighted MRI with the first-pass pharmacokinetic model: correlation with histopathology. *Invest Radiol* 2007; **42**: 629-35.
30. Hermans R, Meijerink M, Van den Bogaert W, Rijnders A, Weltens C, Lambin P. Tumor perfusion rate determined noninvasively by dynamic computed tomography predicts outcome in head-and-neck cancer after radiotherapy. *Int J Radiat Oncol Biol Phys* 2003; **57**: 1351-6.
31. Schmitz S, Hamoir M, Reyckler H, Magremanne M, Weynand B, Lhommel R, et al. Tumour response and safety of cetuximab in a window pre-operative study in patients with squamous cell carcinoma of the head and neck. *Ann Oncol* 2013; **24**: 2261-6.
32. Abramyk A, Wolf G, Shakirin G, Haberland U, Tokalov S, Koch A, et al. Preliminary assessment of dynamic contrast-enhanced CT implementation in pretreatment FDG-PET/CT for outcome prediction in head and neck tumors. *Acta Radiol* 2010; **51**: 793-9.
33. Donaldson SB, West CM, Davidson SE, Carrington BM, Hutchison G, Jones AP, et al. A comparison of tracer kinetic models for T1-weighted dynamic contrast-enhanced MRI: application in carcinoma of the cervix. *Magn Reson Med* 2010; **63**: 691-700.
34. Coleman TF, Li Y. An interior, trust region approach for nonlinear minimization subject to bounds. *SIAM J Optim* 1996; **6**: 418-45.
35. Young H, Baum R, Cremerius U, Herholz K, Hoekstra O, Lammertsma AA, et al. Measurement of clinical and subclinical tumour response using [18F]-fluorodeoxyglucose and positron emission tomography: review and 1999 EORTC recommendations. European Organization for Research and Treatment of Cancer (EORTC) PET Study Group. *Eur J Cancer* 1999; **35**: 1773-82.
36. Thévenaz P, Ruttimann UE, Unser M. A pyramid approach to subpixel registration based on intensity. *IEEE Trans Image Process* 1998; **7**: 27-41.
37. Luwor RB, Lu Y, Li X, Mendelsohn J, Fan Z et al. The antiepidermal growth factor receptor monoclonal antibody cetuximab/C225 reduces hypoxia-inducible factor-1 alpha, leading to transcriptional inhibition of vascular endothelial growth factor expression. *Oncogene* 2005; **24**: 4433-41.
38. Joann-Hureauux V, Boura C, Merlin JL, Faivre B. Modulation of endothelial cell network formation in vitro by molecular signaling of head and neck squamous cell carcinoma (HNSCC) exposed to cetuximab. *Microvasc Res* 2012; **83**: 131-7.
39. Lutgendorf SK, Cole S, Costanzo E, Bradley S, Coffin J, Jabbari S, et al. Stress-related mediators stimulate vascular endothelial growth factor secretion by two ovarian cancer cell lines. *Clin Cancer Res* 2009; **9**: 4514-21.
40. Fan F, Gray MJ, Dallas NA, Yang AD, Van Buren G 2nd, Camp ER, et al. Effect of chemotherapeutic stress on induction of vascular endothelial growth factor family members and receptors in human colorectal cancer cells. *Mol Cancer Ther* 2008; **7**: 3064-70.

Appearance of Hürthle cell carcinoma soon after surgical extirpation of Hürthle cell adenoma and follicular adenoma of the thyroid gland

Nevena Ristevska, Sinisa Stojanoski, Daniela Pop Gjorceva

Institute of Pathophysiology and Nuclear Medicine, Acad. "Isak S. Tadzer", Skopje, Macedonia

Radiol Oncol 2015; 49(1): 26-31.

Received 14 April 2014
Accepted 18 October 2014

Correspondence to: Nevena Ristevska, M.D., Bul. AVNOJ 36-3/6, 1000 Skopje, Republic of Macedonia. Phone: +389 70 398 042; Fax +389 2 3147 203; E-mail: nenaribi@gmail.com

Disclosure: No potential conflicts of interest were disclosed.

Background. Hürthle cell neoplasms could be benign (Hürthle cell adenoma) or malignant (Hürthle cell carcinoma). Hürthle cell carcinoma is a rare tumour, representing 5% of all differentiated thyroid carcinomas. The cytological evaluation of Hürthle cell neoplasms by fine needle aspiration biopsy (FNAB) is complicated because of the presence of Hürthle cells in both Hürthle cell adenoma and Hürthle cell carcinoma. Thus, the preoperative distinction between these two entities is very difficult and possible only with pathohistological findings of the removed tumour.

Case report. A 57-year old female patient was admitted at our Department, for investigation of nodular thyroid gland. She was euthyroid and FNAB of the nodules in both thyroid lobes were consistent of Hürthle cell adenoma with cellular atypias. After thyroidectomy the histopathology revealed Hürthle cell adenoma with high cellular content and discrete cellular atypias in the left lobe and follicular thyroid adenoma without cellular atypias in the right lobe. One year after substitution therapy, a palpable tumour on the left side of the remnant tissue was found, significantly growing with time, presented as hot nodule on ^{99m}Tc-sestamibi scan and conclusive with Hürthle cell adenoma with marked cellularity on FNAB. Tumorectomy was performed and well-differentiated Hürthle cell carcinoma detected. The patient received ablative dose of 100 mCi ¹³¹I. No signs of metastatic disease are present up to date.

Conclusions. The differences between Hürthle cell adenomas and Hürthle cell carcinomas could be clearly made only by histopathological evaluation. Patients with cytological diagnosis of Hürthle cell neoplasms should proceed to total thyroidectomy, especially if tumour size is > 1cm, FNAB findings comprise cellular atypias and/or multiple bilateral nodules are detected in the thyroid gland.

Key words: thyroid; Hürthle cell carcinoma; follicular adenoma; Hürthle cell adenoma; ^{99m}Tc-MIBI scintigraphy; radioiodine therapy

Introduction

Hürthle cell neoplasms (HCN) could be of benign appearance (Hürthle cell adenoma - HCA) or the cells could undergo malignant transformation (Hürthle cell carcinoma - HCC). Hürthle cell carcinomas are rare thyroid tumours, representing about 5% of all differentiated thyroid carcinomas. They originate from the follicular cells of the thyroid gland and in 75% are composed of so called

oncocytes or Hürthle cells. These cells were described for the first time by Askanazy, as cells with polygonal shape, acidophilic granular cytoplasm, hyperchromatic nuclei and abundant mitochondria.¹ Being more aggressive than the papillary and follicular variant, Hürthle cell carcinomas should take an important part in the diagnostic and therapeutic guidelines for thyroid carcinomas. The cytological evaluation of HCN by fine-needle aspiration biopsy (FNAB) is complicated because

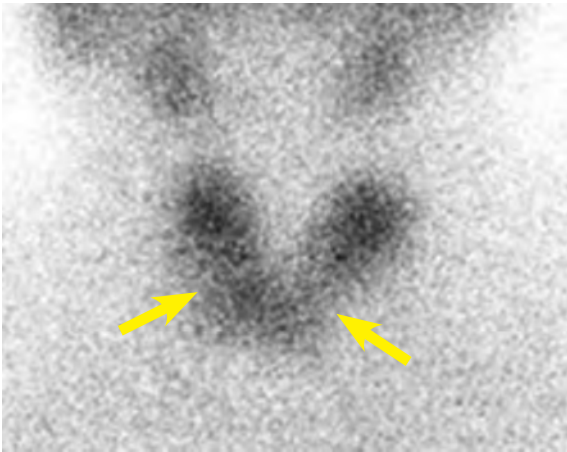


FIGURE 1. $^{99m}\text{TcO}_4$ scan showing "cold" nodules in the both thyroid lobes.

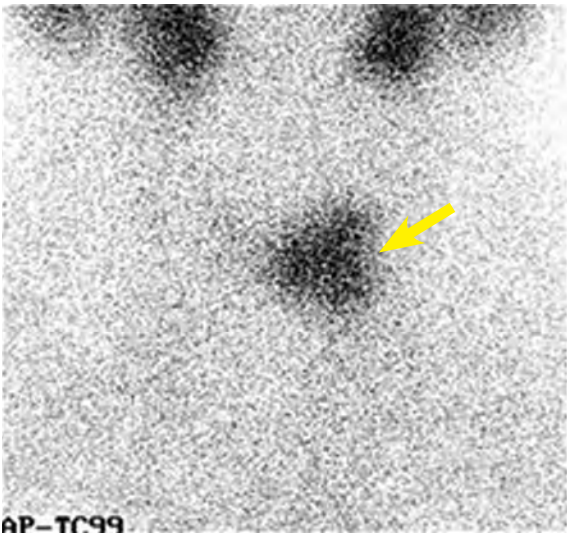


FIGURE 2. $^{99m}\text{TcO}_4$ scan showing remnant thyroid tissue on the left side after the first operation.

of the presence of Hürthle cells in both – HCA and HCC. Thus, the preoperative distinction between these two entities is very difficult and possible only with pathohistological findings of the surgically removed tumours, based on identification of capsular or vascular invasion, or the presence of metastatic disease.²

Case report

A 57-year old female patient was admitted at our Department for investigation of enlarged and nodular thyroid gland in February 2009, noticed firstly by her general practitioner. Written informed con-

sent of patient was obtained for the treatments and for the scientific use of the clinical data according to Declaration of Helsinki.

The patient was euthyroid, had no local or systemic complains, with thyroid functional tests within normal range (FT4 = 17.7 mmol/L, TSH = 1.36 IU/l). Nodules in both thyroid lobes were detected by palpation - smaller one in the right lobe and bigger one in the left lobe. Ultrasound (US) revealed isoechoic, non-homogenic nodule with hypoechoic halo (10 x 12 x 16 mm) in the middle part of the right thyroid lobe and smaller hyperechoic zone above it (7 x 4 x 8 mm). The nodule located in the lower 2/3 of the left lobe was hypoechoic, non-homogenic with cystic degeneration (20 x 27 x 39 mm). A scintiscan was performed, 20 min after intravenous application of 74 MBq of $^{99m}\text{TcO}_4$, that showed reduced uptake of $^{99m}\text{TcO}_4$ in the nodule in the middle of the right lobe and a "cold" nodule in the lower 2/3 of the left lobe (Figure1).

The FNAB of the right thyroid nodule (located in the middle, measured 16mm) detected benign Hürthle cells with abundant basophilic cytoplasm, normochromatic nucleuses and big nucleolus in central position. Some of these cells showed cytological atypias. Hürthle cells with some cytological atypias were also noted by FNAB, in the left thyroid nodule. Both FNAB findings were consistent of Hürthle cell adenomas with cellular atypias.

Because of these findings, total thyroidectomy was suggested. Near total thyroidectomy was performed (November 2009). The extent of the intervention included: *Lobectomy subtotalis l. sin;* *Lobectomy l. dext* and *Isthmectomy subtotalis*. Histopathology revealed HCA with high cellular content and discrete cellular atypias in the nodule, located in the surgically removed tissue fragment (6 x 4.5 x 3.2 cm) of the left lobe and follicular thyroid adenoma without cellular atypias in the nodule located in the surgically removed tissue fragment (4 x 3 x 2.8 cm) of the right lobe. No evidence of malignant cell transformation or capsular invasion was detected. One month after surgery (December 2009), scintiscan with $^{99m}\text{TcO}_4$ showed remnant thyroid tissue (24 mm, isoechoic, non-homogenic oval formation) on the left side, towards isthmic location and no remnant tissue on the right side of the thyroid bed (Figure 2).

Because of the hypothyroid state (FT4 = 5.11 mmol/L, TSH = 36.9 IU/l), substitution therapy with L-thyroxin was administered. Since there was no indication of malignant transformation or capsular invasion on histopathology, removal of the remnant thyroid tissue was not suggested. The size

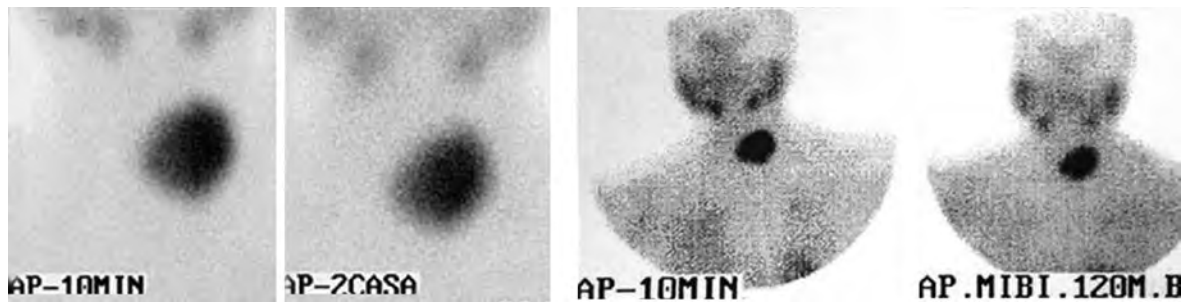


FIGURE 3. ^{99m}Tc -MIBI scan showing intensive accumulation in the newly appeared tumour in the left thyroid lobe.

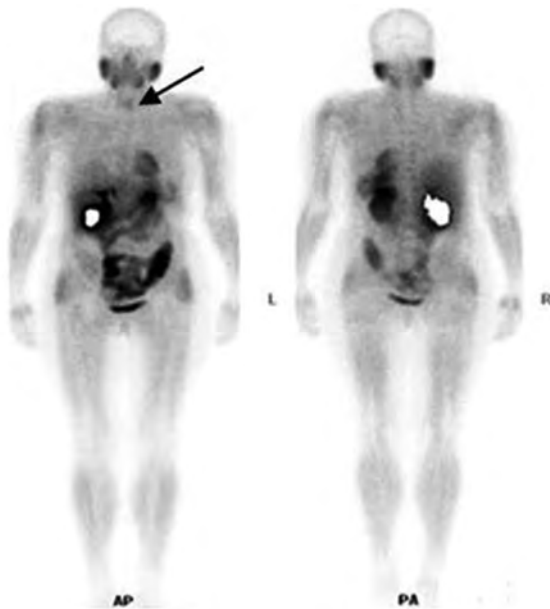


FIGURE 4. Whole-body scan (WBS) with ^{99m}Tc -MIBI showing normal distribution of the tracer in the body as well as the accumulation in the tumor in the left thyroid lobe.

and structure of the remnant tissue on the following regular check-ups was evaluated by US (17 x 11 x 24, isoechoic non-homogeneous structure), without enlargement or nodular presentation on US on the first two regular check-ups. Thereafter, the patient was euthyroid with laboratory findings within normal range.

Almost one year after surgery (patient hasn't come for regular check-ups), at September 2010, a palpable tumour on the side of the remnant thyroid tissue (left side) was found, that showed significant progressive enlargement on US with time (from 22 mm, to 28 mm, to 39 mm). FNAB (April 2011) detected Hürthle cells with big nucleus, big acidophilic nucleolus and poor cytoplasm, cytologically conclusive of HCA with marked cellular-

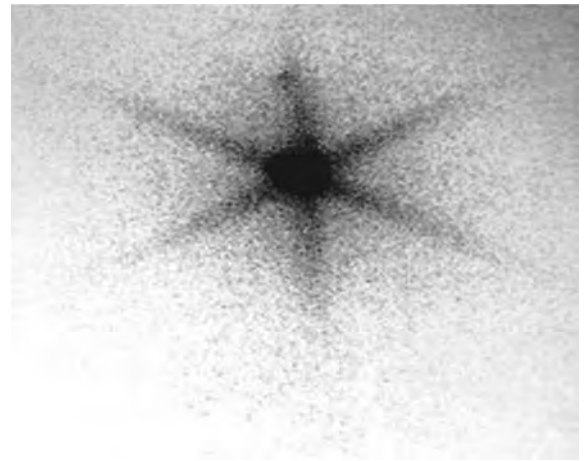


FIGURE 5. Post-therapy whole-body scan (WBS) - after ablative dose of radioiodine - showing uptake only in the thyroid bed.

ity. To evaluate mitochondrial activity and tumour avidity, as a marker of potential malignancy, the double phase ^{99m}Tc - sestamibi (MIBI) scintigraphy was performed. Intensive accumulation was noted in this nodule on the early scintigram (10 min), without washout of the radiotracer on the late (2h) phase (Figure 3).

Considering the FNAB findings, ^{99m}Tc -MIBI scan and tumour size (increasing with time) the patient was suggested and underwent a second operation (August 2012) - tumourectomy and remnant tissue extirpation. Histopathological examination of the extirpated tissue fragment - (comprising the newly detected nodule and the remnant thyroid tissue, sized 5.5 x 4.5 x 4 cm) revealed presence of well-differentiated HCC (stage III, pTNM = pT3 pNx pMx, G1 C1) with large malignant cells rich with eosinophilic cytoplasm, with hyperchromatic nucleuses, and well-differentiated grade 1 nucleus. Necrotic regions and capsular invasion were found as well. US postoperatively revealed only small remnant thyroid tissue on the left side, con-

firmed on the consecutive ^{99m}Tc -MIBI scintigraphy (January 2013) (Figure 4).

One month after, an ablative dose of 100 mCi ^{131}I was given and there was no pathological accumulation of the tracer on the whole-body scan (WBS), except the small accumulation in the region of the remnant thyroid tissue after the second surgical procedure (Figure 5). The patient at present is symptom free, receiving hormonal replacement therapy. No signs of metastatic disease are present up to date and the levels of thyroglobulin (Tg) are within normal range - respectively < 0.2 ng/ml.

Discussion

Hürthle cell carcinomas are oxyphilic type of tumours, with histological features and ability of thyroglobulin production, which suggests that they arise from the follicular cells of the thyroid gland. In the beginning they were considered as a variant of the follicular thyroid carcinomas, but later the morphological findings suggested that they are separate pathological entity. Cellular features on light microscopy include large size, polygonal to square distinct cell borders, voluminous granular and eosinophilic cytoplasm, large hyperchromatic nucleus and cherry pink nucleoli.³ Electron microscopy reveals a granular cytoplasm due to large number of mitochondria within the Hürthle cells.⁴

HCCs comprise 2% to 10% of all differentiated thyroid carcinomas and are usually presented in the fifth to seventh decade of life.⁵⁻⁷ They are mainly slow-growing thyroid nodules, associated with lymphadenopathy, vocal cord paralysis and distant metastasis (usually uncommon). In 15% to 35% of cases, HCC are presented as multifocal and in up to 20% of cases lymph node metastases are presented in the beginning of the disease. About 10% of the metastases from HCCs concentrate iodine, comparing to 75% of the metastases from the follicular carcinomas.⁸

Apart from the findings of other authors, Pu *et al.* in their paper concluded that a diagnosis of HCN does not impart a higher rate of malignancy than a diagnosis of follicular neoplasm by FNAB of thyroid nodules. They also confirm that factors as male gender and older age in general are associated with worse outcome, especially with HCC.⁹

Diagnosis of HCC can be confirmed by histopathology examination of the specimen, through determination of invasiveness of the carcinoma and not only by cytological examination.¹⁰ The verification of invasiveness is based on demonstra-

tion of capsular invasion or angio-invasion that can be assessed only in the resected specimen.¹¹ Furthermore, findings of local invasion, lymph node spread and distant metastases classify HCN as a malignant one. But aside from capsular and vascular invasion, malignancy can be based upon the expression of Ret/PTC or CK-19 gene rearrangements. Considering Ki-67 as an endpoint marker of multiple pathways in cellular proliferation, Hoos *et al.* investigated its role in HCC (vascular invasion, capsular invasion and extrathyroid extension/dissemination). They found that Bcl-2 expression $> 50\%$ was associated with relapse-free survival and disease-specific survival. So Combination of Ki-67 (+) and Bcl-2 (-) phenotype was associated with widely invasive and aggressive HCC, compared to normal tissue. Also they found inactivation of p53 protein, but p21 overexpression in 43–63% of Hürthle cell tumours, suggesting the role of this protein in thyroid tumourogenesis.⁷

HCCs and follicular carcinomas express various oncogenes in different ways. In comparison with follicular carcinomas, HCCs express a greater proportion of Pan-ras, N-myc, transforming growth factor alpha (TGF- α), TGF- β and insulin-like growth factor 1 (IGF-1).¹² So, these findings confirm that HCCs and follicular carcinomas are different entities and not only a subtype one of the other. Recent reports suggest that use of some proliferative cell markers such as Ki-67 or various oncogenes could be useful in distinguishing malignant and benign tumours.¹³

The main procedure of treatment for HCC is thyroidectomy. But a question still prevails about the optimal resection extent for HCC - total thyroidectomy versus lobectomy. Lobectomy could be adequate for smaller tumours (less than 1 cm). There are several advantages when total thyroidectomy is performed:

- In case of multifocal disease, which is found in about 35% of patients;
- Removal of thyroid gland facilitates radioactive iodine uptake in recurrent disease;
- Assessment of Tg is more sensitive for recurrent disease in absence of normal thyroid tissue.

Whenever HCC is diagnosed and thyroidectomy performed, any remaining tissue should be ablated with radioactive iodine. When thyroglobulin is still detectable after total thyroidectomy and ablation with radioiodine or when its value begins to rise, we should think that recurrence could be in question. The problem of distant metastases is still controversial. Treatment with radioactive iodine is of less beneficial results. According to the current

guidelines for treatment of progressive or symptomatic HCC metastatic disease it is recommended:¹⁴

- Use of multikinase inhibitors (MKIs), especially pazopanib, sorafenib or sunitinib;
- Systemic oncological therapeutic protocols;
- Best supportive care.

We report a case of this rare disease where appearance of HCC was documented extremely soon after both HCA and follicular thyroid adenoma were diagnosed on pathohistology of the removed thyroid tissue. This case is an example of rare and complex thyroid pathology concerning two aspects: firstly the concomitant existence of the two entities - follicular thyroid adenoma and HCA (with small cellular atypia), secondly because of the fast growing tumour, probably evolving from the micro multifocal HCC in the remnant thyroid tissue, left over after the surgical removal of HCA.

Knowing the possible multifocal nature of HCC, we assume that in this patient, we see very fast evolution and progression of the micro multicentric HCC in the remnant thyroid tissue. Therefore we verify immediate and last phase of malignant transformation.

HCC are slow progressive neoplasms, with slow evolution, involving a long period of existence and growing of a nodule with HCA and cellular atypia, as in our case (the first nodule in the left thyroid lobe reached a diameter of 5cm). Concerning the short period of malignant transformation (almost 1 year), as well as absence of any malignant cellular characteristics by FNAB (the well-known problem in the distinction between HCA and HCC), the fact of not developing any local metastasis in the neck is not a surprise.

FNAB is simple non-invasive technique for sampling thyroid palpable/non-palpable nodules, but it cannot rule out with certainty the possibility of presence of malignant focus in multifocal HCC. Scintigraphy with ^{99m}Tc-MIBI helps in evaluating metabolic activity in the fast growing tumour (as in our case of HCA/HCC), rising a suspicion of malignant transformation and as a relative indication for surgical operation. WBS with this tracer is a good diagnostic modality for evaluation of distant metastases. Considering the multifocality of the disease with micro variant that was not seen on US, but happened to be present in the remnant thyroid tissue on the left side suggests the total thyroidectomy to be a procedure of first choice in these patients.

The fast growing rate, the size of the thyroid nodule (39 mm) and the presence of necrotic lesions and capsule invasion detected by histopathol-

ogy on one side and not having the opportunity to evaluate the expression for Ret/PTC or CK-19 gene rearrangements and proliferation index Ki-67 on the other side, guided us to post-therapeutic procedure with 100 mCi ¹³¹I for achieving optimal conditions for further evaluation and disease treatment.

Conclusions

The differences between HCAs and HCCs could be clearly made only with histopathological evaluation of the operated specimen, although there are some clinical features used to predict this difference, especially the new molecular markers. This case report confirms the fact that HCC should never be excluded whenever HCA is diagnosed, especially with cellular atypia.

Scintigraphy with ^{99m}TcO₄ usually presents "cold" nodule, and dual phase ^{99m}Tc-MIBI scintigraphy presents "hot" nodule, so in case of HCA/HCC, combination of these two diagnostic modalities could improve the final clinical decision.

Patients with cytological diagnosis of HCNs should proceed to total thyroidectomy, especially if tumour size is > 1 cm, if FNAB findings comprise cellular atypias and / or multiple bilateral nodules are detected in the thyroid, as in our case. Total thyroidectomy allows follow up tests to be more effective thereafter, and also enables better disease prognosis by avoiding the possibility of recidivant HCC appearance.

References

1. Stojadinovic A, Ghossein R, Hoos A, Urist MJ, Spiro RH, Shah JP, et al. Hürthle cell carcinoma: a critical histopathologic appraisal. *J Clin Oncol* 2001; **19**: 2616-25.
2. Maizlin ZV, Wiseman SM, Vora P, Kirby JM, Mason AC, Filipenko D, et al. Hürthle cell Neoplasms of the Thyroid. Sonographic Appearance and Histologic Characteristics. *J Ultrasound Med* 2008; **27**: 751-7.
3. Sandoval MA, Paz-Pacheco E. Hürthle cell carcinoma of the thyroid. *Brit Med Jour Case Reports* 2011; **10**: 1136-72.
4. Sobrino-Simoes MA, Nesland JM, Holm R, Sambade MC, Johannessen JV. Hürthle cell and mitochondrion-rich papillary carcinomas of the thyroid gland: an ultrastructural and immunocytochemical study. *Ultrastruct Pathol* 1985; **8**: 131-42.
5. Agaoglu N. A case report: Hürthle cell carcinoma of the thyroid gland. *Firat Tip Dergisi* 2004; **9**: 28-9.
6. McDonald M, Sanders LE, Silverman ML, Chan HS, Buyske J. Hürthle cell carcinoma: prognostic factors and results of surgical treatment. *Surgery* 1996; **120**: 1004-5.
7. Hoos A, Stojadinovic A, Singh B, Dudas M, Leung HY D, Shaha A. Clinical significance of molecular expression profiles of Hürthle cell tumors of the thyroid analyzed via tissue microarrays. *Am J Pathol* 2002; **160**: 175-83.

8. Grossman RF, Tezleman S, Epstein HD, Novosolov F, Duh QY, Siperstein AE, et al. Total thyroidectomy and central neck lymph node dissection: treatment of choice for Hürthle cell carcinoma. *10th International Congress of Endocrinology*. June 12-15, 1996. San Francisco, California: The Endocrine Society; 1996. p 646.
9. Pu RT, Yang J, Wasserman PG, Bhuiya TT, Griffith KA, Michael CW. Does Hürthle cell lesion/neoplasm predict malignancy more than follicular lesion/neoplasm on thyroid fine-needle aspiration? *Diagn Cytopathol* 2006; **34**: 330-4.
10. Tyler DS, Winchester DJ, Caraway NP, Hickey RC, Evans DB. Indeterminate fine-needle aspiration biopsy of the thyroid identification of subgroup at high risk for invasive carcinoma. *Surgery* 1994; **116**: 1054-60.
11. Massidda B, Nicolosi A, Mura E, Addis E, Esu S, Piga A. Hürthle cell tumors of thyroid. *Minerva Chir* 1992; **47**: 913-7.
12. Masood S, Auguste LJ, Westerband A, Belluco C, Valderama E, Attie J. Differential oncogenic expression in thyroid follicular and Hürthle cell carcinomas. *Am J Surg* 1993; **166**: 366-8.
13. Barnabei A, Ferretti E, Baldelli R, Procaccini A, Spriano G, Appetecchia M. Hürthle cell tumours of the thyroid. Personal experience and review of the literature. *Acta Otorhinolaryngol Ital* 2009; **29**: 305-11.
14. National Comprehensive Cancer Network (NCCN). Version 2.2013, (2013/04/09) Available from: www.nccn.org/professionals/physician_gls/pdf/thyroid.pdf. Accessed 09 April 2013.

Adjuvant TNF- α therapy to electrochemotherapy with intravenous cisplatin in murine sarcoma exerts synergistic antitumor effectiveness

Maja Cemazar^{1,2}, Vesna Todorovic¹, Janez Scancar³, Ursa Lamprecht¹, Monika Stimac¹, Urška Kamensek¹, Simona Kranjc¹, Andrej Coer², Gregor Sersa¹

¹ Department of Experimental Oncology, Institute of Oncology Ljubljana, Ljubljana, Slovenia

² Faculty of Health Sciences, University of Primorska, Izola, Slovenia

³ Jozef Stefan Institute, Ljubljana, Slovenia

Radiol Oncol 2015; 49(1): 32-40.

Received 10 December 2014

Accepted 15 January 2015

Correspondence to: Dr. Maja Čemažar and Dr. Gregor Serša, Institute of Oncology Ljubljana, Department of Experimental Oncology, Zaloška 2, SI-1000 Ljubljana, Slovenia. Phone +386 1 587 95 44; Fax: +386 1 587 94 34; E-mail: mcemazar@onko-i.si or gsersa@onko-i.si

Disclosure: No potential conflicts of interest were disclosed.

Background. Electrochemotherapy is a tumour ablation modality, based on electroporation of the cell membrane, allowing non-permeant anticancer drugs to enter the cell, thus augmenting their cytotoxicity by orders of magnitude. In preclinical studies, bleomycin and cisplatin proved to be the most suitable for clinical use. Intravenous administration of cisplatin for electrochemotherapy is still not widely accepted in the clinics, presumably due to its lower antitumor effectiveness, but adjuvant therapy by immunomodulatory or vascular-targeting agents could provide a way for its potentiation. Hence, the aim of the present study was to explore the possibility of adjuvant tumour necrosis factor α (TNF- α) therapy to potentiate antitumor effectiveness of electrochemotherapy with intravenous cisplatin administration in murine sarcoma.

Materials and methods. *In vivo* study was designed to evaluate the effect of TNF- α applied before or after the electrochemotherapy and to evaluate the effect of adjuvant TNF- α on electrochemotherapy with different cisplatin doses.

Results. A synergistic interaction between TNF- α and electrochemotherapy was observed. Administration of TNF- α before the electrochemotherapy resulted in longer tumour growth delay and increased tumour curability, and was significantly more effective than TNF- α administration after the electrochemotherapy. Tumour analysis revealed increased platinum content in tumours, TNF- α induced blood vessel damage and increased tumour necrosis after combination of TNF- α and electrochemotherapy, indicating an anti-vascular action of TNF- α . In addition, immunomodulatory effect might have contributed to curability rate of the tumours.

Conclusion. Adjuvant intratumoural TNF- α therapy synergistically contributes to electrochemotherapy with intravenous cisplatin administration. Due to its potentiation at all doses of cisplatin, the combined treatment is predicted to be effective also in tumours, where the drug concentration is suboptimal or in bigger tumours, where electrochemotherapy with intravenous cisplatin is not expected to be sufficiently effective.

Key words: TNF- α , electrochemotherapy, cisplatin, adjuvant immunotherapy

Introduction

Electrochemotherapy is a non-thermal tumour ablation modality that is safe and effective in any solid tumour type. Electrochemotherapy is based on the local delivery of electric pulses that permea-

bilize the cell membrane, allowing non-permeant or low-permeant anticancer drugs to enter the cell, thus augmenting their cytotoxicity by orders of magnitude. Treatment is safe, very well tolerated by the patients, and its efficacy is very high on the different tumour nodules.¹ Electrochemotherapy

has gained a role in routine clinical practice for treatment of cutaneous and subcutaneous tumours as local therapy.^{2,3} The development of specialized electrodes has made it possible to apply electrochemotherapy also to deep-seated tumours.^{4,5} The results of the first preclinical and clinical studies using specialized electrodes demonstrated feasibility of this approach for treatment of deep-seated tumours in liver and brain as well as for bone tumours and metastases.^{4,6-11}

Among the drugs that have been tested in preclinical studies, bleomycin and cisplatin (CDDP) proved to be the most suitable for clinical use of electrochemotherapy. In the clinical use, both can be administered locally in the tumour, but only bleomycin systemically, intravenously, to obtain pronounced antitumor effect. Namely, in preclinical studies it was demonstrated that intratumoural administration of CDDP is more effective than systemic administration.¹²⁻¹⁴ The mechanisms of antitumor action of electrochemotherapy using both drugs are multifactorial, including anti-vascular effect and immune response stimulation.^{15,16} The activation of immune response is presumably due to the direct cytotoxic effect on tumour cells leading to immunological cell death.¹⁶ Hence, to potentiate antitumor effectiveness of systemic electrochemotherapy, we explored the possibility of additional intratumoural application of recombinant tumour necrosis factor α (TNF- α). TNF- α is a well-known pro-inflammatory cytokine with a wide range of biological functions.¹⁷ In addition to its immunomodulatory role, it also has an anti-vascular effect.¹⁸ To extend the application of electrochemotherapy with intravenous CDDP administration, addition of TNF- α could enhance the antitumour effectiveness of electrochemotherapy through its biological functions. Therefore, the aim of the present study was to explore the possibility of adjuvant intratumoural TNF- α therapy to electrochemotherapy with intravenous CDDP administration in murine sarcoma.

Materials and methods

Cell line

Murine fibrosarcoma cell line SA-1 (The Jackson Laboratory, Bar Harbor, ME, USA) was grown as monolayer in Eagle Minimum Essential Medium (EMEM) with Glutamax (Invitrogen, Paisley, UK), supplemented with 10% foetal calf serum (FCS) (Invitrogen) and gentamicin (30 $\mu\text{g}/\text{mL}$) (Invitrogen). Cells were routinely subcultured

twice a week and incubated in an atmosphere with 5% CO_2 at 37°C.

Drug

CDDP (Medac, Wedel, Germany) was dissolved in sterile H_2O . For each experiment, a fresh solution of CDDP was prepared. *In vitro*, the final concentrations of CDDP were prepared in EMEM. CDDP concentrations of 0.1 $\mu\text{g}/\text{mL}$ and 0.5 $\mu\text{g}/\text{mL}$ were used in the *in vitro* experiments.

Murine recombinant TNF- α was obtained from Affymetrix eBioscience (Santa Clara, CA, USA). The final concentrations of TNF- α were prepared in phosphate buffered saline (PBS) (Invitrogen). TNF- α concentrations 2.5×10^3 U/mL, 2.5×10^4 U/mL, and 2.5×10^5 U/mL were used in the *in vitro* experiments.

In vitro electroporation

Confluent cell cultures were trypsinized, washed in EMEM with FCS for trypsin inactivation and once in electroporation buffer (125 mM saccharose; 10 mM K_2HPO_4 ; 2.5 mM KH_2PO_4 ; 2 mM $\text{MgCl}_2 \cdot 6\text{H}_2\text{O}$) at 4°C. The final cell suspension (22×10^6 cells/mL) was prepared in electroporation buffer at 4°C. Cells (2×10^6) were mixed with CDDP and/or TNF- α . Half of this mixture (1×10^6 cells) was placed between two parallel stainless steel electrodes with a 2 mm gap in-between and subjected to eight square wave electric pulses (EP) with voltage to distance ratio 1300 V/cm, pulse duration 100 μs and frequency 1 Hz. EP were generated by generator of EP ELECTRO CELL B10 (Betatech, Saint-Orens-de-Gameville, France). The other half of the mixture served as a control for CDDP and/or TNF- α treatment alone. After electroporation, cells were incubated at room temperature for 5 min, diluted in 2 mL of growth medium and then plated for the clonogenic assay.

Clonogenic assay

Sensitivity of SA-1 cells exposed to CDDP or TNF- α alone, a combination of CDDP and TNF- α , EP alone, electrochemotherapy with CDDP (ECT), EP + TNF- α and ECT + TNF- α was determined by clonogenic assay. SA-1 cells were plated at a concentration of 200 cells/dish for exposure to CDDP or TNF- α alone and 500 cells/dish for combination of electroporation and CDDP or TNF- α . After 7 days colonies were fixed, stained with crystal violet and counted. The survival curve for the electro-

chemotherapy-treated cells was normalised for the cytotoxicity of EP treatment alone. The experiment was repeated twice in triplicates.

Tumour and animal model

Murine fibrosarcoma SA-1 cells syngeneic to A/J mice (Harlan, Udine, Italy) were used in the study. Mice were maintained in a specific pathogen-free animal colony at constant room temperature (20–24°C), relative humidity (55±10%), and 12 hour light/dark cycle. Food and water were provided *ad libitum*. Animals were subjected to an adaptation period of 7–10 days before the experiments were carried out. All procedures on animals were performed in accordance with the official guidelines of European Union Directive 2010/63/EU and with the permission of the Ministry of Agriculture and the Environment of the Republic of Slovenia (permission no. 34401-4/2012/2) which was granted based on the approval of Ethical committee for animal experimentation of the Republic of Slovenia. At the beginning of the experiment, the animals were 9–11 weeks old. Solid tumours were induced by subcutaneous injections of SA-1 cells ($5 \cdot 10^5$ cells/0.1 mL 0.9% w/v NaCl) in the right flank prepared from the ascites from donor mouse. When the tumours reached approximately 40 mm³ in volume, the animals were randomly divided into experimental groups and subjected to a specific experimental protocol.

In vivo electroporation

EP were delivered by generator of EP ELECTRO CELL B10 using flat parallel electrodes with 8 mm gap. Electrodes were placed percutaneously at the opposite tumour margins. Electroporation of tumours was performed by applying eight square-wave EP with voltage to distance ratio 1300 V/cm, pulse width 100 μ s and repetition frequency 1 Hz with a perpendicular change of electrode orientation after 4 pulses. Good contact between the electrodes and the overlying skin was ensured by conductive gel (Parker Laboratories, Fairfield, NJ, USA).

In vivo study design

To evaluate the influence of TNF- α on the antitumour effectiveness of electrochemotherapy, TNF- α (1×10^5 U) was applied intratumourally (i.t.) either 5 min before or after the application of EP. CDDP (4 mg/kg) was injected intravenously (i.v.) 3 min before the application of the electric pulses (Figure 1). The pertinent groups were control

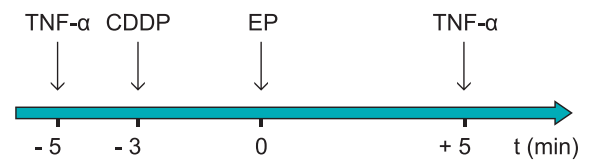


FIGURE 1. Time schedule of the treatment.

(untreated tumours), EP (application of EP only), CDDP (injection of CDDP only), TNF- α (injection of TNF- α only), ECT (electrochemotherapy with CDDP), EP + TNF- α -5 min (injection of TNF- α 5 min before the application of EP), EP + TNF- α +5 min (injection of TNF- α 5 min after the application of EP), CDDP + TNF- α -2 min (injection of TNF- α 2 min before the injection of CDDP), CDDP + TNF- α +8 min (injection of TNF- α 8 min after the injection of CDDP), ECT + TNF- α -5 min (injection of TNF- α 5 min before electrochemotherapy), and ECT + TNF- α +5 min (injection of TNF- α 5 min after electrochemotherapy).

In the second part of the *in vivo* study, the antitumour effect of TNF- α in combination with electrochemotherapy with different CDDP doses was evaluated. TNF- α was injected 2 min before the injection of CDDP (dose range 1 – 8 mg/kg) and 5 min before the application of electric pulses.

After the therapy, tumour growth was followed up by measurements of tumour diameters with a digital calliper. Tumour volume was calculated by the formula $V = a \cdot b \cdot c \cdot \pi / 6$, where a, b and c were three mutually orthogonal tumour diameters. From the calculated volume, arithmetic means and standard error of the means were calculated for each experimental group. Tumour doubling time was determined for each individual tumour, and tumour growth delay was calculated from the mean doubling time of experimental groups. When the tumour volume reached 300 mm³, animals were considered incurable and were humanely euthanized. When the tumours became impalpable, the response to treatment was scored as complete response. Mice that were in complete response 100 days after the treatment were considered as cured. In addition, the weight of the mice was followed as a general toxicity index.

Determination of platinum content in tumours after treatment

Mice were sacrificed 24 h after treatment with CDDP (4 mg/kg), electrochemotherapy, combination of TNF- α and CDDP, and combination of TNF- α and electrochemotherapy. Tumours were excised and

removed from the overlying skin. To determine platinum content in tumours after treatment, tumours were weighed, placed in 15-mL graduated polyethylene tubes and digested in 0.5 mL 65% nitric acid by incubation at 37°C for 2 days to obtain a clear solution. Platinum content in the samples was determined by electrothermal atomic absorption spectrometry on a Hitachi Z-8270 Polarized Zeeman Atomic Absorption Spectrometer, adjusted to a wavelength of 265.9 nm.

Tumour histology

Mice were sacrificed 24 h after treatment with CDDP, electrochemotherapy, combination of TNF- α and CDDP, and combination of TNF- α and electrochemotherapy. Tumours were excised, removed from the overlying skin and fixed in IHC zinc fixative (BD Pharmingen, BD Biosciences, San Diego, CA, USA) for 24 h at room temperature, and embedded in paraffin. Two series of 2 μ m thick tissue sections were cut from each paraffin block with step thicknesses of 20 μ m.

First series of tissue sections were used for immunohistochemical staining of CD31, a marker for endothelial cells. Sections were incubated with rabbit polyclonal antibodies against murine CD31 (ab28364, Abcam, Cambridge, MA, USA) at dilution 1:1000. A peroxidase-conjugated streptavidin-biotin system (Rabbit specific HRP/DAB detection IHC kit, ab64261, Abcam) was used as the colorogenic reagent followed by haematoxylin counterstaining. The immunohistochemically stained sections were examined in blind fashion under light microscopy and 5 images of viable tumour tissue from the same tumour section were captured with a DP72 CCD camera (Olympus, Hamburg, Germany) connected to a BX-51 microscope (Olympus).

Second series of tissue sections were stained with haematoxylin and eosin for evaluation of tumour necrosis. These slides were examined under the microscope Olympus BX-51 and visual light images were recorded with a digital camera DP72 CCD (Olympus). Digital images of haematoxylin and eosin stained tumour sections were analysed in blind fashion and percentage of necrosis was estimated by 4 independent observers.

Statistical analysis

SigmaPlot 11.0 (Systat Software Inc., San Jose, CA, USA) was used for statistical analysis. Normal distribution of the data was tested using Shapiro-Wilk

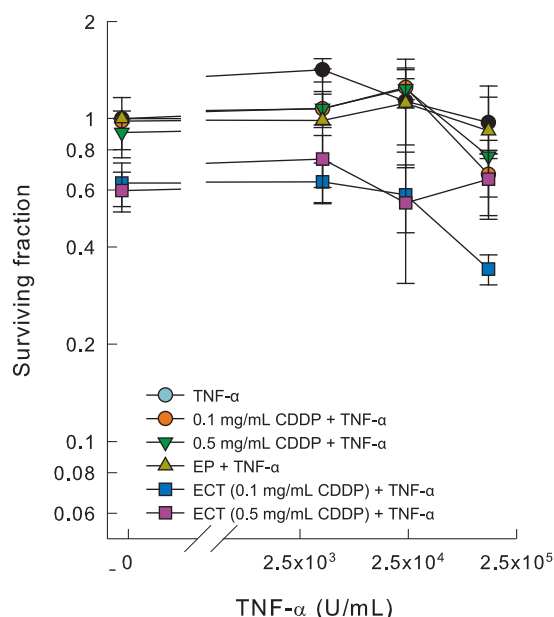


FIGURE 2. Cell survival after electrochemotherapy with TNF- α at different doses. The surviving fraction of cells exposed to electrochemotherapy was normalized to electric pulses alone. Symbols represent median \pm MAD.

test. All pairwise multiple comparisons for normally distributed data were tested with Holm-Sidak test after One Way ANOVA. All pairwise multiple comparisons for data that was not normally distributed were tested using Tukey test or Dunn's test (if treatment group sizes were unequal) after Kruskal-Wallis One-Way ANOVA on ranks. Differences were considered significant when p value was less than 0.05.

Results

TNF- α does not potentiate CDDP cytotoxicity

In vitro sensitivity of SA-1 cells to electrochemotherapy with or without TNF- α was determined by clonogenic assay (Figure 2). TNF- α in all the selected concentrations up to 2.5·10⁵ U/mL did not exert any direct cytotoxic effect on SA-1 cells *in vitro*. Furthermore, no interaction of TNF- α with CDDP or electrochemotherapy was noticed at both concentrations of CDDP tested.

Adjuvant TNF- α before or after ECT *in vivo*?

To determine if TNF- α can potentiate antitumor effectiveness of electrochemotherapy with intra-

TABLE 1. Tumour doubling times and growth delay after different treatments. TNF- α was applied either before (TNF- α +) or after (TNF- α -) treatment

Treatment group	n	Doubling time (mean \pm SEM)	Growth delay (vs. control)	Cures
Control	7	2.2 \pm 0.1		
EP	7	3.2 \pm 0.4	1.0	
CDDP	7	3.1 \pm 0.2	0.9	
TNF- α	7	2.9 \pm 0.1	0.7	
ECT	8	4.1 \pm 0.9	1.9	
TNF- α -5 min + EP	10	7.2 \pm 0.4	5.0	
TNF- α +5 min + EP	10	5.8 \pm 0.5	3.6	
TNF- α -2 min + CDDP	10	3.7 \pm 0.4	1.5	
TNF- α +8 min + CDDP	10	3.5 \pm 0.3	1.3	
TNF- α -5 min + ECT	11	23.7 \pm 2.3*†	21.5	4 (36%)
TNF- α +5 min + ECT	11	15.4 \pm 1.5*	13.2	3 (27%)

* = Significantly increased doubling time in comparison to other treatment groups; † = Significantly increased doubling time in comparison to TNF- α +5 min + ECT. $p < 0.05$

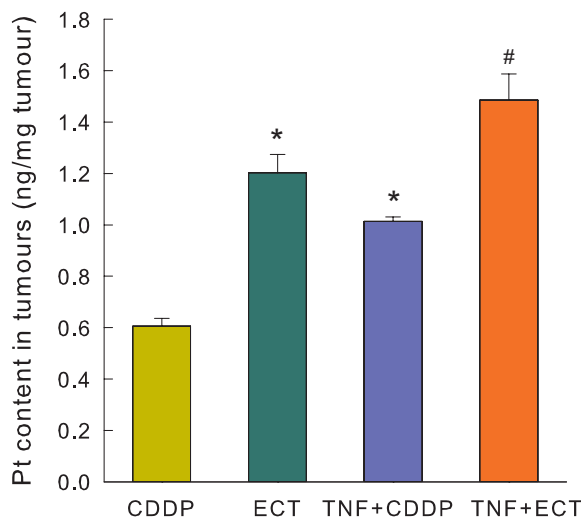


FIGURE 3. Platinum content in tumours 24 h after different treatments. Increased platinum uptake was observed after electrochemotherapy and exposure to TNF- α . Bars represent mean \pm SEM. * $p < 0.05$ vs. CDDP, # $p < 0.05$ vs. CDDP, ECT and TNF+CDDP.

venous CDDP injection *in vivo*, we evaluated the effect of intratumoural TNF- α injection before or after electrochemotherapy on tumour growth (Table 1). A relatively low CDDP dose of 4 mg/kg was selected in order to be able to demonstrate the possible interaction with adjuvant TNF- α therapy.

Among all the combined modality groups only the adjuvant TNF- α therapy to electrochemotherapy produced significant tumour growth delay compared to control tumours and resulted in tumour cures. In these combined treatment groups,

tumour doubling times were greater than the sum of tumour doubling times of single therapies (Table 1). Specifically, the treatment of tumours before the electrochemotherapy was significantly more effective ($p < 0.05$) than treatment with TNF- α after electrochemotherapy, producing longer tumour growth delay, and higher tumour curability rate (36% vs. 27%, respectively) (Table 1). The single or combined therapies did not have toxic side effects or did not induce animal weight loss for more than 10% of the body weight (data not shown).

Platinum content in tumours after treatment

To determine whether TNF- α treatment affects CDDP uptake in tumours, platinum content in whole tumours was determined 24 h post treatment. Significant differences in platinum concentration in tumours were observed after different treatments (Figure 3). Tumour treatment with electrochemotherapy alone or with TNF- α resulted in significantly higher platinum concentration in the whole tumours ($p < 0.05$). Electrochemotherapy increased platinum content in the tumours, as expected, approximately by factor of 2.¹⁹ Furthermore, in the TNF- α with the electrochemotherapy treatment group, platinum content in tumours was further significantly increased compared to tumours treated with either electrochemotherapy or TNF- α in combination with CDDP without EP. Overall 2.2-fold increase in tumour platinum content was observed. The data do not prove the internalisation of the platinum in the cells of tumours, but rather indicate on the overall platinum content in the tumours.

Histological analysis

The effect on tumour blood vessels was demonstrated by immunohistochemical analysis of anti-CD31-stained blood vessels in viable regions of tumours 24 h after treatments (Figure 4). Differences were observed in tumours treated with either CDDP or electrochemotherapy in comparison to tumours treated with TNF- α in combination with CDDP or electrochemotherapy. A strong anti-CD31 staining was observed in tumours treated with either CDDP or electrochemotherapy, while anti-CD31 staining in tumours treated with TNF- α was much weaker. In tumours treated with CDDP alone, typical tumour blood vessels network with thin vessels walls consisting only of endothelial cells was observed

(Figure 4A). After electrochemotherapy, most of the blood vessels were narrowed indicating clearly seen vasoconstriction (Figure 4B). Number of functional blood vessels was significantly reduced in tumours after treatment with TNF- α . In tumours treated with combination of TNF- α and CDDP, tumour vessels were dilated, with stacked erythrocytes (Figure 4C). This effect was more pronounced after treatment with combination of TNF- α and electrochemotherapy, where only few large dilated blood vessels with mostly hyperaemic and occasionally damaged blood vessels and in some areas also extravasated erythrocytes were observed (Figure 4D).

Necrosis of tumour tissue was evaluated histologically in all samples 24 h after different treatments (Figure 5). Cisplatin treatment did not result in significantly increased necrosis compared with control untreated tumours.¹⁹ The degree of necrosis was significantly increased in tumours treated with adjuvant TNF- α and electrochemotherapy in comparison to tumours treated with CDDP, electrochemotherapy or combination of TNF- α and CDDP.

Is TNF- α interaction with electrochemotherapy CDDP dose dependent?

In the second part of the study, the effect of combined TNF- α and electrochemotherapy with different CDDP doses (1-8 mg/kg) on tumour growth was evaluated. Based on the previous experiment, adjuvant TNF- α therapy was given before electrochemotherapy.

As predicted, electroporation significantly potentiated CDDP effectiveness, which was CDDP dose dependent (Figure 6). Electrochemotherapy with the CDDP doses of 6 and 8 mg/kg produced significant tumour growth delay of 8.4 ± 0.8 and 10.3 ± 0.8 days. The adjuvant intratumoural TNF- α therapy significantly potentiated the effectiveness of electrochemotherapy at all the CDDP doses used, also at the lowest CDDP dose of 1 mg/kg that had no effect in electrochemotherapy. Synergistic effect of combined treatment modality was observed at lower CDDP doses (1 and 4 mg/kg), where tumour doubling time of combined treatment modality was greater than the additive effect of single therapies. Addition of TNF- α to electrochemotherapy prolonged tumour doubling time for 5.5 days in comparison to electrochemotherapy treatment alone throughout the tested concentration range. This synergistic effect of the therapies is

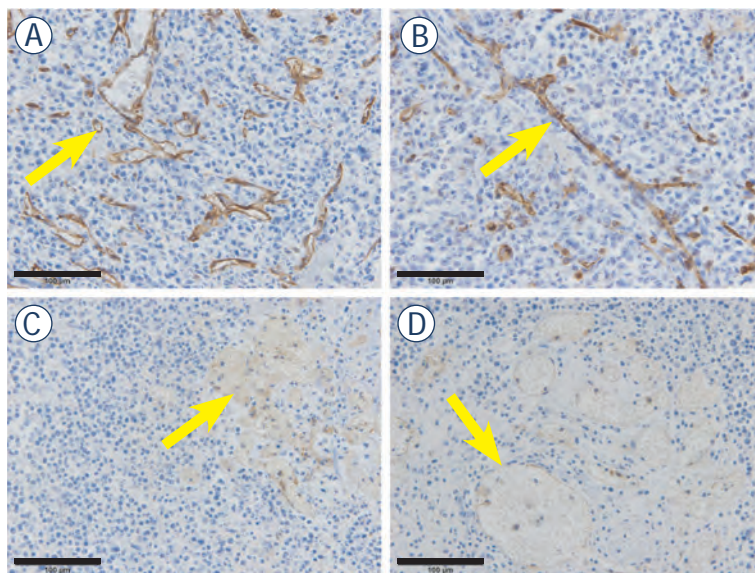


FIGURE 4. Vascular effect of different treatments. Anti-CD31 staining of tumour sections in tumours 24 h after different treatments at 40x magnification. (A) A typical tumour blood vessels network with thin vessels walls consisting only of endothelial cells was observed after CDDP alone (arrow). (B) After electrochemotherapy vasoconstriction of blood vessels was observed (arrow). (C) Dilated tumour vessels with stacked erythrocytes were observed after combination of TNF- α and CDDP (arrow). (D) After combination of TNF- α and electrochemotherapy only few large dilated blood vessels with mostly hyperaemic and occasionally damaged blood vessels were observed. (A) – CDDP; (B) – electrochemotherapy; (C) – TNF- α and CDDP; (D) – TNF- α and electrochemotherapy). Scale bar 100 μ m.

supported by the fact that only the tumours in combined modality protocol were cured and tumours treated with electrochemotherapy alone were not. Namely, after combined treatment of TNF- α and electrochemotherapy with 6 mg/kg CDDP, 2 mice (9.5%) were cured, and after combined treatment of TNF- α and electrochemotherapy with 8 mg/kg CDDP, 1 mouse (4.3%) was cured.

Discussion

In the study, the antitumour effectiveness of TNF- α combined with electrochemotherapy with intravenous CDDP was evaluated in murine fibrosarcoma tumour model. Adjuvant immunotherapy with TNF- α preceding electrochemotherapy, increased antitumor effectiveness of electrochemotherapy with intravenous CDDP. Prolonged tumour growth and increased tumour curability were observed after combined treatment with TNF- α and electrochemotherapy with intravenous CDDP. The underlying mechanism is most likely vascular targeted effect of TNF- α combined with its immunomodulatory effect, as previously proposed for

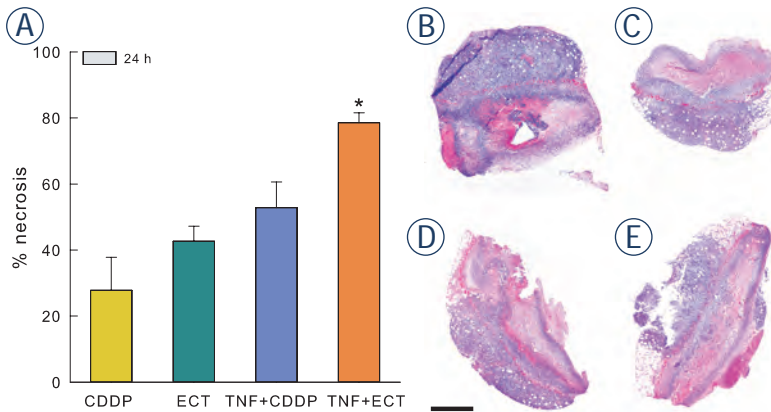


FIGURE 5. Percentage of necrosis in tumours 24 h after different treatments. (A) Increased percentage of necrotic tumour area was observed 24 h after treatment with combination of TNF- α and electrochemotherapy. (B-E) Haematoxylin and eosin staining of tumour sections in tumours 24 h after different treatments at 4x magnification. (B) – CDDP; (C) – electrochemotherapy; (D) – TNF- α and CDDP; (E) – TNF- α and electrochemotherapy. Scale bar 1 mm. Bars represent mean \pm SEM. * $p < 0.05$ vs. CDDP, ECT, and TNF + CDDP.

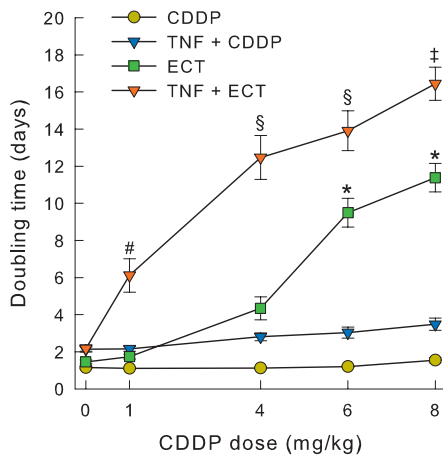


FIGURE 6. *In vivo* application of TNF- α and electrochemotherapy with different CDDP doses. Tumour doubling times after treatment with TNF- α and electrochemotherapy with different doses of CDDP were increased in comparison to electrochemotherapy alone. Symbols represent mean \pm SEM. * $p < 0.05$ vs. EP, ECT 1 mg/kg and ECT 4 mg/kg; # $p < 0.05$ vs. TNF- α + EP; § $p < 0.05$ vs. TNF- α + EP and TNF- α + ECT 1 mg/kg; ‡ $p < 0.05$ vs. TNF- α + EP and TNF- α + ECT 1-4 mg/kg.

combination with electrochemotherapy with bleomycin.¹⁶

Electrochemotherapy gained clinical recognition in the treatment of cutaneous tumours or metastases as well as deep-seated tumours.^{2-4,6-11} Currently, bleomycin is the drug of choice for majority of the electrochemotherapy treatments, although CDDP is also in Standard Operating Procedures, but only if applied intratumoural. CDDP applied intravenously has not been recognized to be sufficiently

effective.¹ However, this was based on a report where EP were applied on large tumours that were not expected to respond to systemic chemotherapy in metastatic melanoma patients.¹³ Due to the size of these treated tumours (the longest diameter of tumours mainly exceeded 3 cm) the response was not comparable to bleomycin data, where predominantly tumours less than 3 cm in diameter were treated.²⁰⁻²³ Nevertheless, it is expected that with time CDDP will gain recognition, predominantly in such situations as in the first study¹³, or when its effectiveness could be potentiated with adjuvant treatment.

Recently, it was demonstrated that tumours larger than 3 cm in size have lower response rate after single electrochemotherapy treatment than smaller ones.^{22,24,25} Furthermore, in preclinical studies, it was shown that electrochemotherapy with bleomycin induces immunological cell death¹⁶, providing additional rationale for combination with immunotherapy. Therefore, one way to potentiate electrochemotherapy effectiveness is adjuvant immunotherapy using different cytokines, such as interleukin 2 and 12, granulocyte-monocyte colony stimulating factor, and TNF- α .²⁶⁻³⁰ All these studies have provided evidence that electrochemotherapy with bleomycin can be potentiated with adjuvant immunotherapy, demonstrating increased tumour growth delay as well as tumour curability. It was already demonstrated that electrochemotherapy with bleomycin can be effectively potentiated in sarcoma model by TNF- α ³⁰, however, combination of electrochemotherapy with CDDP with adjuvant immunotherapy has not been tested yet.

TNF- α is a well-known pro-inflammatory cytokine with a wide range of biological functions, including an immunomodulatory role and anti-vascular action.^{17,18} Due to its side effects, its intravenous administration is not recommended³¹, therefore we decided to use intratumoural route and combined it with electrochemotherapy with intravenous CDDP administration.

Our results demonstrated potentiation of antitumour effectiveness of electrochemotherapy in combination with TNF- α *in vivo*. A synergistic interaction between TNF- α and electrochemotherapy with intravenous CDDP administration was observed. This synergistic interaction cannot be attributed to TNF- α cytotoxicity to tumour cells due to the lack of the effect *in vitro*. Contrary to early speculations of TNF- α cytotoxic action on malignant cells in animal tumour models, it is now accepted that TNF- α is weakly cytotoxic to malignant cells.³² Our *in vitro* results support this, as no cytotoxic effect of TNF- α

alone or in combination with electric pulses on SA-1 fibrosarcoma cells was observed. Similarly, no cytotoxic effect of TNF- α in combination with EP for electrochemotherapy was observed in our previous study.³⁰ Therefore, it is more likely that cell types other than tumour cells, such as endothelial cells or immune cells found in the tumour stroma are responsible for the observed antitumour effect.

In vivo, two distinct and successive effects of TNF- α on tumour-associated vasculature are known. Firstly, TNF- α increases vascular endothelium permeability, resulting in reduction of interstitial fluid pressure and improved penetration of chemotherapeutic agents within the tumour tissue, and secondly, TNF- α causes tumour vessel destruction.³³⁻³⁶ The mechanism whereby these events occur involves rapid perturbation of cell-cell adhesive junctions, leading to loss of intercellular adhesion, and inhibition of $\alpha\text{v}\beta\text{3}$ integrin signalling in tumour-associated vessels.³⁶ Specifically, it selectively damages the integrity of tumour vasculature by disrupting VE-cadherin complexes and thus creates gaps between endothelial cells.³⁷ In addition, the expression of TNF- α receptors is speculated to be up-regulated in tumour vessels in comparison to normal vessels, which makes tumour blood vessels specific targets for TNF- α treatment.³⁸ Binding of TNF- α to its receptors on endothelial cells triggers apoptosis and leads to hyperpermeability of the tumour blood vessels, and extravasation of blood cells.³⁸ In our study, anti-vascular action of TNF- α was confirmed by histological analysis of tumour sections. TNF- α treatment damaged existing blood vessels, resulting in weak anti-CD31 staining. In addition, number of functional blood vessels was significantly reduced after exposure to TNF- α . Blood vessels were dilated with stacked erythrocytes. This effect was even more pronounced after TNF- α combined with electrochemotherapy, where also extravasated erythrocytes were observed. In addition, overall platinum content in tumours was increased 24 h after treatment with TNF- α compared to tumours treated with CDDP alone indicating facilitated uptake of CDDP in TNF- α treated tumours. This correlates well with other studies where improved penetration and increased uptake of anticancer drugs was observed in combination with TNF- α .^{39,40}

Taken together, our results indicate indirect antitumour action of adjuvant TNF- α in SA-1 fibrosarcoma tumours treated with ECT with low CDDP doses. This antitumour action of TNF- α is likely due to hyperpermeability of tumour blood vessels, leading also to increased accumulation of

CDDP in the tumours. Based on these results, we speculate that the mechanism of action of adjuvant TNF- α in electrochemotherapy treated tumours is primarily through a vascular action. Nonetheless, especially at higher CDDP doses, at which tumour cures were obtained, involvement of activated immune response should be taken into account. Namely, in clinical settings, induction of inflammatory response after TNF- α based isolated limb perfusion was observed in the tumour tissue.³⁶ However, involvement of non-immunological antitumour mechanism of TNF- α is also supported by our previous study, where we showed antitumour effect of TNF- α also in immunosuppressed mice.⁴¹ Indeed, in our study, we did not detect the significant infiltration of immune cells into the tumours in histological section, most probably due to the early time of tumours excision after the therapy. Namely, the vascular effect of TNF- α is rapid, while immune adaptive response of the organisms needs the time to develop. Nevertheless, tumour curability after the combined treatment should be attributed to the involvement of adaptive immune system. We speculate that by replacing the recombinant TNF- α with local TNF- α gene therapy, which would result in longer persistence of therapeutic TNF- α concentrations in organism, the immunological components of the synergistic effect would account for higher curability rate.

In conclusion, adjuvant intratumoural TNF- α therapy synergistically contributes to electrochemotherapy with intravenous CDDP administration. Due to its potentiation at all doses of CDDP, the combined treatment is predicted to be effective also in less perfused areas of tumours, where the drug accumulation is not optimal, or in bigger tumours, where the effectiveness of electrochemotherapy with intravenous CDDP is not expected to be sufficiently effective. Its synergistic effectiveness can be attributed to actions of TNF- α ; vascular and also immunomodulatory, that could be further potentiated by replacing the injection of recombinant TNF- α protein with application of gene therapy with TNF- α .

Acknowledgements

This work was financially supported by Slovenian Research Agency (program P3-0003, projects J3-4259, J3-6796 and J3-6793). The research was conducted within the scope of EBAM European Associated Laboratory (LEA) and COST Action TD1104.

References

- Marty M, Sersa G, Garbay J, Gehl J, Collins C, Snoj M, et al. Electrochemotherapy – An easy, highly effective and safe treatment of cutaneous and subcutaneous metastases: Results of ESOPE (European Standard Operating Procedures of Electrochemotherapy) study. *EJC Suppl* 2006; **4**: 3-13.
- Mali B, Jarm T, Snoj M, Sersa G, Miklavcic D. Antitumor effectiveness of electrochemotherapy: A systematic review and meta-analysis. *EJSO* 2013; **39**: 4-16.
- Testori A, Tosti G, Martinoli C, Spadola G, Cataldo F, Verrecchia F, et al. Electrochemotherapy for cutaneous and subcutaneous tumor lesions: A novel therapeutic approach. *Dermatol Ther* 2010; **23**: 651-61.
- Soden DM, Larkin JO, Collins CG, Tangney M, Aarons S, Piggott J, et al. Successful application of targeted electrochemotherapy using novel flexible electrodes and low dose bleomycin to solid tumours. *Cancer Lett* 2006; **232**: 300-10.
- Mahmood F, Gehl J. Optimizing clinical performance and geometrical robustness of a new electrode device for intracranial tumor electroporation. *Bioelectrochem* 2011; **81**: 10-6.
- Agerholm-Larsen B, Iversen HK, Ibsen P, Moller JM, Mahmood F, Jensen KS, et al. Preclinical validation of electrochemotherapy as an effective treatment for brain tumors. *Cancer Res* 2011; **71**: 3753-62.
- Edhemovic I, Gadzjev EM, Breclj E, Miklavcic D, Kos B, Zupanic A, et al. Electrochemotherapy: a new technological approach in treatment of metastases in the liver. *Technol Cancer Res T* 2011; **10**: 475-85.
- Linnert M, Iversen HK, Gehl J. Multiple brain metastases - current management and perspectives for treatment with electrochemotherapy. *Radiol Oncol* 2012; **46**: 271-8.
- Fini M, Salamanna F, Parrilli A, Martini L, Cadossi M, Maglio M, et al. Electrochemotherapy is effective in the treatment of rat bone metastases. *Clin Exp Metastasis* 2013; **30**: 1033-45.
- Fini M, Tschon M, Ronchetti M, Cavani F, Bianchi G, Mercuri M, et al. Ablation of bone cells by electroporation. *J Bone Joint Surg BR* 2010; **92**: 1614-20.
- Edhemovic I, Breclj E, Gasljevic G, Marolt Music M, Gorjup V, Mali B, et al. Intraoperative electrochemotherapy of colorectal liver metastases. *J Surg Oncol* 2014; **110**: 320-7.
- Sersa G, Stabuc B, Cemazar M, Jancar B, Miklavcic D, Rudolf Z. Electrochemotherapy with cisplatin: potentiation of local cisplatin antitumor effectiveness by application of electric pulses in cancer patients. *Eur J Cancer* 1998; **34**: 1213-8.
- Sersa G, Stabuc B, Cemazar M, Miklavcic D, Rudolf Z. Electrochemotherapy with cisplatin: The systemic antitumor effectiveness of cisplatin can be potentiated locally by the application of electric pulses in the treatment of malignant melanoma skin metastases. *Melanoma Res* 2000; **10**: 381-85.
- Cemazar M, Miklavcic D, Vodovnik L, Jarm T, Rudolf Z, Stabuc B, et al. Improved therapeutic effect of electrochemotherapy with cisplatin by intratumoral drug administration and changing of electrode orientation for electropermeabilization on EAT tumors in mice. *Radiol Oncol* 1995; **29**: 121-27.
- Jarm T, Cemazar M, Miklavcic D, Sersa G. Antivasular effects of electrochemotherapy: implications in treatment of bleeding metastases. *Expert Rev Anticancer Ther* 2010; **10**: 729-46.
- Calvet CY, Famin D, Andre FM, Mir LM. Electrochemotherapy with bleomycin induces hallmarks of immunogenic cell death in murine colon cancer cells. *Oncoimmunology* 2014; **3**: e28131.
- Goetz FW, Planas JV, MacKenzie S. Tumor necrosis factors. *Dev Comp Immunol* 2004; **28**: 487-97.
- Mocellin S, Rossi CR, Pilati P, Nitti D. Tumor necrosis factor, cancer and anti-cancer therapy. *Cytokine Growth F R* 2005; **16**: 35-53.
- Cemazar M, Miklavcic D, Scancar J, Dolzan V, Golouh R, Sersa G. Increased platinum accumulation in SA-1 tumour cells after in vivo electrochemotherapy with cisplatin. *Brit J Cancer* 1999; **79**: 1386-91.
- Campana LG, Mali B, Sersa G, Valpione S, Giorgi CA, Strojjan P, et al. Electrochemotherapy in non-melanoma head and neck cancers: a retrospective analysis of the treated cases. *Br J Oral Maxillofac Surg* 2014; **52**: 957-64.
- Campana LG, Valpione S, Falci C, Mocellin S, Basso M, Corti L, et al. The activity and safety of electrochemotherapy in persistent chest wall recurrence from breast cancer after mastectomy: a phase-II study. *Breast Cancer Res Tr* 2012; **134**: 1169-78.
- Campana LG, Mocellin S, Basso M, Puccetti O, De Salvo GL, Chiarion-Sileni V, et al. Bleomycin-based electrochemotherapy: Clinical outcome from a single institution's experience with 52 patients. *Ann Surg Oncol* 2009; **16**: 191-99.
- Campana LG, Valpione S, Mocellin S, Sundararajan R, Granziera E, Sartore L, et al. Electrochemotherapy for disseminated superficial metastases from malignant melanoma. *Brit J Surg* 2012; **99**: 821-30.
- Mali B, Miklavcic D, Campana LG, Cemazar M, Sersa G, Snoj M, et al. Tumor size and effectiveness of electrochemotherapy. *Radiol Oncol* 2013; **47**: 32-41.
- Quagliano P, Mortera C, Osella-Abate S, Barberis M, Illengo M, Rissone M, et al. Electrochemotherapy with intravenous bleomycin in the local treatment of skin melanoma metastases. *Ann Surg Oncol* 2008; **15**: 2215-22.
- Sedlar A, Dolinsek T, Markelc B, Prosen L, Kranjc S, Bosnjak M, et al. Potentiation of electrochemotherapy by intramuscular IL-12 gene electrotransfer in murine sarcoma and carcinoma with different immunogenicity. *Radiol Oncol* 2012; **46**: 302-11.
- Heller L, Pottinger C, Jaroszeski MJ, Gilbert R, Heller R. In vivo electroporation of plasmids encoding GM-CSF or interleukin-2 into existing B16 melanomas combined with electrochemotherapy induces long-term antitumor immunity. *Melanoma Res* 2000; **10**: 577-83.
- Torrero MN, Henk WG, Li S. Regression of high-grade malignancy in mice by bleomycin and interleukin-12 electrochemogenetherapy. *Clin Cancer Res* 2006; **12**: 257-63.
- Ramirez LH, Orłowski S, An D, Bindoula G, Dzodic R, Ardouin P, et al. Electrochemotherapy on liver tumours in rabbits. *Brit J Cancer* 1998; **77**: 2104-11.
- Sersa G, Cemazar M, Menart V, Gaberc-Porekar V, Miklavcic D. Anti-tumor effectiveness of electrochemotherapy with bleomycin is increased by TNF- α on SA-1 tumors in mice. *Cancer Lett* 1997; **116**: 85-92.
- Roberts NJ, Zhou S, Diaz LA, Jr, Holdhoff M. Systemic use of tumor necrosis factor alpha as an anticancer agent. *Oncotarget* 2011; **2**: 739-51.
- Balkwill F. Tumour necrosis factor and cancer. *Nat Rev Cancer* 2009; **9**: 361-71.
- Eisenthal A, Schwartz I, Issakov J, Klausner Y, Misonzhnik F, Lifschitz-Mercer B. Immunohistochemistry evaluation of the effect in vivo of tumor necrosis factor (TNF)- α on blood vessel density in murine fibrosarcoma. *Sarcoma* 2003; **7**: 57-61.
- Nooijen PT, Manusama ER, Eggermont AM, Schalkwijk L, Stavast J, Marquet RL, et al. Synergistic effects of TNF- α and melphalan in an isolated limb perfusion model of rat sarcoma: a histopathological, immunohistochemical and electron microscopical study. *Brit J Cancer* 1996; **74**: 1908-15.
- Kristensen CA, Nozue M, Boucher Y, Jain RK. Reduction of interstitial fluid pressure after TNF- α treatment of three human melanoma xenografts. *Brit J Cancer* 1996; **74**: 533-6.
- Lejeune FJ, Lienard D, Matter M, Ruegg C. Efficiency of recombinant human TNF in human cancer therapy. *Cancer Immunity* 2006; **6**: 6.
- Menon C, Ghartey A, Canter R, Feldman M, Fraker DL. Tumor necrosis factor- α damages tumor blood vessel integrity by targeting VE-cadherin. *Ann Surg* 2006; **244**: 781-91.
- van Horssen R, Ten Hagen TL, Eggermont AM. TNF- α in cancer treatment: molecular insights, antitumor effects, and clinical utility. *Oncologist* 2006; **11**: 397-408.
- Folli S, Pelegri A, Chalandon Y, Yao X, Buchegger F, Lienard D, et al. Tumor necrosis factor can enhance radio-antibody uptake in human colon carcinoma xenografts by increasing vascular permeability. *Int J Cancer* 1993; **53**: 829-36.
- de Wilt JHW, ten Hagen TLM, de Boeck G, van Tiel ST, de Bruijn EA, Eggermont ANM. Tumour necrosis factor alpha increases melphalan concentration in tumour tissue after isolated limb perfusion. *Brit J Cancer* 2000; **82**: 1000-3.
- Sersa G, Willingham V, Milas L. Anti-Tumor Effects of Tumor Necrosis Factor Alone or Combined with Radiotherapy. *Int J Cancer* 1988; **42**: 129-34.

Mild hyperthermia influence on Herceptin[®] properties

Jean-Michel Escoffre, Roel Deckers, Noboru Sasaki, Clemens Bos, Chrit Moonen

Imaging Division, UMC Utrecht, Utrecht, the Netherlands

Radiol Oncol 2015; 49(1): 41-49.

Received 17 August 2014
Accepted 24 October 2014

Correspondence to: Jean-Michel Escoffre, University Medical Center Utrecht, Imaging Division, Heidelberglaan 100, 3584 CX Utrecht, the Netherlands. Phone: +31(0)88 756 9665; Fax: +31(0)88 755 5850; E-mail: j.r.escoffre@umcutrecht.nl and Clemens Bos, University Medical Center Utrecht, Imaging Division, 3584 CX Utrecht, the Netherlands. E-mail: c.bos@umcutrecht.nl

Disclosure: No potential conflicts of interest were disclosed.

Background. Mild hyperthermia (mHT) increases the tumor perfusion and vascular permeability, and reduces the interstitial fluid pressure, resulting in better intra-tumoral bioavailability of low molecular weight drugs. This approach is potentially also attractive for delivery of therapeutic macromolecules, such as antibodies. Here, we investigated the effects of mHT on the stability, immunological and pharmacological properties of Herceptin[®], a clinically approved antibody, targeting the human epidermal growth factor receptor 2 (HER-2) overexpressed in breast cancer.

Results. Herceptin[®] was heated to 37°C (control) and 42°C (mHT) for 1 hour. Formation of Herceptin[®] aggregates was measured using Nile Red assay. mHT did not result in additional Herceptin[®] aggregates compared to 37°C, showing the Herceptin[®] stability is unchanged. Immunological and pharmacological properties of Herceptin[®] were evaluated following mHT using HER-2 positive breast cancer cells (BT-474). Exposure of Herceptin[®] to mHT preserved recognition and binding affinity of Herceptin[®] to HER-2. Western-blot and cell proliferation assays on BT-474 cells showed that mHT left the inhibitory activities of Herceptin[®] unchanged.

Conclusions. The stability, and the immunological and pharmacological properties of Herceptin[®] are not negatively affected by mHT. Further *in-vivo* studies are required to evaluate the influence of mHT on intra-tumoral bioavailability and therapeutic effectiveness of Herceptin[®].

Key words: mild hyperthermia; anticancer antibody; Herceptin[®]; breast cancer

Introduction

Breast cancer is the first most common cancer (464,000 cases in 2012) and is the third cause of death from cancer for women (131,000 in 2012) in Europe.¹ In 25% to 30% of breast cancer, human epidermal growth factor receptor 2 (HER-2) is amplified and overexpressed, which is associated with poor prognostic factors as shown by its highly proliferative and often high-grade histology.^{2,3} Moreover, women with HER-2 positive breast cancer are more likely to develop visceral and central nervous system metastases than those with HER-2 negative breast cancer.⁴ Activation of HER-2 receptors triggers several signaling pathways including phosphoinositide 3-kinase (PI3K) and mitogen-ac-

tivated protein kinase (MAPK) cascades which are intricately involved in multiple processes of breast cancer pathogenesis.⁵

Over the past decades, advances in pharmaceutical research have led to the development of therapeutic monoclonal antibodies (mAbs) which are able to discriminate between healthy and malignant tissue, unlike most conventional cancer treatments.⁶ FDA and EMEA have approved many mAbs for treating hematological malignancies (*e.g.*, Zevalin[®], Rituxan[®]) and solid tumors (*e.g.*, Erbitux[®], Vectibix[®]) for clinical use. Among these antibodies, Herceptin[®] is a clinically approved mAb for treating HER-2 positive breast cancer that specifically binds to the juxtamembrane portion of the extracellular domain of HER-2 receptors. Herceptin[®] exerts its

antitumor effect by two main mechanisms: (i) The Herceptin® binding to the HER-2 receptors induces the internalization and the degradation of HER-2 receptors, therefore inhibiting the phosphorylation of HER-2 receptors.^{7,8} Thus, the PI3K and MAPK signaling pathways are deactivated, promoting cell cycle arrest and apoptosis. (ii) Herceptin® triggers an ADCC (antibody-dependent cellular cytotoxicity) immune response.^{9,10} Furthermore, Herceptin® may suppress tumor neo-angiogenesis by modulating the effects of pro- and anti-angiogenic factors.¹¹ In clinical trials, Herceptin® has shown to decrease mortality in patients with early HER-2 positive and metastatic breast cancer, either as a monotherapy¹² or combined with chemotherapy¹³⁻¹⁵ or with radiotherapy.^{16,17}

Nevertheless, Herceptin®-based immunotherapy, as well as other mAb anticancer treatments, is rarely curative in solid tumors. This is most probably related to their poor intratumoral (i.t.) bioavailability that is compensated for by administration of high or frequent mAb doses to achieve therapeutic effectiveness. These therapeutic doses are given systemically and are associated with undesirable side effects (*e.g.*, cardiotoxicity).¹⁸ The physico-chemical properties of mAbs, as well as the physiological barriers of tumors, limit the success of this approach for treating solid tumors.¹⁹ The large size of mAbs (≈ 150 kDa) does provide a convenient and long circulatory half-life ($t_{1/2} > 21$ days in humans for Herceptin®), but on the other hand restricts its extravasation from the tumor microvasculature, as well as its penetration into tumor interstitium.¹⁹⁻²² To overcome these limitations, the development of efficient delivery methods is required to increase the local concentration of Herceptin® at the desired site while minimizing side effects to healthy tissues.

Mild hyperthermia (41°C – 43°C for 30–60 min) shows great promise in improving the therapeutic effectiveness of drugs by acting on tumor hemodynamics: (i) increasing blood flow, thus increasing drug bioavailability in tumors²³⁻²⁵; (ii) increasing vascular permeability and reducing interstitial fluid pressure, resulting in better drug penetration.^{12,15,26-29} Nowadays, mild hyperthermia (mHT) remains modestly explored as method for improving the i.t. bioavailability of full intact mAbs, such as Herceptin®. Additive or synergetic effects of mHT on mAbs delivery have been successfully reported for mAb fragments²⁸ and reactive haptens with bi-functional mAb fragments.³⁰ In addition, mHT enhanced antigen (Ag) expression, thus enhancing specific binding and retention of mAbs

in tumors.^{31,32} Therefore, mHT may not only improve the i.t. bioavailability of intact mAbs, such as Herceptin®, but also increases the number of binding sites.

However, hyperthermia is known to induce protein aggregation. Indeed, therapeutic proteins, such as mAbs, are physico-chemically unstable and aggregation is one of the key features compromising their physical stability.³³ As previously reported, protein aggregation induces a reduction or loss in biological activity, leading to a decrease in their therapeutic potential.³⁴ Because the Herceptin® needs to be fully active when delivered to patients to be effective, the objective of the present study is to evaluate the influence of mHT on the activation of Herceptin®. Herein, we report on a study of the influence of mHT on the stability, and the immunological and pharmacological properties of Herceptin®. Our methodology, including molecular biology and immunological techniques, addresses the following questions: (i) Does mHT induce Herceptin® aggregation, thus leading to a loss of anticancer activity? (ii) Are the recognition and the affinity of Herceptin® to HER-2 receptors modified by mHT? (iii) Does mHT disturb the Herceptin®-mediated HER-2 degradation and dephosphorylation? and (iv) Are anti-proliferative properties of Herceptin® altered by mHT?

Materials and methods

Chemicals

Propidium iodide and TO-PRO®-3 iodide were purchased from Sigma-Aldrich® (St. Louis, MO) and Life Technologies™ Europe B.V. (Bleiswijk, Netherlands), respectively. Fluorescein isothiocyanate (FITC)-conjugated mouse monoclonal secondary antibody anti-human IgG1-Fc (Ab50473), rabbit polyclonal anti-HER 2 (ab2428), anti-pHER-2 (ab47263), anti-ACTIN (ab1801) antibodies and horseradish peroxidase (HRP)-conjugated goat polyclonal secondary anti-Rabbit IgG Fc (ab97200) were obtained from Abcam® (Cambridge, UK). FITC-conjugated human IgG1 isotype control (ANC-295-040) and human IgG1 isotype control (ANC-295-010) were purchased from Adipogen® International (Liestal, Switzerland).

Cell culture

BT-474, HER-2 positive breast cancer cells were derived from a human ductal carcinoma (ATCC®HTB-20™; LGC Standards GmbH, Wesel,

Germany). The cells were grown as a monolayer in Roswell Park Memorial Institute Medium (RPMI-1640; Sigma-Aldrich®) supplemented with 10% heat-inactivated fetal calf serum (FCS; Sigma-Aldrich®), 10 µg/mL human insulin (Life Technologies™ Europe B.V.), 100 U/mL penicillin and 100 µg/mL streptomycin (Sigma-Aldrich). The cells were routinely sub-cultured every 5 days and incubated at 37 °C in a humidified atmosphere with 5% CO₂.

Herceptin® & mild hyperthermia

Herceptin® was purchased from F. Hoffmann-La Roche Ltd (Pensberg, Germany) and supplied at a concentration of 21 mg/mL (*i.e.*, clinical dose), as a neutral aqueous solution (phosphate-buffered saline, PBS).³⁵ The stock solution of Herceptin® was diluted to a concentration of 0.8 mg/mL or 250 µg/mL in PBS. The diluted solution was incubated at 37°C (*i.e.*, native Herceptin®) and 42°C (*i.e.*, heated Herceptin®) for 1 h in a heat block under gentle agitation (*i.e.*, optimal mHT condition for *in-vivo* antibody delivery^{28,36}).

Antibody aggregation

As previously described, antibody aggregation was evaluated using a Nile Red assay.³³ Nile Red binds to the hydrophobic surfaces of antibodies during aggregate formation. In such a hydrophobic environment, Nile Red exhibits a strong fluorescence whereas in aqueous medium, the fluorescence is quenched. 1 µL of Nile Red solution (100 µM) was added to 100 µL Herceptin® solution (0.8 mg/mL). Subsequently, the antibody solutions were incubated at 37°C (*i.e.*, native Herceptin®), 42°C (*i.e.*, heated Herceptin®) and 90°C (*i.e.*, positive control) for 1 h in a heat block under gentle agitation.

Aggregate counting and size. Antibody sample aliquots were placed on Kova Glasstic slides (Hycor, Garden Grove, USA) and observed using a Keyence BZ-900 fluorescence microscope (Keyence International, Mechelen, Belgium) with a 40× Plan Fluor EL objective (0.6 NA, Ph1). Microscopic images were processed with ImageJ software version 1.42q (NIH, Bethesda, USA).³³ Briefly, microscopic images were first converted to 8-bit grayscale images. Subsequently, the images were calibrated using the “Set Scale” command. An intensity-based threshold was applied manually to delineate the antibody aggregates. A mask was then computed the following magnitudes in the mask were collected with “Analyze Particles” command: number

of aggregates, area and mean fluorescent intensity of aggregate. Data were presented as mean ± standard deviation (SD) from five independent experiments.

Fluorescence measurements. Herceptin® sample aliquots were placed in 96-well plates and the fluorescence was measured by a FLUOstar OPTIMA (BMG Labtech GmbH, Ortenberg, Germany). The antibody aggregation was determined by measuring the intensity of Nile Red fluorescence (Excitation wavelength: 550 ± 10 nm; Emission wavelength: 615 ± 10 nm). Data were presented as mean ± SD from five independent experiments.

Recognition of HER-2 receptors by Herceptin®

The recognition of HER-2 receptors by Herceptin® was assessed by indirect immunofluorescence using confocal microscopy and flow cytometry.

Confocal fluorescence microscopy. BT-474 cells were seeded on a glass coverslip chamber (Ibidi® LLC, Verona, WI) 48 hrs before the immunofluorescence staining. They were washed with ice-cold PBS with Ca²⁺/Mg²⁺ and fixed with 4% paraformaldehyde (Sigma-Aldrich®) in PBS for 10 min at 4°C under gentle agitation. Subsequently, cells were washed twice with cold PBS with Ca²⁺/Mg²⁺ and incubated with PBS supplemented with 2% FCS (PBS-2% FCS) for 20 min at 4°C under gentle agitation (200 rpm). After two additional washing steps with PBS-2% FCS, they were incubated in PBS-2% FCS with native and heated Herceptin®, or human IgG1 isotype control (10 µg/mL), for 1 h at 4°C under gentle agitation. Cells were then washed twice and incubated in the dark for 30 min at 4°C under gentle agitation, with a FITC-conjugated secondary antibody diluted in PBS-2% FCS. Subsequently, cells were washed twice and resuspended in 0.6 mL PBS-2% FCS containing TO-PRO®-3 (1 µM; Life Technologies™) used to localize cell nuclei. The chamber was mounted on the Zeiss LSM 510 live-cell imaging station stage equipped with a 32 PMT meta-detector (Carl Zeiss, MicroImaging GmbH, Gottingen, Germany) and Plan-Apochromat 63× Zeiss objective (1.4 NA, oil immersion). Fifteen different images per experimental condition were acquired (Zen 2008 software, Carl Zeiss) to observe FITC-labeled plasma membrane (excitation laser: 488 nm; emission filter: BP 505-530 nm) and TO-PRO®-3 stained nuclei (excitation laser: 633 nm; emission filter: LP 650 nm). Images of cells were analyzed with the “Measure” and “Cell counter” functions of ImageJ software. The total number of

HER-2 positive breast cancer cells and the associated fluorescence intensity were determined for each image (N = 400 cells/experimental condition). Data were presented as mean \pm SD from three independent experiments.

Flow cytometry: BT-474 cells were harvested using 2 mM EDTA in PBS, washed with cold PBS solution and incubated in PBS-2% FCS for 20 min at 4°C under gentle agitation. Subsequently, cells were centrifuged (150 g, 5 min, 4°C) and washed twice with PBS-2% FCS. The cells were then incubated in PBS-2% FCS with native or heated Herceptin® (10 μ g/mL) for 1 h at 4°C under gentle agitation. Human IgG1 isotype control (10 μ g/mL) was used as nonbinding antibody control. After two additional washing steps, cells were incubated with FITC-conjugated anti-human IgG1-Fc antibody diluted in PBS-2% FCS in the dark, for 30 min at 4°C under gentle agitation. Cells were then washed twice and resuspended in 0.4 mL of PBS-2% FCS containing propidium iodide (0.1 μ g/mL; Sigma-Aldrich®) to stain dead cells. Dot plots were recorded using the BD FACSCanto II flow cytometer (BD Biosciences, Breda, Netherlands) and analyzed using the BD FACS Diva software (v6.1.3., BD Biosciences) supplied by the manufacturer. A minimum of 10,000 events were analyzed to generate each dot plot. Data were presented as mean \pm SD from three independent experiments.

Affinity binding of Herceptin® to HER-2 receptors

BT-474 cells (1.5×10^5) were washed with ice-cold PBS and harvested. The cells were then incubated with unconjugated native or heated Herceptin® (5×10^{-6} to 5×10^{-2} mg/mL) in PBS-2% FCS for 30 min at 4°C under gentle agitation. They were then washed twice with PBS-2% FCS, centrifuged (150 g, 5 min, 4°C) and further incubated with FITC-conjugated Herceptin® or isotype control antibody (5 μ g/mL) for 30 min at 4°C under gentle agitation. After two additional washing steps, the samples were resuspended in 0.4 mL of PBS-2% FCS. Fluorescence intensity was recorded using the BD FACSCanto II flow cytometer and analyzed using the BD FACS Diva software. A minimum of 10,000 events were analyzed to generate each fluorescence histogram. The gate was arbitrarily set for the detection of FITC fluorescence. Data were presented as mean \pm SD from three independent experiments and are fitted with Variable slope model with a 95% confidence interval (GraphPad Prism 6 Software, version 6.01, La Jolla, USA).

Assessment of total and phosphorylated HER-2 receptor levels

BT-474 cells were seeded in 6-well culture plates at 4×10^5 cells per well and grown overnight at 37°C in a humidified atmosphere using a 5% CO₂ incubator. The medium was then removed and cells were washed twice with ice-cold PBS and incubated with or without Herceptin® (50 μ g/mL of native or heated antibody). Six days later, the cells were washed twice with ice-cold PBS and lysed with 200 μ L RIPA buffer (R0278; Sigma-Aldrich®) supplemented with Protease Inhibitor Cocktail (P8340; Sigma-Aldrich®) and Phosphatase Inhibitor Cocktail 2 (P5726; Sigma-Aldrich®) for 10 min at 4°C. Subsequently, protein lysates were collected with a cell scraper and centrifuged at 12,000 g for 15 min. For each sample, the supernatant containing the cell proteins was recovered and protein concentration was determined using the BCA Protein Assay according to manufacturer's instructions (23225; Thermo Fisher Scientific, Etten-Leur, The Netherlands).

Protein samples (10 μ g/well) were separated by 4-12% Bis-Tris gel (NuPAGE® Novex®; Life Technologies™) electrophoresis and transferred onto nitrocellulose membranes (IB3010-02; Life Technologies™) by electroblotting (iBlot® Dry Blotting System; Life Technologies™). Membranes were incubated with 5% bovine serum albumin (BSA, Sigma-Aldrich®) in Tris Buffered Saline - Tween solution (TBST; 20 mM Tris, 150 mM NaCl, 0.1% Tween 20, pH 7.6) for 1 h at room temperature (*i.e.*, to block nonspecific binding) under gentle rolling agitation. Blots were washed once with TBST for 15 min and twice for 5 min under gentle rolling agitation. They were then incubated with either anti-HER-2 (1:10000 dilution) or anti-pHER-2 (1:25000 dilution) or anti-ACTIN (*i.e.*, to control equal protein loading; 1:10000 dilution) antibodies in 1% BSA-TBST overnight at 4°C under gentle rolling agitation. The blots were washed thrice for 5 min under gentle rolling agitation. They were then incubated with HRP-conjugated secondary antibody (1:5000 dilution) for 1 h at room temperature under gentle rolling agitation. After additional washing steps, the membranes were developed using Lumi-Light Western Blotting Substrate (Roche Diagnostic Nederland, B.V. Almere, Netherlands) according to the manufacturer's instructions and visualized using the ChemiDoc™ XRS detection system (Bio-Rad Laboratories B.V., Veenendaal, The Netherlands). Relative densities of HER-2 receptor, phosphorylated HER-2 receptor and

ACTIN were measured using densitometric analysis of western-blots with the “Gels” function of ImageJ software. HER-2 receptor and phosphorylated HER-2 receptor were normalized to ACTIN and the fold change in HER-2 receptor and phosphorylated HER-2 receptor over the control condition was determined. Data were presented as mean \pm SD from three independent experiments.

Cell proliferation

BT-474 cells were seeded in 96-well culture plates at 1.5×10^4 cells per well. The following day, cells were incubated with control and heated Herceptin® (1×10^{-8} to 5×10^{-2} mg/mL) for 6 days at 37°C in a humidified atmosphere using a 5% CO₂ incubator. CellTiter 96® non-radioactive cell proliferation assay was carried out according to the manufacturer’s protocol (Promega Benelux B.V., Leiden, the Netherlands). Mean relative growth was expressed as a ratio of the control mean relative growth (vehicle-treated cells). Data were presented as mean \pm SD from four independent experiments and are fitted with Variable slope model with a 95% confidence interval (GraphPad Prism 6 Software).

Statistical analysis

Descriptive statistics was performed using StatPlus®:mac (version 5.8.3.8. 2001-2009 Analyst Soft Inc., Vancouver, Canada). Statistical analysis was performed using the non-parametric Mann-Whitney test. Significance was defined as $p < 0.05$ (NS, non-significant; * $p < 0.05$; ** $p < 0.01$; *** $p < 0.001$).

Results

mHT influence on Herceptin® stability

The influence of mHT on the Herceptin® stability was investigated by spectrofluorimetry and fluorescence microscopy after Nile Red staining. As shown in Figure 1A, the exposure of Herceptin® to heating at both 37°C and 42°C induced comparable fluorescence levels of Nile Red (3 ± 7 a.u. vs 2 ± 7 a.u.; $p > 0.05$), thus suggesting that similar number and/or size of antibody aggregates were formed. To validate this hypothesis, Herceptin® aggregates were observed using fluorescence microscopy (Figure 1B). The incubation of Herceptin® solution at 37°C for 1 h led to fewer (18 ± 10 aggregates/ μ L) (Figure 1C) and smaller (6 ± 4 μ m²) (Figure 1D) antibody aggregates than the positive control ($2028 \pm$

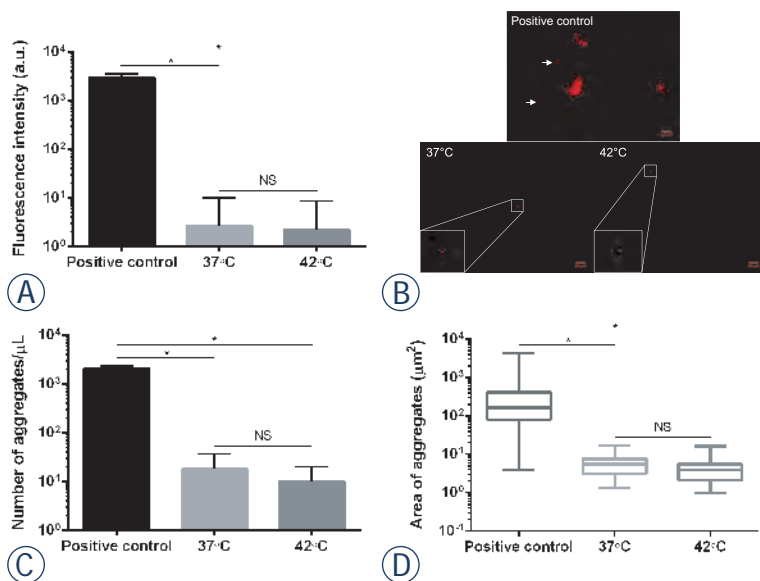


FIGURE 1. Herceptin® stability. Immediately after Nile Red addition (100 μ M), 0.8 mg/mL antibody solution was incubated at 37°C (native antibody), 42°C (heated antibody) and 90°C (positive control) for 1 h. Spectrofluorimetry was used for measuring total fluorescence signal (A), whereas fluorescence images were taken for observing Herceptin® aggregates (B). Representative images of antibody aggregates for each experimental condition are shown. Concentration (C) and area (D) of antibody aggregates are reported. Data expressed as mean \pm SD was calculated from five independent experiments. Statistical analysis was performed using the non-parametric Mann-Whitney test. Significance was defined as $p < 0.05$ (NS, non-significant; * $p < 0.05$ compared to the positive condition).

156 aggregates/ μ L, $p < 0.05$; 419 ± 59 μ m², $p < 0.05$). mHT did not significantly change the number (10 ± 5 aggregates/ μ L; $p > 0.05$) and the area (4 ± 4 μ m²; $p > 0.05$) of Herceptin® aggregates compared to incubation at physiological temperature (Figures 1C–D). These data suggest that mHT does not induce Herceptin® aggregation.

Immunological properties of heated Herceptin®

Breast ductal cancer cells, BT-474, which express high levels of HER-2 receptors and are sensitive to Herceptin® have been commonly used for *in-vitro* and *in-vivo* evaluation of Herceptin®.^{37,38} Therefore, to determine whether mHT altered the recognition of HER-2 receptors by Herceptin®, confocal fluorescence microscopy and flow cytometry analyses were performed on BT-474 cells. Confocal fluorescence images of BT-474 cells revealed a similar percentage of HER-2 positive cells ($98 \pm 2\%$ vs $99 \pm 1\%$; $p > 0.05$) and fluorescence levels ($1.3 \times 10^4 \pm 1.3 \times 10^3$ a.u. vs $1.2 \times 10^4 \pm 0.6 \times 10^3$ a.u.; $p > 0.05$), whether these cells were stained with native (*i.e.*, 37°C, 1 h) or heated (*i.e.*, 42°C, 1 h) Herceptin® (Figure 2A).

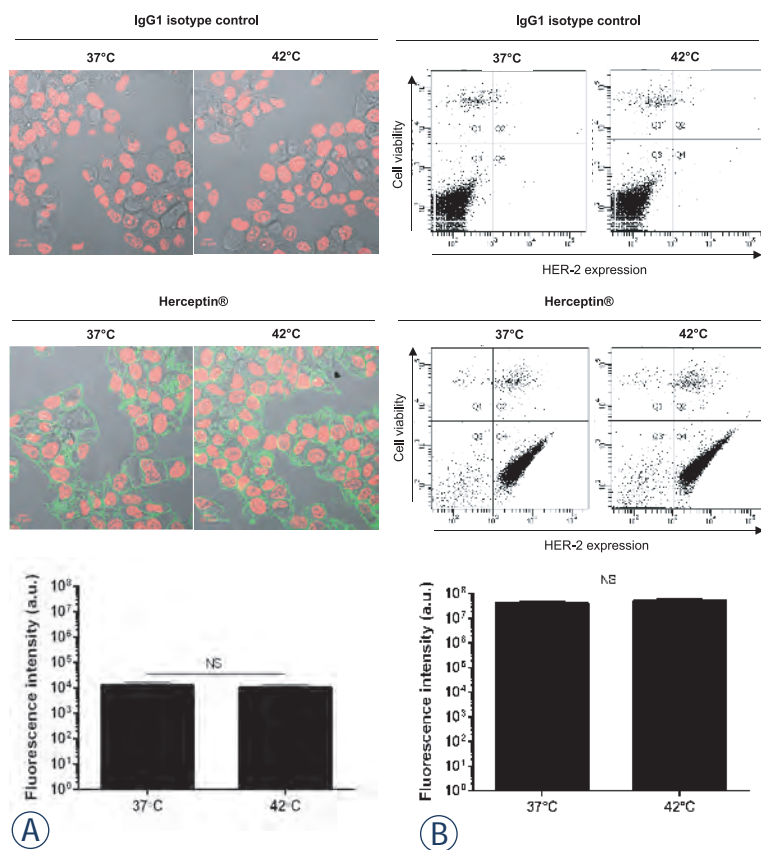


FIGURE 2. Recognition of HER-2 by Herceptin® following mHT. BT-474 cells were incubated with 10 µg/mL native or heated Herceptin®, or matched human isotype control IgG1. Subsequently, the cells were incubated with FITC-conjugated anti-human IgG1-Fc antibody and then analyzed by confocal microscopy (A) and flow cytometry (B). Representative images of BT-474 cells and dot-plots of each experimental condition are shown. Data expressed as mean ± SD was calculated from three independent experiments. Statistical analysis was performed using the non-parametric Mann-Whitney test. Significance was defined as $p < 0.05$ (NS, non-significant).

No HER-2 positive cells were detected with human IgG1 control isotype antibody. In addition, flow cytometry analyses supported these results (Figure 2B). Indeed, the dot plots of BT-474 cells were unchanged with comparable percentages of living HER-2 positive cells ($84 \pm 3\%$ vs $88 \pm 3\%$; $p > 0.05$) and fluorescence intensities ($5.8 \times 10^3 \pm 6 \times 10^2$ a.u. vs $6.1 \times 10^3 \pm 4 \times 10^2$ a.u.; $p > 0.05$) after labeling with native and heated Herceptin® (Figure 2B).

To gain insight into the effect of mHT on the immunological properties of Herceptin®, the binding affinity of this antibody to HER-2 receptors was assessed by a competition assay on BT-474 cells using FITC-coupled Herceptin®. Figure 3 indicates that low concentrations of unlabeled and native Herceptin® (*i.e.*, below 5×10^{-5} mg/mL) did not change the binding of FITC-conjugated Herceptin® to HER-2 receptors, while a concentration range

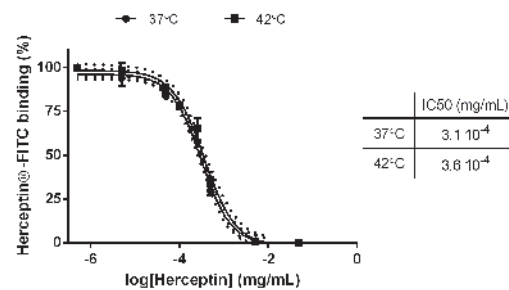


FIGURE 3. Binding affinity of Herceptin® to HER-2. BT-474 cells were first incubated with unconjugated Herceptin® (5×10^{-6} to 5×10^{-2} mg/mL) and subsequently with FITC-Herceptin®. Fluorescence intensity on flow cytometry is plotted as a function of unlabeled Herceptin® concentration used for receptor saturation. Data expressed as mean ± SD calculated from three independent experiments and are fitted with Variable slope model (solid curve: confidence intervals, dotted curve) with a 95% confidence interval. Statistical analysis was performed using the non-parametric Mann-Whitney test. Significance was defined as $p < 0.05$ (NS, non-significant).

from 1×10^{-4} mg/mL to 5×10^{-2} mg/mL of this antibody induced a significant inhibition of the binding of FITC-coupled Herceptin®. Heated Herceptin® led to a similar inhibition of FITC-conjugated Herceptin® as native Herceptin®. Moreover, native and heated Herceptin® show comparable IC50 values, *i.e.*, 3.1×10^{-4} mg/mL and 3.6×10^{-4} mg/mL ($p > 0.05$), respectively. These results indicate that mHT does not modify the recognition and the binding affinity of Herceptin® to HER-2 receptors.

Pharmacological properties of heated Herceptin®

To investigate how the binding of heated Herceptin® to HER-2 receptors affects them, their total and phosphorylated levels were monitored using western-blot assay. As expected, the exposure of BT-474 cells to native Herceptin® (50 µg/mL) resulted in significant decrease in relative densities of HER-2 receptors and phosphorylated HER-2 receptors compared to untreated cells ($p < 0.05$) (Figure 4). These results suggest that native Herceptin® leads to the internalization and the degradation of HER-2 receptors, thus preventing their phosphorylation in BT-474 cells. In addition, heated Herceptin® led to a decrease in total and phosphorylated HER-2 receptor levels that were comparable to the native Herceptin® ($p > 0.05$) (Figure 4).

Using a cell proliferation assay, the anti-proliferative effects of native and heated Herceptin® in BT-474 cells were investigated 6 days after antibody treatment. As shown in Figure 5, low native Herceptin® concentration (1×10^{-8} mg/mL – 1×10^{-5}

mg/mL) slightly affected BT-474 cell proliferation, while antibody concentrations above 1×10^{-4} mg/mL induced a significant decrease in cell proliferation. Heated Herceptin® was similarly potent in suppressing BT-474 cell proliferation (Figure 5). These results suggest that mHT has no significant effect on the anti-proliferative properties of Herceptin®.

Discussion

The present study investigated whether mHT (42°C for 1 h) influences the stability, the immunological and pharmacological properties of Herceptin® *in-vitro*. First, we showed that mHT did not result in additional Herceptin® aggregates compared to the physiological temperature (Figure 1). In agreement with published data, the low number of aggregates observed reflects the good Herceptin® stability under our mHT exposure conditions.^{33,34} Indeed, based on differential scanning calorimetry measurements, previous studies showed that only temperatures above 50°C induced significant number of antibody aggregates.³⁹ However, temperatures between 43°C and 50°C have been shown to cause edema, vascular occlusion and hemorrhage.^{40,41} Thus, the use of appropriate mHT is of great importance with respect to Herceptin® stability and tissue physiology, since the formation of antibody aggregates and tissue damage may induce loss of therapeutic activity^{42,43} and severe side effects^{39,40}, respectively. In addition, the antibody aggregation alters the immunogenicity of the therapeutic antibody. As a result, immune tolerance existing natively to self-antigens (*e.g.*, therapeutic antibodies) breaks down and aggregate-targeting antibodies are produced.⁴³ These antibodies can either have no significant consequences for the patients, or decrease the therapeutic effectiveness of the therapeutic antibodies.

Previous investigations reported that mHT has few incidences on the immunological properties.^{44,45} Indeed, Hauck *et al.* reported that no obvious effects of temperature on kinetic binding parameters of the anti-Tenascin antibody (*i.e.*, 81C6) to human glioma cells were apparent between 37°C and 45°C.⁴⁴ In agreement with these studies, we found that the exposure of Herceptin® to mHT did not modify the recognition and the binding affinity of Herceptin® to HER-2 receptors using human HER-2 positive breast cancer cells such as BT-474 (Figures 2, 3), indicating that mHT has no significant effects on the immunological properties of this therapeutic antibody. The Herceptin®

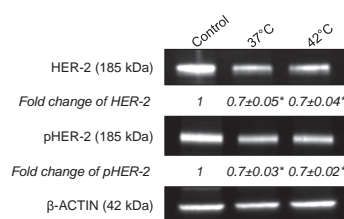


FIGURE 4. Degradation and Dephosphorylation of HER-2 receptors by Herceptin®. 4×10^5 BT-474 cells were seeded in a 6-well plate and treated with Herceptin® (50 µg/mL) for 6 days. Immunoblots of protein lysates were analyzed for total and phosphorylated HER-2 receptors. Representative immunoblots of one experiment out of three independent experiments are shown. The number at the bottom of each lane indicates the relative fold change versus the control after normalization with the β-ACTIN signal. Data expressed as mean ± SD calculated from three independent experiments. Statistical analysis was performed using the non-parametric Mann-Whitney test. Significance was defined as $p < 0.05$ (NS, non-significant; * $p < 0.05$ compared to the positive condition).

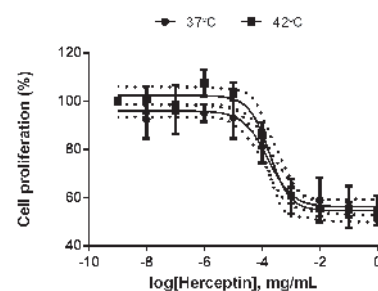


FIGURE 5. Effect of Herceptin® on BT-474 cell proliferation. BT-474 cells were seeded in a 96-well plate at 15,000 cells per well and were treated with native or heated Herceptin® (1×10^{-8} - 5×10^{-2} mg/mL) for 6 days. Cell proliferation assay was performed. The mean relative growth was expressed as a ratio of the mean control relative growth (vehicle-treated cells). Data expressed as mean ± SD calculated from four independent experiments and are fitted with Variable slope model (solid curve; confidence intervals, dotted curve) with a 95% confidence interval. Statistical analysis was performed using the non-parametric Mann-Whitney test. Significance was defined as $p < 0.05$ (NS, non-significant).

binding to HER-2 receptors is expected to induce their internalization^{7,8}, leading to their subsequent degradation.^{38,46} In agreement with these works⁴⁶, we showed that the exposure of BT-474 cells to native Herceptin® as well as heated Herceptin® led to a similar decrease in total and phosphorylated HER-2 receptor levels (Figure 4). As previously shown^{35,38}, this Herceptin®-mediated interference with the HER-2 transduction pathway results in a potent inhibition of the growth of HER-2 positive breast cancer cells (Figure 5). Finally, our data revealed that the anti-proliferating properties of Herceptin® were maintained after mHT.

Since it is preserving the stability, and the immunological and pharmacological properties of Herceptin®, mHT could represent a promising strategy for local delivery of Herceptin® in patients with HER-2 positive breast cancer. Indeed, this method is fully compatible with *i.v.* administration of Herceptin®. In this scenario, the breast tumor would be exposed to local mHT using high intensity focused ultrasound, radiofrequency or infrared radiation.⁴⁷ As the tumor perfusion and the vascular permeability increase as a result of applying mHT and the interstitial fluid pressure is reduced, an improved *i.t.* Herceptin® bioavailability could be obtained. As a result, the tumor response

to Herceptin®-based immunotherapy might be enhanced using this method. This hypothesis is supported by preclinical studies, which reported that combining mHT with intact radiolabelled mAbs improved the tumor mAb uptake⁴⁸, as well as an increase in radio-immunotherapy efficacy in rodent xenograft models.^{31,48} Heating methods, especially focused ultrasound, will be investigated and compared to water-bath in future studies.

Conclusions

In summary, our findings suggest that mHT does not lead to significant changes in the recognition to and the binding affinity of Herceptin® to HER-2 receptors. In addition, the ability of Herceptin® to inhibit the HER-2 signaling pathway and the anti-proliferative properties of Herceptin® remain unchanged. These results are in line with the observed stability of Herceptin® with respect to exposure to mHT. Thus, mHT can also safely be used to improve the i.t. bioavailability of Herceptin® as is already done for nanoparticles.⁴⁹ Further *in-vivo* investigations are required to evaluate the influence of mHT on the anti-tumor effectiveness and the side effects of Herceptin® after exposure of tumors to mHT.

Acknowledgements

The authors acknowledge J.B. van den Dikkenberg and G. Nadibaidze for technical assistance, Dr. M. Bourajaj, Prof. G. Storm (Dept. Pharmaceutics, Utrecht Institute for Pharmaceutical Sciences, Utrecht University, Netherlands), Dr. C.H. Ries (Roche Diagnostics GmbH, Penzberg, Germany), Dr. A. Kong (Dept. Oncology, Weatherall Institute of Molecular Medicine, University of Oxford, UK) and Dr. N. Heuzé-Vourc'h (Inserm U1100, EA 6305, Université de Tours, France) for fruitful discussions, C. ten Brink for her technical assistance (Cell Microscopy Core, Department of Cell Biology, UMC Utrecht). Dr. J. Butterworth professionally proofread the manuscript (Word Perfect Science, <http://www.wordperfectscience.com>). This work was supported by Advanced ERC grant Sound Pharma – 268906 (CM).

Author contributions

JME is responsible for the design of experiments, performance of all experiments, analysis of data

and writing of the manuscript. RD contributed to the analysis of data. NS assisted in flow cytometry experiments. CM and CB are responsible for the reviewing of the manuscript and the supervision of this work.

References

1. Ferlay J, Steliarova-Foucher E, Lortet-Tieulent J, Rosso S, Coebergh JW, Comber H, et al. Cancer incidence and mortality patterns in Europe: estimates for 40 countries in 2012. *Eur J Cancer* 2013; **49**: 1374-403.
2. Arteaga CL, Sliwkowski MX, Osborne CK, Perez EA, Puglisi F, Gianni L. Treatment of HER2-positive breast cancer: current status and future perspectives. *Nat Rev Clin Oncol* 2012; **9**: 16-32.
3. Eroles P, Bosch A, Perez-Fidalgo JA, Lluch A. Molecular biology in breast cancer: intrinsic subtypes and signaling pathways. *Cancer Treat Rev* 2012; **38**: 698-707.
4. Yardley DA, Tripathy D, Brufsky AM, Rugo HS, Kaufman PA, Mayer M, et al. Long-term survivor characteristics in HER2-positive metastatic breast cancer from registHER. *Br J Cancer* 2014; **110**: 2756-64.
5. Hudis CA. Trastuzumab-mechanism of action and use in clinical practice. *N Engl J Med* 2007; **357**: 39-51.
6. Sliwkowski MX, Mellman I. Antibody therapeutics in cancer. *Science* 2013; **341**: 1192-8.
7. Scaltriti M, Verma C, Guzman M, Jimenez J, Parra JL, Pedersen K, et al. Lapatinib, a HER2 tyrosine kinase inhibitor, induces stabilization and accumulation of HER2 and potentiates trastuzumab-dependent cell cytotoxicity. *Oncogene* 2009; **28**: 803-14.
8. Klapper LN, Waterman H, Sela M, Yarden Y. Tumor-inhibitory antibodies to HER-2/ErbB-2 may act by recruiting c-Cbl and enhancing ubiquitination of HER-2. *Cancer Res* 2000; **60**: 3384-8.
9. Clynes RA, Towers TL, Presta LG, Ravetch JV. Inhibitory Fc receptors modulate in vivo cytotoxicity against tumor targets. *Nat Med* 2000; **6**: 443-6.
10. Barok M, Isola J, Palyi-Krekke Z, Nagy P, Juhasz I, Vereb G, et al. Trastuzumab causes antibody-dependent cellular cytotoxicity-mediated growth inhibition of submacroscopic JIMT-1 breast cancer xenografts despite intrinsic drug resistance. *Mol Cancer Ther* 2007; **6**: 2065-72.
11. Izumi Y, Xu L, di Tomaso E, Fukumura D, Jain RK. Tumour biology: herceptin acts as an anti-angiogenic cocktail. *Nature* 2002; **416**: 279-80.
12. Li L, ten Hagen TL, Bolkestein M, Gasselhuber A, Yatvin J, van Rhoon GC, et al. Improved intratumoral nanoparticle extravasation and penetration by mild hyperthermia. *J Control Release* 2013; **167**: 130-7.
13. Seidman AD, Fournier MN, Esteva FJ, Tan L, Kaptain S, Bach A, et al. Weekly trastuzumab and paclitaxel therapy for metastatic breast cancer with analysis of efficacy by HER2 immunophenotype and gene amplification. *J Clin Oncol* 2001; **19**: 2587-95.
14. Joensuu H, Kellokumpu-Lehtinen PL, Bono P, Alanko T, Kataja V, Asola R, et al. Adjuvant docetaxel or vinorelbine with or without trastuzumab for breast cancer. *N Engl J Med* 2006; **354**: 809-20.
15. Friedl J, Turner E, Alexander HR, Jr. Augmentation of endothelial cell monolayer permeability by hyperthermia but not tumor necrosis factor: evidence for disruption of vascular integrity via VE-cadherin down-regulation. *Int J Oncol* 2003; **23**: 611-6.
16. Horton JK, Halle J, Ferraro M, Carey L, Moore DT, Ollila D, et al. Radiosensitization of chemotherapy-refractory, locally advanced or locally recurrent breast cancer with trastuzumab: a phase II trial. *Int J Radiat Oncol Biol Phys* 2010; **76**: 998-1004.
17. Liang K, Lu Y, Jin W, Ang KK, Milas L, Fan Z. Sensitization of breast cancer cells to radiation by trastuzumab. *Mol Cancer Ther* 2003; **2**: 1113-20.
18. Tarantini L, Cioffi G, Gori S, Tuccia F, Boccardi L, Bovelli D, et al. Trastuzumab adjuvant chemotherapy and cardiotoxicity in real-world women with breast cancer. *J Card Fail* 2012; **18**: 113-9.

19. Jain RK. Physiological barriers to delivery of monoclonal antibodies and other macromolecules in tumors. *Cancer Res* 1990; **50**: 814s-9s.
20. Jain RK. Vascular and interstitial barriers to delivery of therapeutic agents in tumors. *Cancer Metastasis Rev* 1990; **9**: 253-66.
21. Jain RK, Baxter LT. Mechanisms of heterogeneous distribution of monoclonal antibodies and other macromolecules in tumors: significance of elevated interstitial pressure. *Cancer Res* 1988; **48**: 7022-032.
22. Baker JH, Lindquist KE, Huxham LA, Kyle AH, Sy JT, Minchinton AI. Direct visualization of heterogeneous extravascular distribution of trastuzumab in human epidermal growth factor receptor type 2 overexpressing xenografts. *Clin Cancer Res* 2008; **14**: 2171-9.
23. Cho CH, Sreenivasa G, Plotkin M, Pietsch H, Wust P, Ludemann L. Tumour perfusion assessment during regional hyperthermia treatment: comparison of temperature probe measurement with H(2)(15)O-PET perfusion. *Int J Hyperthermia* 2010; **26**: 404-11.
24. Song CW. Effect of local hyperthermia on blood flow and microenvironment: a review. *Cancer Res* 1984; **44**: 4721s-30s.
25. Song CW, Park H, Griffin RJ. Improvement of tumor oxygenation by mild hyperthermia. *Radiat Res* 2001; **155**: 515-28.
26. Kirui DK, Koay EJ, Guo X, Cristini V, Shen H, Ferrari M. Tumor vascular permeabilization using localized mild hyperthermia to improve macromolecule transport. *Nanomedicine* 2014; **10**: 1487-96.
27. Kong G, Braun RD, Dewhirst MW. Characterization of the effect of hyperthermia on nanoparticle extravasation from tumor vasculature. *Cancer Res* 2001; **61**: 3027-32.
28. Cope DA, Dewhirst MW, Friedman HS, Bigner DD, Zalutsky MR. Enhanced delivery of a monoclonal antibody F(ab')₂ fragment to subcutaneous human glioma xenografts using local hyperthermia. *Cancer Res* 1990; **50**: 1803-9.
29. Kong G, Dewhirst MW. Hyperthermia and liposomes. *Int J Hyperthermia* 1999; **15**: 345-70.
30. Gridley DS, Ewart KL, Cao JD, Stickney DR. Hyperthermia enhances localization of ¹¹¹In-labeled hapten to bifunctional antibody in human colon tumor xenografts. *Cancer Res* 1991; **51**: 1515-20.
31. Kinuya S, Yokoyama K, Hiramatsu T, Tega H, Tanaka K, Konishi S, et al. Combination radioimmunotherapy with local hyperthermia: increased delivery of radioimmunoconjugate by vascular effect and its retention by increased antigen expression in colon cancer xenografts. *Cancer Lett* 1999; **140**: 209-18.
32. Wong JY, Mivechi NF, Paxton RJ, Williams LE, Beatty BG, Beatty JD, et al. The effects of hyperthermia on tumor carcinoembryonic antigen expression. *Int J Radiat Oncol Biol Phys* 1989; **17**: 803-8.
33. Demeule B, Gurny R, Arvinte T. Detection and characterization of protein aggregates by fluorescence microscopy. *Int J Pharm* 2007; **329**: 37-45.
34. Cudd A, Arvinte T, Das RE, Chinni C, MacIntyre I. Enhanced potency of human calcitonin when fibrillation is avoided. *J Pharm Sci* 1995; **84**: 717-9.
35. Pickl M, Ries CH. Comparison of 3D and 2D tumor models reveals enhanced HER2 activation in 3D associated with an increased response to trastuzumab. *Oncogene* 2009; **28**: 461-8.
36. Hosono MN, Hosono M, Endo K, Ueda R, Onoyama Y. Effect of hyperthermia on tumor uptake of radiolabeled anti-neural cell adhesion molecule antibody in small-cell lung cancer xenografts. *J Nucl Med* 1994; **35**: 504-9.
37. Kramer-Marek G, Gijzen M, Kiesewetter DO, Bennett R, Roxanis I, Zielinski R, et al. Potential of PET to predict the response to trastuzumab treatment in an ErbB2-positive human xenograft tumor model. *J Nucl Med* 2012; **53**: 629-37.
38. Gijzen M, King P, Perera T, Parker PJ, Harris AL, Larijani B, et al. HER2 phosphorylation is maintained by a PKB negative feedback loop in response to anti-HER2 herceptin in breast cancer. *PLoS Biol* 2010; **8**: e1000563.
39. Ishikawa T, Ito T, Endo R, Nakagawa K, Sawa E, Wakamatsu K. Influence of pH on heat-induced aggregation and degradation of therapeutic monoclonal antibodies. *Biol Pharm Bull* 2010; **33**: 1413-7.
40. Landon CD, Park JY, Needham D, Dewhirst MW. Nanoscale Drug Delivery and Hyperthermia: The Materials Design and Preclinical and Clinical Testing of Low Temperature-Sensitive Liposomes Used in Combination with Mild Hyperthermia in the Treatment of Local Cancer. *Open Nanomed J* 2011; **3**: 38-64.
41. Goldberg SN, Gazelle GS, Mueller PR. Thermal ablation therapy for focal malignancy: a unified approach to underlying principles, techniques, and diagnostic imaging guidance. *AJR Am J Roentgenol* 2000; **174**: 323-31.
42. Bucciantini M, Giannoni E, Chiti F, Baroni F, Formigli L, Zurdo J, et al. Inherent toxicity of aggregates implies a common mechanism for protein misfolding diseases. *Nature* 2002; **416**: 507-11.
43. Schellekens H. Factors influencing the immunogenicity of therapeutic proteins. *Nephrol Dial Transplant* 2005; **20** (Suppl 6): vi3-9.
44. Hauck ML, Dewhirst MW, Zalutsky MR. The effects of clinically relevant hyperthermic temperatures on the kinetic binding parameters of a monoclonal antibody. *Nucl Med Biol* 1996; **23**: 551-7.
45. Hauck ML, Larsen RH, Welsh PC, Zalutsky MR. Cytotoxicity of alpha-particle-emitting astatine-211-labelled antibody in tumour spheroids: no effect of hyperthermia. *Br J Cancer* 1998; **77**: 753-9.
46. Koay DC, Zerillo C, Narayan M, Harris LN, DiGiovanna MP. Anti-tumor effects of retinoids combined with trastuzumab or tamoxifen in breast cancer cells: induction of apoptosis by retinoid/trastuzumab combinations. *Breast Cancer Res* 2010; **12**: R62.
47. Ta T, Porter TM. Thermosensitive liposomes for localized delivery and triggered release of chemotherapy. *J Control Release* 2013; **169**: 112-25.
48. Hauck ML, Zalutsky MR. Enhanced tumour uptake of radiolabelled antibodies by hyperthermia: Part I: Timing of injection relative to hyperthermia. *Int J Hyperthermia* 2005; **21**: 1-11.
49. Escoffre JM, Novell A, de Smet M, Bouakaz A. Focused ultrasound mediated drug delivery from temperature-sensitive liposomes: in-vitro characterization and validation. *Phys Med Biol* 2013; **58**: 8135-51.

EGFR-expression in primary urinary bladder cancer and corresponding metastases and the relation to HER2-expression. On the possibility to target these receptors with radionuclides

Jörgen Carlsson¹, Kenneth Wester¹, Manuel De La Torre², Per-Uno Malmström³, Truls Gårdmark⁴

¹ Department of Radiology, Oncology and Radiation Science, Biomedical Radiation Sciences, Rudbeck Laboratory, Uppsala University, Uppsala, Sweden

² Department of Immunology, Genetics and Pathology, Molecular and Morphological Pathology, Rudbeck Laboratory, Uppsala University Hospital, Uppsala, Sweden

³ Department of Surgical Sciences, Urology, Uppsala University Hospital, Uppsala, Sweden

⁴ Department of Clinical Sciences, General Surgery and Urology, Karolinska Institute at Danderyd Hospital, Stockholm, Sweden

Radiol Oncol 2015; 49(1): 50-58.

Received 25 January 2014

Accepted 24 March 2014

Correspondence to: Prof. Jörgen Carlsson, Biomedical Radiation Sciences, Department of Radiology, Oncology and Radiation Science, Rudbeck Laboratory, Uppsala University, SE-75185 Uppsala, Sweden. E-mail: jorgen.carlsson@bms.uu.se

Disclosure: No potential conflicts of interest were disclosed

Background. There is limited effect of tyrosine kinase inhibitors or “naked” antibodies binding EGFR or HER2 for therapy of metastasized urinary bladder cancer and these methods are therefore not routinely used. Targeting radionuclides to the extracellular domain of the receptors is potentially a better possibility.

Methods. EGFR- and HER2-expression was analyzed for primary tumors and corresponding metastases from 72 patients using immunohistochemistry and the internationally recommended HercepTest. Intracellular mutations were not analyzed since only the receptors were considered as targets and intracellular abnormalities should have minor effect on radiation dose.

Results. EGFR was positive in 71% of the primary tumors and 69% of corresponding metastases. Local and distant metastases were EGFR-positive in 75% and 66% of the cases, respectively. The expression frequency of HER2 in related lesions was slightly higher (data from previous study). The EGFR-positive tumors expressed EGFR in metastases in 86% of the cases. The co-expression of EGFR and HER2 was 57% for tumors and 53% for metastases. Only 3% and 10% of the lesions were negative for both receptors in tumors and metastases, respectively. Thus, targeting these receptors with radionuclides might be applied for most patients.

Conclusions. At least one of the EGFR- or HER2-receptors was present in most cases and co-expressed in more than half the cases. It is therefore interesting to deliver radionuclides for whole-body receptor-analysis, dosimetry and therapy. This can hopefully compensate for resistance to other therapies and more patients can hopefully be treated with curative instead of palliative intention.

Key words: EGFR; HER2; radionuclides; resistance; urinary bladder cancer metastases

Introduction

Biological resistance to both EGFR- and HER2-targeted therapies, due to mutations in for example PI3K/AKT, Ras/Raf/Mek/Erk or other intracellular signal pathways has been observed for many types

of cancer.¹⁻⁴ Urinary bladder cancer is at present not generally considered for therapy with EGFR- or HER2-binding agents such as tyrosine kinase inhibitors and “naked” antibodies (e.g. trastuzumab or cetuximab). Evidence for therapy efficacy of such agents in urinary bladder cancer is lacking

and it has been claimed that there might, in several cases, be resistance.⁵⁻⁸ It might therefore be, as an alternative to tyrosine kinase inhibitors and “naked” antibodies, beneficial to target the extracellular domains of EGFR and/or HER2 in metastatic urinary bladder cancer patients with molecules that deliver suitable radionuclides not only for whole body receptor mapping and dosimetry but also for radionuclide therapy. Examples of radionuclides for these purposes are given in the Discussion.

Therapy with radionuclides is of interest since induced resistance to effects of radiation is not a major problem in cancer therapy. The radionuclides can be delivered to cancer cells with various types of molecules, *e.g.* antibodies, antibody fragments and smaller proteins such as affibody molecules and also with peptides.⁹⁻¹² The application of radionuclide labeled molecules for EGFR- and/or HER2-targeted therapy has so far, to the knowledge of the authors, not been clinically applied for therapy of metastatic urinary bladder cancer. If this is tried, the strategy is that the radionuclides can kill cancer cells independent of possible intracellular mutations. This is also why we decided to neither analyze mutations in the intracellular signal pathways nor gene amplifications.

EGFR and HER2 belong to the type 1 tyrosine kinase receptor family consisting of four related receptors, forming dimers with each other, and are important for growth of various cancers.¹³ Several agents binding to EGFR and HER2 aimed to interfere with intracellular downstream signaling, and give therapy effects, are developed or are under development.¹⁴⁻¹⁸ Binders to the other receptors in the EGFR-family, *i.e.* HER3 and HER4, has so far not been introduced for clinical applications so we focus only on EGFR and HER2 in this study.

The worldwide incidence of urinary bladder cancer is high with 350-400.000 new cases per year and the incidence is high also in Europe.¹⁹⁻²¹ Furthermore, approximately one third of all urinary bladder cancers are, at the time of diagnosis, growing invasive through the bladder wall and can form metastases which often are growing in regional (local) lymph nodes and in several distant organs, especially lung, liver and skeleton.²² External radiotherapy and surgery are treatment modalities for the localized tumors. Chemotherapy and tyrosine kinase inhibitors are applied for therapy of the disseminated tumors but such therapy is in most cases not curative.^{5,6,22} Thus, other treatment modalities, *e.g.* receptor targeted radionuclide therapy is of interest to exploit. We analyzed and discussed in this article whether EGFR and

TABLE 1. Characteristics of the urinary bladder cancers and patients with available EGFR and HER2 data for both primary tumors and corresponding metastases (n=72)

Characteristics	Number and (%) patients
Gender	
Male	55 (≈76%)
Female	17 (≈24%)
Primary tumor characteristics	
Histological grade II*	8 (≈11%)
Histological grade III*	64 (≈89%)
Metastatic locations	
<i>Lymph node metastases</i>	
Regional (local) lymph nodes	28 (≈39%)
Distant lymph nodes	7 (≈10%)
<i>Non-lymph node metastases</i>	
Liver	6 (≈8%)
Lung	1 (≈1%)
Skeleton	3 (≈4%)
Intestinal	10 (≈14%)
Prostate	5 (≈7%)
Vagina	1 (≈1%)
Other	11 (≈15%)

The mean age of the patients at diagnosis was ≈ 66 years (span 35-87). The time from diagnosis of the primary tumor to sampling of metastases was on the average ≈ 10 months (span 0-82) (Gårdmark et al [22]).

*WHO 1977.

HER2 are expressed with such high frequencies that targeted radionuclide therapy might be a possibility and an alternative or complement to other modalities in the treatment of metastatic urinary bladder cancers.

Materials and methods

Tissue samples

The study included 72 patients with metastatic urinary bladder carcinoma, where tissue samples from both primary tumors and metastases were available. The study was approved by the institutional review board. In the previous publication 90 patients were analysed²² but samples were not available for 18 of the patients because the paraffin blocks were previously sectioned so much that no

tissue of value could be found. The primary treatment was transurethral resection in 61 (85%) cases and cystectomy in 11 (15%) cases. Patient, tumor and metastasis characteristics are shown in Table 1. All samples were fixated in 10% buffered formalin (4% formaldehyde), paraffin embedded according to standard procedures at our laboratory and sections, 4- μ m thick, were then cut and deparaffinized in xylene and hydrated through graded concentrations of ethanol to distilled water.²³

EGFR-immunohistochemistry

EGFR was assessed by immunohistochemistry, IHC, using a streptavidin-biotin complex technique as previously described.^{23,24} Endogenous peroxidase was blocked in 0.3% H₂O₂ in PBS for 20 min. Then, antigen retrieval was done in 0.05% protease K (Code no. S3020, Dako, Glostrup, Denmark) in PBS for 10 min at room temperature. The tissue sections were preincubated in PBS for 10 min and then the primary mouse monoclonal antibody (clone 31G7, Zymed labs, South San Francisco, CA, USA) directed against the EGF receptor, diluted 1:100, was added and the sections incubated overnight at 4°C. The secondary biotinylated antibody (goat anti-mouse, Dako, Glostrup, Denmark) and the peroxidase-labeled streptavidin-biotin complex (Dako, Glostrup, Denmark), diluted 1:200, were then added and the samples incubated for 30 min at room temperature. All sections were developed in 0.05% diaminobenzidine (Sigma, St Louis, MO, USA) for 5 min and counterstained in Harris haematoxylin (Sigma, St Louis, MO, USA). Finally, the sections were dehydrated through graded alcohol to xylene and mounted in organic mounting medium (Pertex®, HistoLab, Gothenburg, Sweden).

HER2-immunohistochemistry

The IHC staining was made as previously described.^{22,24} The sections were incubated in methanol and hydrogen peroxide for 30 min to quench endogenous peroxidase. Antigen retrieval was done in water bath at 95-98°C, pH 6 for 40 minutes. Thereafter the sections were cooled at room temperature and then washed in distilled water. Staining was performed using the Elite ABC Kit (Vectastain, Vector Laboratories, Burlingame, CA, USA). First blocking serum was applied for 15 min and followed by incubation with polyclonal rabbit anti-human c-erbB-2 oncoprotein (code No. A 0485, Dako, Glostrup, Denmark) diluted 1:350. The samples were then incubated with the biotinylat-

ed secondary antibody and visualized using the peroxidase substrate 3-amino-9-ethyl-carbazole (AEC) (Sigma A-5754, St Louis, MO, USA) as chromogen. Finally, the sections were counterstained with Mayer's haematoxylin and mounted with Aquamount (BDH Ltd, Poole, UK).

Evaluation of immunohistochemistry

Evaluation of the IHC staining was performed by four of the authors. Authors JC and MT evaluated the expression in this study. TG, MT and KW evaluated the HER2 expression in the previously published study.²²

The cellular membrane expression pattern of EGFR is similar to that of HER2. EGFR expression was therefore evaluated using the same scoring criterion as for HER2. Briefly, the EGFR- and HER2-expressions were scored using the HercepTest criterion based on a scale where 0 corresponded to tumor cells that were completely negative, 1+ corresponded to faint perceptible staining of the tumor cell membranes, 2+ corresponded to moderate staining of the entire tumor cell membranes and 3+ was strong circumferential staining of the entire tumor cell membranes creating a fishnet pattern. The Canadian and the DAKO HercepTest guidelines²⁵ were applied, which require $\geq 10\%$ of the tumor cells to be stained. The HER2 data, as published by Gårdmark *et al.*²², also reported on the criterion that $\geq 2/3$ of the tumor cells must be HER2-stained to score a sample HER2-positive. However, in the present study we only considered data applying the $\geq 10\%$ criterion since only the internationally recommended HercepTest scoring²⁵ made the same way as for breast cancer is accepted at our hospital.

Cytoplasmic staining was considered non-specific and was not included in the scoring. As positive controls we used positive tissue sections; epithelial samples from skin for EGFR-positivity and HER2-positive breast cancer samples complemented with HER2-positive sections from DAKO. All positive controls were stained with the same protocol as applied for the urinary bladder cancer sections. As negative controls we used normal tissues which are expected not to express the receptors such as connective tissue, blood cells and lymphocytes seen in the same sections as the tumor cells. In the metastases sections we used lymphocytes, connective tissue and the surrounding capsule of the lymph nodes as negative internal controls. Thus, all tissues used as negative controls were stained with the same protocol as the urinary bladder cancers since they were in the same sections.

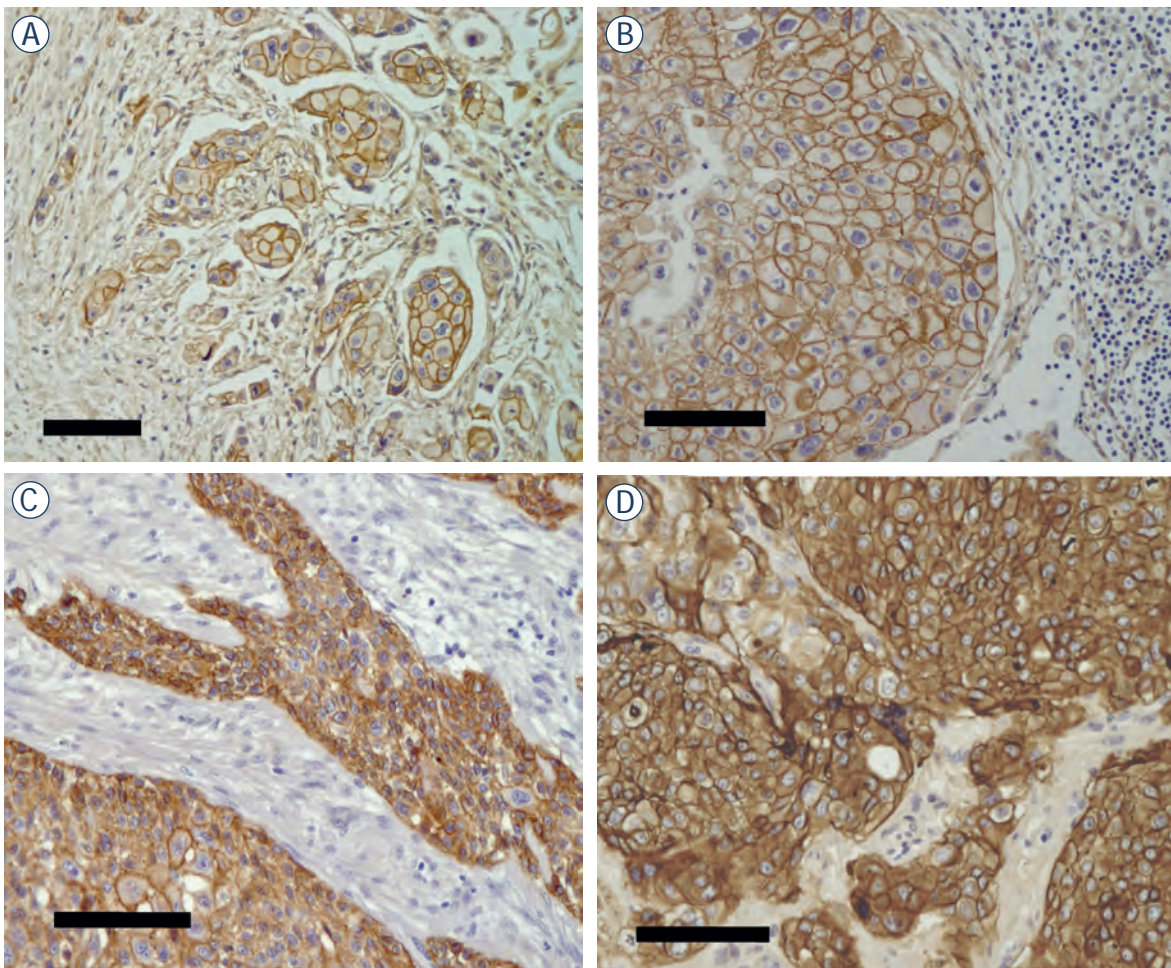


FIGURE 1. Examples of immunohistochemical EGFR-staining (brown) of samples from metastasized urinary bladder cancers. (A) Primary tumor. (B) Regional (local) lymph node metastasis (from the same patient as in A). Note the large number of lymphocytes (small blue haematoxylin stained nuclei to the right). (C) Primary tumor. (D) Colon metastasis (classified as distant). All samples were scored 3+ and EGFR-positive. All bars correspond to 100 μ m.

Positive versus negative receptor expression

Scores 2+ and 3+ were considered receptor positive and scores 0 and 1+ receptor negative. This a “crude” rule but gives an indication of which patients that are candidates for nuclear medicine based receptor analysis and thereafter considered suitable for radionuclide therapy.

Results

Expression of EGFR

The EGFR determinations are shown in Table 2. EGFR was positive in 51/72 (71%) of the primary tumors and 50/72 (69%) of the corresponding metastases. The regional (local) and the distant me-

tastases were EGFR-positive in 21/28 (75%) and 29/44 (66%) of the cases, respectively. Considering only the EGFR-positive primary tumors ($n=51$) the corresponding metastases were EGFR-positive in 44/51 (86%) of the cases. Examples of EGFR-positive tumor cells are shown in Figure 1.

There was good agreement between the expression frequencies in the primary tumors and the corresponding lymph node metastases in the majority of cases. Totally, 13 changes were observed, *i.e.* 6 upregulations and 7 downregulations, in the metastases in relation to the primary tumors and 11 of these changes were in the distant metastases (Table 2). Nine of the regional (local) lymph nodes metastases were characterized as sentinel nodes and 5 of these were EGFR-positive in both the primary tumors and the metastasis while 3 were negative in both. One sentinel node metastasis was

TABLE 2. EGFR-scores for all analyzed primary urinary bladder tumors and corresponding metastases (upper part), regional (local) lymph node metastases (middle part) and distant metastases and non-lymph node metastases (lower part)

Primary tumors EGFR-scores	All metastases, EGFR-scores (n=72)			
	0	1+	2+	3+
0	6	0	2	0
1+	2	7	4	0
2+	0	4	12	2
3+	2	1	5	25

Primary tumors EGFR-scores	Regional (local) lymph node metastases, EGFR-scores (n=28)			
	0	1+	2+	3+
0	3	0	0	0
1+	1	1	0	0
2+	0	2	3	2
3+	0	0	3	13

Primary tumors EGFR-scores	Distant metastases and none-lymph node metastases, EGFR-scores (n=44)			
	0	1+	2+	3+
0	3	0	2	0
1+	1	6	4	0
2+	0	2	9	0
3+	2	1	2	12

negative while the corresponding primary tumor was positive.

Expression of HER2

The values for HER2 positivity in our article from 2005 were 79% for primary tumors and 62% for metastases when $\geq 2/3$ of the tumor cells had to be HER2-stained and the staining should be as intense as for breast cancer sections.²² The internationally recommended DAKO procedure²⁵ which we used this time gave 60/72 (83%) and 53/72 (74%) HER2-positive cases in the analyzed primary tumors and metastases, respectively. The reasons for the different results are discussed below. Eight out of the 9 sentinel nodes were HER2-positive in both the primary tumors and the metastasis and one sentinel node metastasis was HER2 negative while the corresponding primary tumor was positive.

Co-expression of EGFR and HER2

Table 3 shows the relation between EGFR expression and HER2 expression frequencies in primary tumors and metastases. The co-expression of EGFR

TABLE 3. EGFR and HER2 scores for all analyzed primary urinary bladder tumors (upper part) and corresponding metastases (lower part)

Primary tumors EGFR-scores	Primary tumors, HER2-scores (n=72)			
	0	1+	2+	3+
0	0	1	2	5
1+	1	0	3	9
2+	4	0	1	13
3+	3	3	12	15

Metastases EGFR-scores	Metastases, HER2-scores (n=72)			
	0	1+	2+	3+
0	2	0	3	5
1+	3	2	0	7
2+	5	3	4	11
3+	3	1	9	14

and HER2 was 41/72 (57%) for the primary tumors and 38/72 (53%) for the metastases. Only 2/72 (3%) of the patients were negative for both receptors in the primary tumors and in 7/72 (10%) of the metastases. Table 4 shows a summary of relations between positive (2+ and 3+) and negative (0 and 1+) expressions of EGFR and between EGFR and HER2 in primary tumors and metastases.

Discussion

At least one of the receptors, EGFR or HER2, was positive in nearly all cases and co-expression was seen in more than half of the cases and this was valid for both primary tumors and metastases. With such high expression frequencies the number of patients that can be considered for radionuclide based receptor mapping (imaging), dosimetry and therapy is high. Furthermore, targeting of both receptors in the same patient might, in many cases, be a possibility to deliver increased amounts of radionuclides, *i.e.* give higher radiation doses to the tumor cells.

Radionuclide therapy is of special interest when there is "biological resistance" to EGFR- and/or HER2-targeted therapies probably because of intracellular signal pathway mutations¹⁻⁴ and such resistance, or at least lack of therapy efficacy, has been reported for urinary bladder cancer.⁵⁻⁸ The receptors themselves, and not intracellular mutations and gene amplifications, are of main interest in these cases.

It is of methodological interest that discrepancies between gene amplification and receptor expression has actually been reported from studies of urinary bladder cancer.²⁶⁻³⁰ However, since our primary goal was to consider the receptors as targets we focused only on IHC analyses giving receptor expression frequencies. The IHC results indicate which patients that might benefit from EGFR and/or HER2 targeted radionuclide therapy. The limitation is that the samples analyzed with IHC might neither be representative for the whole volume of tumors and metastases and that differences in expression between metastases in the same patient might exist.

Furthermore, IHC analyses cannot be a basis for radionuclide dosimetry and such calculations were of course beyond the scope of this study. Reliable information related to the spatial distribution of receptor expression and dosimetry for each patient, and possibly also for prediction of therapy results, require a well functioning whole body, non-invasive nuclear medicine based method as suggested for other types of tumors.³¹⁻³⁵ However, the high frequencies of expression of both EGFR and HER2 in primary tumors and metastases in our study indicate that many, maybe most, urinary bladder cancers are of interest for targeting with molecules that deliver radionuclides to these receptors.

It is often claimed that positivity for EGFR and HER2 receptors indicate aggressive tumor cells and bad survival prognosis^{26,36-42} and, if so, the most aggressive cells are attacked with the radiation. The expression frequencies in our study are high in comparison to some other studies and this is probably because only patients with verified metastatic growth were considered and their primary tumors were mainly of high grade.

The expression frequency of EGFR in metastatic urinary bladder cancer has in several articles been reported to be in the range 40-100% for both primary tumors and metastases^{23,43-45} that is high enough to make EGFR an interesting target for systemic treatment. However, EGFR is also expressed in various normal tissues and for successful therapy it is required that EGFR is strongly expressed in the tumor cells, as shown in the examples in Figure 1. Favorable tumor to blood and tumor to normal tissue quotients of delivered radioactivity are required to get PET or SPECT images of high quality and this is of course also a requirement for radionuclide therapy. It has recently been reported that delivery molecules with low specific radioactivity (the injection solution containing a large fraction

TABLE 4. Summary of relations between positive (2+ and 3+) and negative (0 and 1+) expressions of EGFR in primary tumors and metastases (upper part), between EGFR and HER2 in primary tumors (middle part) and between EGFR and HER2 in metastases (lower part) (n=72)

EGFR status primary tumors	EGFR status metastases	Number and % cases
positive	positive	44 (61%)
positive	negative	7 (10%)
negative	positive	6 (8%)
negative	negative	15 (21%)
EGFR status primary tumors	HER2 status primary tumors	Number and % cases
positive	positive	41 (57%)
positive	negative	10 (14%)
negative	positive	19 (26%)
negative	negative	2 (3%)
EGFR status metastases	HER2 status metastases	Number and % cases
positive	positive	38 (53%)
positive	negative	12 (17%)
negative	positive	15 (21%)
negative	negative	7 (10%)

non-labeled targeting molecules) and/or delivery molecules giving fast body clearance can give good image quality.^{46,47,48} This aspect is especially important for targeting of EGFR which is expressed in various normal tissues.^{49, 50}

The tendency towards lower HER2-expression frequencies with increasing "distance" from the primary tumor as previously indicated²² was in our study not present considering the EGFR-expression frequencies.

The expression frequency of HER2 has also been reported to often be high and vary a lot, *i.e.* in the range 25-100% in primary tumors^{22,23,37,42,51} and 40-70% in corresponding metastases.^{22,23,38,42,52} It has been indicated that most HER2-positive metastases were from HER2-positive primary tumors.^{22,23,42} HER2 is much less expressed in normal tissues than EGFR, especially in liver, reproductive organs, the digestive tract and bile ducts and various epithelial tissues.^{53,54} Thus, HER2 is an interesting target for therapy with radionuclides since the uptake in normal organs is expected to be low. This also supports the possibility to combine EGFR-targeted therapy with HER2-targeted therapy.

The large differences in reported receptor expression frequencies between different studies are probably due to different patient inclusion criteria

and etiological differences but differences in receptor scoring methods and IHC retrieval techniques might also be explanations. The values for HER2 positivity in our 2005 article on urinary bladder cancer²² were also different from the values in the present article. The reason for the difference between our investigations is unclear but improved retrieval and staining procedures can at least be part of the explanation. We previously also had a criteria that staining intensity should be comparable to that often seen in breast cancer stainings. We do not apply that criteria anymore and instead only use the internationally recommended HercepTest staining and scoring system, i.e. the DAKO procedure.²⁵

Suitable molecules for delivery of radionuclides are antibodies, antibody fragments, affibody molecules and small molecules such as peptides.⁹⁻¹² Bi-functional antibodies or affibody molecules, with capacity to bind two receptors at the same time, is also a possible approach for radionuclide based imaging and therapy. Co-expression may be associated with high-grade malignancy^{15,16} and “double targeting” can hopefully also increase targeting specificity.

Radionuclides suitable for therapy are β -emitters (e.g. ⁶⁷Cu, ⁹⁰Y, ¹³¹I, ¹⁷⁷Lu, ¹⁸⁶Re, ¹⁸⁸Re) and α -emitters (e.g. ²¹¹At, ²¹²Bi, ²¹³Bi, ²²⁵Ac, ²²⁷Th). The requirement is of course that relevant labeling methods are available that not significantly disturb receptor binding. For receptor mapping (imaging) and dosimetry, radionuclides such as ^{99m}Tc, ¹¹¹In and ¹²³I for gamma cameras (including SPECT) or ¹⁸F, ⁶⁴Cu, ⁶⁸Ga, ⁷⁶Br, ⁸⁶Y, ⁸⁹Zr and ¹²⁴I for PET cameras can be applied when relevant labeling methods are at hand.^{9-12,43}

The α - and β -particle emitters can locally give rather homogeneous dose distributions since the radiation from the targeted cells can give therapeutic effects also on non-targeted tumor cells.¹² There are also examples of interesting toxins that are candidates for receptor mediated delivery to tumor cells^{55,56} but these are not discussed in this article.

Targeted radionuclide therapy has been available for many years but few methods are routinely used on a large scale. However, during the past decades promising clinical and preclinical research have been made with therapy using radiolabeled antibodies for therapy of lymphomas^{57,58} (e.g. anti-CD20 antibodies such as ⁹⁰Y-Zevalin) and radiolabeled peptides for therapy of neuroendocrine tumors^{59,60} (e.g. somatostatin analogs such as ¹⁷⁷Lu-Octreotate). There is potential for more and improved clinical studies since preclinical research and early clinical studies have given interesting

results and there is also an intensive search for new targeting agents with advantageous pharmacokinetics and biodistributions.^{11,31-34,61-67} Note that promising results with radionuclide therapy of lymphomas^{57,58} has been achieved although the tumor cells are spread throughout large parts of the patients. This indicates that targeted radionuclide therapy can also be of value for treatment of disseminated solid tumors.

The novelty of our previous article published 2005 was to show the high percentage of HER2 expression in urinary bladder cancers and to indicate a possible value of HER2-targeted therapy (with for example lapatinib and/or trastuzumab).²² However, since then there has been reports on resistance of urinary bladder cancer for both EGFR- and HER2-targeting agents (e.g. cetuximab, trastuzumab, lapatinib).⁵⁻⁸ The novelty of the present article is to suggest targeting of the receptors with agents⁹⁻¹² that deliver radionuclides of therapy interest.

In conclusion, it is of interest to try to target EGFR and/or HER2 for radionuclide based therapy of disseminated urinary bladder cancers to decrease the influence of resistance to other forms of therapy. This might improve therapy effectiveness and hopefully allow that more patients can be treated with curative instead of palliative intention.

Acknowledgement

This study was supported by grants from the Swedish Cancer Society, contracts 11-0565 and 12-0415.

References

1. Yamaguchi H, Chang SS, Hsu JL, Hung MC. Signaling cross-talk in the resistance to HER family receptor targeted therapy. *Oncogene* 2014; **33**: 1073-81.
2. Sen M, Joyce S, Panahandeh M, Li C, Thomas SM, Maxwell J, Wang L, et al. Targeting Stat3 abrogates EGFR inhibitor resistance in cancer. *Clin Cancer Res* 2012; **18**: 4986-96.
3. Nahta R, Esteva FJ. Trastuzumab: triumphs and tribulations. *Oncogene* 2007; **26**: 3637-43.
4. Morgillo F, Bareschino MA, Bianco R, Tortora G, Ciardiello F. Primary and acquired resistance to anti-EGFR targeted drugs in cancer therapy. *Differentiation* 2007; **75**: 788-99.
5. Calabrò F, Sternberg CN. Metastatic bladder cancer: anything new? *Curr Opin Support Palliat Care* 2012; **6**: 304-9.
6. Siefker-Radtke A. Bladder cancer: can we move beyond chemotherapy? *Curr Oncol Rep* 2010; **12**: 278-83.
7. Adam L, Zhong M, Choi W, Qi W, Nicoloso M, Arora A, et al. miR-200 expression regulates epithelial-to-mesenchymal transition in bladder cancer cells and reverses resistance to epidermal growth factor receptor therapy. *Clin Cancer Res* 2009; **15**: 5060-72.

8. Kassouf W, Dinney CP, Brown G, McConkey DJ, Diehl AJ, Bar-Eli M, et al. Uncoupling between epidermal growth factor receptor and downstream signals defines resistance to the antiproliferative effect of Gefitinib in bladder cancer cells. *Cancer Res* 2005; **65**: 10524-35.
9. Goldenberg DM, and Sharkey RM. Using antibodies to target cancer therapeutics *Expert Opin Biol Ther* 2012; **12**: 1173-90.
10. Thomadsen B, Erwin W, Mourtada F. The physics and radiobiology of targeted radionuclide therapy. In: Speer TW, ed. *Targeted radionuclide therapy*. Lippincott Williams & Wilkins, Philadelphia; 2011, Chapter 6, p. 71–87. ISBN 978-0-7817-9693-4.
11. Löfblom J, Feldwisch J, Tolmachev V, Carlsson J, Ståhl S, Frejd FY. Affibody molecules: Engineered proteins for therapeutic, diagnostic and biotechnological applications. *FEBS Lett* 2010; **584**: 2670-80.
12. Carlsson J, Stigbrand T, Adams GP. Introduction to radionuclide therapy. In: Stigbrand T, Adams G, Carlsson J, editors. *Targeted radionuclide tumor therapy, biological aspects*. Springer Verlag. Springer Science+Business Media France; 2008, Chapter 1, p. 1-11. ISBN 978-1-4020-8695-3.
13. Yarden Y, Sliwkowski MX. Untangling the ErbB signalling network. *Nat Rev Mol Cell Biol* 2001; **2**: 127-37.
14. Avraham R, Yarden Y. Feedback regulation of EGFR signalling: decision making by early and delayed loops. *Nat Rev Mol Cell Biol* 2011; **12**: 104-17.
15. Bublil EM, Yarden Y. The EGF receptor family: spearheading a merger of signaling and therapeutics. *Curr Opin Cell Biol* 2007; **19**: 124-34.
16. Citri A, Yarden Y. EGF-ERBB signalling: towards the systems level. *Nat Rev Mol Cell Biol* 2006; **7**: 505-16.
17. Mosesson Y, Yarden Y. Oncogenic growth factor receptors: implications for signal transduction therapy. *Semin Cancer Biol* 2004; **14**: 262-70.
18. Mendelsohn J, Baselga J. The EGF receptor family as targets for cancer therapy. *Oncogene* 2000; **19**: 6550-65.
19. Parkin DM. The global burden of urinary bladder cancer. *Scand J Urol Nephrol Suppl* 2008; **218**: 12-20.
20. Ferlay J, Shin HR, Bray F, Forman D, Mathers C, Parkin DM: Estimates of worldwide burden of cancer in 2008: GLOBOCAN 2008. *Int J Cancer* 2010; **127**: 2893-917.
21. Ferlay J, Steliarova-Foucher E, Lortet-Tieulent J, Rosso S, Coebergh JWW, Comber H, et al. Cancer incidence and mortality patterns in Europe: estimates for 40 countries in 2012. *Eur J Cancer* 2013; **49**: 1374-403.
22. Gardmark T, Wester K, DeLa Torre M, Carlsson J, Malmström PU. Analysis of HER2 expression in primary urinary bladder carcinoma and corresponding metastases. *Brit J Urol (BJU)* 2005; **95**: 982-86.
23. Wester K, Sjöström A, de la Torre M, Carlsson J, Malmström PU. HER-2—a possible target for therapy of metastatic urinary bladder carcinoma. *Acta Oncol* 2002; **41**: 282-88.
24. Wei Q, Chen L, Sheng L, Nordgren H, Wester K, Carlsson J: EGFR, HER2 and HER3 expression in esophageal primary tumours and corresponding metastases. *Int J Oncol* 2007; **31**: 493-9.
25. Bilous M, Dowsett M, Hanna W, Isola J, Lebeau A, Moreno A, et al. Current perspectives on HER2 testing: a review of national testing guidelines. *Mod Pathol* 2003; **16**: 173-182.
26. Fleischmann A, Rotzer D, Seiler R, Studer UE, Thalmann GN. Her2 amplification is significantly more frequent in lymph node metastases from urothelial bladder cancer than in the primary tumours. *Eur Urol* 2011; **60**: 350-7.
27. Caner V, Turk NS, Duzcan F, Tufan NL, Kelten EC, Zencir S, et al. No strong association between HER-2/neu protein overexpression and gene amplification in high-grade invasive urothelial carcinomas. *Pathol Oncol Res* 2008; **14**: 261-6.
28. Hauser-Kronberger C, Peham K, Grall J, Rausch W, Hutarew G, Dietze O. Novel approach of human epidermal growth factor receptor 2 detection in noninvasive and invasive transitional cell carcinoma of the bladder. *J Urol* 2006; **175**(3 Pt 1): 875-80.
29. Latif Z, Watters AD, Dunn I, Grigor K, Underwood MA, Bartlett JM. HER2/neu gene amplification and protein overexpression in G3 pT2 transitional cell carcinoma of the bladder: a role for anti-HER2 therapy? *Eur J Cancer* 2004; **40**: 56-63.
30. Sanchez KM, Sweeney CJ, Mass R, Koch MO, Eckert GJ, Geary WA, et al. Evaluation of HER-2/neu expression in prostatic adenocarcinoma: a requested for a standardized, organ specific methodology. *Cancer* 2002; **95**: 1650-5.
31. Baum RP, Prasad V, Muller D, Schuchardt C, Orlova A, Wennborg A, et al. Molecular imaging of HER2-expressing malignant tumors in breast cancer patients using synthetic ¹¹¹In- or ⁶⁸Ga-labeled Affibody molecules. *J Nucl Med* 2010; **51**: 89-97.
32. Tolmachev V. Imaging of HER-2 overexpression in tumors for guiding therapy. *Curr Pharm Des* 2008; **14**: 2999–3019.
33. Heskamp S, van Laarhoven HW, Oyen WJ, van der Graaf WT, Boerman OC. Tumor-receptor imaging in breast cancer: a tool for patient selection and response monitoring. *Curr Mol Med* 2013; **13**: 1506-22.
34. Fox JJ, Schöder H, Larson SM. Molecular imaging of prostate cancer. *Curr Opin Urol* 2012; **22**: 320-7.
35. Perik PJ, Lub-De Hooge MN, Gietema JA, van der Graaf WT, de Korte MA, Jonkman S et al. Indium-111-labeled trastuzumab scintigraphy in patients with human epidermal growth factor receptor 2-positive metastatic breast cancer. *J Clin Oncol* 2006; **24**: 2276-82.
36. Chen PC, Yu HJ, Chang YH, Pan CC. Her2 amplification distinguishes a subset of non-muscle-invasive bladder cancers with a high risk of progression. *J Clin Pathol* 2013; **66**: 113-9.
37. Bolenz C, Shariat SF, Karakiewicz PI, Ashfaq R, Ho R, Sagalowsky AI, et al. Human epidermal growth factor receptor 2 expression status provides independent prognostic information in patients with urothelial carcinoma of the urinary bladder. *BJU Int.* 2010; **106**: 1216-22.
38. Bolenz C, Lotan Y. Translational research in bladder cancer: from molecular pathogenesis to useful tissue biomarkers. *Cancer Biol Ther* 2010; **10**: 407-15.
39. Kolla SB, Seth A, Singh MK, Gupta NP, Hemal AK, Dogra PN, et al Prognostic significance of Her2/neu overexpression in patients with muscle invasive urinary bladder cancer treated with radical cystectomy. *Int Urol Nephrol* 2008; **40**: 321-7.
40. Black PC, Dinney CP. Growth factors and receptors as prognostic markers in urothelial carcinoma. *Curr Urol Rep* 2008; **9**: 55-61.
41. Krüger S, Weitsch G, Büttner H, Matthiensen A, Böhmer T, Marquardt T, et al. HER2 overexpression in muscle-invasive urothelial carcinoma of the bladder: prognostic implications. *Int J Cancer* 2002; **102**: 514-8.
42. Jimenez RE, Hussain M, Bianco FJ Jr, Valshampayan U, Tabazcka P, Sakr WA, et al. Her-2/neu overexpression in muscle-invasive urothelial carcinoma of the bladder: prognostic significance and comparative analysis in primary and metastatic tumors. *Clin Cancer Res* 2001; **7**: 2440-7.
43. Carlsson J. Potential for clinical radionuclide based imaging and therapy of common cancers expressing EGFR-family receptors. *Tumor Biol* 2012; **33**: 653-9.
44. Chau A, Cohen JS, Schultz L, Albadine R, Jadallah S, Murphy KM, et al. High epidermal growth factor receptor immunohistochemical expression in urothelial carcinoma of the bladder is not associated with EGFR mutations in exons 19 and 21: a study using formalin-fixed, paraffin-embedded archival tissues. *Hum Pathol* 2012; **43**: 1590-5.
45. Carlsson J. EGFR-family expression and implications for targeted radionuclide therapy. In: Stigbrand T, Adams G, Carlsson J, editors. *Targeted radionuclide tumor therapy, biological aspects*. Springer Verlag. Springer Science+Business Media France; 2008, Chapter 3, p. 25-58. ISBN 978-1-4020-8695-3.
46. Velikyan I, Sundin A, Eriksson B, Lundqvist H, Sörensen J, Bergström M, et al. In vivo binding of [⁶⁸Ga]-DOTATOC to somatostatin receptors in neuroendocrine tumours—impact of peptide mass. *Nucl Med Biol* 2010; **37**: 265-75.
47. Tolmachev V, Tran TA, Rosik D, Sjöberg A, Abrahmsen L, Orlova A. Tumor targeting using affibody molecules: interplay of affinity, target expression level, and binding site composition. *J Nucl Med* 2012; **53**: 953-60.
48. Tolmachev V, Wallberg H, Sandström M, Hansson M, Wennborg A, Orlova A. Optimal specific radioactivity of anti-HER2 Affibody molecules enables discrimination between xenografts with high and low HER2 expression levels. *Eur J Nucl Med Mol Imaging* 2011; **38**: 531-39.
49. Damjanov I, Mildner B, Knowles BB. Immunohistochemical localization of the epidermal growth factor receptor in normal human tissues. *Lab Invest* 1986; **55**: 588-92.

50. Gusterson B, Cowley G, Smith JA, Ozanne B. Cellular localisation of human epidermal growth factor receptor. *Cell Biol Int Rep* 1984; **8**: 649-58.
51. Skagias L, Politi E, Karameris A, Sambaziotis D, Archondakis A, Vasou O, et al. Prognostic impact of HER2/neu protein in urothelial bladder cancer. Survival analysis of 80 cases and an overview of almost 20 years' research. *J BUON* 2009; **14**: 457-62.
52. Naik DS, Sharma S, Ray A, Hedau S. Epidermal growth factor receptor expression in urinary bladder cancer. *Indian J Urol* 2011; **27**: 208-14.
53. Natali PG, Nicotra MR, Bigotti A, Ventura I, Slamon DJ, Fendly BM, et al. Expression of the p185 encoded by HER2 oncogene in normal and transformed human tissues. *Int J Cancer* 1990; **45**: 457-61.
54. Press MF, Cordon-Cardo C, Slamon DJ. Expression of the HER-2/neu proto-oncogene in normal human adult and fetal tissues. *Oncogene* 1990; **5**: 953-62.
55. Govindan SV, Goldenberg DM. Designing immunoconjugates for cancer therapy. *Expert Opin Biol Ther* 2012; **12**: 873-90.
56. Verma S, Miles D, Gianni L, Krop IE, Welslau M, Baselga J, et al. Trastuzumab emtansine for HER2-positive advanced breast cancer. *N Engl J Med* 2012; **367**: 1783-91.
57. Witzig TE, Fishkin P, Gordon LI, Gregory SA, Jacobs S, Macklis R, et al. Treatment recommendations for radioimmunotherapy in follicular lymphoma: a consensus conference report. *Leuk Lymphoma* 2011; **52**: 1188-99.
58. Press OW. Radiolabeled antibody therapy of B-cell lymphomas. *Semin Oncol* 1999; **26**(5 Suppl 14): 58-65.
59. Kam BL, Teunissen JJ, Krenning EP, de Herder WW, Khan S, van Vliet EI, et al. Lutetium-labelled peptides for therapy of neuroendocrine tumours. *Eur J Nucl Med Mol Imaging* 2012; **39**(Suppl 1): S103-12.
60. Sandström M, Garske U, Granberg D, Sundin A, Lundqvist H. Individualized dosimetry in patients undergoing therapy with (177)Lu-DOTA-D-Phe (1)-Tyr (3)-octreotate. *Eur J Nucl Med Mol Imaging* 2010; **37**: 212-25.
61. Williams SP. Tissue distribution studies of protein therapeutics using molecular probes: molecular imaging. *AAPS J* 2012; **14**: 389-99.
62. Matthews PM, Rabiner EA, Passchier J, Gunn RN. Positron emission tomography molecular imaging for drug development. *Br J Clin Pharmacol* 2012; **73**: 175-86.
63. Ståhl S, Friedman M, Carlsson J, Tolmachev V, Frejd F. Affibody molecules for targeted radionuclide therapy. In: Speer TW, editor. *Targeted radionuclide therapy*. Lippincott Williams & Wilkins; 2011. Chapter 4, p. 49-58.
64. Gomes CM, Abrunhosa AJ, Ramos P, Pauwels EK. Molecular imaging with SPECT as a tool for drug development. *Adv Drug Deliv Rev* 2011; **63**: 547-54.
65. Fondell A, Edwards K, Ickenstein LM, Sjöberg S, Carlsson J, Gedda L. Nuclisome: A novel concept for radionuclide therapy using targeting liposomes. *Eur J Nucl Med Mol Imaging* 2010; **37**: 114-23.
66. Stigbrand T, Carlsson J, Adams GP. Developmental trends in targeted radionuclide therapy - biological aspects. In: Stigbrand T, Adams G, Carlsson J, editors. *Targeted radionuclide tumor therapy, biological aspects*. Springer verlag. Springer Science+Business Media France; 2008, Chapter 21, p. 387-97. ISBN 978-1-4020-8695-3.
67. Persson M, Gedda L, Lundqvist H, Tolmachev V, Nordgren H, Malmstrom PU et al. [177Lu]pertuzumab: experimental therapy of HER-2-expressing xenografts. *Cancer Res* 2007; **67**: 326-31.

Higher levels of total pepsin and bile acids in the saliva as a possible risk factor for early laryngeal cancer

Maja Sereg-Bahar¹, Ales Jerin², Irena Hocevar-Boltezar¹

¹ University Medical Center Ljubljana, Department of Otorhinolaryngology and Head & Neck Surgery, Ljubljana, Slovenia

² University Medical Center Ljubljana, Institute for Clinical Chemistry and Biochemistry, Ljubljana, Slovenia

Radiol Oncol 2015; 49(1): 59-64.

Received 19 January 2014

Accepted 21 March 2014

Correspondence to: Maja Sereg-Bahar, M.D., M.Sc., University Medical Center Ljubljana, Department of Otorhinolaryngology and Head & Neck Surgery, Zaloška cesta 2, 1000 Ljubljana, Slovenia. Phone: +386 41 884 672; Fax: +386 1 522 48 15; E-mail: maja.sereg@kclj.si

Disclosure: No potential conflicts of interest were disclosed.

Background. Gastroesophageal reflux is suspected to be an etiological factor in laryngeal and pharyngeal cancer. The aim of this study was to establish, using a non-invasive method, whether laryngopharyngeal reflux (LPR) appears more often in patients with early laryngeal cancer than in a control group.

Patients and methods. We compared the pH, the level of bile acids, the total pepsin and the pepsin enzymatic activity in saliva in a group of 30 patients with T1 laryngeal carcinoma and a group of 34 healthy volunteers.

Results. The groups differed significantly in terms of levels of total pepsin and bile acids in the saliva sample. Higher levels of total pepsin and bile acids were detected in the group of cancer patients. No significant impact of other known factors influencing laryngeal mucosa (e.g. smoking, alcohol consumption, and the presence of irritating substances in the workplace) on the results of saliva analysis was found.

Conclusions. A higher level of typical components of LPR in the saliva of patients with early laryngeal cancer than in the controls suggests the possibility that LPR, especially biliary reflux, has a role in the development of laryngeal carcinoma.

Key words: laryngopharyngeal reflux; gastric acid; pepsin; bile acids; laryngeal carcinoma

Introduction

Gastroesophageal reflux (GER) disease is caused by the pathological retrograde flow of gastric contents into the esophagus. In laryngopharyngeal reflux (LPR), the gastric contents pass the upper esophageal sphincter and reach the pharynx and the larynx. It is believed that LPR is never physiological, because the mucosa of the upper respiratory tract is more sensitive to gastric contents than the esophageal mucosa.¹

In LPR, the mucosa of the upper aerodigestive tract is exposed to the effects of gastric contents (acid and non-acid reflux). In the case of even minimal biliary reflux, the non-acid reflux consists of pepsin and conjugated bile acids. Acid and non-

acid reflux have a synergistic effect on the mucosa of the upper aerodigestive tract.²

Laryngeal cancer is mentioned as one of the possible extraesophageal complications of GER disease by some authors.¹ In addition, an association between LPR and laryngeal carcinoma has been suggested, though the causality remains unproven. LPR prevalence among patients with laryngeal cancer has been found to be as high as 67%.³⁻⁸

In the present study we tried to identify which components of LPR are present in the saliva of patients with early laryngeal cancer. For this purpose, the levels of the various components of LPR (pepsin, gastric acid and bile acids) in saliva were determined in patients with early laryngeal cancer and in a control group of healthy volunteers.

REFLUX SYMPTOM INDEX – RSI						
Within the last MONTH, how did the following problems affect you?	0 = no problem 5 = severe problem					
1. Hoarseness or a problem with your voice	0	1	2	3	4	5
2. Clearing your throat	0	1	2	3	4	5
3. Excess throat mucus or postnasal drip	0	1	2	3	4	5
4. Difficulty swallowing food, liquids, or pills	0	1	2	3	4	5
5. Coughing after eating or after lying down	0	1	2	3	4	5
6. Breathing difficulties or choking episodes	0	1	2	3	4	5
7. Troublesome or annoying cough	0	1	2	3	4	5
8. Sensations of something sticking in your throat or a lump in your throat	0	1	2	3	4	5
9. Heartburn, chest pain, indigestion, or stomach acid coming up	0	1	2	3	4	5
	Total					

FIGURE 1. Reflux Symptom Index questionnaire.

TABLE 1. Historical data and the results of the RSI questionnaire for patients with early laryngeal carcinoma and the control group

Parameter	T1 N = 30	C N = 34	P
Gender – male / female	25 / 5	21 / 13	0.055
Age (mean /standard deviation – years)	58.8 / 8.1	57.5 / 15.1	0.676
RSI score (mean /standard deviation)	10.8 / 4.3	3.9 / 3.1	0.000
Smokers	29	16	0.000
Number of cigarettes/ day (mean /standard deviation)	24 / 10.4	16.5 / 7.7	0.005
Smoking years (mean /standard deviation)	34.6 / 9.6	22.6 / 11.8	0.000
Regular alcohol consumers	10	17	0.178
Duration of alcohol consumption (mean /standard deviation – years)	29.5 / 12.9	29 / 12.2	0.914
Occupational exposure to irritating substances	28	6	0.000

T1 = patients with T1 laryngeal carcinoma; C = control group; N = number of subjects

Patients and methods

Patients and controls

Thirty successive patients with early laryngeal cancer (T1 squamocellular carcinoma of the vocal folds) admitted to a tertiary center for their first treatment between 2011–2012 and 34 successive healthy volunteers matched by age +/- 5 years (accompanying persons of patients at the general otorhinolaryngological outpatient clinic having no major health problems according to the results of a questionnaire about past pulmonary, cardiac, gastroenterological, neurological, and renal diseases, i.e. the control group) were included in the study. Only those subjects who were willing to under-

take the proposed examinations were included in the study. The study protocol was approved by the National Medical Ethics Committee / number 44/04/04. In both groups, the data on LPR symptoms were obtained through a standardized Reflux Symptom Index (RSI) questionnaire regarding any extraesophageal reflux problems that had been present for at least 5 years (Figure 1).⁹An RSI score > 13 is considered to be a result of LPR.⁹ The participants were asked to fill in a questionnaire about typical GER symptoms (heartburn, regurgitation) and other factors causing similar symptoms as LPR, i.e. smoking habits (smoker/nonsmoker; for smokers: number of cigarettes per day, years of smoking), regular alcohol consumption (intake of more than 140 mg of alcohol per week in men or 70 mg of alcohol per week in women, years of regular alcohol intake), and exposure to irritating substances (wood dust, concrete dust, asbestos, acid fumes, gas vapors) at the workplace (exposed/not exposed). The data about the localization of the T1 laryngeal tumor (the anterior half of the vocal fold, the posterior half of the vocal fold or the entire vocal fold) were obtained from the medical documentation of the patients.

Biochemical analyses

Saliva samples were taken from all the participants, one from each participant. Participants spit their saliva (2ml) through a straw into a testing tube at least two hours after their last meal. Samples were frozen and kept at a temperature below -20 °C until analysed. The pH, the level of total pepsin, the pepsin enzymatic activity and the level of bile acids of the samples were measured.

The pH measurement was conducted using pH indicator papers (Siemens Healthcare, Erlangen, Germany) and the results were rounded up to the nearest half of a unit. The concentrations of bile acids in the saliva samples were measured via the enzyme method using an Olympus AU600 biochemical analyser (Beckman Coulter, Brea, CA, USA) and appropriate reagents (Alere Ltd, Stockport, UK). Bile acids were converted into 3-keto-steroids and thio-NADH in the presence of thio-NAD and 3- α -hydroxy steroid dehydrogenase enzymes (3- α HSD). The speed of the reaction of origin of thio-NADH at 405 nm, which is proportional to the bile acid concentration in the sample, was measured. Bile acid concentration in saliva is given in μ mol/l.

An ELISA (Enzyme-Linked Immunosorbent Assay) specific for human pepsin (USCN Life, Wuhan, China) was used to determine the total

pepsin concentration in the samples. The sample was immobilized on a solid support. A specific antibody linked to a special enzyme was applied over its surface so it could bind to the antigen (pepsin). A substance containing the enzyme's substrate was added. The subsequent reaction produced a detectable signal, a color change in the substrate. Pepsin concentration in saliva was measured in $\mu\text{g/l}$.

The protease enzyme activity was established with a colorimetric test of enzyme activity (PDQ Protease Assay, Protease Determine Quick Test, Athena Sciences, Baltimore, USA). The test substrate contained proteins bound to a fluorescein pigment. In the presence of active pepsin the substrate changed colour. The protease activity was determined spectrophotometrically or fluorometrically. The increase in optical density of the sample was proportional to the increase in pepsin enzymatic activity. Enzyme activity was measured in numbers of kilo units per liter - kU/L.

Statistics

The general data (gender, age), the results of the questionnaire about factors influencing the larynx (smoking habits, alcohol consumption, and the presence of irritating substances in the workplace), the total score of the RSI questionnaire, and the results of the saliva samples' analysis were compared for the group of T1 laryngeal cancer patients and the control group. In order to assess the influence of other factors on the pH value, the levels of bile acids, total pepsin and pepsin enzymatic activity, correlations between the results of the biochemical analysis of the saliva samples and the known etiologic factors for laryngeal cancer, gender and age were performed in the T1 laryngeal cancer group and in the control group. The SPSS 19.0 statistical package (SPSS Inc., Chicago, IL, USA) was used to perform the analyses. The data were analyzed using the χ^2 -test, the Fisher exact test, Pearson's correlation, the Spearman rank correlation, the t-test, and the nonparametric Mann-Whitney test. All the statistical tests were two-sided and a p-value of ≤ 0.05 was considered to be statistically significant.

Results

Compared to the laryngeal carcinoma patients, there were more females ($p = 0.055$) and significantly fewer smokers and those exposed to irritating substances in the control group. No difference in the mean age was observed between the two groups (Table 1). Among patients, the cancer ap-

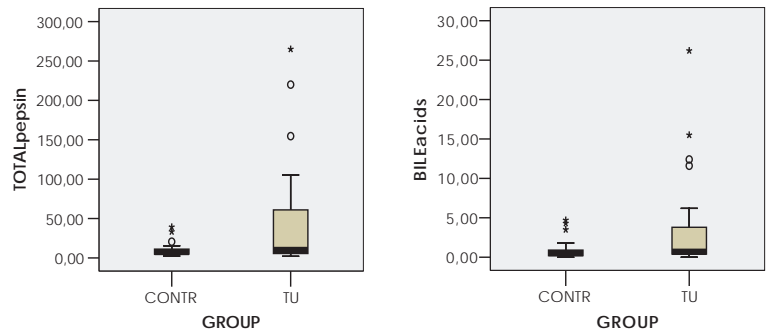


FIGURE 2. Distribution of total pepsin and bile acid concentration in the saliva samples of patients with T1 laryngeal cancer. TU = laryngeal cancer (N = 30); CONTR = control group (N = 34).

TABLE 2. Results of the saliva analysis for patients with T1 laryngeal carcinoma and the control group

Parameter	T1 N = 30	C N = 34	P
Saliva pH / range mean / standard deviation	5.0 - 8.5 7.0 / 0.8	5.0-8.5 7.2 / 0.8	0.382
Bile acids - $\mu\text{mol/L}$ / range mean /standard deviation	0-26.2 3.4 / 5.9	0-4.7 0.9 / 1.2	0.031
Total pepsin - $\mu\text{g/L}$ / range mean / standard deviation	2.1-265 44.6 / 66.8	2.4-39.28 9.6 / 8.1	0.044
Pepsin enzymatic activity - kU/L/ range mean /standard deviation	0.1-35.3 7.7 / 6.9	0.4-30.5 6.2 / 6.3	0.204

T1 = patients with T1 laryngeal carcinoma, C = control group, N = number of participants

peared in the anterior half of a vocal fold in 30 patients (53.6%), in the posterior half of a vocal fold in 3 patients (5.4%), and over the entire vocal fold in 23 patients (41%).

In the group of T1 laryngeal patients, 8 subjects (26.7%) had problems with heartburn and 6 subjects (20%) with regurgitation. There were 8 subjects (26.7%) with at least one typical GER symptom in the T1 laryngeal group. In the control group only one person (2.9%) had problems with regurgitation. In addition, there were 7 patients (23.3%) with an RSI score above 13 whereas none of the controls had an RSI score above 13 (Table 1).

A significant difference between the groups was detected with regard to the level of total pepsin and bile acids in saliva. The mean levels of total pepsin and bile acids in the saliva were more than four times higher in patients with early laryngeal cancer than in the subjects of the control group. No difference in pH or pepsin enzymatic activity was recorded between the two groups (Table 2, Figure 2).

Using correlation analysis we tried to establish whether gender, age, smoking, alcohol intake and exposure to irritants have an impact on the biochemically determined levels of pH, total pepsin,

TABLE 3. Correlations between gender, age, smoking, alcohol intake, presence of irritating substances in the workplace, and the pH value, the levels of bile acids, total pepsin and pepsin enzymatic activity in the patients with T1 laryngeal carcinoma (N = 30)

Parameter	Saliva pH	Bile acids	Total pepsin	Pepsin enzymatic activity
Gender	p=0.753	U=54.5 p=0.776	U=73 p=0.146	U=36 p=0.1,000
Age	r=0.096 p=0.619	rho=-0.014 p=0.943	rho= 0.033 p=0.864	rho=0.080 p=0.693
Smoking	p=1,000	U=14.5 p=0.952	U=13 p=0.905	U=3 p=0.199
Alcohol intake	p=0.820	U=93.5 p=0.945	U=85 p=0.646	U=56 p=0.145
Irritating substances in the workplace	p=0.102	U=94 p=0.963	U=78 p=0.435	U=64 p=0.382

U = Mann Whitney U; r = Pearson's coefficient; rho = Spearman's coefficient

TABLE 4. Correlations between gender, age, smoking, alcohol intake, presence of irritating substances in the workplace, and the pH value, the levels of bile acids, total pepsin and pepsin enzymatic activity in the control group (N = 34)

Parameter	Saliva pH	Bile acids	Total pepsin	Pepsin enzymatic activity
Gender	p=0.873	U=65 p=0.054	U=136.5 p=0.811	U=117 p=0.313
Age	r=0.348 p=0.053	rho=-0.072 p=0.699	rho= -0.245 p=0.170	rho=0.027 p=0.891
Smoking	p=0.099	U=99 p=0.425	U=122.5 p=0.651	U=82 p=0.315
Alcohol intake	p=0.364	U=126 p=0.812	U=144.5 p=0.759	U=130 p=0.275
Irritating substances in the workplace	p=0.053	U=54.5 p=0.571	U=37 p=0.097	U=43 p=0.326

U = Mann Whitney U; r = Pearson's coefficient; rho = Spearman's coefficient

bile acids, and pepsin enzymatic activity in the laryngeal cancer group and in the control group. No significant correlations were found in either group (Table 3).

Discussion

The results of our study established a much higher mean level of bile acids and total pepsin in the saliva of the patients with T1 squamous cell laryngeal carcinoma than in the control group of healthy volunteers. The scores of the standardized RSI questionnaire were also significantly higher in the group of T1 laryngeal carcinoma patients than in the controls. As pepsin and bile acids are excreted only in the gastrointestinal tract below the level of the pharynx, all these results indicate greater retrograde movement of the gastric contents to the level

of the upper aerodigestive tract in patients with early laryngeal carcinoma than in the control group.

Our results confirm the results of other studies that detected LPR in a considerable number of patients with laryngeal cancer using 24-hour ambulatory double pH monitoring.³⁻⁸ However, the exact mode of influence of LPR on laryngeal mucosa has yet to be revealed. The first of the studied parameters, the pH value, was very similar in the group of patients with T1 laryngeal cancer and in the controls. We believe that a much larger volume of saliva excreted in the oral cavity in comparison with the volume of LPR was the reason for such result.

Pepsin enzymatic activity did not differ significantly in the two groups, which could be attributed to the rather similar pH values found among patients and controls. Pepsinogen, the enzymatically inactive precursor of pepsin, is secreted by gastric mucosa cells and transformed into enzymatically active pepsin by gastric acid. However, at a mean pH value of 7.0–7.2, which was the level measured in our patients and controls, pepsin is mostly inactivated.¹⁰

In our study, the level of total pepsin was significantly higher in the T1 laryngeal cancer patients than in the controls. Total pepsin includes active and inactivated pepsin and is, as previously mentioned, a good indicator of LPR. An immunologic pepsin assay of combined sputum and saliva was determined to be 100% sensitive and 89% specific for detection of extraesophageal reflux (based on pH-metry).¹¹

The level of bile acids was also significantly higher in our patients with T1 laryngeal cancer than in the control group. Several studies have shown a significant correlation between subtotal gastrectomy and an increased risk of the development of laryngeal carcinoma. Such patients have pyloric dysfunction, which enables large quantities of biliary reflux to reach the upper aerodigestive tract, causing the occurrence of malignant disease. It has been estimated that 20 years after gastric surgery, patients have a ten times higher risk of laryngeal cancer than the population who had not undergone gastric surgery.^{6, 12}

Smoking, excessive alcohol consumption and occupational exposure to irritating substances are all known etiological factors for laryngeal cancer¹³⁻¹⁵, which case relative high incidence of the disease.¹⁶ It is also known that alcohol intake increases the distal oesophagus exposure to acid reflux.¹⁷ High body mass index (BMI) and longer duration of reflux symptoms are also risk factors for the occurrence of LPR.¹⁹ BMI data were not obtained from

our participants, therefore we cannot discuss the role of BMI in the aetiology of LPR in our study.

In the present study, the group of patients with T1 laryngeal cancer and the control group differed with regard to smoking and exposure to irritants in the workplace, as expected. Because correlation analysis excluded any relationship between these risk factors and the results of biochemical analyses in our participants, it is suggested that the differences in levels of total pepsin and bile acids in saliva between cancer patients and controls are the result of LPR rather than the activity of the above-mentioned factors.

Only subjects considered healthy according to data from the questionnaire about their possible diseases were included in the control group. Of these, only one control subject showed a typical GER symptom (*e.g.* regurgitation). The participants were asked about any extraoesophageal symptoms (RSI protocol) lasting for at least five years. None of the controls had an RSI score above 13. Nevertheless, a certain level of total pepsin, bile acids and pepsin enzymatic activity was also found in the saliva of the majority of the control group. It is possible that the presence of pepsin and bile acids is a sign of flow of the gastric contents to the oesophagus and up to the level of the oral cavity even in completely asymptomatic patients, but the concentrations are lower. A study including a large asymptomatic group would help to determine what levels of the pepsin and bile acids in saliva constitute a normal range.

Laryngeal cancer typically develops in the membranous portion of the vocal folds and rarely in the posterior part of the larynx. It has been suggested that malignant alteration is rare in the posterior part of the larynx where carbonic anhydrase is expressed in the mucosal cells and neutralizes any acid, thereby protecting the mucosa.³ Actually, it has not yet been proven that the gastric contents come in contact with the mucosa of the anterior part of the vocal folds. It has been shown, however, that the hypersensibility of the laryngeal mucosa to the chemical (acid) stimulation of reflux causes the adduction of the vocal folds and closure of the larynx²⁰, thus not allowing the reflux to reach the anterior parts of the vocal folds. There are no data on the effect of biliary reflux on laryngeal sensibility. In the present study, malignant tumors appeared on the posterior part of the vocal fold in only 3 patients. In all other patients, cancers extended over the anterior half or over entire vocal fold. This raises the question of how reflux can directly act on vocal folds' mucosa causing malignant changes.

The main drawback of our study is that there were some differences between the cancer patient group and the control group. A different gender ratio in both groups was noticed. There were 83% men and 17% women in the T1 cancer group, and 62% men and 38% women in the control group. Although the difference was noticeable, it was not statistically significant.

The groups also differed with regard to smoking habits and exposure to irritating substances in the work place. Smoking is a known risk factor for laryngeal cancer. Therefore it was expected that the majority of the laryngeal cancer patients would be smokers. The data on smoking, alcohol intake and workplace were obtained because these factors can cause similar laryngeal and pharyngeal symptoms as LPR. When the correlations between smoking, irritating substances in the workplace, and the results of saliva testing were performed, no significant results were found.

A larger number of included subjects would give firmer proof of the role of LPR in the etio-pathogenesis of laryngeal cancer. Our results for the group of 30 patients and 34 controls suggest a possible role for LPR. In order to really prove that LPR is a risk factor for laryngeal cancer, only those patients with laryngeal cancer who are nonsmokers and not exposed to noxious substances in the workplace should be included in the study.

Furthermore, it remains unclear how pepsin and bile acids, which can cause malignant alteration in the mucosa, come in contact with the vocal folds.

Conclusions

Significantly higher levels of LPR components in the saliva of patients with T1 laryngeal carcinoma may indicate that LPR plays a role in the development of laryngeal carcinoma.

A further study of LPR's role in the etiology of laryngeal carcinoma is necessary, especially in patients with no other known cancer risk factors, *i.e.* smoking, alcohol consumption or exposure to irritating substances in the workplace.

References

1. Koufman JA, Dettmar PW, Johnston N. Laryngopharyngeal reflux (LPR). *ENT News* 2005; **14**: 42-5.
2. De Corso E, Baroni S, Agostino S, Cammarota G, Mascagna G, Mannocci A, et al. Bile acids and total bilirubin detection in saliva of patients submitted to gastric surgery and in particular to subtotal billroth II resection. *Ann Surg* 2007; **245**: 880-5.

3. Tae K, Jin BJ, Ji YB, Jeong JH, Cho SH. The role of laryngopharyngeal reflux as a risk factor in laryngeal cancer: A preliminar report. *Clin Exp Otorhinolaryngol* 2011; **4**: 101-4.
4. Dagli S, Dagli U, Kurtaran H, Alkim C, Sahin B. Laryngopharyngeal reflux in laryngeal cancer. *Turk J Gastroenterol* 2004; **15**: 77-81.
5. Lewin JS, GillenwaterAM, Garret JD. Characterization of laryngopharyngeal reflux in patients with premalignant or early carcinomas of the larynx. *Cancer* 2003; **97**: 1010-4.
6. Galli J, Cammarota G, Volante M, De Corso E, Almadori G, PaludettiG. Laryngeal carcinoma and laryngo-pharyngeal reflux disease. *Acta Otorhinolaryngol Ital* 2006; **26**: 260-3.
7. Quadeer MA, Lopez R, Wood BG. Does acid suppressive therapy reduce the risk of laryngeal cancer recurrence? *Laryngoscope* 2005; **115**: 1877-81.
8. Copper MP, Smit CF, Stanojic LD, Devriese PP, Schouwenburg PF Mathus-Vliegen LM. High incidence of laryngeal reflux in patients with head and neck cancer. *Laryngoscope* 2000; **110**: 1007-11.
9. Belafsky PC, Postma GN, Koufman JA. Validity and reliability of the reflux Symptom Index (RSI). *J Voice* 2002; **16**: 274-7.
10. Samuels TL, Johnston N. Pepsin as a marker of extraesophageal reflux. *Ann Otol Rhinol Laryngol* 2010; **119**: 203-8.
11. Knight J, Liveloy MO, Johnston N, Dettmar PW, Koufman JA. Sensitive Pepsin immunoassay for detection of laryngopharyngeal reflux. *Laryngoscope* 2005; **115**: 1473-8.
12. Buyukasik O, Hasdemir AO, Gulnerman Y, Col C, Ikiz O. Second primary cancers in patients with gastric cancer. *Radiol Oncol* 2010; **44**: 239-43.
13. La Vecchia C, Zhang ZF, Altieri A. Alcohol and laryngeal cancer: an update. *Eur J Cancer Prev* 2008; **17**: 116-24.
14. Hashibe M, Boffetta P, Zaridze D, Shangina O, Szeszenia-Dabrowska N, Mates IN, et al. Contribution of tobacco and alcohol to the high rates of squamous cell carcinoma of the supraglottic and glottic in Central Europe. *Am J Epidemiol* 2007; **165**: 814-20.
15. Elci OC, Akpınar-Elci M. Occupational exposures and laryngeal cancer among non-smoking and non-drinking men. *Int J Occup Environ Health* 2009; **15**: 370-3.
16. Peszynska-Piorun M, Malicki J, Golusinski W. Doses in organs at risk during head and neck radiotherapy using IMRT and 3D-CRT. *Radiol Oncol* 2012; **46**: 328-36.
17. Vitale GC, Cheadle WG, Patel B, Sadek Sa, Michel ME, Cusechieri A. The effect of alcohol on nocturnal gastroesophagealrefluku. *JAMA* 1987; **16**: **258**: 2077-9.
18. Majchrzak E, Szybiak B, Wegner A, Pienkowski P, Pazdrowski J, Luczewski L, et al. Oral cavity and oropharyngeal squamous cell carcinoma in young adults: a review of the literature. *Radiol Oncol* 2014; **48**: 1-10.
19. Saruc M, Aksoy EA, Vardereeli E, Karaaslan M, Cicek B, Ince U et al. Risk factors for laryngopharyngeal reflux. *Eur Arch Otorhinolaryngol* 2012; **269**: 1189-96.
20. Phua SY, McGarvey L, Ngu M, Ing A. The differential effect of gastroesophageal reflux disease on mechanostimulation and chemostimulation of the laryngopharynx. *Chest* 2010; **138**: 180-5.

Hypodontia phenotype in patients with epithelial ovarian cancer

Anita Fekonja¹, Andrej Cretnik², Danijel Zerdoner^{2,3}, Iztok Takac^{2,4}

¹ Department of Orthodontics, Health Centre Maribor, Maribor, Slovenia

² Medical Faculty, University of Maribor, Maribor, Slovenia

³ Department of Maxillofacial and Oral Surgery, Teaching Hospital Celje, Celje, Slovenia

⁴ Department of Gynaecologic and Breast Oncology, Clinical Department of Gynaecology and Perinatology, University Clinical Centre Maribor, Maribor, Slovenia

Radiol Oncol 2015; 49(1): 65-70.

Received: 31 December 2013

Accepted: 27 April 2014

Correspondence to: Anita Fekonja, D.M.D., Department of Orthodontics, Health Centre Maribor, Ulica Talcev 9, SI-2000 Maribor, Slovenia.
E-mail: anita.fekonja1@guest.arnes.si

Disclosure: No potential conflicts of interest were disclosed.

Background. Ovarian cancer is usually diagnosed in an advanced stage and the present clinical and diagnostic molecular markers for early OC screening are insufficient. The aim of this study was to identify potential relationship between the hypodontia and epithelial ovarian cancer (EOC).

Patients and methods. A retrospective study was conducted on 120 patients with EOC treated at the Department of Gynaecologic and Breast Oncology at the University Clinical Centre and 120 gynaecological healthy women (control group) of the same mean age. Women in both groups were reviewed for the presence of hypodontia and the patients with EOC also for clinicopathological characteristics of EOC according to hypodontia phenotype.

Results. Hypodontia was diagnosed in 23 (19.2%) of patients with EOC and 8 (6.7%) controls ($p = 0.004$; odds ratio [OR] = 3.32; confidence interval [CI], 1.42–7.76). There was no statistically significant difference in patients with EOC with or without hypodontia regarding histological subtype ($p = 0.220$); they differed in regard to FIGO stage ($p = 0.014$; OR = 3.26; CI, 1.23–8.64) and tumour differentiation grade ($p = 0.042$; OR = 3.1; CI, 1.01–9.53). Also, bilateral occurrence of EOC was more common than unilateral occurrence in women with hypodontia ($p = 0.021$; OR = 2.9; CI, 1.15–7.36).

We also found statistically significant difference between the ovarian cancer group and control group in presence of other malignant tumours in subjects ($p < 0.001$).

Conclusions. The results of the study suggest a statistical association between EOC and hypodontia phenotype. Hypodontia might serve as a risk factor for EOC detection.

Key words: hypodontia; epithelial ovarian cancer; risk factor; early stage diagnosis

Introduction

Ovarian cancer is the most fatal malignancy of the female genital tract in the Western world.¹⁻³ In Slovenia, ovarian cancer is the eighth overall and the second most common gynaecologic cancer (after endometrial one).¹ Nonspecific symptoms, lack of reliable (bio)markers, frequent diagnosis in advanced stage (approximately 75–80% of ovarian cancers are diagnosed in stage III–IV), and the presence of drug-resistant histologic types limit the long-term cure rates and prognosis of the dis-

ease.^{4,7} Ovarian cancer is usually seen in peri- or postmenopausal women.^{1,5} Multiple reproductive, demographic and lifestyle factors are known to influence a woman's risk of developing this cancer, but, the strongest known risk factor is a positive family history.^{5,8-11} Approximately 5–10% of ovarian cancer occurs in those known to carry BRCA mutations, depending on the population or ethnic group. In women with a family history of breast or ovarian cancer and a known BRCA mutation, the cumulative lifetime risk of developing the disease has been estimated to be approximately 40–50% for

BRCA1 and 20–30% for BRCA2, compared with an approximate 1.6% lifetime risk in the general population.^{11,12} In hereditary nonpolyposis colorectal cancer families (also known as Lynch II syndrome) lifetime risk of ovarian cancer in carriers of mismatch repair gene mutation is around 6.7–12%.^{5,11} However, these known gene faults do not account for all of the inherited risk in women with a family history of ovarian cancer. Other »high risk« ovarian cancer genes may exist, although mutations in these genes are probably less common than BRCA1 and BRCA2. It is likely that much of the remaining familial risk is due to a combination of several genes that each individual contributes, rise to a low or moderate risk.¹¹

In our (dental) clinical practice we have seen more frequent positive self-reported family history of some disease (colorectal cancer, ovarian cancer, thyroid disease) in patients with hypodontia than those without hypodontia.

A congenital anomaly affecting the formation of the dentition that results in a reduction of the usual number of the human deciduous dentition (20 total teeth in both jaws) and/or the permanent dentition (a total of 32 teeth in both jaws) is commonly referred to as aplasia. The term hypodontia is used when one to five teeth, excluding the third molar, are absent. The condition, when more than five teeth, excluding the third molar, are absent, is called oligodontia. Anodontia is an extreme case, denoting the complete absence of teeth.¹³

Dental agenesis is an important clinical and public health problem. Patients with hypodontia may suffer from a reduced chewing ability, inarticulate speech, and an unfavourable aesthetic appearance. Comprehensive management often requires a multidisciplinary approach. The reported prevalence of hypodontia in the permanent dentition in population vary from 2.6% to 11.3%^{14,15}, being lower in North America than in European countries.¹⁶ In the Caucasian population the most frequently affected teeth were lower second premolars, followed by the maxillary lateral incisors and the upper second premolars. Most studies showed a higher prevalence of hypodontia in females.¹⁵⁻¹⁷

The aetiology of hypodontia is multifactorial with major genetic and environmental factors. Hereditary or family history has been suggested as the primary cause for hypodontia.¹⁶ In familial hypodontia, the type of inheritance in the majority of families seems to be autosomal dominant with incomplete penetrance and variable expression. Sex-linked and polygenic models of inheritance are also possible.¹⁸ Various genes including

PAX9, MSX1 and AXIN2 have been implicated in the aetiology of hypodontia.^{19,20} The AXIN2 gene regulates the *Wnt* signalling pathway, which plays an important role in the cellular proliferation, differentiation and morphogenesis of most organs, and control of β -catenin stability is central to *Wnt* signalling. Defects that interfere with β -catenin regulation have been reported in various human cancers. The *Wnt* pathway has been well studied in a number of cancers where β -catenin mutations could be identified (like in colorectal cancer).²⁰⁻²² In ovarian cancer, however, the detection of a high-rate of β -catenin mutations (approximately 40%) was confined to the endometrioid subtype of epithelial ovarian cancer.²³

On the other hand, it has been suggested that a major hereditary contribution to cancer is given by largely unknown alleles of low penetrance and some of these alleles may also contribute to the background of tooth agenesis. It is conceivable that defects in other genes, in addition to AXIN2, involved in *Wnt* signalling and regulation of β -catenin level may also show a link between tooth agenesis and cancer predisposition. However, relationship among hypodontia and other pathological conditions, such as the colorectal cancer, has already been shown²¹ and if a link between hypodontia and ovarian cancer could be established, this could serve as a potential risk factor for detection of ovarian cancer, particularly in earlier stages.

The aim of the study was to identify a possible correlation between hypodontia phenotype and epithelial ovarian cancer (EOC). Therefore, this study sought to evaluate and compare the International Federation of Gynecology and Obstetrics (FIGO) stage, the histologic subtype, the grade, the side of tumour according to the presence of hypodontia phenotype. We also analysed the family history of ovarian cancer and other cancer in both groups.

Patients and methods

The study included 120 consecutive patients with histologically proven EOC who were treated at the Department of Gynaecologic and Breast Oncology at the University Clinical Centre Maribor, and 120 gynaecological healthy women who had given their formal consent after receiving an explanation about the aim of this study. The study was approved by the Ethics Committee at the Ministry of Health of Slovenia.

Clinic pathological characteristics of patients, including age at diagnosis of the EOC, definitive

FIGO stage, postoperative histologic subtypes, postoperative tumour grade, and side of tumour (unilateral/bilateral) were collected from medical records. Tumours were classified as FIGO stage, using the grading system proposed by Benedet.²⁴

One-hundred-twenty gynaecological healthy women (of the same mean age as study group) represented control group, which was confirmed by general gynaecological examination, including the transvaginal ultrasound. In the control group exclusionary criteria included women with any ovarian abnormalities as assessed by transvaginal ultrasound to detect abnormal ovarian morphology, which is an indicator of a potential malignancy. Dental examination for all subjects was conducted at the Department of Orthodontics in Health Centre Maribor. A tooth was registered as congenitally missing when no trace could be found on the radiograph and the dental treatment records confirmed that the tooth had not been extracted. Third molars were not included in the research. Other teeth abnormalities, such as microdontia, were excluded from criteria to denote hypodontia phenotype. Women with dentures or women in whom we can not determine the cause of missing teeth were not included in the study. No subjects had cleft lip/palat or any syndrome. We interviewed each subject about her family history of cancer. If at least one family member had had cancer, that participant was considered to have a family history of cancer. Data were collected between December 1st, 2010 and October 24th, 2013 and analysed statistically.

Statistical analysis

Descriptive statistics were used to present baseline characteristics. Unpaired (two-sample) t-test at a significance level of < 0.05 was used to assess the differences in age between the EOC patients and the control group. We analysed the difference in prevalence rates of hypodontia among the EOC patients and the gynaecological healthy women (control group), and the difference in FIGO stage, histologic subtypes, tumour differentiation grades, and the tumour bilateralism between EOC patients with and without hypodontia using chi-square test or Fisher exact test with a p value of < 0.05 as a standard for a statistically significant difference. To determine the relationship between hypodontia and ovarian cancer we used logistic regression model. The results were presented as odds ratios (OR) with corresponding 95% confidence interval (CI).

TABLE 1. FIGO stage and histologic types of tumours in study groups

CHARACTERISTICS	WITH HYPODONTIA	WITHOUT HYPODONTIA
FIGO STAGE*		
Stage I	7 (30.4%)	57 (58.8%)
Stage II	4 (17.4%)	7 (7.2%)
Stage III	8 (34.8%)	28 (28.9%)
Stage IV	4 (17.4%)	5 (5.1%)
HISTOLOGIC SUBTYPES**		
Papillary serous adenocarcinoma	18 (78.3%)	63 (64.9%)
Mucinous cystadenocarcinoma	1 (4.3%)	15 (15.5%)
Endometrioid carcinoma	3 (13.1%)	13 (13.4%)
Clear cell carcinoma	1 (4.3%)	0 (0%)
Malignant Brenner tumour	0 (0%)	3 (3.1%)
Mixed tumour	0 (0%)	2 (2.1%)
Undifferentiated carcinoma	0 (0%)	1 (1.0%)

* $\chi^2 = 8.826$; $p = 0.014$

** $\chi^2 = 7.853$; $p = 0.220$

Results

The mean (standard deviation [SD]) age of the EOC patients at time of diagnosis was 53.1 (11.1) with a median of 53 years, and mean (SD) age of the control group was 53.3 (10.7) with a median of 54 years ($p = 0.878$).

In 120 patients with EOC, hypodontia phenotype was found in 23 (19.2%) patients and in eight out of 120 healthy individuals (6.7%). The difference between these two hypodontia rates was statistically significant ($p = 0.004$). The data also showed that the OR was 3.32 (95% CI, 1.42–7.76).

In Table 1 further analysis of the women with EOC (study group) with or without hypodontia is presented (FIGO stage and histology). Statistically significant difference was found in FIGO stage ($p = 0.014$; OR = 3.26; 95% CI, 1.23–8.64). Histopathological analysis showed predominantly serous subtype of epithelial ovarian cancer in women with and without hypodontia and no significant differences between groups regarding definitive histology ($p = 0.220$).

Most (64.7%) of the invasive tumours in patients with hypodontia were poorly differentiated tumours, 17.6 % moderately and 17.6 % highly differentiated, whether in women without hypodontia poorly differentiated, moderately differentiated, and highly differentiated ones were observed almost at the same range (37.1 %, 37.1 %, and 25.8 %).

TABLE 2. Distribution of tumors according to its presence unilaterally or bilaterally

Study group	Unilaterally		Bilaterally
	Right	Left	
With hypodontia (n=23)	7 (30.4%)	3 (13.1%)	13 (56.5%)
Without hypodontia (n=97)	34 (35.1%)	33 (34%)	30 (30.9%)

$\chi^2 = 5.296$; $p = 0.021$

TABLE 3. Presence of malignant tumours in subjects and family members according to hypodontia

	Study group	Control group	P-value
All other malignant tumours in subjects	32 (26.7%)	9 (7.5%)	< 0.001
Family history of ovarian cancer	9 (7.5%)	7 (5.8%)	0.617
Family history of other malignant tumour	65 (54.2%)	62 (51.7%)	0.698

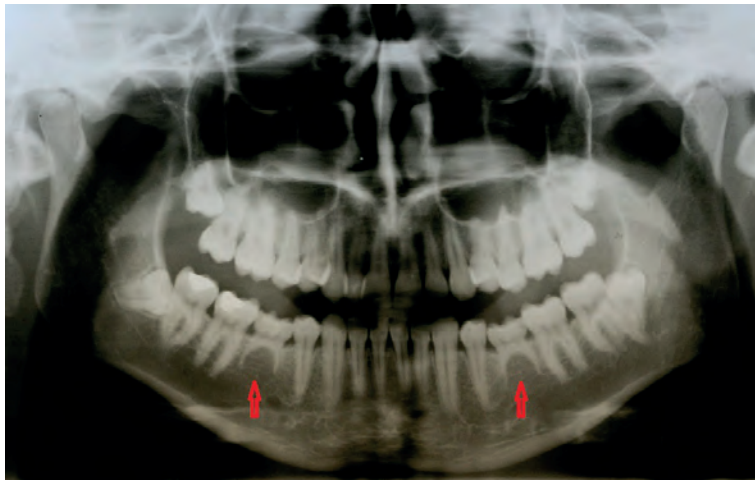


FIGURE 1. Hypodontia of both lower second premolars (persistent deciduous second molars).

In patients with epithelial ovarian cancer and hypodontia, we observed a significantly higher proportion of poorly differentiated tumours (high-grade tumour malignancy, gradus 3) than in patients without hypodontia (64.7 % in 37.1 %, $p = 0.042$). Patients with hypodontia have 3.1 (95% CI, 1.01–9.53) times the odds ratio as patients without hypodontia of having poorly differentiated tumours (gradus 3).

In 56.5% of our patients with hypodontia and in 30.9% of patients without hypodontia ovarian cancer was bilateral ($p = 0.021$; OR = 2.9; 95 % CI, 1.15–7.36) (Table 2).

We also found statistically significant difference in presence of other malignant tumours in sub-

jects between the ovarian cancer group and control group ($p < 0.001$). Most commonly reported additional malignant tumours in study group were breast, uterus, intestine and colon, and thyroid carcinoma and breast carcinoma in control group, but without statistically significant difference in tumours types between groups. Otherwise no other statistically significant differences were found in family history (Table 3).

Discussion

Ovarian cancer, known as the silent killer in women, is difficult to diagnosis due to a lack of effective early screening markers for this disease. Without improvements in the current early detection protocols, over 75% of women diagnosed with ovarian cancer will be identified in late stage of disease with a significantly reduced chance of survival.

Lopes *et al.*²⁵ reported that anomalies of the teeth may be present in many diseases and dentists may be the first to notice them particularly through the preventive children screening programmes (obligatory in Slovenia). Previous studies have demonstrated that the genes that control the tooth development may have an important function in other organs and cancer diseases.^{21,26} Zhai *et al.*²⁷ indicated in their study that β -catenin and TCF plays a vital role in the activation of AXIN2 expression in colon and ovarian cancer cells. Lammi *et al.*²¹ reported about evidence of the expression of association AXIN2 in colorectal tissue leading to carcinoma and hypodontia in a Finnish family. It is interesting that one gene mutation can cause tooth agenesis and predispose to colorectal cancer. Although 10% of ovarian cancer is familial and the majority of the inherited types are related to mutations in the BRCA1 and BRCA2 genes⁸, other unknown genetic mutations may play a crucial role as well.

We found only one paper in the literature showing possible association between teeth anomalies and epithelial ovarian cancer (EOC) by Chalothorn *et al.*²⁸ Authors found low prevalence of hypodontia in control group (3%; 3/100), despite they included patients with microdontia and hypodontia and 20% prevalence (10/50) in patients with EOC with statistically significant difference between groups. In our study only patients with hypodontia were included. The present study revealed hypodontia phenotype prevalence in 19.2% and 6.7% for the EOC group and control group, respectively.

The prevalence of hypodontia in population varies quite a lot. Mattheeuws *et al.*¹⁶ reported

prevalence of hypodontia in meta-analysis in the Caucasian population within 3.9–10.1%. Study by Fekonja²⁹ showed 6.9% (7.8% in female and 5.9% in male) hypodontia prevalence in Maribor population (Slovenia). Results of our study show higher hypodontia prevalence in women with EOC, while the prevalence of control group was similar to Slovenian population.²⁹ As hypodontia can be diagnosed early in the life (by radiographs as early as age nine), a possible association between hypodontia phenotype and EOC could serve as the earliest possible quantifying risk factor for the EOC, before the development of clinical evident disease (Figure 1).

In the study we also evaluated the FIGO stages, the histological subtypes, and tumour grades. Other authors reported that over 75% of patients are diagnosed at the advanced stage, when cancer has already metastasized, because of non-specific clinical symptoms.^{4,7} In our study 69.6% patients with hypodontia and 41.2% patients without hypodontia were diagnosed in stage II, III, or IV. Screening protocols for women with hypodontia could be of a great help in detecting ovarian cancer in earlier stage with potential better curing possibilities and prognosis.

As reported by other authors³⁰, serous carcinoma is the most common histological subtype of ovarian cancer, what was also found in our study (78.3% ovarian serous carcinoma in patients with hypodontia corresponding to 64.9% in the group without hypodontia).

But³¹ reported that 46 % EOC were poorly differentiated, 38.1% moderately and 15.9% highly differentiated tumours. In our study also predominated poorly differentiated tumours (43%), followed by moderately (33%) and highly (24%) differentiated. According to the hypodontia we founded the majority (64.7%) of poorly differentiated tumours in patients with hypodontia, whether in women without hypodontia moderately differentiated, highly differentiated and poorly differentiated ones were observed almost at the same range.

In our study we also evaluated the uni- or bilateralism of EOC occurrence. In 23 patients with hypodontia the tumour was bilateral in 13 patients (56.5%) and unilateral in 10 patients (43.5%). In 97 patients without hypodontia the tumours were bilateral in 30 subjects (30.9%) and unilateral in 67 subjects (69.1%). We can conclude that there might be a trend toward more frequent bilateralism in patients with hypodontia.

In our study there was statistically significant difference in patients with EOC with or without hypodontia regarding FIGO stage ($p = 0.014$; OR

$= 3.26$; CI, 1.23–8.64), tumour differentiation grade ($p = 0.042$; OR = 3.1; CI, 1.01–9.53), and bilateralism ($p = 0.021$; OR = 2.9; CI, 1.15–7.36), but no statistically significant difference was found in histological subtype ($p = 0.220$). However, in the multivariate model the relationship of hypodontia with the FIGO stage, tumour differentiation grade, bilateralism and histological subtype of EOC could not be confirmed ($p = 0.368$). Chalothorn *et al.*²⁸ did not report of any clinicopathological characteristics of the tumour in their study so we can not compare their findings with our results.

Kücher *et al.*²⁶ reported that individuals with hypodontia had an increased risk of having a family history of breast, ovarian, and cervical uterine cancer. In our study we confirmed the correlation between hypodontia and other malignant tumours, but no significant difference between hypodontia and family history of ovarian or other malignant tumours.

In conclusion, this study indicated statistically significant association between EOC and hypodontia phenotype. Congenital absence of permanent teeth has direct visual implication and could identify patients with hypodontia phenotype and serve as a possible risk factor for EOC detection. The results of this study suggest that more research in this topic is needed to be able to identify genetic markers, which, combined with the presence of missing teeth, could identify women of greatest risk for developing EOC in their lifetime at a much younger age than previously possible.

References

1. *Cancer in Slovenia 2010*. Ljubljana: Institute of Oncology Ljubljana, Epidemiology and Cancer Registry, Cancer Registry of Republic of Slovenia; 2011. p. 37.
2. *Cancer Research UK*. Statistical Information Team; 2012. Available at: <http://www.info.cancerresearchuk.org/cancerstats>
3. *United States cancer statistics: 1999-2008 incidence and mortality Wb-based report*. Atlanta (GA): Department of Health and Human Services, Centers for Disease Control and Prevention, and National Cancer Institute; 2010. Available at: <http://www.cdc.gov/uscs>
4. Zhang B, Cai FF, Zhong XY. An overview of biomarkers for the ovarian cancer diagnosis. *Eur J Obstet Gynecol Reprod Biol* 2011; **158**: 119-23.
5. Lalwani N, Prasad SR, Vikram R, Shanbhogue AK, Huetter PC, Fasih N. Histologic, molecular, and cytogenetic features of ovarian cancers: implications for diagnosis and treatment. *Radio Graphics* 2011; **31**: 625-46.
6. Paulsen T, Kaern J, Kjaerheim K, Tropé C, Tretli S. Symptoms and referral of women with epithelial ovarian tumors. *Int J Gynecol Obstet* 2005; **88**: 31-7.
7. Wikborn C, Pettersson F, Silfverswärd C, Moberg PJ. Symptoms and diagnostic difficulties in ovarian epithelial cancer. *Int J Gynecol Obstet* 1993; **42**: 261-4.
8. Stratton JF, Pharoah P, Smith SK, Easton D, Ponder BA. A systematic review and meta-analysis of family history and risk of ovarian cancer. *Br J Obstet Gynaecol* 1998; **105**: 493-9.

9. Takač I, Arko D. Diagnosis and treatment of ovarian cancer. In: Štabuc B, editor. *Gynecological cancer/ XVI. Course in memoriam dr. Dušana Reje*. Ljubljana: Zveza slovenskih društev proti raku; 2008. p. 41-8.
10. Benedet JL. Progres in gynecologic cancer detection and treatment. *Int J Gynecol Obstet* 2000; **70**: 135-47.
11. Bolton KL, Ganda C, Berchuck A, Pharaoh PDP, Gayther SA. Role of common genetic variants in ovarian cancer susceptibility and outcome: progress to date from the ovarian cancer association consortium (OCAC). *J Intern Med* 2012; **271**: 366-78.
12. Zweemer RP, Verheijen RHM, Menko FH. Differences between hereditary and sporadic ovarian cancer. *Eur J Obstet Gynecol Reprod Biol* 1999; **82**: 151-3.
13. Peker I, Kaya E, Darendeliler-Yaman S. Clinic and radiographical evaluation of non - syndromic hypodontia and hyperdontia in permanent dentition. *Med Oral Patol Oral Cir Bucal* 2009; **14**: 393-7.
14. Silva Meza R. Radiographic assessment of congenitally missing teeth in orthodontic patients. *Int J Pediatr Dent* 2003; **13**: 112-6.
15. Pemberton TJ, Das P, Patel PI. Hypodontia: genes and future perspectives. *Braz J Oral Sci* 2005; **4**: 695-706.
16. Mattheeuws N, Dermaut L, Martens G. Has hypodontia increased in Caucasians during the 20th century? A meta-analysis. *Eur J Orthod* 2004; **26**: 99-103.
17. Poldner BJ, Van't Hof MA, Van der Linden FP, Kuijpers Jagtmas AM. A meta-analysis of the prevalence of dental agenesis of permanent teeth. *Community Dent Oral Epidemiol* 2004; **32**: 217-26.
18. Peck L, Peck S, Attia Y. Maxillary canine-first premolar transposition, associated dental anomalies and genetic basis. *Angle Orthod* 1993; **63**: 99-109.
19. Thesleff I. Epithelial-mesenchymal signalling regulating tooth morphogenesis. *J Cell Science* 2003; **116**: 1647-8.
20. Mostowska A, Biedziak B, Jagodzinski PP. Axis inhibition protein 2 (AXIN2) polymorphisms may be a risk factor for selective tooth agenesis. *J Hum Genet* 2006; **51**: 262-6.
21. Lammi L, Arte S, Somer M, Järvinen H, Lahermo P, Thesleff I, et al. Mutations in AXIN2 cause familial tooth agenesis and predispose to colorectal cancer. *Am J Hum Genet* 2004; **74**: 1043-50.
22. Schmid S, Bieber M, Zhang F, Zhang M, He B, Jablons D, et al. Wnt and Hedgehog gene pathway expression in serous ovarian cancer. *Int J Gynecol Cancer* 2011; **21**: 975-80.
23. Wu R, Zhai Y, Fearon ER, Cho KR. Diverse mechanisms of beta-catenin deregulation in ovarian endometrioid adenocarcinomas. *Cancer Res* 2001; **61**: 8247-55.
24. Benedet JL. Staging classifications and practice guidelines for gynecologic cancer. *Int J Gynecol Obstet* 2000; **70**: 207-312.
25. Lopes NN, Petrilli AS, Caran Em, França CM, Chilvarquer I, Lederman H. Dental abnormalities in children submitted to antineoplastic therapy. *J Dent Child* 2006; **73**: 210-3.
26. Küchler EC, Lips A, Tannure PN, Ho B, Costa MC, Granjeiro JM, et al. Tooth agenesis association with self-reported family history of cancer. *J Dent Res* 2013; **92**: 149-55.
27. Zhai Y, Wu R, Schwartz DR, Darrah D, Reed H, Kolligs FT, et al. Role of β -Catenin /T-Cell Factor-regulate genes in ovarian endometrioid adenocarcinoma. *Am J Pathol* 2002; **160**: 1229-38.
28. Chalothorn LA, Beeman CS, Ebersole JL, Kluemper GT, Hicks EP, Kryscio RJ, et al. Hypodontia as a risk marker for epithelial ovarian cancer: a case-controlled study. *J Am Dent Assoc* 2008; **139**: 163-9.
29. Fekonja A. Hypodontia prevalence over four decades in Slovenian population. *J Esthet Restor Dent* 2013; doi: 10.1111/jerd.12076. [Epub ahead of print].
30. Lurie G, Wilkens LR, Thompson PJ, Matsuno RK, Carney ME, Goodman MT. Symptom presentation in invasive ovarian carcinoma by tumor histological type and grade in a multiethnic population: a case analysis. *Gynecol Oncol* 2010; **119**: 278-84.
31. But I. *DNA ploidy and CA 125 in serous ovarian carcinoma* [Doctoral Thesis]. Ljubljana: Faculty of Medicine, University of Ljubljana; 1998.

Consolidation electrochemotherapy with bleomycin in metastatic melanoma during treatment with dabrafenib

Sara Valpione¹, Luca G. Campana², Jacopo Pigozzo¹, Vanna Chiarion-Sileni¹

¹ Melanoma Oncology Unit, Veneto Region Oncology Research Institute (IOV-IRCCS), Padova, Italy

² Melanoma and Sarcoma Unit, Veneto Region Oncology Research Institute (IOV-IRCCS), Padova, Italy

Radiol Oncol 2015; 49(1): 71-74.

Received 10 June 2014

Accepted 31 July 2014

Correspondence to: Dr. Sara Valpione, 64 Gattamelata St, 35128 Padova, Italy. E-mail: sara.valpione@unipd.it

Disclosure: No potential conflicts of interest were disclosed.

Background. Small molecules that inhibit V600 mutated BRAF protein, such as vemurafenib and dabrafenib, are effective in treatment of metastatic melanoma.

Case report. We here describe the clinical course of a V600E BRAF mutated metastatic melanoma patient with systemic disease, who developed tumor progression on superficial soft-tissue metastases during treatment with dabrafenib. Bleomycin electrochemotherapy during dabrafenib treatment was administered to control the soft-tissue progressing metastases and ensured sustained local control without significant toxicity.

Conclusions. The new combined approach maintained the patient quality of life and allowed for the prosecution of the target therapy, which proved to be still effective on systemic disease, up to 17 months.

Key words: dabrafenib; electrochemotherapy; melanoma; BRAF inhibitors; bleomycin

Background

In the last years, the treatment of V600 BRAF mutated metastatic melanoma patients has radically changed. Small molecules that inhibit V600 mutated BRAF protein, such as vemurafenib and dabrafenib, are now available and provide unprecedented response rates ranging to 50%^{1,2}, with median progression free survival of approximately 6 months. Further, the combination of BRAF inhibitors (BRAFi) and MEK inhibitors (*i.e.*, trametinib or cobimetinib) ensured even more striking results, with response rates ranging to 70% and progression free-survival raising to approximately 10 months.³ The main toxicity related to BRAFi treatment is cutaneous, which, despite being not dose limiting in most cases, may impact on patient quality of life, that should instead be a priority in the context of the advanced phase of the disease.⁴

In order to further improve the outcome of patients with metastatic melanoma, researchers are

exploring BRAFi in combination with other approaches. Unfortunately, the attempt of combining BRAFi with new immunoregulatory molecules such as anti-CTLA4 ipilimumab failed due to the increase of liver and skin toxicities⁵, and no data are available about combination with chemotherapy.

Another approach under active investigation is represented by the association of BRAFi with other locoregional treatments as radiotherapy and isolated limb perfusion. Although the best schedule of radiation and BRAFi remains to be established, this approach has shown an acceptable tolerability in preliminary experiences in patients with brain metastases.⁶ In this context, a sensitizing effect leading to enhanced cutaneous toxicity has been reported when BRAFi was concomitant with radiation and therefore should be carefully considered.⁷

Electrochemotherapy (ECT) is a combined locoregional treatment which has shown sustained activity in different tumor histotypes, including

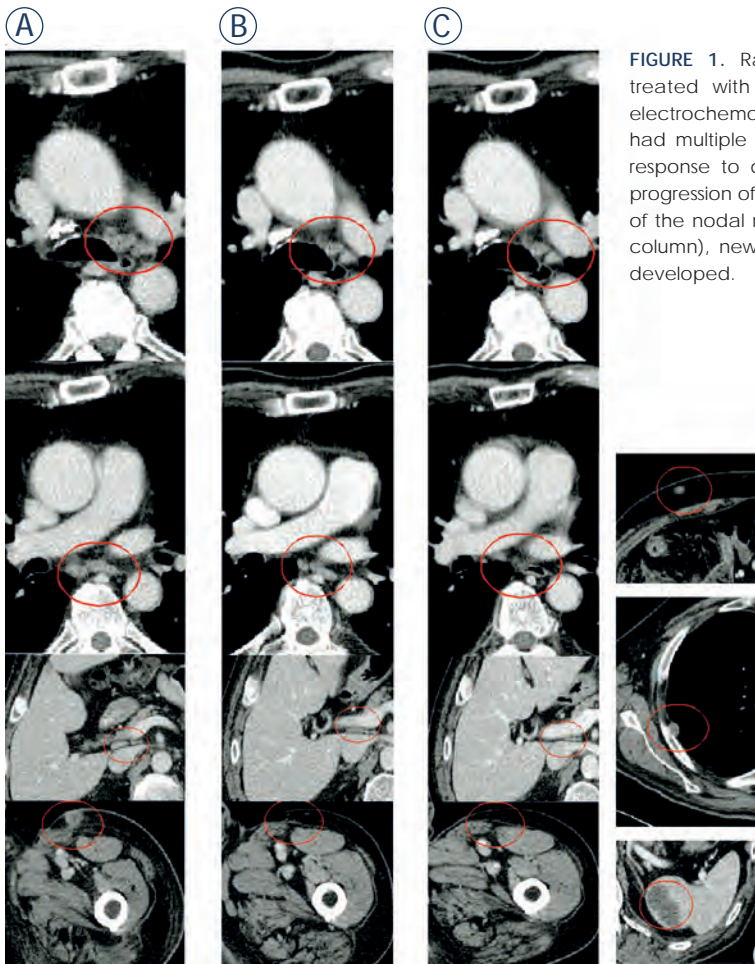


FIGURE 1. Radiological course of a metastatic melanoma patient initially treated with dabrafenib and subsequently temozolomide, combined with electrochemotherapy on superficial tumor nodules. (A) In July 2013 the patient had multiple nodal metastases; (B) in January 2013 was appreciated a good response to dabrafenib on visceral metastases (despite superficial soft tissue progression of the left leg); (C) in November 2013, despite the maintained control of the nodal metastases present at the beginning of dabrafenib treatment (left column), new deep (soft tissue, pleural and splenic, right column) metastases developed.

Case report

A 72-year-old metastatic melanoma male patient treated with dabrafenib 150 mg twice daily within the compassionate programme of Glaxo Smith Kline BRF115252. Bleomycin-ECT was administered in accordance with the ESOPE protocol. Treatment side effects were graded according to the Common Toxicity Criteria for Adverse Events (CTCAE), version 4. Written informed consent was obtained for the treatments and for the scientific use of clinical data, according to EC and Italian law requirements.

The patient received the first diagnosis of cutaneous melanoma of the left leg (stage IIA, T2b N0), in May 2007. From Dec 2010 to February 2011 he developed a single in-transit metastasis associated with inguinal lymph node recurrence, both managed by surgical excision. Thereafter, the patient was enrolled in an adjuvant trial with ipilimumab (CA184-029). Treatment was discontinued after four cycles owing to persistent G2 skin toxicity (pruritus), G2 diarrhoea and G2 hyphophysitis (he remained on therapy with corticosteroids for recurrence of hyphophysitis when he tried to discontinue them).

In May, two additional local recurrences were resected. In October 2011, temozolomide treatment was started for inoperable local recurrence. In May 2012, after an initial stabilization of the disease, he developed pathological mediastinal and abdominal lymph nodes (Figure 1A), and soft tissue progression in the left leg, rapidly increasing in size and number, requiring frequent dressing for bleeding and impairing the patient's quality of life. Molecular analysis of BRAF gene was positive for V600E mutation. In June 2012, dabrafenib treatment (150mg per os twice daily, continuously) was started, obtaining in two weeks a partial response on superficial disease and complete re-

melanoma.⁸⁻¹¹ The mechanism of action of ECT relies on the association of a poorly permeant anticancer agent (bleomycin or cisplatin) followed by locally-applied electric voltages which open transient pores on the cell membrane and increase drug entry into neoplastic tissues. Most common side effects of ECT include local erythema, skin ulceration and persistent pigmentation. This treatment permits a local complete response in 15-58% of patients with superficial metastases, according to the most recent experiences^{9,12,13} with ECT applied according to a shared protocol (European Standard Operative procedures of Electrochemotherapy, ESOPE).¹⁰

We here describe the clinical course of a metastatic melanoma patient who achieved durable tumor control by concomitant treatment with dabrafenib and bleomycin-ECT, administered to control isolated soft tissue metastases increasing during dabrafenib treatment.



FIGURE 2. Clinical course of a metastatic melanoma patient initially treated with dabrafenib and subsequently temozolomide, combined with electrochemotherapy on superficial tumor nodules.

In July 2013 the patient had multiple nodal and soft tissue metastases; (A) in October 2012 the left thigh of the patient was covered with white spots in the site of the metastases responsive to dabrafenib (white dotted arrows); at that time, only two bulging nodules were appreciable (black arrows); (B) despite

the good response to dabrafenib on visceral metastases, in January 2013 three of these lesions worsened and one was ulcerated (black arrows); (C) in June 2013, after the first ECT course the metastases of the left thigh shrank; (D) in November 2013, new multiple skin metastases developed. Nevertheless, tumor control at the site of initial metastases that were responsive to dabrafenib and ECT was maintained (white arrows).

Jagged arrows symbolize ECT courses.

sponse in mediastinal and abdominal lymph nodes (Figure 1B).

The treatment was well tolerated. In particular, despite previous skin toxicity during the adjuvant trial with ipilimumab, no significant cutaneous toxicity appeared during dabrafenib; the only reported adverse events were G1 plantar hyperkeratosis (from June 2012, controlled with acetylsalicylic acid based topical treatment) and a temporary G1 rhinitis (from October to December 2012).

In January 2013, the majority of subcutaneous lesions were stable except three, which progressively increased becoming symptomatic (Figure 2A and 2B).

Treatment with dabrafenib was maintained, considering the good tolerance and the systemic control of the disease, and ECT was applied in progressing nodules (the maximum diameter of the lesions was 3.5cm) under mild general sedation using systemic Bleomycin (15MUI).^{14,15} After one month, the lesions regressed to be classified as partial response (Figure 2C) without significant cutaneous toxicity; a second ECT cycle was administered in July 2013 without additive toxicity except for transient G1 erythema. Dabrafenib was stopped in November 2013 because of new soft tissue lesions and lymph node progression (Figure 1C and 2D). To assess whether a new clone with BRAF

V600E mutation loss could have developed we performed a tumor biopsy, that confirmed the diagnosis of melanoma metastases and, interestingly, the maintenance of BRAF V600E mutation in the new soft tissue nodules. A third ECT cycle was applied with palliative intent in the new soft tissue lesions obtaining, again, a partial response on treated nodules; systemic therapy was switched to temozolomide, considering the previous efficacy and the impossibility to use immunomodulating therapy due to the corticosteroid need.

In March 2014, the patient is still mostly asymptomatic and fully-active with controlled disease and continues chemotherapy with temozolomide.

Discussion

This is, to our knowledge, the first report of ECT combined with a BRAFi in a patient with metastatic melanoma. Actually, no consistent data are available about the prosecution of BRAFi treatment beyond progression in metastatic melanoma patients, but this case suggests that a multidisciplinary approach with locoregional treatments in addition to BRAFi therapy could be useful in some patients and should be tested more extensively. ECT seems a reliable and safe approach to control isolated skin

and/or subcutaneous lesions in patients with systemic or visceral disease control. The combination of BRAFi and ECT allowed the control of disease and preservation of PS and quality of life for 17 months, which is almost three times the usual progression free survival time observed with the use of BRAFi.

This was a clear benefit for the patient, particularly in a disease like metastatic melanoma, where treatment options, despite the promising recent advances, are still numbered and long survival is difficult to obtain. The most important finding emerging from the presented case is the tolerability of the combined treatment approach. Radiotherapy is demonstrated to be effective in patients receiving BRAFi treatments, but a cautious evaluation, and interruption of the therapy during radiation, is recommended to avoid significant worsening of cutaneous toxicity.

We cannot elucidate whether the combination of dabrafenib and ECT had an additive effect, or whether ECT, thanks to its sustained local cytotoxic activity, may enhance tumor antigen presentation and promote lymphocyte tumor infiltration, as previously reported.^{16,17} Moreover, the immunological benefits could have been enhanced through the silencing of the aberrant immune-depressant pathways driven by the BRAF constitutive activation.^{18,19}

This may be a possible explanation for the benefit observed in this patient despite the multiple and rapid recurrences. Nevertheless, we cannot exclude that the disease course could be favored by the previous immunotherapy with ipilimumab.

In conclusion, we recommend further investigations to assess the following open issues: (a) whether the maintenance of BRAFi after tumor progression could give advantage to patients compared to its discontinuation when locoregional treatment, to control isolated tumor relapse, is possible; (b) to evaluate the most effective and tolerable locoregional treatment (*i.e.* radiotherapy, isolated limb perfusion/infusion, ECT).

In our experience, the association of ECT during dabrafenib proved to be a safe and valuable option in a challenging patient who developed tumor resistance exclusively on superficial disease. ECT ensured sustained local control on skin metastases without significant toxicity, maintained patient quality of life and allowed for the prosecution of target therapy which proved to be still effective on systemic disease. As a result, we encourage the study of this association in an adequate number of patients.

References

- Chapman PB, Hauschild A, Robert C, Haanen JB, Ascierto P, Larkin J, et al. Improved survival with vemurafenib in melanoma with BRAF V600E mutation. *N Engl J Med* 2011; **364**: 2507-16.
- Hauschild A, Grob JJ, Demidov LV, Jouary T, Gutzmer R, Millward M, et al. Dabrafenib in BRAF-mutated metastatic melanoma: a multicentre, open-label, phase 3 randomised controlled trial. *Lancet* 2012; **380**: 358-65.
- Flaherty KT, Infante JR, Daud A, Gonzalez R, Kefford RF, Sosman J, et al. Combined BRAF and MEK inhibition in melanoma with BRAF V600 mutations. *N Engl J Med* 2012; **367**: 1694-703.
- Mattei PL, Alora-Palli MB, Kraft S, Lawrence DP, Flaherty KT, Kimball AB. Cutaneous effects of BRAF inhibitor therapy: a case series. *Ann Oncol* 2013; **24**: 530-7.
- Ribas A, Hodi FS, Callahan M, Kondo C, Wolchok J. Hepatotoxicity with combination of vemurafenib and ipilimumab. *N Engl J Med* 2013; **368**: 1365-6.
- Rompoti N, Schilling B, Livingstone E, Griewank K, Hillen U, Sauerwein W, et al. Combination of BRAF inhibitors and brain radiotherapy in patients with metastatic melanoma shows minimal acute toxicity. *J Clin Oncol* 2013; **31**: 3844-5.
- Ducassou A, David I, Delannes M, Chevreau C, Sibaud V. Radiosensitization induced by vemurafenib. *Cancer Radiother* 2013; **17**: 304-7.
- Sersa G, Miklavcic D, Cemazar M, Rudolf Z, Pucihar G, Snoj M. Electrochemotherapy in treatment of tumours. *Eur J Surg Oncol* 2008; **34**: 232-40.
- Campana LG, Valpione S, Mocellin S, Sundararajan R, Granziera E, Sartore L, et al. Electrochemotherapy for disseminated superficial metastases from malignant melanoma. *Br J Surg* 2012; **99**: 821-30.
- Mir LG, L; Sersa, G; Collins, CG; Garbaya, GR; Billard, V; Geertsend, PF; et al. Standard operating procedures of the electrochemotherapy: Instructions for the use of bleomycin or cisplatin administered either systemically or locally and electric pulses delivered by the Cliniporator™ by means of invasive or non-invasive electrodes. *EJC Suppl* 2006; **4**: 14-25.
- Belehradek M, Domenge C, Luboinski B, Orlowski S, Behlradek J, Jr., Mir LM. Electrochemotherapy, a new antitumor treatment. First clinical phase I-II trial. *Cancer* 1993; **72**: 3694-700.
- Matthiessen LW, Chalmers RL, Sainsbury DC, Veeramani S, Kessell G, Humphreys AC, et al. Management of cutaneous metastases using electrochemotherapy. *Acta Oncol* 2011; **50**: 621-9.
- Campana LG, Testori A, Mozzillo N, Rossi CR. Treatment of metastatic melanoma with electrochemotherapy. *J Surg Oncol* 2014; **109**: 301-7.
- Mali B, Jarm T, Snoj M, Sersa G, Miklavcic D. Antitumor effectiveness of electrochemotherapy: a systematic review and meta-analysis. *Eur J Surg Oncol* 2013; **39**: 4-16.
- Mali B, Miklavcic D, Campana LG, Cemazar M, Sersa G, Snoj M, et al. Tumor size and effectiveness of electrochemotherapy. *Radiol Oncol* 2013; **47**: 32-41.
- Gerlini G, Sestini S, Di Gennaro P, Urso C, Pimpinelli N, Borgognoni L. Dendritic cells recruitment in melanoma metastasis treated by electrochemotherapy. *Clin Exp Metastasis* 2013; **30**: 37-45.
- Sersa G, Kotnik V, Cemazar M, Miklavcic D, Kotnik A. Electrochemotherapy with bleomycin in SA-1 tumor-bearing mice—natural resistance and immune responsiveness. *Anticancer Drugs* 1996; **7**: 785-91.
- Wilmott JS, Long GV, Howle JR, Haydu LE, Sharma RN, Thompson JF, et al. Selective BRAF inhibitors induce marked T-cell infiltration into human metastatic melanoma. *Clin Cancer Res* 2012; **18**: 1386-94.
- Schilling B, Paschen A. Immunological consequences of selective BRAF inhibitors in malignant melanoma: Neutralization of myeloid-derived suppressor cells. *Oncoimmunology* 2013; **2**: e25218.

Treatment of tongue cavernous haemangioma with direct puncture and sclerotization with ethanol

Tomaz Seruga, Jernej Lucev, Marko Jevsek

Radiology Department, University Medical Centre Maribor, Slovenia

Radiol Oncol 2015; 49(1): 75-79.

Received 3 October 2013

Accepted 6 December 2013

Correspondence to: Tomaz Seruga, M.D., Ph.D., Radiology Department, University Medical Centre Maribor, Ljubljanska ulica 5, SI-2000 Maribor, Slovenia. Tel: +386 2 321 29 77; E-mail: tomaz.seruga@ukc-mb.si

Disclosure: No potential conflicts of interest were disclosed.

Background. Haemangiomas of tongue are rare type of malformations. They can be treated mostly conservatively but in some cases they need more aggressive treatment with preoperative intra arterial embolization and surgical resection. Lesions of tongue that are localized superficially can also be treated with direct puncture and injection of sclerosing agent (absolute ethanol).

Case report. We present a case of a 48 years old female patient, where we performed embolization of cavernous haemangioma with mixture of absolute ethanol and oil contrast. After the procedure the patient received analgetics and antioedematous therapy. After the sclerotization the planned surgery was abandoned. Control MRI examinations 6 and 12 months after the procedure showed only a small remnant of haemangioma and no signs of a larger relapse.

Conclusions. In our case the direct puncture of haemangioma and sclerotherapy with ethanol proved to be a safe and effective method to achieve preoperative devascularization of the lesion. Direct puncture of the lesion is not limited by the anatomy of the vessels or vasospasm, which can occur during the intra-arterial approach.

Key words: vascular abnormalities; cavernous haemangioma; direct puncture; ethanol; oil contrast media

Introduction

Vascular malformations of the tongue are relatively rare disorders. According to Mulliken and Glowacki they are divided into haemangiomas and vascular malformations (Table 1).¹

The nomenclature in this field is very problematic, particularly in assessing benign vascular anomalies. Currently a variety of systems adapted for and by distinct clinical subgroups, like pathologists, clinicians, radiologist, are in use. In 1982, Mulliken and Glowacki proposed a binary classification system (Table 1) for vascular anomalies based on pathologic features.¹ These system was adopted by the International Society for the Study of Vascular Anomalies (ISSVA) and has since been expanded and is now widely accepted. The importance of the ISSVA system is that it allows a systematic approach to vascular lesions that correlates

predictably with clinical history, disease course, and treatment options, making it clinically useful.²

The ISSVA classification system divides vascular anomalies into 2 primary biological categories (Table 2). The major distinction between the 2 categories is whether there is increased endothelial cell turnover, which is ultimately determined by the identification of mitoses seen on histopathology. Vasoproliferative neoplasms have increased endothelial cell turnover. Vascular malformations do not have increased endothelial cell turnover. Instead, vascular malformations are structural abnormalities of the capillary, venous, lymphatic, and arterial system that grow in proportion to the child.² Although ISSVA classification system is widely accepted, other nomenclatures are in use, but none of the current classification schemes are universally accepted. That continues to cause confusion, misunderstood diagnoses, and poten-



FIGURE 1. T2 weighted MR image in sagittal plane before treatment shows 35 x 25 mm big lesion (white arrow) identified as submucosal cavernous haemangioma of the tongue. The lesion is expansive and does not involve the radix of the tongue.



FIGURE 2. T2 weighted MR image of the same lesion (white arrow) in coronal plane before treatment shows that the majority of lesion is located on the left side of the tongue.

tial mismanagement. In order to avoid excessive entanglement, we decided to use Mulliken and Glowacki classification in our article, because de-

TABLE 1. Classification of vascular abnormalities according to Mulliken and Glowacki

Vascular abnormalities	
Haemangiomas (tumour):	Vascular Malformations:
<ul style="list-style-type: none"> • Usually not present at birth • Rapidly increase in size • Involute • F:M = 3:1 • 60% Head and Neck • Most common tumour of infancy • "strawberry naevus" 	<ul style="list-style-type: none"> • Present at birth (may not be clinically apparent) • Grow in proportion to body size • Can degenerate • Can hypertrophy (AVM)

tailed classification for the understanding of the article is not necessary.

Haemangiomas are the most common tumour of infancy and typically appear as a small reddish macule. About 80% occur within the first month of life. The macule quickly grows and becomes raised and lobulated. Majority of haemangiomas involve the skin, they can occur subcutaneously, appearing as a bluish patch under the skin. This can cause a rapidly developing swelling which then involutes as in the cutaneous lesion.

The term vascular malformations (VM) refer to lesions where the anatomy and morphology of the vessels are abnormal although the vascular endothelium is normal. These lesions can either be high, low or mixed flow lesions.

Classification that considers also clinical symptoms is named after Schobinger and has four stages, where stage 1 presents as a blue-skin blush, stage 2 as a mass associated with a bruit and a thrill, stage 3 as a mass associated with ulceration, bleeding and pain and stage 4 as a stage 3 lesions producing heart failure.¹

Each vascular abnormality requires a serious diagnostic approach. Based on the findings the most appropriate method of treatment is selected.³ Location of the lesion, its topography, the size and geometry can be best shown by the contrast enhanced magnetic resonance imaging (MRI).⁴ Next diagnostic method is a digital subtractal angiography (DSA), which can show us the angioarchitecture of the malformations and flow dynamic within the lesion.

The invasive treatment of the tongue vascular abnormalities is usually the preoperative endovascular embolization followed by the surgical resection of the lesion or partial resection of the tongue,

TABLE 2. International Society for the Study of Vascular Anomalies Classification System

Vascular (or vasoproliferative) Neoplasms	Vascular Malformations
Infantile haemangioma	Slow-flow vascular malformations <ul style="list-style-type: none"> • Capillary malformation • Venous malformation • Lymphatic malformation
Congenital haemangiomas <ul style="list-style-type: none"> • RICH • NICH 	
Kaposiform haemangioendothelioma and tufted angiomas (with or without Kasabach-Merritt syndrome)	Fast-flow vascular malformations <ul style="list-style-type: none"> • Arterial malformation • Arteriovenous fistula • Arteriovenous malformation
Spindle cell haemangioendothelioma	
Epithelioid haemangioendotheliomas	
Other rare haemangioendotheliomas (i.e., composite, retiform, and others)	Combined vascular malformations (various combination of the above)
Angiosarcoma	
Dermatologic acquired vascular tumors (i.e., pyogenic granuloma)	

RICH = rapidly involuting congenital haemangioma; NICH = noninvoluting congenital haemangioma

depending on the size of the lesion.^{5,6} Preoperative embolization is preformed because intraoperative bleeding can significantly influence the outcome of the surgical treatment. Intra-arterial catheter embolization can be technically difficult because of the complex vascular anatomy and the vasospasm.⁵ Problems connected with the intra-arterial catheter embolization can be solved by direct puncture and injection of alcohol into the lesion. In doing so, care must be taken that the injection of the embolization material is limited to the lesion and that there is no recourse to the venous side of the malformation.⁷ The success of the therapy is evaluated clinically, later follow up is provided by MR examinations.¹

Case report

A 48 years old female patient was admitted to our institution because of the difficulties in swallowing food and the swelling of the tongue. The otorhinolaryngology exam showed bluish, localized, approximately 35 × 25 mm big swelling on the upper side of tongue, with vessels shining through the glossal mucosa. The lesion was localised on the right side of the tongue in the middle part. The ra-

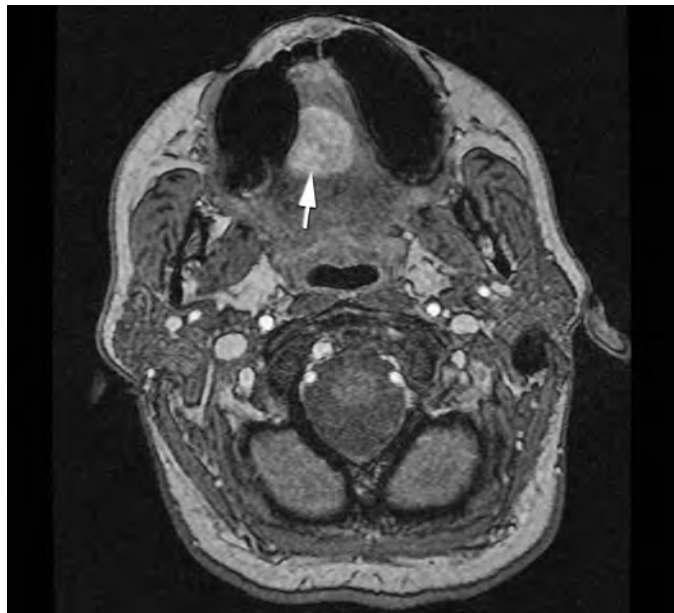


FIGURE 3. Axial plane of the lesion (white arrow) shown with MR angiography with time resolved imaging of contrast kinetics (TRICKS) before treatment.

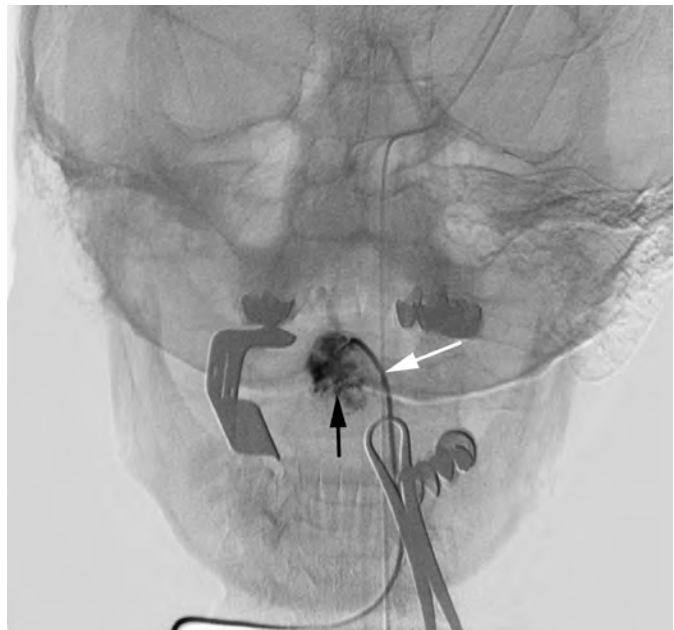


FIGURE 4. Digital, nonsubtracted, image of tongue parenchymography during sclerotization with opened mouth with distractor and cannula (white arrow) placed in haemangioma (black arrow).

dix of the tongue was free. After the biopsy the histological examination of the tissue was performed and cavernous haemangioma was diagnosed.

Contrast enhanced MRI with time resolved imaging of contrast kinetics sequence (TRICKS) was



FIGURE 5. Digital subtracted image during the procedure enabled us a more controlled injection of ethanol and gave us a possibility to avoid the reflux to the venous side. The haemangioma of tongue is indicated with the white arrow.

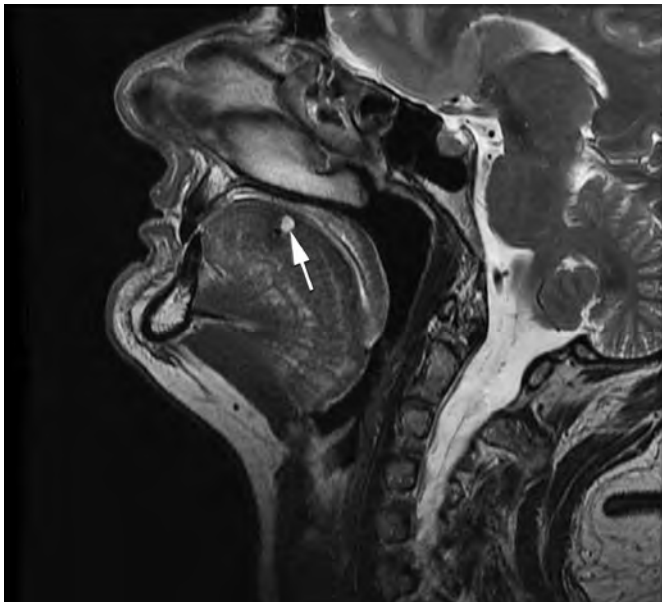


FIGURE 6. Control postcontrast sagittal T2 weighted image of tongue, six months after the procedure, showing a small remnant of the cavernous haemangioma (white arrow).

performed, so that the best method of treatment could be selected (Figure 1, Figure 2 and Figure 3). The maxillofacial surgeon planned a surgery, so we

were asked to perform a preoperative intra-arterial embolization. Because of the superficial localization of the lesion, we chose a direct puncture as the most appropriate approach.

The procedure was performed under general anaesthesia. This provided us the complete analgesia and prevention of tongue movement during the puncture and the injection of the ethanol and the contrast media.

We performed parenchymography of the lesion using several projections to reach an optimal view of the lesion and to evaluate the potential extravasation of contrast from haemangioma (Figure 4, Figure 5). This enabled us a more controlled injection of ethanol and gave us a possibility to avoid the reflux to the venous side. For the puncture we used 10 to 12 G needle (Terumo, Tokyo, Japan). After the puncture the proper position of the needle was verified with a continuous reflux of blood. Then the cannula was flushed with a 5% glucose solution. Under fluoroscopy control 96% alcohol diluted with Lipiodol (ratio 1:5) was injected. The cannula was removed and next puncture was performed. All together we performed six punctures and injected approximately 6 ml of ethanol. There were no technical complications during the procedure (Figure 3). No major bleeding was observed after the procedure. After the procedure the patient received analgetics and antioedematous therapy. After the sclerotization the planned surgery was abandoned. Control MRI examinations 6 and 12 months after the procedure showed only a small remnant of haemangioma and no signs of a larger relapse (Figure 6).

Discussion

Most haemangiomas can be treated conservatively with an expectant strategy.¹ However there are occasions when haemangiomas need more active intervention with sclerotization or preoperative embolization followed by surgery.⁸ The correct diagnosis has to be made and the decision to intervene has to be balanced against non-intervention and spontaneous involution. The outcome has to be considered and treatment with sclerosants should be limited to haemangiomas where the site is not of a major aesthetic concern. Surgical debulking has to be considered in the same context with regard to the long term effects. Surgery involving extensive scarring should be avoided if the alternative is awaiting natural resolution and lesser scarring.

Usually treatment of the tongue vascular abnormalities is performed by the intra-arterial catheterisation and embolization with particles or n-butyl cyanoacrylate (NBCA). Such a treatment has good results, but it is not suitable for all types of malformations.⁹ Intra-arterial endovascular embolization therapy is limited by the number of arteries, technical problems related to the difficult vascular anatomy or by the occurrence of vasospasm, which can lead to the failure of the procedure.

Direct puncture and the application of ethanol were initially described as an alternative method in cases where conventional intra-arterial catheter embolization was technically not possible.^{9,10} In such cases the direct injection of the sclerosing agent results in a higher level of devascularization compared to the intra-arterial embolization. The relative simplicity and good results have led to a wider implementation and application of the method. Absolute ethanol has been accepted as a new sclerosing agent associated with a substantial reduction of lesion recurrence, which induces denaturation of tissue protein, precipitating protoplasm and subsequent permanent obliteration of the vessel lumen.¹¹

Sclerotization must be carried out slowly so that the amount of ethanol entering the haemangioma vascular bed can be maximized. The movement of the sclerosing agent to avoid the passing to the venous side must be constantly monitored.^{7,12,13}

With our intervention we allowed a patient, which was intended to undergo a mutilant surgery with the resection of the tongue, a year and a half of normal life until now.

Direct puncture of the cavernous haemangioma and sclerotherapy with alcohol proved to be a safe and effective method to achieve devascularization of the lesion and postpone or even avoid surgical resection.

References

- Mulliken JB, Glowacki J. Hemangiomas and vascular malformations in infants and children: a classification based on the key driver characteristics. *Plast Reconstr Surg* 1982; **69**: 412-22.
- Lowe LH, Marchant TC, Rivard DC, Scherbel AJ. Vascular malformations: classification and terminology the radiologist needs to know. *Semin Roentgenol* 2012; **47**: 106-17.
- Pekkola J, Lapalainen K, Voula P, Salminen Kloockars T, Pitkeranta A. Head and neck malformation: results of ethanol sclerotherapy. *AJNR Am J Neuroradiol* 2013; **34**: 198-204.
- Hyodoh H, Hori M, Akiba H, Tamakawa M, Hyodoh K, Hareyama M. Peripheral vascular malformations: imaging, treatment and therapeutic approaches issues. *Radiographics* 2005; **25** (Suppl 1): 159-71.
- Perez D, Leibold D, Liddell A, Duraini M. Vascular lesions of the maxillofacial region: a case report and review of literature. *Tex Dent J* 2010; **127**: 1045-57.
- Cho SK, Do YS, Shin SW, Kim DJ, Kim YW, Park KB et al. Peripheral arteriovenous malformations with dominant outflow vein: results of ethanol embolization. *Korean J Radiol* 2008; **9**: 258-67.
- Do YS, Park KB, Park HS, Cho SK, Shin SW, Moon JW, et al. Extremity arteriovenous malformations involving the bone: therapeutic outcomes of ethanol embolotherapy. *J Vasc Interv Radiol* 2010; **21**: 807-16.
- Jeong HS, Baek CH, Son YI, Kim TW, Lee BB, Byun HS. Treatment for extracranial arteriovenous malformations: preliminary results of 17 cases. *AJNR Am J Neuroradiol* 2009; **30**: 1679-84.
- Mueller-Forrell W, Valavanis A. How angioarchitecture of cerebral arteriovenous malformations should influence the therapeutic considerations. *Minim Invasive Neurosurg* 1995; **38**: 32-40.
- Park HS, Do YS, Park KB, Kim DJ, Kim YW, Kim MJ, et al. Ethanol embolotherapy of hand arteriovenous malformations. *J Vasc Surg* 2011; **53**: 725-31.
- Jin Y, Lin X, Chen H, Hu X, Fan X, Li W, et al. Auricular arteriovenous malformations: Potential success of superselective ethanol embolotherapy. *J Vasc Interv Radiol* 2009; **20**: 736-43.
- Fan XD, Su LX, Zheng JW, Zheng LZ, Zhang ZY. Ethanol embolization of arteriovenous malformations of the mandible. *AJNR Am J Neuroradiol* 2009; **30**: 1178-83.
- Zheng LZ, Fan XD, Zheng JW, Su LX. Ethanol embolization of auricular arteriovenous malformation: preliminary results of 17 cases. *AJNR Am J Neuroradiol* 2009; **30**: 1679-84.

Bevacizumab and irinotecan in recurrent malignant glioma, a single institution experience

Tanja Mesti, Maja Ebert Moltara, Marko Boc, Martina Rebersek, Janja Ocvirk

Department of Medical Oncology, Institute of Oncology Ljubljana, Ljubljana, Slovenia

Radiol Oncol 2015; 49(1): 80-85.

Received 9 September 2013

Accepted 8 November 2013

Correspondence to: Asist. Prof. Janja Ocvirk, M.D., Ph.D., Institute of Oncology Ljubljana, Zaloška 2, Ljubljana. Phone: +386 1 5879 220; Fax: +386 1 5879 305; E-mail: jocvirk@onko-i.si

Disclosure: No potential conflicts of interest were disclosed.

Background. Treatment options of recurrent malignant gliomas are very limited and with a poor survival benefit. The results from phase II trials suggest that the combination of bevacizumab and irinotecan is beneficial.

Patients and methods. The medical documentation of 19 adult patients with recurrent malignant gliomas was retrospectively reviewed. All patients received bevacizumab (10 mg/kg) and irinotecan (340 mg/m² or 125 mg/m²) every two weeks. Patient clinical characteristics, drug toxicities, response rate, progression free survival (PFS) and overall survival (OS) were evaluated.

Results. Between August 2008 and November 2011, 19 patients with recurrent malignant gliomas (median age 44.7, male 73.7%, WHO performance status 0–2) were treated with bevacizumab/irinotecan regimen. Thirteen patients had glioblastoma, 5 anaplastic astrocytoma and 1 anaplastic oligoastrocytoma. With exception of one patient, all patients had initially a standard therapy with primary resection followed by postoperative chemoradiotherapy. Radiological response was confirmed after 3 months in 9 patients (1 complete response, 8 partial responses), seven patients had stable disease and three patients have progressed. The median PFS was 6.8 months (95% confidence interval [CI]: 5.3-8.3) with six-month PFS rate 52.6%. The median OS was 7.7 months (95% CI: 6.6-8.7), while six-month and twelve-month survival rates were 68.4% and 31.6%, respectively. There were 16 cases of hematopoietic toxicity grade (G) 1-2. Non-hematopoietic toxicity was present in 14 cases, all G1-2, except for one patient with proteinuria G3. No grade 4 toxicities, no thromboembolic event and no intracranial hemorrhage were observed.

Conclusions. In recurrent malignant gliomas combination of bevacizumab and irinotecan might be an active regimen with acceptable toxicity.

Key words: recurrent malignant glioma; bevacizumab; irinotecan; systemic therapy

Introduction

Malignant (high-grade) gliomas are rapidly progressive brain tumors comprising of anaplastic oligodendroglioma, anaplastic astrocytoma, mixed anaplastic oligoastrocytoma (all grade III, World Health Organization [WHO]) and glioblastoma (grade IV, WHO).¹

The incidence of malignant gliomas is approximately 5/100,000. Malignant gliomas constitute 35–45% of primary brain tumors. Glioblastomas account for approximately 60 to 70% of malignant

gliomas, while anaplastic astrocytomas represent 10 to 15%, and anaplastic oligodendrogliomas and anaplastic oligoastrocytomas 10% of malignant gliomas.¹⁻³ The incidence of these tumors has increased slightly over past two decades, especially in the elderly. The peak incidence is in the fifth and sixth decade of life. The median age of patients at the time of diagnosis in the case of glioblastoma is 64 years and in the case of anaplastic gliomas is 45 years. Malignant gliomas are 40% more frequent in man than in woman and twice more frequent in white population than in black.^{2,4,5}

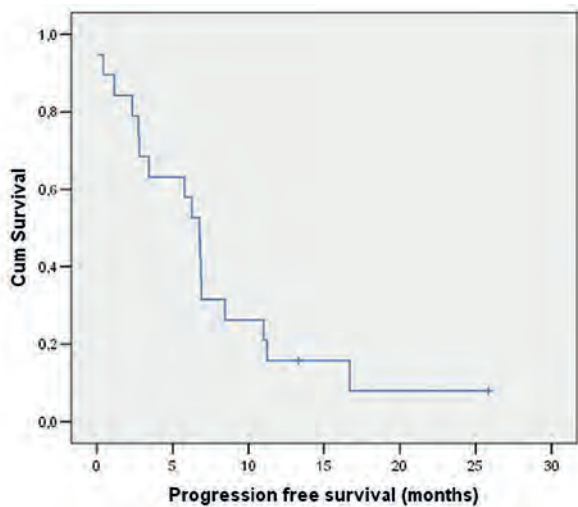


FIGURE 1. The median progression free survival (PFS).

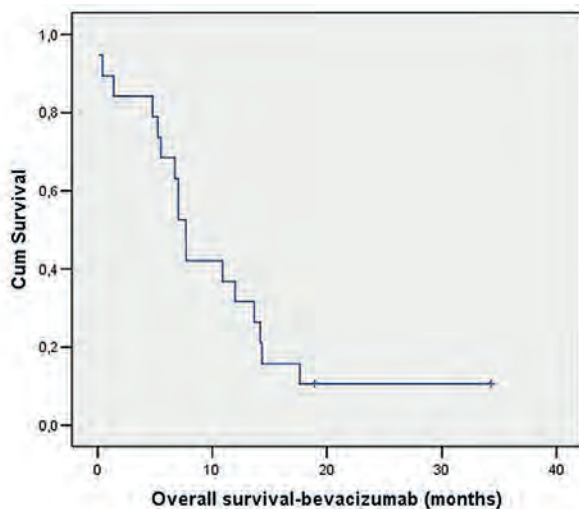


FIGURE 2. The median overall survival (OS).

In Slovenia from 1991 till 2005, a total of 1636 patients (878 males and 758 females) were diagnosed with brain cancer. Since 2001 till 2005 the microscopical verification was performed in 83% of cases: 82% were gliomas, of which two thirds were glioblastoma, 14% astrocytoma and 10% oligodendroglioma. Approximately 60% of the patients were diagnosed at age between 50 to 74 years, and 25% at age between 20 to 49 years.⁶

Glioblastoma tumors are gliomas of highest malignancy (grade IV), characterized by uncontrolled, aggressive cell proliferation and infiltrative growth within the brain and general resistance to conventional treatment. Despite the efforts to improve treatment outcome, the survival of patients with

malignant gliomas is poor, with median survival of about 14 months.^{7,8} For glioblastoma, median time to progression after postoperative treatment with radiotherapy (RT) and temozolomide (TMZ) is 6,9 months and after RT alone 5.0 months.⁹ Although the 5-year OS analysis of the EORTC-NCIC trial has shown benefit for patients treated with RT and TMZ compared with only irradiated patients (9.8% vs. 1.9%), the median survival after progression remains only 6.2 months¹⁰, regardless of the initial treatment.

We present single institution experience of treating recurrent malignant gliomas with combination of bevacizumab and irinotecan.

Patients and methods

We retrospectively reviewed medical documentation of 19 adult patients with recurrent malignant gliomas treated with bevacizumab and irinotecan at our center. All patients received bevacizumab at 10 mg/kg in combination with irinotecan 340 mg/m² or 125 mg/m² (with or without concomitant enzyme inducing antiepileptic drugs, respectively) every two weeks. Patient clinical characteristics (pre-recurrence treatment, performance status at the baseline), drug toxicities, response rate (RR), progression free survival (PFS) and overall survival (OS) were evaluated.

Statistical analysis was performed using the SPSS software, version 17.0. (SPSS Inc® Fulfillment center Haverhill MA, SPSS 17.0).

The study was approved by the Institutional Review Board Committee and was conducted in accordance with the Declaration of Helsinki.

Results

Patient characteristics

Fourteen (73.7%) males and five (26.3%) females were included. Median age was 44.7 years (range 27-74). Thirteen patients had glioblastoma, 5 anaplastic astrocytoma and 1 anaplastic oligoastrocytoma. In our group WHO performance status was 0-2. As an initial therapy all patients had a standard therapy with primary resection followed by postoperative chemoradiotherapy, with three-dimensional (3D) conformal radiation therapy (3D CRT), with 56 Gy in 28 fractions, combined with TMZ 75mg/m², and followed with TMZ 150-200mg/m² (4-20 cycles), except for one patient, with anaplastic astrocytoma of medullary cone, who had only biopsy.

TABLE 1. Systemic treatment of choice after disease progression

Recurrence	Cht (number of patients)
First	Bevacizumab + Irinotecan 12 (63.2%) BCNU 2 TMZ 4 PCV 1
Second	Bevacizumab + Irinotecan 5 (26.3%) BCNU 1 PCV 1
Third	Bevacizumab + Irinotecan 2 (10.5%)

BCNU = Carmustine (BCNU), 80 mg/m² BCNU on days 1 on 3; Cht = chemotherapy; PCV = lomustine (CCNU), 110 mg/m², on day 1; procarbazine, 60 mg/m² on days 8 to 21; and vincristine, 1.5 mg/m² (maximum dose, 2 mg), on days 8 and 29; TMZ = temozolomide, 150-200 mg/m²/day on days 1 to 5 of each subsequent 28-day cycle

TABLE 2. Radiological response after 3 months and 6 months of concomitant irinotecan and bevacizumab treatment

Response (n=19)	after 3 months	after 6 months
Complete Response (CR)	1	1
Partial Response (PR)	8	5
Stable Disease (SD)	7	5
Progression of Disease (PD)	3	8

Treatment of recurrence

Bevacizumab and irinotecan systemic treatment was introduced after 1st, 2nd and 3rd recurrence in 12 (63.2%), 5 (26.3%) and 2 (10.5%) patients, respectively (Table 1). No patient received additional RT at the time of disease recurrence.

Efficacy

Average number of chemotherapy applications was 9.3 (range 1-17). Median follow up of the patients was 10 months (range 0-34 months). Radiological response was confirmed after 3 months in nine patients (1 complete response, 8 partial responses), seven patients had stable disease, and 3 patients have progressed. After 6 months, one patient remained in complete response, five had partial response, five had stable disease and eight have progressed (Table 2).

The median PFS was 6.8 months (95% confidence interval [CI]: 5.3-8.3) (Figure 1) and the estimated six-month and twelve-month- PFS rates

were 52.6% and 15.8%, respectively. The median OS was 7.7 months (95% CI: 6.6-8.7) (Figure 2), while the six-month and twelve-month survival rates were 68.4% and 31.6%, respectively.

Toxicity

Toxicity was graded according to the National Cancer Institute Common Toxicity Criteria for Adverse Events (NCI-CTCAE) version 4.0. There were 16 cases of hematopoietic toxicity, only one patient had G2 neutropenia whereas in others only G1 toxic events were recorded. Two patients had neutropenia, six had lymphopenia, two had thrombocytopenia and one patient had anemia. No febrile neutropenia was observed. Non-hematopoietic toxicity G1-2 was present in 14 patients, with exception of one patient with proteinuria G3. Non-hematopoietic adverse events were: arterial hypertension (3), proteinuria (7), vomiting (2), diarrhea (1) and muscle pain (1). There was no G4 toxicity, no thromboembolic events and no intracranial hemorrhage observed (Table 3).

Discussion

Everyday reality is that, despite efforts to improve therapies or to develop new ones, the outcome of treatment in malignant gliomas is poor with median survival of 14 months.²

The treatment of recurrent malignant gliomas with RT is controversial. Some data have suggested that fractionated stereotactic reirradiation (SRT) and stereotactic radiosurgery (SRS), which are also effective in another diseases, may be beneficial.^{11,12} Observational series of patients with recurrent malignant gliomas, treated with SRT showed the median survival of 16 months for patients with grade III tumors and eight months for those with grade IV lesions.¹³ The one-year survival rates were 65% and 23% for patients with grade III and IV lesions, respectively. Kong *et al.* in a patients with recurrent gliomas treated with SRS has achieved progression free survival for patients with grade III and grade IV gliomas of 8.6 and 4.6 months, respectively.¹⁴ All patients were treated with SRS treatments delivered by gamma knife, except for 5 patients treated by linear accelerator.

Chemotherapy treatment is more effective for anaplastic gliomas than for glioblastoma, and in general has modest value for recurrent malignant gliomas. There is no established chemotherapy regimen available and patients are best treated within investigational clinical protocols.

TMZ was evaluated in a phase II study in patients with recurrent anaplastic gliomas who had previously been treated with nitrosoureas.¹⁵ The response rate was 35%, and the 6-month PFS rate was 46%, comparing favorably with the 6-month PFS rate of 31% for therapies that were generally considered ineffective.¹⁶ In patients with recurrent glioblastoma, TMZ has only limited activity, with response rate of 5.4% and 6-month rate of PFS of 21%.¹⁷

Other chemotherapeutic agents that are used for recurrent gliomas include nitrosoureas, carboplatin, procarbazine, irinotecan, and etoposide. Nitrosoureas (carmustine, fotemustine) either as single agents or in combination regimens as procarbazine, lomustine and vincristine (PCV) have shown activity in phase II studies in previously treated patients. Brandes AA *et al.*, conducted a phase II study on 40 patients with recurrent glioblastoma following surgery and standard radiotherapy, treated with carmustine as monotherapy. Median time to progression was 13.3 weeks and progression-free survival at 6-months was 17.5%.¹⁸ Schmidt F *et al.*, has applied PCV, as combined regimen, to 86 patients with recurrent glioblastoma. There were three partial responses, but no complete responses. Median progression-free survival was 17.1 weeks and progression-free survival at 6 months was 38.4%.¹⁹

Bevacizumab is a monoclonal antibody, which binds to VEGF, the key driver of neovascularization, and thereby inhibits the binding of VEGF to its receptors, VEGFR-1 and VEGFR-2, on the surface of endothelial cells.

Anti-VEGF therapy, including bevacizumab, acts by binding to VEGF and preventing its cellular effects. However, this linear interaction represents only a partial view of the pathobiology of the disease and treatment processes. Consequently, the classical concept of linear interactions is being replaced by the concept of networks of interactions, emphasizing the importance of interactions between different components of a biologic system.²⁰

In phase II studies Bevacizumab as a single agent or in combination with chemotherapy agents such as irinotecan demonstrated clinical activity for patients with grade 3 and grade 4 malignant gliomas (higher objective response, progression-free survival and overall survival) in recurrent glioblastoma²¹⁻³² and in May 2009, it has been approved by FDA for the secondary treatment of glioblastoma in USA³², but it is not approved yet by EMA in Europe.³⁴

According to the meta-analysis of phase II trials with bevacizumab and irinotecan treatment

TABLE 3. Adverse events

	Without AE n (%)	G1 n (%)	G2 n (%)	G3 n (%)	G4 n (%)
Hematopoietic toxicity					
leukopenia	16 (84)	2 (10.5)	1 (5.3)	0	0
neutropenia	17 (89.5)	1 (5.3)	1 (5.3)	0	0
lymphopenia	13 (68.4)	6 (31.6)	0	0	0
thrombocytopenia	17 (89.5)	2 (10.5)	0	0	0
anemia	16 (84.2)	3 (15.8)	0	0	0
febrile neutropenia	0	/	/	/	0
Non-hematopoietic toxicity					
arterial hypertension	16 (84.2)	2 (10.5)	1 (5.3)	0	0
proteinuria	12 (63.2)	3 (15.8)	3 (15.8)	1 (5.2)	/
sepsis	0	/	/	/	0
diarrhea	18 (94.7)	1 (5.3)	0	0	0
vomiting	17 (89.5)	1 (5.3)	1 (5.3)	0	0
muscle pain	18 (84.7)	1 (5.3)	0	/	/
intracranial hemorrhage	0	0	0	0	0
tromboembolic event	0	0	0	0	0

0 = no adverse side effects; / = adverse events of this grade doesn't exist

TABLE 4. Comparison of our study data with other studies

	Patients	Response rate	PFS at 6 months	Median survival (months)
Bev+Irinotecan (Vredenburg) ²⁵	35	57%	46%	9.7
Bev→Bev+Irinotecan (Kreisl) ²¹	85	35%	29%	7.2
Bev+Irinotecan (Friedman) ²²	167	28% / 38%	43% / 53%	9.2 / 8.7
Bev+Irinotecan (IO Lj study)	19	47.4%	52.6%	7.7

IO Lj = Institute of Oncology Ljubljana

in recurrent malignant gliomas³⁵, which included 411 patients, the median progression-free survival time ranged from 2.4 to 13.4 months and the median overall survival time ranged from 6.2 to 14.9 months, with response rates ranging from 28% to 86%. The improvement in tumor response rate observed in patients with recurrent malignant gliomas treated with bevacizumab and irinotecan combination to those on other systemic drugs protocols was highly statistically significant ($P = 0.00002$), and so was the same with the OS ($P = 0.024$).

The most extensive experience with bevacizumab comes from a noncomparative phase II trial, in which 167 patients with recurrent glioblastoma, previously treated with chemotherapy with temozolomide were randomly assigned to bevacizumab, either as a single agent or at the same dose in conjunction with irinotecan.²⁴ Treatment cycles were repeated every two weeks. The objective response rates with bevacizumab alone or in combination with irinotecan were 28% and 38%, respectively, the 6-month PFS rates were 43% and

50%, respectively and mOS times were 9.2 and 8.7 months, respectively. An update of the results was presented at the 2010 American Society of Clinical Oncology meeting.²³ Overall safety and efficacy were similar to that previously presented; the 12 and 24-month survival rates were 38% and 16% to 17% on both treatment arms, which appear to be better than historical control series.

We treated 19 patients with recurrent malignant gliomas with bevacizumab and irinotecan, from August 2008 to November 2011. The objective response rates were 47.4% and 31.6% after 3 and 6 months respectively. The 6-month PFS and OS rate and interval were 52.6% and 68.4% and 6.8 and 7.7 months, respectively. One third of the patients (31.6%) reached twelve-month OS. Regarding toxicity, 78.9% patients experienced hematopoietic toxicity G1, with only one patient experiencing G2 neutropenia. As for the non-hematopoietic toxicity, 42.1% patients had adverse events G1, 26.3% G2 and one patient had G3 proteinuria. There were no grade 4 toxicities, no febrile neutropenia, no thromboembolic event and no intracranial hemorrhage observed. Comparison of our data with other studies is presented in the Table 4.

Conclusions

In patients with recurrent malignant gliomas the combination of bevacizumab and irinotecan shows promising activity with acceptable toxicity although survival outcome is far from desired. Our results of the treatment of patients with recurrent malignant gliomas, regarding response rate, PFS and OS are comparable with the previously published data.

As all data about efficacy and safety of bevacizumab and irinotecan therapy in recurrent malignant gliomas are coming from phase II trials, larger phase III randomized controlled studies comparing bevacizumab plus irinotecan with other treatment protocols are warranted so that the efficacy can be assessed properly.

References

1. WHO Classification of tumours of the central nervous system. Louis DN, Ohgaki H, Wiestler OD, Cavenee WK, editors. Lyon: IARC Press; 2007.
2. CBTRUS, Central Brain Tumor Registry of the United States. 2007–2008. Primary brain tumors in the United States. Statistical report. 2000–2004 years of data collected. Available from: <http://www.cbtrus.org/reports/2007-2008/2007report.pdf>. Accessed on 10 November 2013.
3. Kase M, Minajeva A, Niinepuu K, Kase S, Vardja M, Asser T, et al. Impact of CD133 positive stem cell proportion on survival in patients with glioblastoma multiforme. *Radiol Oncol* 2013; **47**: 405-10.
4. Fisher JL, Schwartzbaum JA, Wrensch M, Wiemels JL. Epidemiology of brain tumors. *Neurol Clin* 2007; **25**: 867-90.
5. Smrdel U, Kovac V, Popovic M, Zwitter M. Glioblastoma patients in Slovenia from 1997 to 2008. *Radiol Oncol* 2014; **48**: 72-9.
6. Zakej MP, Zadnik V, Zagar T, Zakotnik B. *Survival of cancer patients, diagnosed in 1991-2005 in Slovenia*. Ljubljana: Institute of Oncology Ljubljana, Epidemiology and Cancer Registry, Cancer Registry of Republic of Slovenia; 2009. p. 229.
7. Van Meir EG, Hadjipanayis CG, Norden AD, Shu HK, Wen PY, Olson JJ. Exciting new advances in neuro-oncology: the avenue to a cure for malignant glioma. *CA Cancer J Clin* 2010; **60**: 166-93.
8. Podergajs N, Brekka N, Radlwimmer B, Herold-Mende C, Talasila KM, Tiemann K, et al. Expansive growth of two glioblastoma stem-like cell lines is mediated by bFGF and not by EGF. *Radiol Oncol* 2013; **47**: 330-7.
9. Stupp R, Mason PW, van den Bent MJ, Weller M, Fisher B, Taphoorn MJB, et al. Radiotherapy plus concomitant and adjuvant temozolomide for glioblastoma. *N Engl J Med* 2005; **352**: 987-96.
10. Stupp R, Hegi EM, Mason PW, van den Bent MJ, Taphoorn JBM, Janzer CR, et al. Effects of radiotherapy with concomitant and adjuvant temozolomide versus radiotherapy alone on survival in glioblastoma in a randomised phase III study: 5-year analysis of the EORTC-NCIC trial. *Lancet Oncol* 2009; **10**: 459-66.
11. Tsao MN, Mehta MP, Whelan TJ, Morris DE, Hayman JA, Flickinger JC, et al. The American Society for Therapeutic Radiology and Oncology (ASTRO) evidence-based review of the role of radiosurgery for malignant glioma. *Int J Radiat Oncol Biol Phys* 2005; **63**: 47-55.
12. Blamek S, Larysz D, Miszczyk L, Idasiak A, Rudnik A, Tarnawski R. Hypofractionated stereotactic radiotherapy for large or involving critical organs cerebral arteriovenous malformations. *Radiol Oncol* 2013; **47**: 50-6.
13. Combs SE, Thilmann C, Edler L, Debus J, Schulz-Ertner D. Efficacy of fractionated stereotactic reirradiation in recurrent gliomas: long-term results in 172 patients treated in a single institution. *J Clin Oncol* 2005; **23**: 8863-9.
14. Kong DS, Lee JI, Park K, Kim JH, Lim DH, Nam DH. Efficacy of stereotactic radiosurgery as a salvage treatment for recurrent malignant gliomas. *Cancer* 2008; **112**: 2046-51.
15. Yung WK, Prados MD, Yaya-Tur R, Rosenfeld SS, Brada M, Friedman HS, et al. Multicenter phase II trial of temozolomide in patients with anaplastic astrocytoma or anaplastic oligoastrocytoma at first relapse: Temodal Brain Tumor Group. *J Clin Oncol* 1999; **17**: 2762-71. [Erratum in *J Clin Oncol* 1999; **17**: 3693.]
16. Wong ET, Hess KR, Gleason MJ, Jaeckle KA, Kyritsis AP, Prados MD, et al. Outcomes and prognostic factors in recurrent glioma patients enrolled onto phase II clinical trials. *J Clin Oncol* 1999; **17**: 2572-8.
17. Yung WK, Albright RE, Olson J, Fredericks R, Fink K, Prados MD, et al. A phase II study of temozolomide vs. procarbazine in patients with glioblastoma multiforme at first relapse. *Br J Cancer* 2000; **83**: 588-93.
18. Brandes AA, Tosoni A, Amistà P, Nicolardi L, Grosso D, Berti F, Ermani M. How effective is BCNU in recurrent glioblastoma in the modern era? A phase II trial. *Neurology* 2004; **63**: 1281-4.
19. Schmidt F, Fischer J, Herrlinger U, Dietz K, Dichgans J, Weller M. PCV chemotherapy for recurrent glioblastoma. *Neurology* 2006; **66**: 587-9.
20. Loscalzo J, Kohane I, Barabasi AL. Human disease classification in the post-genomic era: a complex systems approach to human pathobiology. *Mol Syst Biol* 2007; **3**: 124.
21. Kreisl TN, Kim L, Moore K, Duic P, Royce C, Stroud I, et al. Phase II trial of single-agent bevacizumab followed by bevacizumab plus irinotecan at tumor progression in recurrent glioblastoma. *J Clin Oncol* 2009; **27**: 740-5.
22. Friedman HS, Prados MD, Wen PY, Mikkelsen T, Schiff D, Abrey LE, et al. Bevacizumab alone and in combination with irinotecan in recurrent glioblastoma. *J Clin Oncol* 2009; **27**: 4733-40.
23. Cloughesy T, Vredenburgh JJ, Day B, Das A, Friedman HS. Updated safety and survival of patients with relapsed glioblastoma treated with bevacizumab in the BRAIN study. [Abstract]. *J Clin Oncol* 2010; **28**(Suppl 15): No. 2008.
24. Chen W, Delaloye S, Silverman DH, Geist C, Czernin J, Sayre J, et al. Predicting treatment response of malignant gliomas to bevacizumab and irinotecan by imaging proliferation with [18F] fluorothymidine positron emission tomography: a pilot study. *J Clin Oncol* 2007; **25**: 4714-21.

25. Vredenburgh JJ, Desjardins AHJE, Marcello J, Reardon DA, Quinn JA, Rich JN, et al. Bevacizumab plus irinotecan in recurrent glioblastoma multiforme. *J Clin Oncol* 2007; **25**: 4722-9.
26. Bokstein F, Shpigel S, Blumenthal DT. Treatment with bevacizumab and irinotecan for recurrent high-grade glial tumors. *Cancer* 2008; **112**: 2267-73.
27. Guiu S, Taillibert S, Chinot O, Taillandier L, Honnorat J, Dietrich PY, et al. [Bevacizumab/irinotecan. An active treatment for recurrent high grade gliomas: preliminary results of an ANOCEF Multicenter Study]. [French]. *Rev Neurol (Paris)* 2008, **164**: 588-94.
28. Ali SA, McHayleh WM, Ahmad A, Sehgal R, Braffet M, Rahman M, et al. Bevacizumab and irinotecan therapy in glioblastoma multiforme: a series of 13 cases. *J Neurosurg* 2008; **109**: 268-72.
29. Desjardins A, Reardon DA, Herndon JE, Marcello J, Quinn JA, Rich JN, et al. Bevacizumab Plus Irinotecan in Recurrent WHO Grade 3 Malignant Gliomas. *Clin Cancer Res* 2008; **14**: 7068-73.
30. Kang TY, Jin T, Elinzano H, Peereboom D. Irinotecan and bevacizumab in progressive primary brain tumors, an evaluation of efficacy and safety. *J Neurooncol* 2008; **89**: 113-8.
31. Poulsen HS, Grunnet K, Sorensen M, Olsen P, Hasselbalch B, Nelausen K, et al. Bevacizumab plus irinotecan in the treatment patients with progressive recurrent malignant brain tumours. *Acta Oncol* 2009; **48**: 52-8.
32. Zuniga RM, Torcuator R, Jain R, Anderson J, Doyle T, Ellika S, et al. Efficacy, safety and patterns of response and recurrence in patients with recurrent high-grade gliomas treated with bevacizumab plus irinotecan. *J Neurooncol* 2009; **91**: 329-36.
33. NCCN clinical practical guidelines in oncology. Central nervous system cancer. Version 2.2013. Available from: http://www.nccn.org/professionals/physician_gls/f_guidelines.asp#site. Accessed on 4 November 2013.
34. Stupp R, Tonn JC, Brada M, Pentheroudakis G. High grade malignant glioma: ESMO Clinical Practice Guidelines for diagnosis, treatment and follow-up. *Ann Oncol* 2010; **21(Suppl 5)**: v190-3.
35. Xu T, Chen J, Lu Y, Wolff JEA. Effectstof bevacizumab plus irinotecan on response and survival in patients with recurrent malignant glioma: a systematic review and survival-gain analysis. *BMC Cancer* 2010, **10**: 252.

A new instrument for estimating the survival of patients with metastatic epidural spinal cord compression from esophageal cancer

Dirk Rades¹, Stefan Huttenlocher¹, Amira Bajrovic², Johann H. Karstens³, Tobias Bartscht⁴

¹ Department of Radiation Oncology, University of Lubeck, Lubeck, Germany

² Department of Radiation Oncology, University Medical Center Eppendorf, Hamburg, Germany

³ Department of Radiation Oncology, Hannover Medical School, Hannover, Germany

⁴ Department of Hematology and Medical Oncology, University of Lubeck, Lubeck, Germany

Radiol Oncol 2015; 49(1): 86-90.

Received 29 June 2014

Accepted 29 September 2014

Correspondence to: Prof. Dirk Rades, M.D., Department of Radiation Oncology, University of Lubeck, Ratzeburger Allee 160, 23538 Lubeck, Germany. Phone: +49 451 500 6661; Fax: +49 451 500 3324; E-mail: rades.dirk@gmx.net

Disclosure: No potential conflicts of interest were disclosed.

Background. This study was initiated to create a predictive instrument for estimating the survival of patients with metastatic epidural spinal cord compression (MESCC) from esophageal cancer.

Methods. In 27 patients irradiated for MESCC from esophageal cancer, the following nine characteristics were evaluated for potential impact on survival: age, gender, Eastern Cooperative Oncology Group (ECOG) performance score, histology, number of involved vertebrae, ambulatory status before irradiation, further bone metastases, visceral metastases, and dynamic of developing motor deficits before irradiation. In addition, the impact of the radiation regimen was investigated. According to Bonferroni correction, p-values of < 0.006 were significant representing an alpha level of < 0.05.

Results. ECOG performance score ($p < 0.001$), number of involved vertebrae ($p = 0.005$), and visceral metastases ($p = 0.004$) had a significant impact on survival and were included in the predictive instrument. Scoring points for each characteristic were calculated by dividing the 6-months survival rates (in %) by 10. The prognostic score for each patient was obtained by adding the scoring points of the three characteristics. The prognostic scores were 4, 9, 10, 14 or 20 points. Three prognostic groups were formed, 4 points ($n = 11$), 9–14 points ($n = 12$) and 20 points ($n = 4$). The corresponding 6-months survival rates were 0%, 33% and 100%, respectively ($p < 0.001$). Median survival times were 1 month, 5 months and 16.5 months, respectively.

Conclusions. This new instrument allows the physician estimate the 6-months survival probability of an individual patient presenting with MESCC from esophageal cancer. This is important to know for optimally personalizing the treatment of these patients.

Key words: esophageal cancer; spinal cord compression; metastatic; epidural; irradiation; survival; predictive instrument

Introduction

In cancer patients, the treatment of loco-regional disease is constantly improving. Therefore, one can expect an increasing number of patients presenting with distant metastases in the future. Bone metastases are quite common in cancer patients and may be associated with complications such as

pathological fractures and metastatic epidural spinal cord compression (MESCC).^{1,2} Different options are available for treating spinal metastases causing MESCC. These options include decompressive surgery, stereotactic body radiotherapy (SBRT), and different regimens of conventional radiotherapy.² During recent years, personalization of treatment has gained importance, particular for palliative

settings and metastatic disease. An optimal personalized treatment approach likely cannot be realized without being able to estimate the patient's remaining lifespan. Therefore, oncologists have focused more strongly on the development of predictive instruments. Also for MESCC, survival scores have already been developed.³ Since each tumor entity leading to spinal metastasis and consequent MESCC has its own biological behavior and metastatic patterns, optimal treatment personalization can only be realized if specific scores are available for each of these entities.^{1,2}

In the current study, we have created a predictive instrument that allows estimating a patient's probability to survive at least 6 months following irradiation for MESCC from esophageal cancer.

Patients and methods

The data of 27 patients irradiated for MESCC were retrospectively analyzed. All patients presented with motor deficits of the legs caused by MESCC. They did not have surgery or irradiation to the involved spinal region before. The diagnosis of MESCC was based on computed tomography or magnetic resonance imaging. Patients were presented to a surgeon prior to irradiation. Dexamethasone was started when MESCC was diagnosed, given during the period of radiation treatment, and tapered down afterwards. Radiotherapy was delivered using a linear accelerator and 6–10 MV photon beams. The treatment volumes encompassed one normal vertebra above and below those vertebrae involved by metastatic disease.

The following nine characteristics were investigated for a potential impact on survival: Age (< 60 years *vs.* ≥ 60 years, median age: 59 years), gender, Eastern Cooperative Oncology Group (ECOG) performance score (1–2 *vs.* 3–4), histology (squamous cell carcinoma *vs.* adenocarcinoma), number of involved vertebrae (1 vertebra *vs.* ≥ 2 vertebrae), ambulatory status before irradiation (ambulatory *vs.* not ambulatory), further bone metastases at the time of irradiation (no *vs.* yes), visceral metastases at the time of irradiation (no *vs.* yes), and the dynamic of the development of motor deficits before irradiation (fast: ≤ 7 days *vs.* slower: > 7 days) (Table 1). Separately, the potential impact of the radiation regimen (short-course: 1 × 8 Gy / 5 × 4 Gy *vs.* longer-course: 10 × 3 Gy / 15 × 2.5 Gy / 20 × 2 Gy) on survival was looked at. For the survival analysis, the Kaplan-Meier method and the log-rank test were used. According to Bonferroni correction for

TABLE 1. Characteristics investigated for survival

	N patients	(%)
Age		
< 60 years	15	56
≥ 60 years	12	44
Gender		
female	5	19
male	22	81
ECOG performance score		
1–2	11	41
3–4	16	59
Histology		
squamous cell carcinoma	11	41
adenocarcinoma	16	59
Number of involved vertebrae		
1 vertebra	6	22
≥ 2 vertebrae	21	78
Ambulatory status before irradiation		
ambulatory	12	44
not ambulatory	15	56
Further bone metastases		
no	9	33
yes	18	67
Visceral metastases		
no	9	33
yes	18	67
Dynamic of developing motor deficits		
fast (≤ 7 days)	10	37
slower (> 7 days)	17	63

ECOG = Eastern Cooperative Oncology Group

multiple tests, results were considered significant for $p < 0.006$ representing an overall alpha level of < 0.05. Characteristics achieving a p-value of < 0.006 were included in the instrument developed for estimation of survival. The study was carried out according to the Helsinki Declaration.

Results

Of the investigated nine characteristic, the following three had a significant impact on survival: ECOG performance score ($p < 0.001$), number of involved vertebrae ($p = 0.005$), and visceral metastases ($p = 0.004$). The results of the survival analysis are presented in Table 2. The additional analysis of the radiation regimen did not reveal a significant association with survival ($p = 0.72$). Six-months survival rates were 25% after short-course irradiation (3 of 12 patients) and 33% (5 of 15 patients) after longer-course irradiation, respectively. The 12-months survival rates were 8% and 13%, respectively.

The three significant characteristics were included in the predictive instrument as follows. Scoring points for each characteristic were calculated by

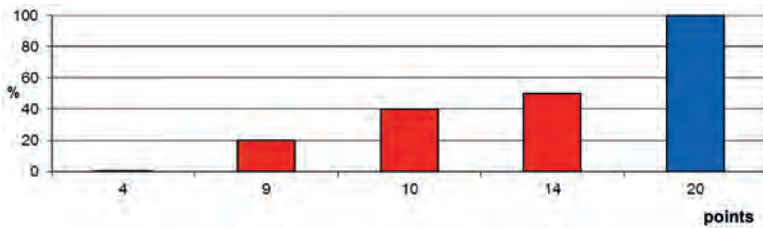


FIGURE 1. The 6-months survival rates of the prognostic scores (4, 9, 10, 14 or 20 points).

TABLE 2. Survival rates at 6 and 12 months

	At 6 months (%)	At 12 months (%)	P
Age			
< 60 years	27	7	0.34
≥ 60 years	33	17	
Gender			
Female	40	20	0.61
Male	27	9	
ECOG performance score			
1–2	55	27	< 0.001
3–4	13	0	
Histology			
squamous cell carcinoma	27	9	0.65
adenocarcinoma	31	13	
Number of involved vertebrae			
1 vertebra	67	50	0.005
≥ 2 vertebrae	19	0	
Ambulatory status before irradiation			
ambulatory	40	20	0.006
not ambulatory	17	0	
Further bone metastases			
no	56	33	0.007
yes	17	0	
Visceral metastases			
no	67	33	0.004
yes	11	0	
Dynamic of developing motor deficits			
fast (≤ 7 days)	20	10	0.19
slower (> 7 days)	35	12	

According to Bonferroni correction, p-values < 0.006 were considered significant. ECOG = Eastern Cooperative Oncology Group

TABLE 3. Survival rates at 6 and the corresponding scoring points

	Survival rate at 6 months (%)	Scoring points
ECOG performance score		
1–2	55	6
3–4	13	1
Number of involved vertebrae		
1 vertebra	67	7
≥ 2 vertebrae	19	2
Visceral metastases		
no	67	7
yes	11	1

ECOG = Eastern Cooperative Oncology Group

dividing the 6-months survival rate (in %) by 10 (Table 3). The prognostic score for each patient was calculated by adding the scoring points of the three significant characteristics. The addition resulted in prognostic scores of 4, 9, 10, 14 or 20 points. The 6-months survival rates of the prognostic scores are shown in Figure 1. Taking into account the 6-months survival rates of the prognostic scores, the following three survival groups were formed: 4 points (n = 11), 9–14 points (n = 12), and 20 points (n = 4). The corresponding survival rates at 6 months were 0%, 33% and 100%, respectively (p < 0.001). Median survival times following irradiation were 1 month (range: 0–3 months), 5 months (range: 2–11 months) and 16.5 months (range: 8–19 months), respectively.

Discussion

In order to achieve the best results of anticancer therapies, personalized treatment approaches are increasingly used. Individual strategies are particularly important for patients with metastatic disease, since each metastatic situation is quite unique. MESCC is not uncommon in oncology and may occur in up to 10% of adult cancer patients^{1,2} “Real” MESCC is associated with neurologic deficits, mostly with motor deficits of the legs. These deficits may range from very mild symptoms to complete paraplegia. Many patients with MESCC are heavily debilitated, whereas others can manage their daily life quite well. In order to optimally tailor the treatment regimen to a patient’s needs, one has to take into account both his current impairment and his remaining lifetime. To choose the most appropriate treatment strategy, it is very important to be able to rate the patient’s survival prognosis as precise as possible. This can be achieved with the application of predictive tools based on prognostic factors. Primary tumors can vary considerably with respect to biological behavior, metastatic spread, response to anticancer treatment, and prognosis. Taking into account these aspects, it becomes obvious that separate predictive tools are important to optimally personalize the treatment. In the present study, we created a survival score specifically for patients with MESCC from esophageal cancer. When using this instrument, the retrospective study design and the relatively small number of patients must be considered. However, since patients with MESCC from esophageal cancer are rare, a larger prospective series will not be available soon.^{1,2,4}

In the current study, three characteristics, ECOG performance score, number of affected vertebrae and visceral metastases, were identified that had a significant impact on survival in such patients. Based on these three characteristics, a predictive instrument including three prognostic groups was developed. The 6-months survival rates of these groups varied considerably. Of the group of patients achieving only 4 points, no patient survived longer than three months. Therefore, these patients are no candidates for decompressive surgery prior to irradiation. They should receive a short course of irradiation, preferably a single fraction of 8 Gy. Several studies have shown that 1 x 8 Gy is not inferior to multi-fraction programs with respect to pain relief and improvement of motor deficits. In a meta-analysis including 5,617 patients from randomized trials, overall pain relief was observed in 60% of patients after single-fraction treatment and 61% after multi-fraction treatment, respectively ($p = 0.36$).⁵ Complete pain relief was achieved in 23% of patients and 24% of patients, respectively ($p = 0.57$). In a randomized trial of 276 patients from Italy, 1 x 8 Gy resulted in similar functional outcomes when compared to a longer (two-and-a-half weeks) split-course regimen (3 x 5 Gy followed by one week rest and 5 x 3 Gy).⁶ Sixty-eight per cent and 71% of patients, respectively, were able to walk after irradiation. In a large retrospective study of 1,304 patients from several European countries, 1 x 8 Gy was similarly effective as 5 x 4 Gy in one week, 10 x 3 Gy in two weeks, 15 x 2.5 Gy in three weeks and 20 x 2 Gy in four weeks with respect to improvement of motor function.⁷ Improvement rates at one month after radiotherapy were 26% (1 x 8 Gy), 28% (5 x 4 Gy), 27% (10 x 3 Gy), 31% (15 x 2.5 Gy), and 28% (20 x 2 Gy), respectively ($p = 0.90$). The post-treatment ambulatory rates were 69%, 68%, 63%, 66% and 74%, respectively ($p = 0.58$).

Patients achieving 9–14 points in the predictive instrument presented here had a 6-months survival probability of 33% and a median survival time of five months. To be suitable for decompressive surgery, a survival prognosis of at least three months was required in a randomized study from the United States.⁸ Therefore, in selected patients (spinal instability, vertebral fracture, sphincter dysfunction) of this prognostic group the option of surgery followed by longer-course irradiation should be discussed. If surgery is not indicated, these patients should receive fractionated irradiation, for example 5 x 4 Gy or 10 x 3 Gy. One has to be aware that in-field recurrences of MESCC

occur more frequently after 5 x 4 Gy than after 10 x 3 Gy.^{9,10}

Those patients who achieved 20 points in the current score had a favorable survival prognosis of median 16.5 months. All patients survived longer than 6 months. Unfortunately, this prognostic group represented only 15% of the patients in the present study. However, it is important to identify these patients, since they are at a considerably higher risk of developing an in-field recurrence of MESCC than patients achieving ≤ 14 points. MESCC patients with such a favorable survival prognosis were shown in a retrospective study of 382 patients to benefit from 15 x 2.5 Gy or 20 x 2 Gy when compared to 10 x 3 Gy in terms of better local control (risk ratio: 2.42; $p = 0.011$) and better survival (risk ratio: 1.64; $p = 0.014$).¹¹ Therefore, these patients should receive longer-course irradiation with doses beyond 30 Gy. In addition, these patients should be presented to a surgeon prior to irradiation to discuss whether upfront decompressive surgery is indicated and possible. For highly selected patients, even radiosurgery and SBRT may be considered. When delivering radiosurgery or SBRT, it is mandatory to regard the tolerance doses of spinal cord and vertebral bone, since rates of treatment-related vertebral fractures up to 39% and neurologic deficits up to 8% were reported.^{12,13} In an international practice guideline, SBRT was recommended to be used for MESCC only within clinical trials, which was also supported by a recent review article.^{14,15}

Conclusions

New predictive instrument has been designed that allows estimating the survival time of patients with MESCC from esophageal cancer. This instrument can assist the physician in selecting the appropriate radiation regimen and in making a decision for or against upfront decompressive surgery.

References

1. Prasad D, Schiff D. Malignant spinal cord compression. *Lancet Oncol* 2005; **6**: 15-24.
2. Rades D, Abraham JL. The role of radiotherapy for metastatic epidural spinal cord compression. *Nat Rev Clin Oncol* 2010; **7**: 590-8.
3. Rades D, Douglas S, Veninga T, Stalpers LJA, Hoskin PJ, Bajrovic A, et al. Validation and simplification of a score predicting survival in patients irradiated for metastatic spinal cord compression. *Cancer* 2010; **116**: 3670-3.
4. Rades D, Rudat V, Veninga T, Stalpers LJA, Bazic H, Karstens JH, et al. A score predicting post-treatment ambulatory status in patients irradiated for metastatic spinal cord compression. *Int J Radiat Oncol Biol Phys* 2008; **72**: 905-8.

5. Chow E, Zeng L, Salvo N, Dennis K, Tsao M, Lutz S. Update on the systematic review of palliative radiotherapy trials for bone metastases. *Clin Oncol (R Coll Radiol)* 2012; **24**: 112-24.
6. Maranzano E, Bellavita R, Rossi R, De Angelis V, Frattegiani A, Bagnoli R, et al. Short-course versus split-course radiotherapy in metastatic spinal cord compression: results of a phase III, randomized, multicenter trial. *J Clin Oncol* 2005; **23**: 3358-65.
7. Rades D, Stalpers LJ, Veninga T, Schulte R, Hoskin PJ, Obralic N, et al. Evaluation of five radiation schedules and prognostic factors for metastatic spinal cord compression. *J Clin Oncol* 2005; **23**: 3366-75.
8. Patchell R, Tibbs PA, Regine WF, Payne R, Saris S, Kryscio RJ, et al. Direct decompressive surgical resection in the treatment of spinal cord compression caused by metastatic cancer: a randomised trial. *Lancet* 2005; **366**: 643-8.
9. Rades D, Fehlaue F, Schulte R, Veninga T, Stalpers LJ, Basic H, et al. Prognostic factors for local control and survival after radiotherapy of metastatic spinal cord compression. *J Clin Oncol* 2006; **24**: 3388-93.
10. Rades D, Lange M, Veninga T, Stalpers LJA, Bajrovic A, Adamietz IA, et al. Final results of a prospective study comparing the local control of short-course and long-course radiotherapy for metastatic spinal cord compression. *Int J Radiat Oncol Biol Phys* 2011; **79**: 524-30.
11. Rades D, Panzner A, Rudat V, Karstens JH, Schild SE. Dose escalation of radiotherapy for metastatic spinal cord compression (MSCC) in patients with relatively favorable survival prognosis. *Strahlenther Onkol* 2011; **187**: 729-35.
12. Rose PS, Laufer I, Boland PJ, Hanover A, Bilsky MH, Yamada J, et al. Risk of fracture after single fraction image-guided intensity-modulated radiation therapy to spinal metastases. *J Clin Oncol* 2009; **27**: 5075-9.
13. Garg AK, Shiu AS, Yang J, Wang XS, Allen P, Brown BW, et al. Phase 1/2 trial of single-session stereotactic body radiotherapy for previously unirradiated spinal metastases. *Cancer* 2012; **118**: 5069-77.
14. Lutz S, Berk L, Chang E, Chow E, Hahn C, Hoskin P, et al. Palliative radiotherapy for bone metastases: an ASTRO evidence-based guideline. *Int J Radiat Oncol Biol Phys* 2011; **79**: 965-76.
15. Chawla S, Schell MC, Milano MT. Stereotactic body radiation for the spine: a review. *Am J Clin Oncol* 2013; **36**: 630-6.

Dosimetric comparison for volumetric modulated arc therapy and intensity-modulated radiotherapy on the left-sided chest wall and internal mammary nodes irradiation in treating post-mastectomy breast cancer

Qian Zhang¹, Xiao Li Yu¹, Wei Gang Hu¹, Jia Yi Chen¹, Jia Zhou Wang¹, Jin Song Ye², Xiao Mao Guo¹

¹ Department of Radiation Oncology, Fudan University Shanghai Cancer Center; Department of Oncology, Shanghai Medical College, Fudan University, 270 Dong An Road, Shanghai 200032, China

² Swedish Cancer Institute, 747 Broadway, Seattle, USA

Radiol Oncol 2015; 49(1): 91-98.

Received 11 October 2013

Accepted 7 July 2014

Correspondence to: Xiao Mao Guo M.D., Department of Radiation Oncology, Fudan University Shanghai Cancer Center; Department of Oncology, Shanghai Medical College, Fudan University, 270 Dong An Road, Shanghai 200032, China. 8621 64175590 6602; Fax: 86 21 6403 6901; E-mail: xiaomaoguo@hotmail.com

Qian Zhang and Xiao Li Yu contributed equally to this work.

Disclosure: No potential conflicts of interest were disclosed.

Background. The aim of the study was to evaluate the dosimetric benefit of applying volumetric modulated arc therapy (VMAT) on the post-mastectomy left-sided breast cancer patients, with the involvement of internal mammary nodes (IMN).

Patients and methods. The prescription dose was 50 Gy delivered in 25 fractions, and the clinical target volume included the left chest wall (CW) and IMN. VMAT plans were created and compared with intensity-modulated radiotherapy (IMRT) plans on Pinnacle treatment planning system. Comparative endpoints were dose homogeneity within planning target volume (PTV), target dose coverage, doses to the critical structures including heart, lungs and the contralateral breast, number of monitor units and treatment delivery time.

Results. VMAT and IMRT plans showed similar PTV dose homogeneity, but, VMAT provided a better dose coverage for IMN than IMRT ($p = 0.017$). The mean dose (Gy), V_{30} (%) and V_{10} (%) for the heart were 13.5 ± 5.0 Gy, $9.9\% \pm 5.9\%$ and $50.2\% \pm 29.0\%$ by VMAT, and 14.0 ± 5.4 Gy, $10.6\% \pm 5.8\%$ and $55.7\% \pm 29.6\%$ by IMRT, respectively. The left lung mean dose (Gy), V_{20} (%), V_{10} (%) and the right lung V_5 (%) were significantly reduced from 14.1 ± 2.3 Gy, $24.2\% \pm 5.9\%$, $42.4\% \pm 11.9\%$ and $41.2\% \pm 12.3\%$ with IMRT to 12.8 ± 1.9 Gy, $21.0\% \pm 3.8\%$, $37.1\% \pm 8.4\%$ and $32.1\% \pm 18.2\%$ with VMAT, respectively. The mean dose to the contralateral breast was 1.7 ± 1.2 Gy with VMAT and 2.3 ± 1.6 Gy with IMRT. Finally, VMAT reduced the number of monitor units by 24% and the treatment time by 53%, as compared to IMRT.

Conclusions. Compared to 5-beam step-and-shot IMRT, VMAT achieves similar or superior target coverage and a better normal tissue sparing, with fewer monitor units and shorter delivery time.

Key words: breast cancer; radiotherapy; VMAT; IMRT

Introduction

Among the most commonly diagnosed cancers, breast cancer alone accounts for 29% of all new cancers among women in 2014.¹ Most early-stage

patients can be treated with breast conserving surgery, adjuvant radiotherapy or systemic treatment combined with neoadjuvant chemotherapy.² However, patients with the advanced conditions usually receive mastectomy and postoperative ra-

diotherapy. It has been shown that adjuvant post mastectomy radiotherapy (PMRT) is efficient in reducing locoregional recurrence rate, and improving 10-year overall survival rate in patients with lymph node-positive breast cancer.^{3,4,8}

However, there is a dosimetric challenge to deliver an uniform target dose to the patient with three-dimensional conformal radiotherapy (3D-CRT) if internal mammary node (IMN) is involved, especially in the patients with left-sided breast cancer.^{9,10} In order to achieve better cosmetic results and decrease the toxicity in normal tissues, the intensity modulated radiation therapy (IMRT) has been widely implemented in the clinic to improve the target dose homogeneity and conformity for breast cancer treatment as well as spare the irradiation doses of normal tissues.¹¹⁻¹³ Compared to the 3D-CRT, Van der Laan *et al.* reported that the IMRT technique improved the chest wall (CW) and IMN dose coverage and reduced the cardiac dose. Previously, we conducted a similar study in 30 patients with left-sided post-mastectomy breast cancer, and the results showed that the conformity index of IMRT was better than that of 3D-CRT and IMRT increased the low-dose volume of normal tissue.^{14,15}

Volumetric modulated arc therapy (VMAT), a novel technique that delivers the radiation dose to the target in a single or multiple gantry rotations, has been used in the treatment of many cancers sites, such as prostate, head and neck, and Hodgkin lymphoma.¹⁶⁻²⁰ Some dosimetric studies compared VMAT with other techniques in treating breast cancer patients.^{21,22} Also, one study compared the rapid arc (a VMAT technique), IMRT and modified wide-tangent techniques in the left-sided breast cancer and found that the rapid arc could achieve similar target coverage as IMRT but with better organ at risks sparing and shorter treatment time, though only one patient received mastectomy in their 5-patient study.²³ To master the application of VMAT with better efficacy, we investigated the dosimetric difference between the VMAT and IMRT in patients with left-sided breast cancer in the present study.

Patients and methods

Patients

From April 2009, the first fifteen left-sided breast cancer patients (T3/4, metastatic axillary lymph nodes > 4) treated in our department, with the mean age of 48 years (39 to 58), were enrolled in the study. All patients had undergone post-mastectomy and

Level I-II nodal dissection and received the combined chemotherapy with or without trastuzumab. Patients were set up on a breast board (Med-Tec Corporation, USA) with the sternum parallel to the table and the left arms elevated above their heads. The patient's head turned to the right side. The radio-opaque markers were placed on the patient's midline, mid axillary line, the inferior aspect of the clavicle head, the inferior border at 1 cm below the contralateral infra mammary fold and the superior aspect of the fourth rib. CT images were acquired from the level of mandible to the lung base on a large bore CT scanner (Philips Medical, Fitchburg, WI, USA) with a slice thickness of 5 mm. All the images were exported to the Pinnacle treatment planning system (Pinnacle³ version 9.0, Philips Radiation Oncology Systems, Andover, MA) for contouring and treatment planning.

Target definitions

The clinical target volume (CTV) of CW (CTV_{CW}) and IMN (CTV_{IMN}) was delineated according to the Radiation Therapy Oncology Group (RTOG) breast cancer consensus definitions. The CTV_{IMN} was contoured from the superior aspect of the medial first rib to the fourth one by encompassing the internal mammary/thoracic vessels. A margin of 10 mm was added to CTV_{CW} and CTV_{IMN} to define the planning target volume of CW (PTV_{CW}) and IMN (PTV_{IMN}). Total PTV (PTV_{total}) consisted of PTV_{CW} and PTV_{IMN}. All the PTV_{CW}, PTV_{IMN} and PTV_{total} were limited to the skin surface. The organs at risk were also outlined: the heart contoured from the first CT slice below the pulmonary artery to the apex inferiorly; the entire ipsilateral and contralateral lung contoured; and the contralateral breast outlined based on the visible breast parenchyma.

Treatments

The treatments were planned for delivery on an Elekta Synergy linear accelerator (Elekta Oncology System, Crawley, UK) with 1-cm width multileaf collimator (MLC). A 5 mm tissue-equivalent bolus was placed on the patient's skin with the coverage of PTV and surgical scar to increase the skin dose. The dose was calculated using the collapse cone superposition convolution algorithm with inhomogeneity correction.

In the present dosimetric study, one step-and-shoot IMRT and one VMAT treatment plan were created for each patient within the Pinnacle treatment planning system with the same dose optimi-

zation objectives. The isocenter was placed at the center of the PTV. The prescription dose was 50 Gy in 25 fractions. The plan quality for both treatment techniques was evaluated against the following criteria: at least 95% of the PTV volume receiving 50 Gy, 95% of the prescription dose ($V_{95\%}$) covering at least 99% of the PTV volume; the hot spot defined as PTV receiving more than 110% of prescription dose as little as possible; less than 20% of the left lung to 20 Gy (V_{20}); less than 10% of the heart to 30 Gy (V_{30}); a minimized dose to the contralateral lung and breast since some of the beams could penetrate the patient's right lung and right breast.

A step-and-shoot IMRT plan with 5 beams (300, 0, 40, 80 and 110 degree) was created for each patient. The optimization was performed using the direct machine parameter optimization (DMPO) technique with preset parameters of minimum 3 monitor units, minimum 3 cm² segment area and maximum 50 segments. Before the final dose calculation, the MLC leaves were manually pushed outside of the patient's skin by 1 cm if they blocked only the air part in the beam's eye view.

The SmartArc in Pinnacle was used for the VMAT planning. One or two 200 degree partial arcs (gantry rotated from 310 to 150 degrees) and 15 degree collimator rotation were utilized to generate VMAT plans. A 4-degree resolution was used for the final dose calculation. For the purpose of fair plan comparison, several step-and-shoot IMRT and SmartArc VMAT plans were created for the initial 3 patients and the best IMRT and VMAT plans were selected for dose volume histogram (DVH) data analysis. Then, the optimization parameters for the best plans were used for the following patients and all the required DVH data were obtained.

The DVHs of the PTV_{total}, PTV_{IMN}, lungs, heart and contralateral breast were derived from the IMRT and VMAT plans. For the targets were calculated the D_{98} (the minimum dose received by 98% of the target volume), $D_{2\%}$, mean dose, dose homogeneity index (HI), $V_{90\%}$ (percentage of the PTV receiving at least 90% of the prescription dose) and $V_{95\%} \cdot D_{98}$ and D_2 were used to evaluate the minimal and maximal dose to the target, respectively. The homogeneity index was calculated as follows:

$$HI = \frac{(D_2 - D_{98})}{D_p} * 100\%$$

where the D_p is the prescription dose, and lower HI means better homogeneity. Additionally, the $V_{110\%}$ and $V_{115\%}$ for the PTV_{IMN} were also recorded. For the critical structures, the mean dose, $V_{30\%}$, $V_{5\%}$ and V_{10} of the heart, and $V_{20\%}$, $V_{5\%}$, V_{10} and mean dose

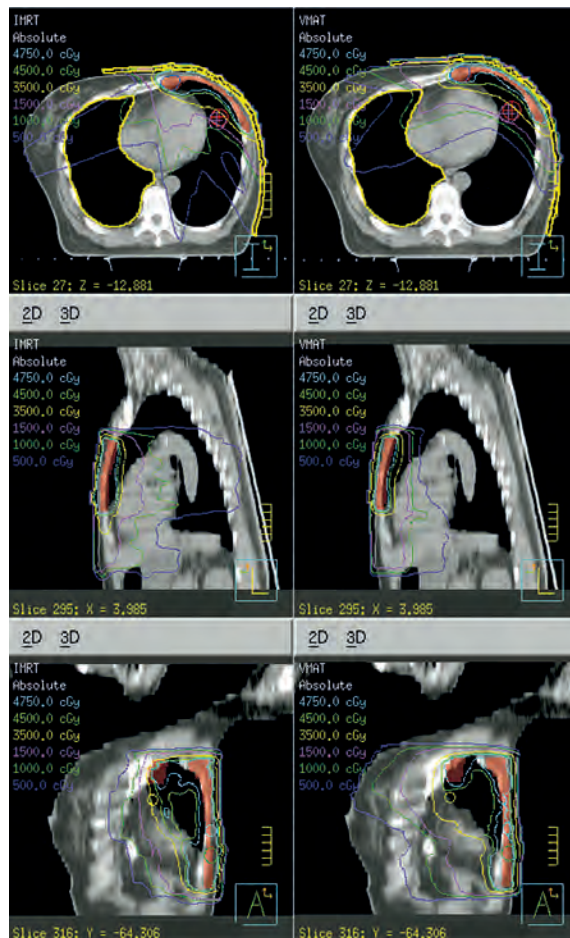


FIGURE 1. Comparison between volumetric modulated arc therapy (VMAT) and intensity-modulated radiotherapy (IMRT) on dose distribution on the transverse plane at isocenter (from one representative case). The VMAT plan is on the right side and the IMRT on the left side.

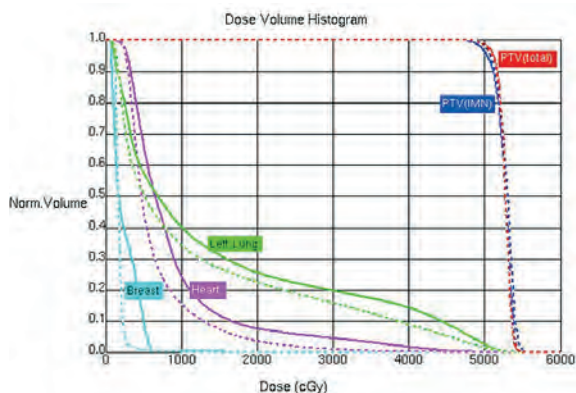


FIGURE 2. Comparison between volumetric modulated arc therapy (VMAT) and intensity-modulated radiotherapy (IMRT) on dose volume histogram for PTV_{total}, PTV_{IMN}, heart, left lung and the contralateral breast (from one representative case shown in Figure 1). The VMAT plan is displayed as dashed line, IMRT plan as solid line.

TABLE 1. Comparison of the dose coverage for the PTV_{total} and the PTV_{IMN} (mean ± SD)

PTV _{total}		IMRT	VMAT	p value
Max dose (D ₂)	(Gy)	55.6 ± 2.2	55.4 ± 1.7	0.760
Min dose (D ₉₈)	(Gy)	48.8 ± 1.0	48.5 ± 2.2	0.616
Mean dose	(Gy)	52.6 ± 1.2	52.4 ± 1.7	0.344
HI		0.15 ± 0.05	0.15 ± 0.01	0.602
V ₄₅	(%)	99.8 ± 0.3	100.0 ± 0.1	0.524
V _{47.5}	(%)	98.9 ± 1.1	99.1 ± 1.1	0.363
PTV _{IMN}				
Max dose (D ₂)	(Gy)	56.8 ± 2.0	56.2 ± 1.6	0.126
Min dose (D ₉₈)	(Gy)	41.7 ± 5.4	45.3 ± 6.9	0.016
Mean dose	(Gy)	52.6 ± 1.8	53.1 ± 1.1	0.207
HI		0.15 ± 0.06	0.13 ± 0.06	0.048
V ₄₅	(%)	99.3 ± 1.5	100.0 ± 0.1	0.017
V _{47.5}	(%)	98.1 ± 2.9	99.2 ± 1.8	0.017
V ₅₅	(%)	14.6 ± 24.6	15.7 ± 19.9	0.787
V _{57.5}	(%)	4.0 ± 16.3	2.0 ± 3.6	0.421

HI = homogeneity index; IMRT = intensity-modulated radiotherapy; Max = maximal; Min = minimal; PTV_{IMN} = internal mammary node planning target volume; PTV_{total} = planning target volume; SD = standard deviation; V₄₅ = the percentage of the lung volume which receives radiation doses of 45 Gy; VMAT = volumetric modulated arc therapy

of the ipsilateral lung, V₅ and mean dose of the contralateral lung and mean dose of the contralateral breast were calculated. Number of monitor units and treatment delivery time were also calculated. Dry runs were performed for all the plans.

Statistical analysis

The results were represented as mean ± standard deviation (SD). Statistical analysis was performed using SPSS 17.0 software (Chicago, IL, USA). The two-sided paired t test was used when the datasets were normally distributed. Otherwise, datasets were compared by Wilcoxon Cox test. The p value less than 0.05 was considered statistically significant.

Results

Target coverage

The mean volume of PTV_{total} was 212cm³ (90 to 425 cm³). A dose distribution is shown in Figure 1 and the corresponding DVHs in Figure 2 for a typical patient. The differences in the PTV_{total} coverage and

dose homogeneity between two techniques were of no statistical significance, V_{95%} being 99.1% ± 1.1% with VMAT and 98.9% ± 1.1% with IMRT (p = 0.363); the similar maximum dose of PTV_{total} defined as one in 2% of the target volume, i.e. D₂, 55.6 ± 2.2 Gy with IMRT and 55.4 ± 1.7 Gy with VMAT, respectively; and the dose homogeneity index being 0.15 with both VMAT and IMRT (Table 1).

As for the dosimetric comparison data for the smaller PTV_{IMN}, the VMAT plans provided a better IMN coverage than the IMRT ones, the mean values of V_{95%} were 99.2% ± 1.8% and 98.1% ± 2.9% with VMAT and IMRT, respectively (p = 0.017). Although there was no significant difference in PTV_{IMN} mean doses, the VMAT plans seemed to develop more homogeneous dose distribution in the IMN. The minimal dose to PTV_{IMN} (D₉₈) with VMAT was higher than that with IMRT (45.3 ± 6.9 Gy for VMAT vs 41.7 ± 5.4 Gy for IMRT) (p = 0.016). The mean HI was found to be 0.13 ± 0.06 with VMAT and 0.15 ± 0.06 with IMRT (p = 0.048). Both techniques presented comparable hot spots as the p values for V_{110%} and V_{115%} were 0.421 and 0.334, respectively (Table 1).

Normal tissue sparing

In terms of the doses to the normal tissues for the two treatment techniques, VMAT slightly reduced the mean dose to the heart, 13.5 ± 5.5 Gy for VMAT vs. 14.0 ± 5.3 Gy for IMRT (p = 0.792). Meanwhile, it did not show any significant differences in heart V₃₀ and V₅₇ as well as in V₁₀ compared with IMRT (50.2% ± 29.0% with VMAT vs. 55.7% ± 29.6% with IMRT, p = 0.611) (Table 2).

It was also found that the VMAT plans achieved lower mean dose to the left lung than the IMRT ones, i.e., 12.8 ± 1.9 Gy vs. 14.1 ± 2.3 Gy (p = 0.001). Moreover, the values of left lung V_{20%}, V₁₀ and V₅ were 21.0% ± 3.8%, 37.1% ± 8.4%, 61.1% ± 18.0% for VMAT, and 24.2% ± 5.9%, 42.4% ± 11.9%, 66.0% ± 15.5% for IMRT. There was no significant difference in the mean dose of right lung, but VMAT plans achieved lower V₅ to the right lung, as compared to IMRT (32.1% ± 18.2% with VMAT vs. 41.2% ± 12.3% with IMRT, p = 0.034). The mean dose to the contralateral breast was 1.7 ± 1.2 Gy and 2.3 ± 1.6 Gy, respectively (p = 0.001) (Table 2).

Monitor units and treatment delivery time

The dose rate for IMRT was 512 MU/min, and the maximum dose rate for VMAT was 512 MU/min.

TABLE 2. Comparison parameters of normal tissue with VMAT or IMRT (mean \pm SD)

Structure	Parameters		IMRT	VMAT	VMAT/IMRT	p value
Heart	Mean dose	(Gy)	14.0 \pm 5.3	13.5 \pm 5.0	0.97 \pm 0.05	0.792
	V ₃₀	(%)	10.6 \pm 5.8	9.9 \pm 5.9	0.91 \pm 0.30	0.251
	V ₁₀	(%)	55.7 \pm 29.6	50.2 \pm 29.0	0.89 \pm 0.12	0.611
	V ₅	(%)	77.0 \pm 21.1	78.0 \pm 20.1	1.02 \pm 0.06	0.355
Left Lung	Mean dose	(Gy)	14.1 \pm 2.3	12.8 \pm 1.9	0.91 \pm 0.05	0.001
	V ₂₀	(%)	24.2 \pm 5.9	21.0 \pm 3.8	0.89 \pm 0.09	0.002
	V ₁₀	(%)	42.4 \pm 11.9	37.1 \pm 8.4	0.89 \pm 0.09	0.001
	V ₅	(%)	66.0 \pm 15.5	61.1 \pm 18.0	0.92 \pm 0.07	0.001
Right Lung	Mean dose	(Gy)	4.67 \pm 0.93	4.49 \pm 1.06	0.94 \pm 0.14	0.409
	V ₅	(%)	41.2 \pm 12.3	32.1 \pm 18.2	0.71 \pm 0.31	0.034
Right Breast	Mean dose	(Gy)	2.3 \pm 1.6	1.7 \pm 1.2	0.70 \pm 0.04	0.002

IMRT = intensity-modulated radiotherapy; SD = standard deviation; V₃₀ = the percentage of the lung volume which receives radiation doses of 30 Gy; VMAT = volumetric modulated arc therapy

The mean number of MU for VMAT plans was 462 (range, 380 to 590 MU) compared to 604 (range, 488 to 850 MU) for IMRT. The mean treatment time for one arc was 2.0 minutes, and the mean treatment time to deliver two arcs was 4.20 minutes (range, 4.1 to 4.3 minutes) compared to 9.0 minutes (range, 8.7 to 11.2 minutes) for IMRT.

Discussion

IMRT and VMAT can shape the dose to the concave target in the CW and IMN in breast cancer radiotherapy. In the current study, we reported a dosimetric comparison between the two techniques on 15 cases of left-sided breast cancer. The step-and-shoot IMRT plans using DMPO technique and the VMAT plans using the SmartArc were used in the Pinnacle treatment planning system. In our study, CT images were acquired base on a CT scanner with a slice thickness of 5 mm. Though the widths of slices are usually 2-3 mm, CT scan could also be

performed using 5 mm slice thickness to evaluate the dose distribution of IMRT.³⁻⁷

Target coverage

It has a benefit in maximizing efficacy and improving local control to ensuring homogeneous dose coverage of PTV by avoiding areas of under dose ('cold spots', PTV receiving less than 90% of prescription dose), and at the same time eliminating areas of relative overdose ('hot spots'), minimizing normal long-term tissue toxicity (skin changes and fibrosis) which negatively affect cosmesis. In our study, the IMRT and VMAT plans showed similar PTV_{total} coverages and both avoided the hot spots successfully. However, the VMAT had a better dose homogeneity in the PTV_{IMN} by reducing the "cold spot", which might decrease the local recurrence in the IMN area.

The radiotherapy target volume includes the CW, supraclavicular fossa and IMN with or without the axilla.^{24,25} Though the inclusion of the supraclavicular region in the post-mastectomy

radiotherapy has an influence on the dose to the ipsilateral lung, it is still reasonable and significant to compare the dose coverage between IMRT and VMAT when the supraclavicular region was not considered for all the patients. On the other hand, PTV should be a few millimetres below the skin surface. In our study, the PTVs were limited to the skin surface due to that chest has thinner wall with a few millimetres and bolus was placed on the patient's chest skin surface to increase the skin dose. Therefore, the skin could provide the dose we needed and it is unnecessary to subtract a few millimetres from the skin surface.

Organs at risk dose

It has been shown that the V_{20} and mean dose to the lung are good predictors for radiation induced lung toxicity.²⁶ Also, an analysis of non-small-cell lung cancer has shown that the V_5 is a significant cut off point for the subsequent development of pneumonitis.²⁷ When it comes to the breast cancer, it was found that clinically significant pneumonitis was rare if the V_{20} of ipsilateral lung was less than 30% for breast cancer patients.²⁸ It has been also reported that the complication rate could be expected to be 20% if more than 50% of the lung volume received 10 Gy.²⁹ We selected $V_{20} < 20\%$ as a criterion since it is also an optimization parameter in our centre. We found that the VMAT plan had a significant reduction in the V_{20} , V_{10} , V_5 or the mean dose in the left lung than IMRT. Also, the VMAT showed the superior or similar right lung sparing compared with IMRT. These results strongly suggested that the VMAT technique could achieve better sparing of the lung.

It has been reported that the use of 3D-CRT and IMRT techniques in the treatment of breast cancer could reduce the cardiac dose and cardiac mortality.^{30,31} However, the potential cardiac toxicity was increased dramatically owing to the widespread use of anthracyclines, taxanes and trastuzumab.^{32,33} Therefore, it is critical to limit the heart dose in patients, especially those with left-sided breast cancer. It has been reported that the heart V_{30} of IMRT was significantly lower than 3D-CRT levels for patients underwent left-sided mastectomy.¹⁴ Rudat *et al.* have found that IMRT significantly reduced the ipsilateral lung dose and heart dose in 20 subsequent post mastectomy breast cancer patients.³⁴ Moreover, VMAT has been revealed to deliver lower doses to the ipsilateral breast and lung and offer better dose conformity than 3D-CRT technique for partial breast irradiation patients.³⁵ In this study,

the dose to the heart for IMRT and VMAT was similar.

The dose to the contralateral breast is another critical factor to consider, especially in younger women who received RT. Previous studies showed that there was an elevated long-term risk of developing the secondary contralateral breast cancer, and the mean dose to the contralateral breast was 3.2 Gy with RapidArc.^{23,36} In our study, a slightly lower mean dose of 1.7 Gy was observed with VMAT, which may be the results of different dose calculation algorithms or inhomogeneity correction in the two treatment planning systems. We also found that the average mean dose to the contralateral breast was 2.3 Gy in the IMRT, suggesting that VMAT might have dosimetric effect in reducing the risk of contralateral breast cancer occurrence.

Organ motion

It is well known that the respiration-induced target motion can lead to variation between the planned and delivered dose. A 10 mm margin was applied in the study for expanding the CTV to PTV. We then evaluated the intra-fraction motion of the chest wall using the fluoroscopic imaging on the simulator and found that the maximum displacement was around 3 mm. It's been reported that the respiratory movements of the breast during normal breathing were negligible, and at 80% of the tidal capacity the mean displacement of the breast and chest wall from the exhale was less than 1 mm in the anterior and superior directions.^{37,38} The 5 mm margin may extend the PTV to the outside of skin. With limited segments of the step-and-shot IMRT plans (maximum 50 segments), the MLC leaves can be pushed outwards from the patient's skin by 1 or 2 cm if only the air part in BEV was blocked. However, such manual adjustment is unfeasible in the VMAT plans. Therefore, the solutions with improved target coverage for possible changes in size and position of target and rest tissues caused by respiration or oedema are to use the third-party software to move the block-air MLC away from the skin, or manually add 10-mm tissue around the skin for optimization but removing it in the final dose calculation.³⁹ Another clinical advantage of VMAT is that it generally takes fewer MUs to deliver a VMAT treatment than IMRT for the same plan quality. Our results showed that the MUs for the fifteen chest walls examined by VMAT plans were about 2/3 to 3/4 of those by IMRT plans. Obviously, fewer MUs are always favourable as to

shorten the treatment delivery time and reduce the whole body dose.

Conclusions

Overall, our results showed that VMAT achieved similar or superior target coverage, better normal tissue sparing, fewer monitor units and shortened delivery time, as compared with 5-beam step-and-shot IMRT.

Acknowledgements

This study was supported by the National Natural Science Foundation of China (Grant No. 81072164)

References

- Siegel R, Ma J, Zou Z, Jemal A. Cancer statistics, 2014. *CA Cancer J Clin* 2014; **64**: 9-29.
- Caudell JJ, De Los Santos JF, Keene KS, Fiveash JB, Wang W, Carlisle JD, et al. A dosimetric comparison of electronic compensation, conventional intensity modulated radiotherapy, and tomotherapy in patients with early-stage carcinoma of the left breast. *Int J Radiat Oncol Biol Phys* 2007; **68**: 1505-11.
- Chung CS, Harris JR. Post-mastectomy radiation therapy: translating local benefits into improved survival. *Breast* 2007; **16** (Suppl 2): S78-83.
- Overgaard M, Hansen PS, Overgaard J, Rose C, Andersson M, Bach F, et al. Postoperative radiotherapy in high-risk premenopausal women with breast cancer who receive adjuvant chemotherapy. Danish Breast Cancer Cooperative Group 82b Trial. *N Engl J Med* 1997; **337**: 949-55.
- Overgaard M, Jensen MB, Overgaard J, Hansen PS, Rose C, Andersson M, et al. Postoperative radiotherapy in high-risk postmenopausal breast-cancer patients given adjuvant tamoxifen: Danish Breast Cancer Cooperative Group DBCG 82c randomised trial. *Lancet* 1999; **353**: 1641-8.
- Ragaz J, Jackson SM, Le N, Plenderleith IH, Spinelli JJ, Basco VE, et al. Adjuvant radiotherapy and chemotherapy in node-positive premenopausal women with breast cancer. *N Engl J Med* 1997; **337**: 956-62.
- Moo T-A, El-Tamer M. Use of postmastectomy radiation therapy in the treatment of breast cancer. *Breast Cancer Management* 2012; **1**: 177-80.
- Duraker N, Demir D, Bati B, Yilmaz BD, Bati Y, Caynak ZC, et al. Survival benefit of post-mastectomy radiotherapy in breast carcinoma patients with T1-2 tumor and 1-3 axillary lymph node(s) metastasis. *Jpn J Clin Oncol* 2012; **42**: 601-8.
- Coskun M, Ozsahin M, Sozzi WJ, Tsoutsou P. Application of Tomotherapy in Breast Cancer Patients. In: Haydaroglu A, Ozyigit G, editors. *Principles and practice of modern radiotherapy techniques in breast cancer*. New York: Springer Science and Business Media; 2013. p. 299-318.
- Hjelstuen MH, Mjaaland I, Vikstrom J, Dybvik KI. Radiation during deep inspiration allows loco-regional treatment of left breast and axillary-, supraclavicular- and internal mammary lymph nodes without compromising target coverage or dose restrictions to organs at risk. *Acta Oncol* 2012; **51**: 333-44.
- Dogan N, Cuttino L, Lloyd R, Bump EA, Arthur DW. Optimized dose coverage of regional lymph nodes in breast cancer: the role of intensity-modulated radiotherapy. *Int J Radiat Oncol Biol Phys* 2007; **68**: 1238-50.
- Beckham WA, Popescu CC, Patenaude VV, Wai ES, Olivetto IA. Is multibeam IMRT better than standard treatment for patients with left-sided breast cancer? *Int J Radiat Oncol Biol Phys* 2007; **69**: 918-24.
- Coles CE, Moody AM, Wilson CB, Burnet NG. Reduction of radiotherapy-induced late complications in early breast cancer: the role of intensity-modulated radiation therapy and partial breast irradiation. Part II--Radiotherapy strategies to reduce radiation-induced late effects. *Clin Oncol (R Coll Radiol)* 2005; **17**: 98-110.
- van der Laan HP, Korevaar EW, Dolsma WV, Maduro JH, Langendijk JA. Minimising contralateral breast dose in post-mastectomy intensity-modulated radiotherapy by incorporating conformal electron irradiation. *Radiother Oncol* 2010; **94**: 235-40.
- Zhang Q, Chen JY, Hu WG, Guo XM. Modified partially wide tangents technique in post-mastectomy radiotherapy for patients with left-sided breast cancer. *Chin Med J (Engl)* 2010; **123**: 2825-31.
- Palma D, Vollans E, James K, Nakano S, Moiseenko V, Shaffer R, et al. Volumetric modulated arc therapy for delivery of prostate radiotherapy: comparison with intensity-modulated radiotherapy and three-dimensional conformal radiotherapy. *Int J Radiat Oncol Biol Phys* 2008; **72**: 996-1001.
- Verbakel WF, Cuijpers JP, Hoffmans D, Bieker M, Slotman BJ, Senan S. Volumetric intensity-modulated arc therapy vs. conventional IMRT in head-and-neck cancer: a comparative planning and dosimetric study. *Int J Radiat Oncol Biol Phys* 2009; **74**: 252-9.
- Weber DC, Peguret N, Dipasquale G, Cozzi L. Involved-node and involved-field volumetric modulated arc vs. fixed beam intensity-modulated radiotherapy for female patients with early-stage supra-diaphragmatic Hodgkin lymphoma: a comparative planning study. *Int J Radiat Oncol Biol Phys* 2009; **75**: 1578-86.
- Teoh M, Clark CH, Wood K, Whitaker S, Nisbet A. Volumetric modulated arc therapy: a review of current literature and clinical use in practice. *Br J Radiol* 2011; **84**: 967-96.
- Bhide SA, Nutting CM. Advances in radiotherapy for head and neck cancer. *Oral Oncol* 2010; **46**: 439-41.
- Sakumi A, Shiraishi K, Onoe T, Yamamoto K, Haga A, Yoda K, et al. Single-arc volumetric modulated arc therapy planning for left breast cancer and regional nodes. *J Radiat Res* 2012; **53**: 151-3.
- Shaitelman SF, Kim LH, Yan D, Martinez AA, Vicini FA, Grills IS. Continuous arc rotation of the couch therapy for the delivery of accelerated partial breast irradiation: a treatment planning analysis. *Int J Radiat Oncol Biol Phys* 2011; **80**: 771-8.
- Popescu CC, Olivetto IA, Beckham WA, Ansbacher W, Zavgorodni S, Shaffer R, et al. Volumetric modulated arc therapy improves dosimetry and reduces treatment time compared to conventional intensity-modulated radiotherapy for locoregional radiotherapy of left-sided breast cancer and internal mammary nodes. *Int J Radiat Oncol Biol Phys* 2010; **76**: 287-95.
- Yang B, Wei XD, Zhao YT, Ma CM. Dosimetric evaluation of integrated IMRT treatment of the chest wall and supraclavicular region for breast cancer after modified radical mastectomy. *Med Dosim* 2014; **39**: 185-9.
- Krueger EA, Fraass BA, McShan DL, Marsh R, Pierce LJ. Potential gains for irradiation of chest wall and regional nodes with intensity modulated radiotherapy. *Int J Radiat Oncol Biol Phys* 2003; **56**: 1023-37.
- Kimura T, Togami T, Takashima H, Nishiyama Y, Ohkawa M, Nagata Y. Radiation pneumonitis in patients with lung and mediastinal tumours: a retrospective study of risk factors focused on pulmonary emphysema. *Br J Radiol* 2012; **85**: 135-41.
- Wang S, Liao Z, Wei X, Liu HH, Tucker SL, Hu CS, et al. Analysis of clinical and dosimetric factors associated with treatment-related pneumonitis (TRP) in patients with non-small-cell lung cancer (NSCLC) treated with concurrent chemotherapy and three-dimensional conformal radiotherapy (3D-CRT). *Int J Radiat Oncol Biol Phys* 2006; **66**: 1399-407.
- Blom Goldman U, Wennberg B, Svane G, Bylund H, Lind P. Reduction of radiation pneumonitis by V20-constraints in breast cancer. *Radiat Oncol* 2010; **5**: 99.
- Yorke ED, Jackson A, Rosenzweig KE, Braban L, Leibel SA, Ling CC. Correlation of dosimetric factors and radiation pneumonitis for non-small-cell lung cancer patients in a recently completed dose escalation study. *Int J Radiat Oncol Biol Phys* 2005; **63**: 672-82.
- Harris EE, Correa C, Hwang WT, Liao J, Litt HI, Ferrari VA, et al. Late cardiac mortality and morbidity in early-stage breast cancer patients after breast-conservation treatment. *J Clin Oncol* 2006; **24**: 4100-6.

31. Lohr F, El-Haddad M, Dobler B, Grau R, Wertz HJ, Kraus-Tiefenbacher U, et al. Potential effect of robust and simple IMRT approach for left-sided breast cancer on cardiac mortality. *Int J Radiat Oncol Biol Phys* 2009; **74**: 73-80.
32. Yardley DA. Integrating bevacizumab into the treatment of patients with early-stage breast cancer: focus on cardiac safety. *Clin Breast Cancer* 2010; **10**: 119-29.
33. Marinko T, Dolenc J, Bilban-Jakopin C. Cardiotoxicity of concomitant radiotherapy and trastuzumab for early breast cancer. *Radiat Oncol* 2014; **48**: 105-12.
34. Rudat V, Alaradi AA, Mohamed A, Ai-Yahya K, Altuwaijri S. Tangential beam IMRT versus tangential beam 3D-CRT of the chest wall in postmastectomy breast cancer patients: a dosimetric comparison. *Radiat Oncol* 2011; **6**: 26.
35. Qiu J-J, Chang Z, Wu QJ, Yoo S, Horton J, Yin F-F. Impact of volumetric modulated arc therapy technique on treatment with partial breast irradiation. *Int J Radiat Oncol Biol Phys* 2010; **78**: 288-96.
36. Stovall M, Smith SA, Langholz BM, Boice JD, Jr., Shore RE, Andersson M, et al. Dose to the contralateral breast from radiotherapy and risk of second primary breast cancer in the WECARE study. *Int J Radiat Oncol Biol Phys* 2008; **72**: 1021-30.
37. Chopra S, Dinshaw KA, Kamble R, Sarin R. Breast movement during normal and deep breathing, respiratory training and set up errors: implications for external beam partial breast irradiation. *Br J Radiol* 2006; **79**: 766-73.
38. Moran JM, Balter JM, Ben-David MA, Marsh RB, Van Herk M, Pierce LJ. Short-term displacement and reproducibility of the breast and nodal targets under active breathing control. *Int J Radiat Oncol Biol Phys* 2007; **68**: 541-6.
39. Nicolini G, Fogliata A, Clivio A, Vanetti E, Cozzi L. Planning strategies in volumetric modulated arc therapy for breast. *Medical physics* 2011; **38**: 4025-31.

Estimated collective effective dose to the population from radiological examinations in Slovenia

Dejan Zontar¹, Urban Zdesar², Dimitrij Kuhelj³, Dean Pekarovic³, Damijan Skrk¹

¹ Slovenian Radiation Protection Administration, Ljubljana, Slovenia

² Institute of Occupational Safety, Ljubljana, Slovenia

³ Clinical Radiology Institute, University Medical Center Ljubljana, Ljubljana, Slovenia

Radiol Oncol 2015; 49(1): 99-106.

Received 24 April 2014

Accepted 11 June 2014

Correspondence to: Assist. Prof. Dejan Žontar, Ph.D., Slovenian Radiation Protection Administration Ljubljana, Ajdovščina 4, SI-1000 Ljubljana, Slovenia, EU. E-mail: dejan.zontar@gov.si

Disclosure: No potential conflicts of interest were disclosed.

Background. The aim of the study was to systematically evaluate population exposure from diagnostic and interventional radiological procedures in Slovenia.

Methods. The study was conducted in scope of the “Dose Datamed 2” project. A standard methodology based on 20 selected radiological procedures was adopted. Frequencies of the procedures were determined via questionnaires that were sent to all providers of radiological procedures while data about patient exposure per procedure were collected from existing databases. Collective effective dose to the population and effective dose per capita were estimated from the collected data (DLP for CT, MGD for mammography and DAP for other procedures) using dose conversion factors.

Results. The total collective effective dose to the population from radiological in 2011 was estimated to 1300 manSv and an effective dose per capita to 0.6 mSv of which approximately 2/3 are due to CT procedures.

Conclusions. The first systematic study of population exposure to ionising radiation from radiological procedures in Slovenia was performed. The results show that the exposure in Slovenia is under the European average. It confirmed large contributions of computed tomography and interventional procedures, identifying them as the areas that deserve special attention when it comes to justification and optimisation.

Key words: collective effective dose; population exposure; dose per capita; radiological procedures; diagnostic procedures

Introduction

Medical procedures using ionizing radiation represent by far the largest source of manmade population exposure to ionizing radiation in most developed countries. In the USA the effective dose from medical exposure already exceeded the contribution from the natural background.¹ As exposure is related to cancer risk² it is important to determine the contribution of doses from medical exposure to the population as required by the legislation of European Union.^{3,4} While numerous studies were carried out in the past^{1,5-11} and the results from European coun-

tries⁵ show that in Europe contribution of medical procedures to the population exposure is significantly lower than in the USA², no systematic study has been previously performed in Slovenia.

This article reports the findings of the first systematic study, carried out in 2011 by the Slovenian Radiation Protection Administration (SRPA) in scope of the European Commission project “Study on European Population Doses from Medical Exposure” or “Dose Datamed 2”. A standard methodology⁵ developed by the first “Dose Datamed” project and recommended by the European Commission was adopted.

Materials and methods

A precise determination of population exposure from medical use of radiation would require detailed knowledge of number of procedures and patient doses for all procedures. As full information is not realistically obtainable, three models for data collection were proposed by the Dose DataMed 2 project. They were based on TOP20 types of examination, 70 examination categories or 225 specific examinations.⁵ Based on the available informational infrastructure the TOP20 approach was chosen for Slovenia. It is based on collecting frequency and dose information for 20 examination types as listed in guidance RP154⁵ that were determined to present major contribution to the total population exposure. They consist of 7 examination types belonging to conventional radiography (without contrast media), 5 radiography/fluoroscopy examination types (mostly involving contrast), 7 categories of computed tomography examinations and coronary angioplasty (PTCA) as a representative of interventional procedures. All 20 examination types are listed in the first column of Table 1. The results obtained by the TOP20 methodology were extrapolated to the overall collective effective dose using correction factors proposed by the Dose DataMed 2 project. To determine the effective dose per capita the overall collective effective dose was divided by the total population of Slovenia at the end of 2011 *i.e.* 2.05 million.¹²

Frequency estimation

Data on the frequencies of the selected procedures were collected using a questionnaire based on the RP154⁵ guidance. In order to minimise an error originating from different classification of the procedures appropriate instructions were included. For each of the 20 types of examination information on typical examinations, common techniques and common indications were provided. A single procedure was defined as one examination that may consist of more projections or, in case of CT, phases. In case of mammography both projections on both breasts were defined as one examination. For examinations that may consist of more projections, frequencies were requested for all projections. For CT procedures the average number of phases used for each type of examination was required.

Review of SRPA databases identified 90 providers that can perform those types of examinations. The questionnaire was sent to all of them and the response rate was 80% (72 providers), covering ap-

proximately 90% of the total workload. Only two of the major institutions (General hospitals Brežice and Murska Sobota) did not provide the data so the frequencies had to be estimated. For CT procedures, health insurance agency data for the year 2009 were available and adopted. For other procedures, frequencies were estimated from the CT frequencies by using an average ratio between CT and other procedures as determined for the general hospitals that reported full data. For the remaining providers the frequencies were estimated from the (generally conservative) workload information as obtained during licensing procedures. The influence of those estimations on the cumulative dose will be discussed in the section dedicated to the uncertainty of the results.

Dose estimation

The average effective dose for each examination type was determined from measurements of the relevant dose quantities on a sample of patients during regular practice. Dose Area Product (DAP) was used for conventional, fluoroscopic and interventional procedures, Dose Length product (DLP) for CT procedures and Mean Glandular Dose (MGD) for mammography. The measurements were performed by the Institute of Occupational Safety during the previous years and were available for approximately 2/3 of institutions performing conventional radiography, for about 80% of CT units, for all mammography units (MGD from phantom measurements) and for all units performing PTCA (cumulative DAP) and cardiac angiography. Data were very scarce (available only for one to four providers per procedure) for the remaining fluoroscopy procedures (DAP per procedure). For examinations that may consist of more projections, the average cumulative quantity was determined by summing the relevant values for all projections weighted by the fraction of the examinations for which each projection was carried out. For example, in case of chest x-ray total DAP would be determined as $DAP_{\text{chest}} = DAP_{\text{PA}} + F_{\text{LAT}} * DAP_{\text{LAT}}$ where DAP_{PA} and DAP_{LAT} are average DAP values for PA and lateral projection and F_{LAT} is the fraction of all examinations where imaging is also performed in lateral projection. For CT examinations the average DLP per phase was multiplied by the average number of phases used for a given type of examination. Average values of the relevant dosimetric quantities for each type of examination were then converted to the average effective dose per procedure using conversion coefficients recommended

by the guidance RP154⁵, except for mammography where conversion coefficient of 0.12 mSv/mGy was used following ICRP publication 103.⁴ Considering that mammography is mostly performed on older patients conversion coefficient of 0.05 mSv/mGy as recommended by the ICRP publication 60 could be used instead.¹³ In that case the total dose from mammography would be reduced by a factor 2.4 and the overall cumulative dose by approximately 2%. Values of the conversion coefficients for all 20 examination types as used in this research are listed in Table 2.

Collective effective dose $D_{col, ex}$ for each examination was calculated as a sum of the frequencies of that examination type in each institution $N_{ex, inst}$ multiplied by the effective dose for that examination in the corresponding institution $D_{ex, inst}$ i.e. $D_{col, ex} = \sum_{inst} N_{ex, inst} \cdot D_{ex, inst}$.

For institutions for which an effective dose for any given type of examination was not known the average effective dose for that type of examination over all institutions was used instead. The total collective effective dose for the TOP20 procedures was determined as a sum of collective effective doses over all 20 examinations.

Results

Frequency data

Frequency data for all 20 procedures as collected by this study are shown in Table 1. For the purpose of this article the radiology providers were categorised into 5 groups: university medical centres (2), general hospitals (10), specialised hospitals and larger practices (13), public health centres (38) and other institutions including mostly smaller private practices (27). As it was not possible to present full data such grouping was considered as a useful compromise that still provides some insight into contributions of different types of providers. For each group the frequencies are reported for each type of procedure and summed up for each group of procedures. Total number of procedures for each type of examination is given in the seventh column of Table 1. In the last column some basic information about the procedures that influence the patient exposure are listed: in case of conventional radiography the fraction of examinations for which lateral projection is used (except for mammography where both projections on both breasts are assumed for all examinations), for radiography/fluoroscopy number of images per examination and for CT procedures the average number of

phases used per examination. In all cases the average value over all institutions, not weighted by their workload, is listed.

The results show that in 2011 nearly 1 million of the TOP20 types of examinations were performed in Slovenia. Approximately 88% of them belong to conventional radiography, approximately 10% were CT procedures, radiography/fluoroscopy examinations contributed about 1.5% and interventional procedures approximately 0.5%.

Data obtained by the TOP20 methodology can be used to estimate the overall number of radiological procedures (including dental) using correction factors as determined by the Dose Datamed 2 project.¹⁴ They were determined from results of the countries that collected data based on both TOP20 types of examination and 225 specific examinations. The values of the correction factors and the resulting estimates for the overall number of radiological procedures are listed in Table 2. The extrapolation of data shows that about 2 millions of radiological procedures were performed in Slovenia in 2011, corresponding to one procedure per capita. The relative contributions of each group of procedures are slightly modified when looking at the overall numbers instead of the TOP20 procedures with the contribution of conventional radiography being increased to about 92% and contribution of CT procedures reduced to about 5%. Contributions of radiography/fluoroscopy and interventional procedures remain at almost the same values of around 1.5% and 0.5% respectively.

Dose data

To determine the cumulative dose the frequency data were combined with the dose information as described in the section about methodology of the study. The average values of the relevant dose quantities i.e. DAP per projection for conventional radiography, DAP per examination for radiography/fluoroscopy and interventional procedures, DLP per phase for CT procedures and MGD per breast (both projections) for mammography are listed in Table 3. For the first five procedures from the conventional radiography group separate DAP values were used for AP/PA and lateral projections so average values are listed for both projections. In the analysis the DAP value for each lateral projection was properly weighted with the frequency of examinations in which both projections were taken (overall averages are listed in the last column of Table 1). For mammography, the listed values were multiplied by 2 to obtain MGD per examina-

TABLE 1. Number of radiology procedures performed in 2011 for the selected 20 types of procedures

Type of examination	University medical centres (2) [x1000]	General hospitals (10) [x1000]	Other hospitals (13) [x1000]	Public health centres (38) [x1000]	Other institutions (27) [x1000]	Total (90) [x1000]	Average no. of per examination
Conventional radiography	196	279	120	226	45	865	Side proj.
Chest/lung	109	116	47	100	27	399	0.45
Cervical spine	17	37	6.2	23	2.7	86	0.91
Thoracic spine	10	14	3.1	10	1.2	39	0.94
Lumbar spine	24	39	12	43	3.3	121	0.87
Mammography	0.6	27	39	28	8.8	104	
Abdomen	11	25	2.5	0.6	0.1	39	0.17
Pelvis & hip	24	22	9.8	21	2.1	79	0.26
Radiography/ fluoroscopy	8.3	4.2	2.5	<0,1	0	15	Images
Ba meal	0.3	0.8	1.0	<0.1	0	2.1	4.93
Ba enema	0.5	0.8	0.1	0	0	1.4	5.26
Ba follow	0.3	0.2	0.6	0	0	1.1	5.25
Intravenous urography (IVU)	1.1	1.4	0.1	0	0	2.6	4.58
Cardiac angiography	6.2	0.9	0.7	0	0	7.8	
Computed tomography	27	44	24	0	0	96	Phases
CT head	16	25	8.7	0	0	49	1.57
CT neck	1.2	1.0	0.7	0	0	2.9	1.13
CT chest	3.2	4.1	5.9	0	0	13	1.47
CT spine	0.5	2.6	3.3	0	0	6.4	1.00
CT abdomen	4.7	9.2	3.9	0	0	18	2.24
CT pelvis	0.2	0.6	0.3	0	0	1.1	1.48
CT trunk	1.4	2.1	1.5	0	0	5.1	2.00
Interventional procedures	3.2	0.5	0.2	0	0	3.9	
PTCA	3.2	0.5	0.2	0	0	3.9	
Total	234	328	147	226	45	980	

TABLE 2. Estimated total number of radiological procedures performed in Slovenia in 2011

Type of examination	Number of TOP20 examinations [x1000]	Correction factor	No. of overall examinations [x1000]	Relative contribution to overall number [%]
Conventional radiography	865	2.25	1947	92.8
Radiography/ fluoroscopy	15	2.04	31	1.5
Computed tomography	96	1.13	108	5.1
Interventional procedures	3.9	3.23	12	0.6
Total	980		2098	

tion *i.e.* imaging of both breasts. For CT examinations DLP per phase was multiplied by the average number of phases (overall averages in Table 1) to obtain DLP per examination as defined by the Dose Dated 2.

The third column in Table 3 lists the conversion coefficients for all TOP20 examinations as used in this study and in the fourth column cumulative effective doses for all TOP20 types of procedures and for each of group of procedures are given in units of man-Sv. The last column lists the average effective dose per examination for all TOP20 types of examinations. They were determined by dividing the cumulative effective dose from each type of examination by the corresponding number of

examinations and thus represent averages weighted by the workload of each institution. While not directly relevant for the evaluation of collective dose of the general population they offer a good insight into both absolute and relative dose burden of a patient subjected to radiology examinations in Slovenia.

As it was done for the frequency data, cumulative dose from the TOP20 procedures can be extrapolated to estimate an overall cumulative dose using correction factors as determined by the Dose Datamed 2 project.¹⁴ The correction factors for dose and the resulting overall cumulative doses for each group of procedures are given in Table 4. The extrapolated data indicate that the overall dose to the population of Slovenia from radiological procedures in 2011 was about 1300 manSv or 0.65 mSv per capita. The main contribution, almost 2/3, is due to computed tomography, conventional radiography contributes approximately 20%, interventional procedures around 10% and radiography/fluoroscopy only about 5%.

Uncertainties of the results

Three main contributions to the uncertainty of the overall cumulative effective dose are: uncertainty on the frequencies of procedures, uncertainty in dose estimation and uncertainty of the extrapolation to the overall cumulative dose from the TOP20 data.

Frequency data as reported in the survey were mostly extracted from databases of each provider. Depending on the available technology either exact numbers were extracted from an electronic system or yearly workload was extrapolated from a shorter (usually a few months) time period. Another source of frequency uncertainty could be procedure mismatching. A 10% uncertainty was conservatively assumed for institutions that reported frequency data. For the institutions for which frequencies had to be estimated from other sources a 50% uncertainty was assumed. Uncertainties for each institution and for each type of examinations were assumed to be uncorrelated and absolute values were summed in quadrature. Using this methodology a 2% uncertainty on the frequencies of the TOP20 examinations was estimated for conventional radiography, around 4% uncertainty for radiography/fluoroscopy procedures, around 3% uncertainty for CT procedures and approximately 6% uncertainty for interventional procedures. Relative uncertainty on the total number of the TOP20 radiological procedures was around 2%.

TABLE 3. Summary of the dose information for the selected 20 types of procedures

Type of examination	Average value of the relevant dose quantity		Conversion coefficient		Collective effective dose [manSv]	Average effective dose per procedure [mSv]	
	CT: DLP [mGycm]	Mamo: MGD [mGy]	Other: DAP [μ Gym ²]	CT: Sv/Gycm	Mamo: Sv/Gy	Other: Sv/Gym ²	
Conventional radiography	PA/AP	LAT					225
Chest/lung	11.0	33.3		1.80			18.2
Cervical spine	24.5	23.1		1.30			5.5
Thoracic spine	101	93		1.90			13.8
Lumbar spine	124	219		2.10			91.9
Mammography		1.5			0.12		38.7
Abdomen		170			2.60		16.2
Pelvis & hip		197			2.90		40.2
Radiography/fluoroscopy							55.6
Ba meal		700			2.00		2.9
Ba enema		2800			2.80		11.2
Ba follow		2400			2.20		5.8
Intravenous urography (IVU)		483			1.80		2.4
Cardiac angiography		2110			2.00		33.4
Computed tomography							675
CT head		875			2.10		142
CT neck		580			5.90		8.6
CT chest		385			14.0		88.7
CT spine		650			15.0		64.0
CT abdomen		467			15.0		273
CT pelvis		415			15.0		10.7
CT trunk		852			15.0		88.8
Interventional procedures							47.8
PTCA		6000			2.00		12.4
Total							1004

TABLE 4. Cumulative dose from radiological procedures extrapolated to all examinations

Type of examination	Collective effective dose from TOP20 methodology [manSv]	Correction coefficient for extrapolation to all examinations	Extrapolated collective effective dose to all examinations [manSv]	Contribution to total collective effective dose [%]
Conventional radiography	225	1.12	252	19
Radiography/fluoroscopy	55.6	1.40	78	6
Computed tomography	675	1.23	831	64
Interventional procedures	47.8	2.97	142	11
Total	1004		1302	

As reported in a previous section, values of the relevant dose quantities were known for most institutions from previous studies. For majority of the examinations the effect of the uncertainty on dose per procedure was estimated by substituting individual matching of dose data and frequencies for each institution with using the average dose value of each type of examination for Slovenia for all institutions. Such approach gave approximately 5% uncertainty on cumulative dose from conventional radiography, 3% for CT procedures and 3% for interventional procedures. For the four radiography/fluoroscopy examinations (excluding coronary angiography) where the data were very scarce a 100% uncertainty on the dose was assumed, leading to a 25% uncertainty on the cumulative dose from radiography/fluoroscopy examinations (including coronary angiography). Combining all those uncertainties in quadrature gives less than 3% overall uncertainty due to dose data. Uncertainty on the dose conversion coefficients was ignored for the purpose of this study.

To estimate the uncertainty on the overall cumulative effective dose from radiological procedures uncertainties on frequency and dose estimations for the TOP20 procedures had to be combined with the uncertainty of the correction factors used to extrapolate the TOP20 data to all examinations. The values of those correction factors as proposed by the Dose Datamed 2 project were given in Table 4. Unfortunately the Dose Datamed 2 report¹⁴ provided no uncertainty values for those factors. The uncertainty on the conversion factors was thus estimated from the data available in the report to around 25% for conventional radiography group, 40% for radiography/fluoroscopy group, 13% for CT group and 20% for interventional procedures group. It can be seen that the total uncertainty on the overall effective dose from radiography procedures in Slovenia is dominated by the uncertainty of the correction factors. Combining all three main sources of uncertainty for each group of examinations separately and then combining data from all four groups of examinations, assuming the uncertainties were uncorrelated, the total uncertainty on collective effective dose from radiology procedures was estimated to be around 11% (1 standard deviation).

Discussion

The results presented above provide an estimate of the collective effective dose to the population

of Slovenia from radiological examinations. They show that computed tomography, while only representing about 5% of all radiology procedures in Slovenia, contributes approximately 2/3 of the total dose and is thus a major source of exposure to the population. CT was therefore identified as the main area towards which further efforts for increasing optimisation and justification should be directed. Another area that deserves special attention are interventional procedures that only represent around 0.5% of all radiology procedures but contribute approximately 10% to the overall cumulative effective dose. While those conclusions could be expected based on the previous studies from other developed countries this is the first time that reliable information are available about the situation in Slovenia.

The study shows that in conventional radiography workload is about equally distributed between public health centres and other small providers (approximately 1/3), general hospitals and university medical centres (another third) and specialised hospitals and larger providers (the last third). Among CT examinations approximately 30% are performed in the university medical centres, 45% in general hospitals and the remaining 25% in specialised hospitals and larger private centres with the later contributing approximately 10%. As for the interventional procedures, approximately 80% are performed in the university medical centres and the remaining 20% in 2 general hospitals and one private centre. The above sharing is expected to be somewhat modified if the TOP20 list is expanded to all procedures, particularly if dental radiography is included in conventional radiography.

The presented study was conducted according to a well defined and internationally accepted methodology. Such approach provided a well developed methodology and ensured that the results can be reliably compared with other European countries.^{5,14} The comparison shows that the overall effective collective dose per capita in Slovenia is below average for European countries (around 1.1 mSv per capita¹⁴ for 2011) and places Slovenia among the countries with the lowest overall effective collective dose per capita. Comparison of the overall total frequencies per 1000 population¹⁴ places Slovenia into the middle of distribution with 20 countries having higher and 15 countries lower overall total frequencies. The relative frequency of computed tomography in Slovenia (5%) tends to be lower than in many countries (only 8 out of 36 countries evaluated in the Dose Datamed

2 report¹⁴ show lower relative frequency of CT procedures than Slovenia with only two of them lower than 4%). This indicates either good use of the principle of justification when referring to CT examinations or somewhat limited access to this modality caused by lower number of CT units per capita than the European average.¹⁵ On the other hand the relative contribution of CT procedures to the overall effective dose (63.8%) is higher from the reported mean value (57%) for all countries. This is consistent with the observation that the average doses for most CT examinations from the TOP20 group in Slovenia significantly exceed the mean over the countries included in the study. It is thus necessary to put more efforts into optimisation of CT procedures in Slovenia. On the other hand the average doses for conventional radiography in Slovenia are significantly lower from the mean values as given in the Dose Datamed 2 report. Thus the relative contribution of conventional procedures to the cumulative effective dose (19.3%) is comparable to the reported mean value (19.5%) while the relative frequency (92.8%) is above the reported mean of 87.4%. Interventional procedures have comparable contribution to the cumulative effective dose (0.6%) to the mean (0.6%) despite slightly larger relative frequency (11% *vs.* 8.7%). The relative contribution of the radiography/fluoroscopy group in Slovenia is lower from the mean both in frequency (1.5% *vs.* 3.3%) and in cumulative dose (6.0% *vs.* 14.8%).

Although it was not the main goal of the study the extensive data collection on which it was based provided a wealth of other information about the radiology practice in Slovenia. An example is information about the relative frequency of using lateral projection in chest imaging. The data show that both PA and lateral projection are in average taken in 45% of all chest x-rays. If we take under investigation public health centres where similar clinical questions can be assumed it can be seen that in approximately 1/3 of all public health centres both projections are performed in over 80% of all chest x-rays while in about 1/3 of them lateral projection is taken in less than 20% of all chest x-rays. Another side result of the study is information about the average patient doses for the TOP20 procedures in Slovenia (Table 3 last column). While not relevant for optimisation purposes the values are still indicative for evaluation of the relative risk of different procedures and could be useful for educational purposes. The authors are aware that the full potential of the data collected in this study data was not yet explored. Such analysis exceeds

the scope of this article and may become a topic of a separate study.

Conclusions

Results of the first systematic study of population exposure in Slovenia due to radiological medical procedures are presented. They show that total collective effective dose from radiological procedures in 2011 was approximately 1300 manSv. By far the largest share is due to computed tomography that contributes approximately 830 manSv or almost 2/3 of the total dose, although it only represents approximately 5% of all diagnostic procedures. Another important group are interventional procedures that represent approximately 0.5% of the total workload but contribute approximately 10% of the cumulative dose. Those two groups were thus identified as the areas that deserve special attention when it comes to justification and optimisation. Results of the study on nuclear medicine that was reported in a previous article¹⁶ showed that the total collective effective dose from nuclear medicine procedures in 2011 was approximately 100 manSv or 0.05 mSv per capita. Adding the nuclear medicine contributions the overall collective effective dose from medical examinations in Slovenia in 2011 was approximately $1400 \times (1 \pm 0,1)$ manSv or $0.7 \times (1 \pm 0,1)$ mSv per capita.

Presented results show that population exposure from medical procedures in Slovenia is in most aspects comparable to, or even lower than in most European countries. The one exception is computed tomography that represents much lower fraction of the total frequency yet still has a relatively high contribution to the cumulative dose.

Due to the rapid technological development and ever-increasing utilisation of radiological examinations, particularly the high-dose procedures such as CT, surveys and analysis of the doses from medical procedures should be performed regularly. The results of the presented study provided reliable information about the contribution of various types of radiological examinations to the population exposure, contributions of various radiology providers as well as some insight into the differences in everyday practice among them. This information can and should be used to direct the efforts of radiology specialists and regulators to the most critical areas while regularly updated information would provide insight into the impact of the changing technologies and guidelines.

Acknowledgement

The authors would like to express gratitude to all radiology departments in Slovenia participating in the study for providing the frequency data.

References

1. NCRP Report No. 160: Ionizing Radiation Exposure of the Population of the United States National Council on Radiation Protection and Measurements, Bethesda, MD (2009)
2. Berrington de González A, Darby S. Risk of cancer from diagnostic X-rays: estimates for the UK and 14 other countries. *The Lancet* 2004; **363**: 345-51.
3. European Commission. *Council Directive 97/43/EURATOM of 30 June 1997 on health protection of individuals against the danger of ionizing radiation in relation to medical exposure (Official Journal of the European Commission, No- L 180)*. Luxemburg: Office for Official Publications of the European Communities; 1997.
4. International Commission on Radiological Protection ICRP. *The 2007 recommendations of the International Commission on Radiological Protection*. Orlando: Elsevier, published for the International Commission on Radiological Protection; 2007.
5. European Commission. *European Commission guidance on estimating population doses from medical X-ray procedures (Radiation Protection No 154)*. Luxemburg: Office for Official Publications of the European Communities; 2008.
6. Brugmans MJ, Buijs WC, Geleijns J, Lembrechts J. Population exposure to diagnostic use of ionizing radiation in The Netherlands. *Health Phys* 2002; **82**: 500-9.
7. Hart D, Wall BF. UK population dose from medical X-ray examinations. *EJR* 2004; **50**: 285-91.
8. Wise KN, Thomson JEM. Changes in CT radiation doses in Australia from 1994 to 2002. *Journal of Medical Radiation Sciences* 2004; **51**: 81-5.
9. Shannoun F, Zeeb H, Back C, Blettner M. Medical exposure of the population from diagnostic use of ionizing radiation in Luxembourg between 1994 and 2002. *Health Phys* 2006; **91**: 154-62.
10. Mettler FA Jr, Thomadsen BR, Bhargavan M, Gilley DB, Gray JE, Lipoti AJ, et al. Medical radiation exposure in the U.S. in 2006: Preliminary results. *Health Physics* 2008; **95**: 502-7.
11. Tung CJ1, Yang CH, Yeh CY, Chen TR. Population dose from medical diagnostic exposure in Taiwan. *Radiat Prot Dosimetry*. 2011; **146**: 248-51.
12. Statistical office of the Republic of Slovenia. *Slovenia in Figures 2012*, Ljubljana: Littera picta d.o.o.; 2012.
13. International Commission on Radiological Protection ICRP. *The 1990 recommendations of the International Commission on Radiological Protection*. Orlando: Elsevier, published for the International Commission on Radiological Protection; 2007.
14. *DDM2 Project Report on European Population Dose Estimation*. Draft report for internal use (<http://ddmed.eu/>); 2013. To be published by the European Commission.
15. OECD iLibrary, Health at glance: Europe 2012: Medical Technologies: CT scanners and MRI Units. [http://www.oecd-ilibrary.org/sites/9789264183896-en/03/04/index.html;jsessionid=2be6smve97uv8.x-oecd-live-02?contentTy pe=&itemId=%2Fcontent%2Fchapter%2F9789264183896-31-en&mimeType=text%2Fhtml&containerItemId=%2Fcontent%2Fserial%2F23056088&accessItemIds=%2Fcontent%2Fbook%2F9789264183896-en \(10.5.2014](http://www.oecd-ilibrary.org/sites/9789264183896-en/03/04/index.html;jsessionid=2be6smve97uv8.x-oecd-live-02?contentTy pe=&itemId=%2Fcontent%2Fchapter%2F9789264183896-31-en&mimeType=text%2Fhtml&containerItemId=%2Fcontent%2Fserial%2F23056088&accessItemIds=%2Fcontent%2Fbook%2F9789264183896-en (10.5.2014)
16. Škrk D, Zontar D. Estimated collective effective dose to the population from nuclear medicine examinations in Slovenia. *Radiol Oncol* 2013; **47**: 304-10.

Radiol Oncol 2015; 49(1): 1-9.
doi:10.2478/raon-2013-0071

Uporaba PET-CT pri načrtovanju zdravljenja z obsevanjem

Jelerčič S, Rajer M

Izhodišča. PET-CT je postala nepogrešljiva preiskava pri diagnostiki malignih tumorjev. Uporabljamo jo za določanje obsežnosti maligne bolezni in za spremljanje odgovora na zdravljenje. Z razvojem radioterapije je preiskava PET-CT postala del priprav in načrtovanja obsevanja. Poleg anatomskih značilnosti tumorja, ki nam jih prikažejo klasične slikovne preiskave (računalniška tomografija ali magnetna resonanca), lahko PET-CT ovrednoti tudi biološke značilnosti tumorja. V prispevku obravnavamo vlogo PET-CT-ja pri načrtovanju obsevanja nekaterih pogostih solidnih tumorjev.

Zaključki. V bližnji prihodnosti bo PET-CT sestavni del večine postopkov radioterapevtskega načrtovanja v vsakodnevni klinični praksi. Danes ima jasno vlogo v radioterapevtskem planiranju pri raku pljuč. Pričakujemo pa, da bodo prihajajoče klinične raziskave pokazale optimalno uporabo PET CT-ja pri načrtovanju obsevanja drugih solidnih tumorjev.

Radiol Oncol 2015; 49(1): 10-16.
doi:10.2478/raon-2014-0031

Klinični pomen slikanja celega telesa z magnetno resonanco pri zdravi odrasli populaciji

Tarnoki DL, Tarnoki AD, Richter A, Karlinger K, Berczi V, Pickuth D

Izhodišča. Magnetnoresonančno slikanje celega telesa (WB-MRI) in magnetnoresonančna angiografija (WB-MRA) postajata vse bolj uveljavljeni slikovni metodi v diagnostiki in raziskavah. Retrospektivno smo ugotavljali pogostnost potencialno pomembnih najdb pri zdravi populaciji.

Preiskovanci in metode. 22-tim zdravim osebam, vodilnim delavcem (18 moških, povprečne starosti 47±9 let) smo med marcem 2012 in septembrom 2013 naredili preiskavi magnetnoresonančno slikanje celega telesa in magnetnoresonančno angiografijo. Uporabili smo magnetnoresonančno napravo Discovery MR750w wide bore 3 Tesla (GE Healthcare). Naredili smo obtežene sekvence T1 ter sekvence z magnetno resonančno metodo izločanja signalov maščobe (STIR) in sekvence z difuzijskim poudarkom slikanja (DWI) po standardiziranih protokolih.

Rezultati. Pri eni osebi smo našli sumljivo pararektalno tvorbo, ki smo jo potrdili z endorektalnim ultrazvočnim pregledom. Pri 20 osebah smo opisali naključne najdbe, med njimi hidrocele (11 oseb), benigne kostne lezije (7 oseb) in nespecifično povečane bezgavke (5 oseb). Nadaljnjo diagnostiko smo priporočili pri 68 % preiskovancev (UZ preiskava pri 36 %, CT pri 28 %, mamografija pri 9 %). Magnetnoresonančna angiografija je bila negativna pri 16 osebah. Nekaj je bilo variant poteka žil, pri eni osebi pa smo našli 40-procentno stenozo leve skupne karotidne arterije.

Zaključki. V raziskavi smo z magnetnoresonančnim slikanjem celega telesa in magnetnoresonančno angiografijo diagnosticirali klinično pomembne bolezni in nepričakovane najdbe pri naključni skupini zdrave populacije, kar je zahtevalo nadaljnjo diagnostiko ali nadzor pri 68 % pregledovancev. Magnetnoresonančna preiskava celega telesa bo tako lahko imela nadvse pomembno vlogo pri presejanju zdrave populacije, posebej pri prihodnjih generacijah, ko bomo iskali maligne in aterosklerotične spremembe. Naša raziskava je prva, ki je pri zdravi populaciji uporabila za presejalno metodo 3-T magnetno napravo s T1, sekvence STIR, magnetnoresonančno angiografijo in sekvence DWI.

Radiol Oncol 2015; 49(1): 17-25.
doi:10.2478/raon-2014-0030

Ocenjevanje zgodnje aktivnosti Cetuksimaba z dinamično in kontrastno ojačano tomografijo pri bolnikih, ki so zboleli zaradi skvamozno celičnega raka glave in vratu

Schmitz S, Rommel D, Michoux N, Lhommel R, Hanin FX, Duprez T, Machiels JP

Izhodišča. Cetuksimab je monoklonsko protitelo, usmerjeno proti receptorju za epidermalni rastni dejavnik (EGFR), ki je pokazal pri različnih vrstah tumorjev. Z uporabo dinamične, s kontrastom ojačene računalniške tomografije (DCE-CT) smo preučevali zgodnjo aktivnost monoterapije s cetuksimabom pri predhodno še nezdravljenih bolnikih s ploščatoceličnim karcinomom glave in vratu (PCKGV).

Metode. Še nezdravljeni bolniki s PCKG so prejeli cetuksimab 2 tedna pred operacijo z namenom ozdravitve. Terapevtska aktivnost smo ocenjevali z DCE-CT ob vključitvi bolnika in pred operacijo. Za ocena tumorskega žilja in značilnosti intersticija smo uporabili Brixov dvokomponentni kinetični model. Spremembe perfuzijskih dejavnikov (pretok krvi F_p , zunajžilni prostor V_e , žilni prostor V_p , konstanta prehoda PS) smo analizirali med obema časovnima točkama. Podatke DCE smo primerjali s rezultati FDG-PET in histopatološkim pregledom, ki sta bila izvedena sočasno. Plazemske žilne označevalce smo preučili ob različnih časih.

Rezultati. Štirinajst bolnikov je imelo razpoložljive podatke DCE-CT ob obeh časovnih točkah. Ugotovili smo značilen porast sledilcu dosegljivega zunajžilnega značeličnega prostora V_e ; v primeru drugih kinetičnih dejavnikov (F_p , V_p ali PS) ni bilo najti značilnih razlik. Značilna ujemanje smo ugotovili med dejavniki DCE in drugima dvema modalitetama. Plazemski VEGF, PDGF-BB in IL-8 so bili znižani že 2 uri po infuziji cetuksimaba.

Zaključki. DCE-CT je zaznal zgodnje učinkovanje cetuksimaba na značilnosti tumorskega intersticija. Spremembe plazemskih žilnih označevalcev niso zadostne za potrditev antiangiogene aktivnosti cetuksimaba *in vivo*. Potrebne so nadaljnje raziskave za določitev obsega sprememb dejavnikov DCE-CT in za oceno, ali z njimi lahko napovemo izhod zdravljenja.

Radiol Oncol 2015; 49(1): 26-31.
doi:10.2478/raon-2014-0047

Rak Hürthlovih celic kmalu po kirurški odstranitvi adenoma Hürthlovih celic in folikularnega adenoma žleze ščitnice

Ristevska N, Stojanoski S, Pop Gjorceva D

Izhodišča. Novotvorbe Hürthlovih celic so lahko benigne, kot so adenomi, ali pa so maligne, kot je rak Hürthlovih celic. Ta je redek tumor, predstavlja 5 % vseh diferenciranih ščitničnih rakov. Citološka opredelitev novotvorb Hürthlovih celic s tankoigelno aspiracijsko biopsijo je težavna, ker Hürthlove celice najdemo tako pri takšnih adenomih kot pri takšnih rakih. Ker je predoperativno izjemno težko ločiti obe vrsti novotvorb, nam le patohistološki pregled kirurško odstranjenega tumorja da dokončni odgovor.

Prikaz primera. 57-letno bolnico so napotili na skopski Inštitut za patofiziologijo in nuklearno medicino zaradi opredelitve vozličastih sprememb v ščitni žlezi. Bila je eutireotična. Tankoigelna aspiracijska biopsija vozličev v obeh ščitničnih režnjih je pokazala adenom Hürthlovih celic z atipičnimi celicami. Po tiroidektomiji je histopatološki pregled levega ščitničnega režnja potrdil adenom Hürthlovih celic z obilno citoplazmo in diskretno celično atipijo, vozlič v desnem ščitničnem režnju pa opredelil kot folikularni adenom brez celične atipije. Bolnico smo eno leto zdravili s substitucijskimi zdravili, nato pa odkrili tipljiv tumor na levi strani preostanka ščitnice. S scintigrafijo z radiofarmakom ^{99m}Tc -sestamibi smo tumor opredelili kot vroč nodule, s tankoigelno aspiracijsko biopsijo pa smo ponovno ugotovili adenom Hürthlovih celic z izrazitejšimi celularnimi spremembami. Naredili smo tumorrektomijo in patohistološko potrdili dobro diferenciran rak Hürthlovih celic. Bolnica je nato prejela ablativno dozo obsevanja z 100 mCi izotopa ^{131}I . v štirih letih, ob rednem sledenju bolnice nismo ugotovili morebitnih zasevkov.

Zaključki. Samo s histopatološkim pregledom lahko ločimo adenom in rak Hürthlovih celic. Bolnike, pri katerih smo citološko ugotovili novotvorbo Hürthlovih celic moramo zdraviti s totalno tiroidektomijo, zlasti če je tumor večji kot 1 cm, če ugotovimo atipične celice ali če ugotovimo multiple vozličke v obeh ščitničnih režnjih.

Radiol Oncol 2015; 49(1): 32-40.
doi:10.1515/raon-2015-0005

Sinergistično protitumorsko delovanje dopolnilnega zdravljenja TNF- α in elektrokemoterapije z intravenoznim apliciranjem cisplatina pri sarkomih

Čemažar M, Todorović V, Ščančar J, Lamprecht U, Štimac M, Kamenshek U, Kranjc S, Coer A, Serša G

Izhodišča. Elektrokemoterapija je vrsta ablacijske terapije za zdravljenje tumorjev, ki temelji na elektroporaciji celične membrane. Ta omogoči vstop nekaterim kemoterapevtikom, za katere je celična membrana slabo prepustna, ter tako močno poveča njihovo citotoksičnost. Kot najprimernejša kemoterapevtika za klinično uporabo elektrokemoterapije sta se v predkliničnih raziskavah pokazala bleomicin in cisplatin. Intravenozni vnos cisplatina za elektrokemoterapijo še vedno ni del širše klinične prakse, verjetno zaradi slabše protitumorske učinkovitosti. Učinkovitost pa bi lahko povečali z dopolnilno imunsko-ali žilno ciljano terapijo. Cilj raziskave je bil proučiti, ali lahko z dopolnilno terapijo s tumorskim nekrotizirajočim faktorjem α (TNF- α) povečamo protitumorsko učinkovitost intravenske elektrokemoterapije s cisplatinom na modelu mišjega sarkoma.

Metode. S pomočjo raziskave, ki je potekala *in vivo*, smo ocenili učinek TNF- α . Aplicirali smo ga pred ali po elektrokemoterapiji. Ocenili smo tudi učinek dopolnilnega zdravljenja s TNF- α na elektrokemoterapijo, pri kateri smo vnašali različne odmerke cisplatina.

Rezultati. Z raziskavo smo dokazali sinergistično delovanje TNF- α in elektrokemoterapije. Aplikacija TNF- α pred elektrokemoterapijo je povzročila daljši zaostanek v rasti tumorjev in povišala delež ozdravljenih miši ter je bila tako značilno bolj učinkovita kot aplikacija po elektrokemoterapiji. Analiza tumorjev po elektrokemoterapiji kombinirani z aplikacijo TNF- α je pokazala povišane koncentracije platine v tumorjih, obsežne poškodbe žil in obsežna nekrotična področja.

Zaključki. Rezultati kažejo na protizilno delovanje TNF- α , k ozdravitvam pa je verjetno prispeval tudi imunomodulatorni učinek TNF- α . Dopolnilna intratumorska terapija s TNF- α sinergistično deluje z intravenozno elektrokemoterapijo s cisplatinom. Sinergistično delovanje smo dosegli pri vseh odmerkih cisplatina. Zato predvidevamo, da bi bila kombinirana terapija učinkovita tudi za zdravljenje tumorjev, kjer so koncentracije zdravila suboptimalne, ali večjih tumorjev, kjer intravenozna elektrokemoterapija s cisplatinom ni dovolj učinkovita.

Radiol Oncol 2015; 49(1): 41-49.
doi:10.2478/raon-2014-0045

Blaga hipertermija vpliva na biološke lastnosti Herceptina[®]

Escoffre JM, Deckers R, Sasaki N, Bos C, Moonen C

Izhodišča. Blaga hipertermija (rHT) poveča krvni prekok v tumorjih, prepustnost žil in zmanjša medcelični pritisk, kar lahko vpliva na boljšo aktivnost in dostavo učinkovin z majhno molekulsko maso. Ta pojav je potencialno uporaben tudi za dostavo učinkovin z veliko molekulsko maso in tudi za protitelesa. V raziskavi smo preučevali učinek blage hipertermije na stabilnost ter imunološke in farmakološke lastnosti Herceptina[®]. Zdravilo Herceptin[®] je klinično potrjeno učinkovito protitelo proti receptorjem humanega epidermalnega ravnega faktorja 2 (HER-2). Ti receptorji so lahko v večji meri izraženi pri raku dojke.

Rezultati. Herceptin[®] smo ogreli do 37 °C (kontrola) ali na 42 °C (blaga hipertermija) za eno uro. Merili smo tvorbo agregatov Herceptin[®]-a z metodo nilsko rdeče (Nile Red). Blaga hipertermija ni povzročila povečane agregacije Herceptin[®]-a v primerjavi z inkubacijo pri 37 °C. Imunološke in farmakološke lastnosti Herceptin[®]-a smo preučevali na HER-2 pozitivni celični liniji raka dojke (BT-474). Metoda Western blot in analiza proliferacije celic je pokazala, da blaga hipertermija ni vplivala na biološke lastnosti Herceptina[®]-a na celicah BT-474.

Zaključki. Rahla hipertermija ne vpliva negativno na stabilnost ter imunološke in farmakološke lastnosti Herceptin[®]-a. Potrebno pa bi bilo preučiti tudi *in vivo* na tumorskih modelih vpliv blage hipertermije na intratumorsko bioviabilnost in terapevtsko učinkovitost Herceptin[®]-a.

Radiol Oncol 2015; 49(1): 50-58.

doi:10.2478/raon-2014-0015

Izražanje receptorjev EGFR v primarnih tumorjih mehurja in njihovih zasevkih glede na izražanje receptorjev HER2. Možnosti tarčnega zdravljenja z radionuklidi

Carlsson J, Wester K, De La Torre M, Malmström PU, Gårdmark T

Izhodišča. Delovanje inhibitorjev tirozinskih kinaz ali monoklonskih protiteles proti receptorjem epidermalnega rastnega dejavnika (EGFR) ali receptorjev humanega epidermalnega dejavnika 2 (HER2) je pri zdravljenju metastatskega raka mehurja omejeno. Zato jih ne uporabljamo pri standardnem zdravljenju. Bolj učinkovito bi lahko bilo tarčno zdravljenje z radionuklidi na izvencelične domene teh receptorjev.

Bolniki in metode. Izražanje EGFR in HER2 smo določili na primarnih tumorjih in njihovih zasevkih pri 72 bolnikih. Uporabili smo imunohistokemično metodo in mednarodno priporočeni HerceptTest. Nismo določili znotrajcelične mutacije, ker smo predpostavili, da nimajo večjega vpliva na obsevalno zdravljenje.

Rezultati. Izražanje EGFR je bilo pozitivno v 71 % primarnih tumorjev in v 69 % njihovih zasevkov. Lokalni zasevki so bili EGFR pozitivni v 75 % in oddaljeni zasevki v 66 %. Izražanje HER2 v lezijah smo določili v prejšnji raziskavi. EGFR pozitivni tumorji so imeli tudi EGFR pozitivne zasevke v 86 %. Sočasno izražanje receptorjev EGFR in HER2 pa je bilo v 57 % tumorjev in 53 % zasevkov. Samo 3 % tumorjev je bilo negativnih za oba receptorja in 10 % zasevkov. Zato bi sočasno tarčno zdravljenje obeh receptorjev bilo možno pri večini bolnikov.

Zaključki. Vsaj eden od receptorjev EGFR in HER2 je bil izražen pri večini bolnikov in pri več kot polovici bolnikov sta bila izražena oba receptorja. Zato bi bila zanimiva uporaba radionuklidov za določitev receptorjev v telesu, dozimetrijo in za zdravljenje. Takšno zdravljenje bi morda lahko uporabili ob rezistenci na druga zdravila in z namenom ozdravitve bolnika, ne pa samo kot paliativno zdravljenje.

Radiol Oncol 2015; 49(1): 59-64.

doi:10.2478/raon-2014-0020

Visoke vrednosti celokupnega pepsina in žolčnih kislin v slini kot možen dejavnik tveganja za razvoj raka grla

Šereg-Bahar M, Jerin A, Hočevár-Boltežar I

Izhodišča. Gastroezofagealni refluks je možen dejavnik tveganja pri nastanku raka grla in žrela. Namen raziskave je bil z neinvazivnimi diagnostičnimi metodami ugotoviti, ali je laringofaringealni refluks pogostejši pri bolnikih z zgodnjim rakom grla, kot pri kontrolni skupini zdravih prostovoljcev.

Bolniki in metode. Primerjali smo pH, nivo žolčnih kislin, nivo celokupnega pepsina in encimsko aktivnost pepsina v slini med skupino 30 bolnikov z začetnim rakom grla T1 in skupino 34 zdravih prostovoljcev.

Rezultati. Skupini sta se značilno razlikovali pri meritvah nivoja žolčnih kislin in celokupnega pepsina v slini. Višjo vrednost nivoja celokupnega pepsina in žolčnih kislin v slini so imeli bolniki z rakom grla. Na rezultate analize sline niso pomembno vplivali znani dejavniki tveganja za nastanek raka grla (npr. kajenje, uživanje alkoholnih pijač, prisotnost dražečih snovi na delovnem mestu).

Zaključki. Višji nivo sestavin želodčne vsebine v slini bolnikov z zgodnjim rakom grla v primerjavi s kontrolno skupino nakazuje možnost, da ima laringofaringealni refluks, še posebno bilijarni refluks, pomen pri nastanku raka grla.

Radiol Oncol 2015; 49(1): 65-70.
doi:10.2478/raon-2014-0034

Hipodontija pri bolnicah z epitelnim rakom jajčnikov

Fekonja A, Čretnik A, Žerdoner D, Takač I

Izhodišča. Rak jajčnikov običajno odkrijemo v napredovali obliki. Sedanji klinični in diagnostični molekularni označevalci za zgodnje ugotavljanje raka jajčnikov so nezadostni. Namen raziskave je bil ugotoviti, ali obstaja povezava med hipodontijo in epitelnim rakom jajčnikov.

Bolniki in metode. V retrospektivno raziskavo smo vključili 120 bolnic z epitelnim rakom jajčnikov, ki so bile zdravljene na Oddelku za ginekološko onkologijo in onkologijo dojke UKC Maribor ter 120 zdravih žensk (kontrolna skupina) z enako srednjo starostjo. Pri obeh skupinah preiskovank smo ugotavljali prisotnost hipodontije, pri bolnicah z epitelnim rakom jajčnikov pa tudi klinične in patohistološke značilnosti glede na prisotnost hipodontije.

Rezultati. Hipodontijo smo ugotovili pri 23 (19,2 %) bolnicah z epitelnim rakom jajčnikov in pri 8 (6,7 %) preiskovankah iz kontrolne skupine ($p = 0,004$; razmerje obolevnosti [OR] = 3,32; interval zaupanja [CI], 1,42–7,76). Med bolnicami z epitelnim rakom jajčnikov glede na prisotnost hipodontije nismo ugotovili statistično značilne razlike med histološkimi podvrstami ($p = 0,220$); razliko smo ugotovili glede na stadij FIGO ($p = 0,014$; OR = 3,26; CI, 1,23–8,64) in diferenciacijo tumorja ($p = 0,042$; OR = 3,1; CI, 1,01–9,53). Poleg tega je bilo pri bolnicah s hipodontijo pogostejše bilateralno pojavljanje epitelnega raka jajčnikov ($p = 0,021$; OR = 2,9; CI, 1,15–7,36). Prav tako smo med skupino preiskovank z epitelnim rakom jajčnikov in kontrolno skupino ugotovili statistično značilno razliko v prisotnosti drugih malignih tumorjev ($p < 0,001$).

Zaključki. Rezultati raziskave nakazujejo povezavo med epitelnim rakom jajčnikov in hipodontijo. Hipodontija bi lahko služila kot dejavnik tveganja za prepoznavo epitelnega raka jajčnikov.

Radiol Oncol 2015; 49(1): 71-74.
doi:10.2478/raon-2014-0035

Uporaba elektrokemoterapije z bleomicinom pri zdravljenju metastatskega melanoma med zdravljenjem z dabrafenibom

Valpione S, Campana LG, Pigozzo J, Chiarion-Sileni V

Izhodišča. Male molekule, kot sta vemurafenib in dabrafenib, zavirajo protein, ki nastane zaradi mutacije gena V600 BRAF. So zelo učinkovite pri zdravljenju razširjenega melanoma.

Prikaz primera. Opisujemo klinični potek zdravljenja metastatskega melanoma V600E BRAF pri bolniku z sistemsko boleznijo. Bolezen je napredovala s površinsko metastazo med zdravljenjem z dabrafenibom. Namen zdravljenja z elektrokemoterapijo je bil kontrolirati rast metastaze v mehkem tkivu med zdravljenjem z dabrafenibom in zagotoviti dobro lokalno kontrolo rasti metastaze brez stranskih pojavov.

Zaključki. Rezultati zdravljenja so pokazali, da je elektrokemoterapija omogočila dobro kakovost življenja tega bolnika in nemoteno zdravljenje s tarčno terapijo, ki se je tudi pokazala za učinkovito do 17 mesecev po zdravljenju.

Radiol Oncol 2015; 49(1): 75-79.
doi:10.2478/raon-2014-0006

Neposredna punkcija in sklerozacija kavernoznega hemangioma jezika z etanolom

Šeruga T, Lučev J, Jevšek M

Izhodišča. Hemangiomi jezika so dokaj redke bolezenske spremembe ožilja. Večinoma jih lahko zdravimo konzervativno, v nekaterih primerih pa je potrebno bolj agresivno zdravljenje s predoperativno znotraj arterijsko embolizacijo in kirurško odstranitvijo. Lezije jezika, ki so lokalizirane površno lahko zdravimo tudi z neposredno punkcijo in aplikacijo sklerozantnega sredstva (absolutni etanol).

Predstavitev primera. Predstavljamo primer 48 let stare bolnice, pri kateri smo opravili embolizacijo kavernoznega haemangioma z mešanico absolutnega etanola in oljnega kontrastnega sredstva. Po posegu je pacientka prejela protibolečinsko in antiedematozno terapijo. Rezultat embolizacije je bil tako dober, da načrtovana operacija ni bila potrebna. Kontrolna MRI pregleda 6 in 12 mesecev po posegu sta pokazala le majhen ostanek hemangioma, brez znakov ponovnega razraščanja.

Zaključki. V našem primeru se je neposredna punkcija hemangioma s sklerozacijo z etanolom izkazala kot varna in učinkovita metoda za doseg predoperativnega zmanjšanja in devaskularizacije lezije. Neposredna punkcija lezije ni omejena z anatomijo polnitvenega ožilja ali vazospazmom, do katerega lahko pride med znotraj arterijskim pristopom.

Radiol Oncol 2015; 49(1): 80-85.
doi:10.2478/raon-2014-0021

Bevacizumab in irinotekan pri ponavljajočih malignih gliomih. Slovenske izkušnje

Mesti T, Ebert Moltara M, Boc M, Reberšek M, Ocvirk J

Izhodišča. Možnosti zdravljenja ponavljajočih malignih gliomov so zelo omejene in ne omogočajo daljših preživetij. Maligni gliomi so močno ožiljeni tumorji in zato so obetajoča tarča za zdravila usmerjena proti rastnemu dejavniku za žilni endotelij. Rezultati raziskav II. faze kažejo na prednost kombiniranega zdravljenja z bevacizumabom in irinotekanom.

Bolniki in metode. Napravili smo retrospektivno raziskavo 19 bolnikov s ponavljajočim malignim gliomom, ki so bili zdravljeni z bevacizumabom in irinotekanom. Vsi bolniki so prejeli bevacizumab v odmerku 10 mg/kg v kombinaciji z irinotekanom v odmerku 340 mg/m² ali 125 mg/m² (z ali brez antiepileptične terapije) vsaka dva tedna. Analizirali smo klinične karakteristike bolnikov, toksičnost zdravljenja, odgovor na zdravljenje, preživetje brez napredovanja bolezni in celokupno preživetje.

Rezultati. Zdravili smo 14 (73,7 %) moških in 5 (26,3 %) žensk. Povprečna starost bolnikov je bila 44,7 let (27-74). Trinajst bolnikov je imelo multiformni glioblastom, 5 bolnikov anaplastični astroцитom in 1 bolnik anaplastični oligoastroцитom. Primarno so bili vsi bolniki razen enega zdravljeni z operacijo in pooperativno kemoradioterapijo. Klinični status po Svetovni zdravstveni organizaciji (WHO) je bil pri vseh bolnikih 0-2. Povprečno število aplikacij je bilo 9,3 (1-17). Po treh mesecih zdravljenja smo objektivni odgovor na zdravljenje dosegli pri 9 bolnikih (1 popolni odgovor, 8 delnih odgovorov), 7 bolnikov je imelo stabilno bolezen, pri 3 bolnikih je bolezen napredovala. Srednji čas preživetja brez napredovanja bolezni je bil 6,8 mesecev (95 % interval zaupanja [CI]: 5,3-8,3); po šestih mesecih je bilo brez napredovanja bolezni še vedno 52,6 % bolnikov. Srednje celokupno preživetje je bilo 7,7 mesecev (95 % CI: 6,6-8,7); po 6 mesecih je bilo živih še 68,4 % in po 12 mesecih še 31,6 % bolnikov. Pri 16 bolnikih smo ugotovili hematološko toksičnost, pri vseh stopnje (G) 1-2. Ostale toksičnosti so bile prisotne pri 14 bolnikih, pri vseh G1-2, le en bolnik je imel proteinurijo G3. G4 toksičnosti ni bilo, prav tako ni bilo nobenega primera tromboemboličnih zapletov ali intrakranialne krvavitve.

Zaključki. Kombinirano zdravljenje z bevacizumabom in irinotekanom pri bolnikih z malignimi gliomi je lahko učinkovito zdravljenje s sprejemljivo toksičnostjo. Potrebne so dodatne randomizirane raziskave za potrditev izboljšane preživetja bolnikov zdravljenih z tovrstno kombinacijo zdravil.

Radiol Oncol 2015; 49(1): 86-90.
doi:10.2478/raon-2014-0043

Novi model ocenjevanja preživetja bolnikov z metastatsko epiduralno kompresijo hrbtenjačne zaradi raka požiralnika

Rades D, Huttenlocher S, Bajrovic A, Karstens JH, Bartscht T

Izhodišča. Namen raziskave je bil oblikovati predvidljiv model ocenjevanja preživetja bolnikov z metastatsko epiduralno kompresijo hrbtenjače zaradi raka požiralnika.

Metode. Pri 27 bolnikih, obsevanih zaradi metastatske epiduralne kompresije hrbtenjače zaradi raka požiralnika, smo analizirali devet značilnosti, da bi ugotovili njihovo vlogo na preživetje: starost, spol, stanje splošne zmogljivosti ocenjeno po ECOG (*Easteren Cooperative Oncology Group*), histologijo, število prizadetih vretenc, pokretnost bolnika pred obsevanjem, preostale kostne metastaze, visceralne metastaze in dinamiko razvoja motoričnega primanjkljaja pred obsevanjem. Poleg tega smo analizirali vpliv predpisanega načina obsevanja. Glede na korekcijo po Bonferroniju so vrednosti $p < 0,006$ predstavljale značilni nivo alfa $< 0,05$.

Rezultati. Stanje splošne zmogljivosti ocenjeno po ECOG ($p < 0,001$), število prizadetih vretenc ($p = 0,005$) in visceralne metastaze ($p = 0,004$) so se pokazali kot statistično značilni za preživetje bolnikov in smo jih vključili v model ocenjevanja. Vrednosti za vsako od treh značilnosti smo izračunali tako, da smo 6-mesečno preživetje (v %) delili z 10. Za vsakega bolnika smo določili napovedno oceno kot vsoto vrednosti vseh treh značilnosti. Vrednosti napovednih ocen so bile 4, 9, 10, 14 in 20 točk. Bolnike smo glede na napovedne ocene razdelili v tri skupine: skupino z oceno 4 točke ($n = 11$), skupino z oceno 9–14 točk ($n = 12$) in skupino z oceno 20 točk ($n = 4$). Šest mesečno preživetje je bilo 0 % za prvo skupino (srednji čas preživetja 1 mesec), 33 % za drugo skupino (srednji čas preživetja 5 mescev) in 100 % za tretjo skupino (srednji čas preživetja 16,5 mescev) ($p < 0,001$).

Zaključki. Predstavljeni model omogoča oceno verjetnosti 6-mesečnega preživetja bolnikov z metastatsko epiduralno kompresijo hrbtenjače zaradi raka požiralnika, kar je pomembno za načrtovanje zdravljenja posameznega bolnika.

Radiol Oncol 2015; 49(1): 91-98.

doi:10.2478/raon-2014-0033

Dozimetrična primerjava volumetričnega modulirajočega ločnega obsevanja in intenzitetno modulirajočega obsevanja na levostransko prsno steno pri obsevanju internih mamarnih bezgavk bolnic z rakom dojke po mastektomiji

Zhang Q, Yu XL, Hu WG, Chen JY, Wang JZ, Ye JS, Guo XM

Izhodišča. Namen raziskave je bil oceniti dozimetrično prednost volumetričnega modulirajočega ločnega obsevanja (VMAT) pri bolnicah s prizadetostjo internih mamarnih bezgavk (IMB) po levostranski mastektomiji.

Bolniki in metode. Predpisali smo obsevalno dozo 50 Gy v 25 frakcijah. Klinični tarčni volumen je zajemal levo prsno steno in IMB. Za pripravo in primerjavo planov VMAT in planov z intenzitetno modulirajočim obsevanjem (IMRT) smo uporabili planirni sistem Pinnacle. Primerjali smo homogenost doze znotraj planiranega tarčnega volumna (PTV), pokritje tarčne doze, dozo na kritične organe vključno s srcem, pljuči in nasprotno ležečo dojko, število monitorskih enot in čas obsevanja.

Rezultati. Plani VMAT in IMRT so pokazali podobno homogenost doze PTV, toda VMAT je zagotavljal boljše pokritje doze za IMB kot IMRT ($p = 0,017$). Povprečna doza (Gy), V30 (%) in V10 (%) za srce je bila $13,5 \pm 5,0$ Gy, $9,9 \% \pm 5,9 \%$ in $50,2 \% \pm 29,0 \%$ z VMAT ter $14,0 \pm 5,4$ Gy, $10,6 \% \pm 5,8 \%$ in $55,7 \% \pm 29,6 \%$ z IMRT. Povprečna doza na leva pljuča (Gy), V20 (%), V10 (%) ter doza na desna pljuča V5 (%) se je značilno zmanjšala iz $14,1 \pm 2,3$ Gy, $24,2 \% \pm 5,9 \%$, $42,4 \% \pm 11,9 \%$ in $41,2 \% \pm 12,3 \%$ z IMRT na $12,8 \pm 1,9$ Gy, $21,0 \% \pm 3,8 \%$, $37,1 \% \pm 8,4 \%$ in $32,1 \% \pm 18,2 \%$ z VMAT. VMAT je tudi znižal število monitorskih enot za 24 % in čas obsevanja za 53 % v primerjavi z IMRT.

Zaključki. V primerjavi s 5-žarkovnim stopenjskim zapiranjem lističev z IMRT je tehnika VMAT dala podobne ali boljše rezultate v pokritju tarče ter boljše varovanje normalnih tkiv ob uporabi manjšega števila monitorskih enot in s krajšim časom obsevanja.

Radiol Oncol 2015; 49(1): 99-106.

doi:10.2478/raon-2014-0029

Ocena kolektivne efektivne doze zaradi radioloških posegov v Sloveniji

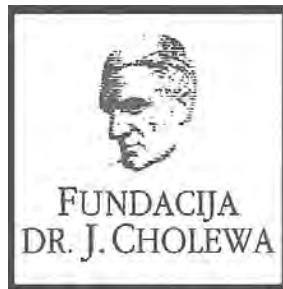
Žontar D, Zdešar U, Kuhelj D, Pekarovič D, Škrk D

Izhodišča. Cilj raziskave je bil izvesti prvo sistematično oceno izpostavljenosti prebivalstva zaradi diagnostičnih in intervencijskih radioloških posegov v Sloveniji.

Metode. Raziskavo smo naredili v projektu "Dose Datamed 2". Uporabili smo standardno metodologijo na osnovi 20 izbranih radioloških posegov. Pogostost posegov smo določili na podlagi vprašalnikov, ki smo jih poslali vsem izvajalcem radioloških posegov v Sloveniji, podatke o izpostavljenosti pacientov pri posameznih posegih (produkt doze in dolžine preiskovanega področja [DLP] za CT, povprečno žlezno dozo [MGD] za mamografijo in produkt doze in površine [DAP] za ostale posege) pa smo ugotovili iz podatkovnih baz. Na podlagi zbranih podatkov in z uporabo konverzijskih količnikov smo ocenili kolektivno efektivno dozo za prebivalstvo in za posameznika.

Rezultati. Skupna kolektivna efektivna doza zaradi radioloških posegov v letu 2011 je bila ocenjena na 1300 človekSv, efektivna doza na prebivalca pa na 0,6 mSv. K skupni dozi je približno 2/3 prispevala računalniška tomografija.

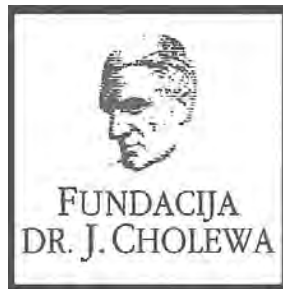
Zaključki. Naredili smo prvo sistematično raziskavo izpostavljenosti prebivalstva ionizirajočemu sevanju zaradi radioloških posegov v Sloveniji. Rezultati kažejo, da je izpostavljenost pod evropskim povprečjem ter potrdili visoka prispevka računalniške tomografije in intervencijskih posegov k skupni dozi. Raziskava je tako navedeni področji opredelila kot področji, ki jima moramo posvetiti posebno pozornost z vidikov optimizacije in upravičenosti.



FUNDACIJA "DOCENT DR. J. CHOLEWA"
JE NEPROFITNO, NEINSTITUCIONALNO IN NESTRANKARSKO
ZDRUŽENJE POSAMEZNIKOV, USTANOV IN ORGANIZACIJ, KI ŽELIJO
MATERIALNO SPODBUJATI IN POGLABLJATI RAZISKOVALNO
DEJAVNOST V ONKOLOGIJI.

DUNAJSKA 106
1000 LJUBLJANA

IBAN: SI56 0203 3001 7879 431



Activity of "Dr. J. Cholewa" Foundation for Cancer Research and Education - a report for the first quarter of 2015

The "Docent Dr. J. Cholewa Foundation for Cancer Research and Education" is a non-profit, non-political and non-government organisation that helps professionals, institutions and individuals obtaining financial help for cancer research and education in the Republic of Slovenia. It carries the name of Dr. Josip Cholewa, one of the first researchers in cancer in Slovenia and the founder of the "Banovinski Inštitut za raziskovanje in zdravljenje novotvorb", that later became the Institute of Oncology in Ljubljana, Slovenia. Already as a Head Physician in Brežice General Hospital in the early twenties of the previous century, he established an experimental cancer research laboratory. His research was based on multisectorial approach to prevention, detection and treatment of cancer, in which various experts collaborate and constantly exchange news and views.

High quality cancer research demands a lot of money and many excellent ideas cannot come into being for the simple lack of it. The most important activity of the Foundation is thus to provide at least some of the financial support needed by qualified individuals and organisations interested in cancer research. With this in mind, the Foundation also aims to help with the transmission of the latest diagnostic and therapy procedures to the everyday research and clinical environment in Slovenia. This part of Foundation's activity represents the most direct benefit for the ever increasing number of patients with various types of cancer in Slovenia, since the incidence rates of many cancers have kept raising in recent decades.

The Foundation continues to provide financial support to "Radiology and Oncology", an international scientific journal that is edited and published in Ljubljana, Slovenia. It publishes scientific research articles, reviews, case reports, short reports and letters to the editor about research and studies in experimental and clinical oncology, supportive therapy, radiology, radiophysics, prevention and early diagnostics of different types of cancer. It is an open access journal available in pdf format and with a respectable Science Citation Index Impact factor. All the abstracts in "Radiology and Oncology" are available in Slovenian and the journal can thus provide sufficient scientific information from various fields of high quality cancer research to interested lay public in Slovenia.

In cancer research natural inquisitiveness, curiosity, persistence and acquired knowledge usually are not enough. In a number of developed countries with extensive cancer research capabilities, the researchers can count on financial assistance in the form of grants and scholarships, provided by an ever growing number of government and independent institutions and charities. The "Docent Dr. J. Cholewa Foundation for Cancer Research and Education" has thus an important role in support of many scientists involved in cancer research, cancer education and in many of the related fields in the Republic of Slovenia.

Andrej Plesničar, MD, MSc
Borut Štabuc, MD, PhD
Tomaž Benulič, MD
Viljem Kovač, MD, PhD

TANTUM VERDE®



Lajšanje bolečine in oteklin pri vnetju v ustni votlini in žrelu, ki nastanejo zaradi okužb in stanj po operaciji in kot posledica radioterapije (t.i. radiomukozitis).



Imetnik dovoljenja za promet
CSC Pharma d.o.o.
Jana Husa 1a
1000 Ljubljana



www.tantum-verde.si

Tantum Verde 1,5 mg/ml oralno pršilo, raztopina

Kakovostna in količinska sestava

1 ml raztopine vsebuje 1,5 mg benzidaminijevega klorida, kar ustreza 1,34 mg benzidamina. V enem razpršku je 0,17 ml raztopine. En razpršek vsebuje 0,255 mg benzidaminijevega klorida, kar ustreza 0,2278 mg benzidamina. En razpršek vsebuje 13,6 mg 96 odstotnega etanola, kar ustreza 12,728 mg 100 odstotnega etanola, in 0,17 mg metilparahidroksibenzoata (E218).

Terapevtske indikacije

Samozdravljenje: lajšanje bolečine in oteklin pri vnetju v ustni votlini in žrelu, ki so lahko posledica okužb in stanj po operaciji. Po nasvetu in navodilu zdravnika: lajšanje bolečine in oteklin v ustni votlini in žrelu, ki so posledica radiomukozitisa.

Odmerjanje in način uporabe

Uporaba 2- do 6-krat na dan (vsake 1,5 do 3 ure). Odrasli: 4 do 8 razprškov 2- do 6-krat na dan. Otroci od 6 do 12 let: 4 razprški 2- do 6-krat na dan. Otroci, mlajši od 6 let: 1 razpršek na 4 kg telesne mase; do največ 4 razprške 2 do 6-krat na dan.

Kontraindikacije

Znana preobčutljivost za zdravilno učinkovino ali katerokoli pomožno snov.

Posebna opozorila in previdnostni ukrepi

Pri manjšini bolnikov lahko resne bolezni povzročijo ustne/žrelne ulceracije. Če se simptomi v treh dneh ne izboljšajo, se mora bolnik posvetovati z zdravnikom ali zobozdravnikom, kot je primerno. Zdravilo vsebuje aspartam (E951) (vir fenilalanina), ki je lahko škodljiv za bolnike s fenilketonurijo. Zdravilo vsebuje izomalt (E953) (sinonim: izomaltitol (E953)). Bolniki z redko dedno intoleranco za fruktozo ne smejo jemati tega zdravila. Uporaba benzidamina ni priporočljiva za bolnike s preobčutljivostjo za salicilno kislino ali druga nesteroidna protivnetna zdravila. Pri bolnikih, ki imajo ali so imeli bronhialno astmo, lahko pride do bronhospazma. Pri takih bolnikih je potrebna previdnost.

Medsebojno delovanje z drugimi zdravili in druge oblike interakcij

Pri ljudeh raziskav o interakcijah niso opravljali.

Nosečnost in dojenje

Tantum Verde z okusom mentola 3 mg pastile se med nosečnostjo in dojenjem ne smejo uporabljati.

Vpliv na sposobnost vožnje in upravljanja s stroji

Uporaba benzidamina lokalno v priporočenem odmerku ne vpliva na sposobnost vožnje in upravljanja s stroji.

Neželeni učinki

Bolezni prebavil Redki: pekoč občutek v ustih, suha usta.

Bolezni imunskega sistema Redki: preobčutljivostna reakcija.

Bolezni dihal, prsnega koša in mediastinalnega prostora Zelo redki: laringospazem.

Bolezni kože in podkožja Občasni: fotosenzitivnost. Zelo redki: angioedem.

Rok uporabnosti

4 leta. Zdravila ne smejo uporabljati po datumu izteka roka uporabnosti, ki je naveden na ovojnjini. Posebna navodila za shranjevanje Za shranjevanje pastil niso potrebna posebna navodila. Platenko z raztopino shranjujte v zunanji ovojnjini za zagotovitev zaščite pred svetlobo. Shranjujte pri temperaturi do 25°C. Shranjujte v originalni ovojnjini in nedosegljivo otrokom.

Individualizirano zdravljenje za bolnike z metastatskim kolorektalnim rakom



Merck Serono Onkologija | Ključ je v kombinaciji

Erbitux 5 mg/ml raztopina za infundiranje

Skrajšan povzetek glavnih značilnosti zdravila

Sestava: En ml raztopine za infundiranje vsebuje 5 mg cetuksimaba in pomožne snovi. Cetuksimab je himerno monoklonsko IgG₁ protitelo. **Terapevtske indikacije:** Zdravilo Erbitux je indicirano za zdravljenje bolnikov z metastatskim kolorektalnim rakom z ekspresijo receptorjev EGFR in nemutiranim tipom RAS v kombinaciji s kemoterapijo na osnovi irinotekana, kot primarno zdravljenje v kombinaciji s FOLFOX in kot samostojno zdravilo pri bolnikih, pri katerih zdravljenje z oksaliplatinom in zdravljenje na osnovi irinotekana ni bilo uspešno in pri bolnikih, ki ne prenašajo irinotekana. Zdravilo Erbitux je indicirano za zdravljenje bolnikov z rakom skvamoznih celic glave in vratu v kombinaciji z radioterapijo za lokalno napredovalo bolezen in v kombinaciji s kemoterapijo na osnovi platine za ponavljajočo se in/ali metastatsko bolezen. **Odmerjanje in način uporabe:** Zdravilo Erbitux pri vseh indikacijah infundirajte enkrat na teden. Pred prvo infuzijo mora bolnik prejeti premedikacijo z antihistaminikom in kortikosteroidom najmanj 1 uro pred uporabo cetuksimaba. Začetni odmerek je 400 mg cetuksimaba na m² telesne površine. Vsi naslednji tedenski odmerki so vsak po 250 mg/m². **Kontraindikacije:** Zdravilo Erbitux je kontraindicirano pri bolnikih z znano hudo preobčutljivostno reakcijo (3. ali 4. stopnje) na cetuksimab. Kombinacija zdravila Erbitux s kemoterapijo, ki vsebuje oksaliplatin, je kontraindicirana pri bolnikih z metastatskim kolorektalnim rakom z mutiranim tipom RAS ali kadar status RAS ni znan. **Posebna opozorila in previdnostni ukrepi:** Pojav hude reakcije, povezane z infundiranjem, zahteva takojšnjo in stalno ukinitvev terapije s cetuksimabom. Če pri bolniku nastopi blaga ali zmerna reakcija, povezana z infundiranjem, lahko zmanjšate hitrost infundiranja. Priporočljivo je, da ostane hitrost infundiranja na nižji vrednosti tudi pri vseh naslednjih infuzijah. Če se pri bolniku pojavi kožna reakcija, ki je ne more prenašati, ali huda kožna reakcija (≥ 3. stopnje po kriterijih CTCAE), morate prekiniti terapijo s cetuksimabom. Z zdravljenjem smete nadaljevati le, če se je reakcija izboljšala do 2. stopnje. Če ugotovite intersticijsko bolezen pljuč, morate zdravljenje s cetuksimabom prekiniti, in bolnika ustrezno zdraviti. Zaradi možnosti pojava znižanja nivoja elektrolitov v serumu se pred in periodično med zdravljenjem s cetuksimabom priporoča določanje koncentracije elektrolitov v serumu. Pri bolnikih, ki prejemajo cetuksimab v kombinaciji s kemoterapijo na osnovi platine, obstaja večje

tveganje za pojav hude nevropenije. Takšne bolnike je potrebno skrbno nadzorovati. Pri predpisovanju cetuksimaba je treba upoštevati kardiovaskularno stanje in indeks zmogljivosti bolnika in sočasno dajanje kardiotoksičnih učinkovin kot so fluoropirimidini. Če je diagnoza ulcerativnega keratitisa potrjena, je treba zdravljenje s cetuksimabom prekiniti ali ukiniti. Cetuksimab je treba uporabljati previdno pri bolnikih z anamnezo keratitisa, ulcerativnega keratitisa ali zelo suhih oči. Cetuksimaba ne uporabljajte za zdravljenje bolnikov s kolorektalnim rakom, če imajo tumorje z mutacijo RAS ali pri katerih je tumorski status RAS neznan. **Interakcije:** Pri kombinaciji s fluoropirimidini se je v primerjavi z uporabo fluoropirimidinov, kot monoterapije, povečala pogostnost srčne ishemije, vključno z miokardnim infarktom in kongestivno srčno odpovedjo ter pogostnost sindroma dlani in stopal. V kombinaciji s kemoterapijo na osnovi platine se lahko poveča pogostnost hude levkopenije ali hude nevropenije. V kombinaciji s kapecitabinom in oksaliplatinom (XELOX) se lahko poveča pogostnost hude driske. **Neželeni učinki:** Zelo pogosti (≥ 1/10): hipomagnezija, povečanje ravnih jetrnih encimov, kožne reakcije, blage ali zmerno reakcije povezane z infundiranjem, mukozitis, v nekaterih primerih resen. Pogosti (≥ 1/100 do < 1/10): dehidracija, hipokalcemija, anoreksija, glavobol, konjunktivitis, driska, navzeja, bruhanje, hude reakcije povezane z infundiranjem, utrujenost. **Posebna navodila za shranjevanje:** Shranjujte v hladilniku (2 °C - 8 °C). **Pakiranje:** 1 viala z 20 ml ali 100 ml raztopine. **Način in režim izdaje:** Izdaja zdravila je le na recept-H. **Imetnik dovoljenja za promet:** Merck KGaA, 64271 Darmstadt, Nemčija.

Datum zadnje revizije besedila: junij 2014.

Pred predpisovanjem zdravila natančno preberite celoten Povzetek glavnih značilnosti zdravila.

Samo za strokovno javnost.

Podrobnejše informacije so na voljo pri predstavniku imetnika dovoljenja za promet z zdravilom:
Merck d.o.o., Ameriška ulica 8, 1000 Ljubljana, tel.: 01 560 3810, faks: 01 560 3830, el. pošta: info@merck.si
www.merckserono.net
www.Erbitux-international.com

SKRAJŠAN POVZETEK GLAVNIH ZNAČILNOSTI ZDRAVILA

Samo za strokovno javnost.

Ime zdravila: Tarceva 25 mg/100 mg/150 mg filmsko obložene tablete

Kakovostna in količinska sestava: Ena filmsko obložena tableta vsebuje 25 mg, 100 mg ali 150 mg erlotiniba (v obliki erlotinibijevga klorida).

Terapevtske indikacije: **Nedrobnocelični rak pljuč:** Zdravilo Tarceva je indicirano za prvo linijo zdravljenja bolnikov z lokalno napredovalim ali metastatskim nedrobnoceličnim rakom pljuč z EGFR-aktivirajočimi mutacijami. Zdravilo Tarceva je indicirano tudi za samostojno vzdrževalno zdravljenje bolnikov z lokalno napredovalim ali metastatskim nedrobnoceličnim rakom pljuč s stabilno boleznijo po 4 ciklih standardne kemoterapije na osnovi platine v prvi liniji zdravljenja. Zdravilo Tarceva je indicirano tudi za zdravljenje bolnikov z lokalno napredovalim ali metastatskim nedrobnoceličnim rakom pljuč po neuspehu vsaj ene predhodne kemoterapije. Pri predpisovanju zdravila Tarceva je treba upoštevati dejavnike, povezane s podaljšanim preživetjem. Koristnega vpliva na podaljšanje preživetja ali drugih klinično pomembnih učinkov zdravljenja niso dokazali pri bolnikih z EGFR-negativnimi tumorji (glede na rezultat imunohistokemije). **Rak trebušne slinavke:** Zdravilo Tarceva je v kombinaciji z gemcitabinom indicirano za zdravljenje bolnikov z metastatskim rakom trebušne slinavke. Pri predpisovanju zdravila Tarceva je treba upoštevati dejavnike, povezane s podaljšanim preživetjem. Koristnega vpliva na podaljšanje preživetja niso dokazali za bolnike z lokalno napredovalo boleznijo.

Odmerjanje in način uporabe: Zdravljenje z zdravilom Tarceva mora nadzorovati zdravnik z izkušnjami pri zdravljenju raka. Pri bolnikih z lokalno napredovalim ali metastatskim nedrobnoceličnim rakom pljuč, ki še niso prejeli kemoterapije, je treba testiranje za določanje mutacij EGFR opraviti pred začetkom zdravljenja z zdravilom Tarceva. Zdravilo Tarceva vzamemo najmanj eno uro pred zaužitjem hrane ali dve uri po tem. Kadar je potrebno odmerke prilagoditi, ga je treba zmanjševati v korakih po 50 mg. Pri sočasnem jemanju substratov in modulatorjev CYP3A4 bo morda potrebna prilagoditev odmerka. Pri dajanju zdravila Tarceva bolnikom z jetrno okvaro je potrebna previdnost. Če se pojavijo hudi neželeni učinki, pride v poštev zmanjšanje odmerka ali prekinitev zdravljenja z zdravilom Tarceva. Uporaba zdravila Tarceva pri bolnikih s hudo jetrno ali ledvično okvaro ter pri otrocih ni priporočljiva. Bolnikom kadilcem je treba svetovati, naj prenehajo kaditi, saj so plazemske koncentracije erlotiniba pri kadilcih manjše kot pri nekadilcih. **Nedrobnocelični rak pljuč:** Priporočeni dnevni odmerki zdravila Tarceva je 150 mg. **Rak trebušne slinavke:** Priporočeni dnevni odmerki zdravila Tarceva je 100 mg, v kombinaciji z gemcitabinom. Pri bolnikih, pri katerih se kožni izpuščaj v prvih 4 do 8 tednih zdravljenja ne pojavi, je treba ponovno pretehati nadaljnje zdravljenje z zdravilom Tarceva.

Kontraindikacije: Preobčutljivost na erlotinib ali katero koli pomožno snov.

Posebna opozorila in previdnostni ukrepi: Pri določanju bolnikovega statusa mutacij EGFR je pomembno izbrati dobro validirano in robustno metodologijo, da se izognemo lažno negativnim ali lažno pozitivnim rezultatom. **Kadilci:** Bolnikom, ki kadijo, je treba svetovati, naj prenehajo kaditi, saj so plazemske koncentracije erlotiniba pri kadilcih zmanjšane v primerjavi s plazemskimi koncentracijami pri nekadilcih. Verjetno je, da je velikost zmanjšanja klinično pomembna. **Intersticijska bolezen pljuč:** Pri bolnikih, pri katerih se akutno pojavijo novi in/ali poslabšajo nepojasneni pljučni simptomi, kot so dispneja, kašelj in vročina, je treba zdravljenje z zdravilom Tarceva prekiniti, dokler ni znana diagnoza. Bolnike, ki se sočasno zdravijo z erlotinibom in gemcitabinom, je treba skrbno spremljati zaradi možnosti pojavnosti toksičnosti, podobni intersticijski bolezni pljuč. Če je ugotovljena intersticijska bolezen pljuč, zdravilo Tarceva ukinemo in uvedemo ustrezno zdravljenje. **Driska, dehidracija, neravnovesje elektrolitov in ledvična odpoved:** Pri približno polovici bolnikov, ki so se zdravili z zdravilom Tarceva, se je pojavila driska (vključno z zelo redkimi primeri, ki so se končali s smrtnim izidom). Zmerno do hudo drisko zdravimo z loperamidom. V nekaterih primerih bo morda potrebno zmanjšanje odmerka. V primeru hude ali dolgotrajne driske, navzee, anoreksije ali bruhanja, povezanih z dehidracijo, je treba zdravljenje z zdravilom Tarceva prekiniti in dehidracijo ustrezno zdraviti. O hipokalemiji in ledvični odpovedi so poročali redko. Posebno pri bolnikih z dejavniki tveganja (zlasti sočasnim jemanjem kemoterapevtikov in drugih zdravil, simptomi ali boleznimi ali drugimi dejavniki, vključno z visoko starostjo) moramo, če je driska huda ali dolgotrajna oziroma vodi v dehidracijo, zdravljenje z zdravilom Tarceva prekiniti in bolnikom zagotoviti intenzivno intravensko rehidracijo. Dodatno je treba pri bolnikih s prisotnim tveganjem za razvoj dehidracije spremljati ledvično delovanje in serumske elektrolite, vključno s kalijem. **Hepatitis, jetrna odpoved:** Pri uporabi zdravila Tarceva so poročali o redkih primerih jetrne odpovedi (vključno s smrtnimi). K njenemu nastanku je lahko pripomogla predhodno obstoječa jetrna bolezen ali sočasno jemanje hepatotoksičnih zdravil. Pri teh bolnikih je treba zato premisliti o rednem spremljanju jetrnega delovanja. Dajanje zdravila Tarceva je treba prekiniti, če so spremembe jetrnega delovanja hude. **Perforacije v prebavilih:** Bolniki, ki prejemajo zdravilo Tarceva, imajo večje tveganje za razvoj perforacij v prebavilih, ki so jih opazili občasno (vključno z nekaterimi primeri, ki so se končali s smrtnim izidom). Pri bolnikih, ki sočasno prejemajo zdravila, ki zavirajo angiogenezo, kortikosteroide, nesteroidna protivnetna zdravila (NSAID) in/ali kemoterapijo na osnovi takсанov, ali so v preteklosti imeli peptični ulkus ali divertikularno bolezen, je tveganje večje. Če pride do tega, je treba zdravljenje z zdravilom Tarceva dokončno ukiniti. **Kožne bolezni, pri katerih so prisotni mehurji in luščenje kože:** Poročali so o primerih kožnih bolezni z mehurji in luščenjem kože, vključno z zelo redkimi primeri, ki so nakazovali na Stevens-Johnsonov sindrom/toksično epidermalno nekrolizo in so bili v nekaterih primerih smrtni. Zdravljenje z zdravilom Tarceva je treba prekiniti ali ukiniti, če se pri bolniku pojavijo hude oblike mehurjev ali luščenja kože. Pri bolnikih s kožnimi boleznimi z mehurji in luščenjem kože je treba preveriti prisotnost okužbe kože in jih zdraviti v skladu z lokalnimi smernicami. **Očesne bolezni:** Bolniki, pri katerih se pojavijo znaki in simptomi, ki nakazujejo na keratitis in so lahko akutni ali se poslabšujejo: vnetje očesa, solzenje, občutljivost na svetlobo, zamegljen vid, bolečine v očesu in/ali rdeče oči, se morajo takoj obrniti na specialista oftalmologije. V primeru, da je diagnoza ulcerativnega keratitisa potrjena, je treba zdravljenje z zdravilom Tarceva prekiniti ali ukiniti. V primeru,

da se postavi diagnoza keratitisa, je treba skrbno razmisliti o koristih in tveganjih nadaljnega zdravljenja. Zdravilo Tarceva je pri bolnikih, ki so v preteklosti imeli keratitis, ulcerativni keratitis ali zelo suhe oči, uporabljati previdno. Uporaba kontaktnih leč je prav tako dejavnik tveganja za keratitis in ulceracijo. Med uporabo zdravila Tarceva so zelo redko poročali o primerih perforacije ali ulceracije roženice. **Medsebojno delovanje z drugimi zdravili:** Močni induktorji CYP3A4 lahko zmanjšajo učinkovitost erlotiniba, močni zaviralci CYP3A4 pa lahko povečajo toksičnost. Sočasnemu zdravljenju s temi zdravili se je treba izogibati. Tablete vsebujejo laktozo in jih ne smemo dajati bolnikom z redkimi dednimi stanji: intoleranco za galaktozo, laponsko obliko zmanjšane aktivnosti laktaze ali malabsorpcijo glukoze/galaktoze.

Medsebojno delovanje z drugimi zdravili in druge oblike interakcij: Erlotinib se pri ljudeh presnavlja v jetrih z jetrnimi citokromi, primarno s CYP3A4 in v manjši meri s CYP1A2. Presnova erlotiniba zunaj jeter poteka s CYP3A4 v črevesju, CYP1A1 v pljučih in CYP1B1 v tumorskih tkivih. Z zdravilnimi učinkovinami, ki se presnavljajo s temi encimi, jih zavirajo ali pa so njihovi induktorji, lahko pride do interakcij. Erlotinib je srednje močan zaviralec CYP3A4 in CYP2C8, kot tudi močan zaviralec glukuronidacije z UGT1A1 *in vitro*. Pri kombinaciji ciprofloksacina ali močnega zaviralca CYP1A2 (npr. fluvoksamina) z erlotinibom je potrebna previdnost. V primeru pojavnosti neželenih učinkov, povezanih z erlotinibom, lahko odmerek erlotiniba zmanjšamo. Predhodno ali sočasno zdravljenje z zdravilom Tarceva ni spremenilo čistostne prototipov substratov CYP3A4, midazolama in eritromicina. Inhibicija glukuronidacije lahko povzroči interakcije z zdravili, ki so substrati UGT1A1 in se izločajo samo po tej poti. Močni zaviralci aktivnosti CYP3A4 zmanjšajo presnovo erlotiniba in zvečajo koncentracije erlotiniba v plazmi. Pri sočasnem jemanju erlotiniba in močnih zaviralcev CYP3A4 je zato potrebna previdnost. Če je treba, odmerek erlotiniba zmanjšamo, še posebno pri pojavu toksičnosti. Močni spodbujevalci aktivnosti CYP3A4 zvečajo presnovo erlotiniba in pomembno zmanjšajo plazemske koncentracije erlotiniba. Sočasno dajanje zdravila Tarceva in induktorjev CYP3A4 se je treba izogibati. Pri bolnikih, ki potrebujejo sočasno zdravljenje z zdravilom Tarceva in močnim induktorjem CYP3A4, je treba premisliti o povečanju odmerka do 300 mg ob skrbnem spremljanju njihove varnosti. Zmanjšana izpostavljenost se lahko pojavi tudi z drugimi induktorji, kot so fenitoin, karbamazepin, barbiturati ali šentjanževka. Če te zdravilne učinkovine kombiniramo z erlotinibom, je potrebna previdnost. Kadar je mogoče, je treba razmisliti o drugih načinih zdravljenja, ki ne vključujejo močnega spodbujanja aktivnosti CYP3A4. Bolnikom, ki jemljejo *kumarinske antikoagulate*, je treba redno kontrolirati protrombinski čas ali INR. Sočasno zdravljenje z zdravilom Tarceva in *statinom* lahko poveča tveganje za miopatijo, povzročeno s statini, vključno z rabdomiolizo; to so opazili redko. Sočasna uporaba *zaviralcev P-glikoproteina*, kot sta ciklosporin in verapamil, lahko vodi v spremenjeno porazdelitev in/ali spremenjeno izločanje erlotiniba. Za erlotinib je značilno zmanjšanje topnosti pri pH nad 5. *Zdravila, ki spremenijo pH v zgornjem delu prebavil*, lahko spremenijo topnost erlotiniba in posledično njegovo biološko uporabnost. Učinka antacidov na absorpcijo erlotiniba niso preučevali, vendar je ta lahko zmanjšana, kar vodi v nižje plazemske koncentracije. Kombinaciji erlotiniba in zaviralca protonske črpalke se je treba izogibati. Če menimo, da je uporaba antacidov med zdravljenjem z zdravilom Tarceva potrebna, jih je treba jemati najmanj 4 ure pred ali 2 uri po dnevnem odmerku zdravila Tarceva. Če razmišljamo o uporabi ranitidina, moramo zdravili jemati ločeno: zdravilo Tarceva je treba vzeti najmanj 2 uri pred ali 10 ur po odmerku ranitidina. V študiji faze Ib ni bilo pomembnih učinkov *gemcitabina* na farmakokinetiko erlotiniba, prav tako ni bilo pomembnih učinkov erlotiniba na farmakokinetiko *gemcitabina*. Erlotinib poveča koncentracijo platine. Pomembnih učinkov *karboplatina* ali paklitaksela na farmakokinetiko erlotiniba ni bilo. *Kapecitabin* lahko poveča koncentracijo erlotiniba. Pomembnih učinkov erlotiniba na farmakokinetiko *kapecitabina* ni bilo. Zaradi mehazma delovanja lahko od *zaviralcev proteasomov*, vključno z bortezomibom, pričakujemo, da vplivajo na učinek zaviralcev EGFR, vključno z erlotinibom.

Neželeni učinki: *Zelo pogosti neželeni učinki* so kožni izpuščaj in driska, kot tudi utrujenost, anoreksija, dispneja, kašelj, okužba, navzea, bruhanje, stomatitis, bolečina v trebuhu, pruritus, suha koža, suhi keratokonjunktivitis, konjunktivitis, zmanjšanje telesne mase, depresija, glavobol, nevropatija, dispneja, flatulenca, alopecija, okorelost, piroksija, nenormalnosti testov jetrne funkcije. *Pogosti neželeni učinki* so krvavitve v prebavilih, epistaksa, resna intersticijska bolezen pljuč, keratitis, paronihija, folikulitis, akne/akneiformni dermatitis, fisure na koži in ledvična insuficienca. *Občasno* so poročali o perforacijah v prebavilih, hirzutizmu, spremembah obrvi, krhkih nohtih, odstopanju nohtov od kože, blagih reakcijah na koži (npr. hiperpigmentaciji), spremembah trepalnic, nefritisu in proteinuriji. *Redko* pa so poročali o jetrni odpovedi in sindromu palmarno-planarne eritrodisezije. *Zelo redko* so poročali o Stevens-Johnsonovem sindromu/toksični epidermalni nekrolizi ter o ulceracijah in perforacijah roženice.

Režim izdaje zdravila: H/Rp.

Imetnik dovoljenja za promet: Roche Registration Limited, 6 Falcon Way, Shire Park, Welwyn Garden City, AL7 1TW, Velika Britanija.

Verzija: 2.0/13

Informacija pripravljena: Januar 2015

DODATNE INFORMACIJE SO NA VOLJO PRI:

Roche farmacevtska družba d.o.o., Vodovodna cesta 109, 1000 Ljubljana.

Povzetek glavnih značilnosti zdravila je dosegljiv na www.roche.si ali www.onkologija.si.

Referenca:

1 Povzetek glavnih značilnosti zdravila Tarceva. Dostopano 05.01.2015 na: http://www.ema.europa.eu/docs/sl_Sl/document_library/EPAR_-_Product_Information/human/000618/WC500033994.pdf



ČAS ZA ŽIVLJENJE.

**TARCEVA® PODALJŠA PREŽIVETJE BREZ
NAPREDOVANJA BOLEZNI PRI BOLNIKI**

z lokalno napredovalim ali metastatskim
nedrobnoceličnim rakom pljuč¹



Instructions for authors

The editorial policy

Radiology and Oncology is a multidisciplinary journal devoted to the publishing original and high quality scientific papers and review articles, pertinent to diagnostic and interventional radiology, computerized tomography, magnetic resonance, ultrasound, nuclear medicine, radiotherapy, clinical and experimental oncology, radiobiology, radiophysics and radiation protection. Therefore, the scope of the journal is to cover beside radiology the diagnostic and therapeutic aspects in oncology, which distinguishes it from other journals in the field.

The Editorial Board requires that the paper has not been published or submitted for publication elsewhere; the authors are responsible for all statements in their papers. Accepted articles become the property of the journal and, therefore cannot be published elsewhere without the written permission of the editors.

Submission of the manuscript

The manuscript written in English should be submitted to the journal via online submission system Editorial Manager available for this journal at: www.radioloncol.com.

In case of problems, please contact Sašo Trupej at saso.trupej@computing.si or the Editor of this journal at gsera@onko-i.si

All articles are subjected to the editorial review and when the articles are appropriated they are reviewed by independent referees. In the cover letter, which must accompany the article, the authors are requested to suggest 3-4 researchers, competent to review their manuscript. However, please note that this will be treated only as a suggestion; the final selection of reviewers is exclusively the Editor's decision. The authors' names are revealed to the referees, but not vice versa.

Manuscripts which do not comply with the technical requirements stated herein will be returned to the authors for the correction before peer-review. The editorial board reserves the right to ask authors to make appropriate changes of the contents as well as grammatical and stylistic corrections when necessary. Page charges will be charged for manuscripts exceeding the recommended length, as well as additional editorial work and requests for printed reprints.

Articles are published printed and on-line as the open access (www.degruyter.com/view/j/raon).

All articles are subject to 700 EUR + VAT publication fee. Exceptionally, waiver of payment may be negotiated with editorial office, upon lack of funds.

Manuscripts submitted under multiple authorship are reviewed on the assumption that all listed authors concur in the submission and are responsible for its content; they must have agreed to its publication and have given the corresponding author the authority to act on their behalf in all matters pertaining to publication. The corresponding author is responsible for informing the coauthors of the manuscript status throughout the submission, review, and production process.

Preparation of manuscripts

Radiology and Oncology will consider manuscripts prepared according to the Uniform Requirements for Manuscripts Submitted to Biomedical Journals by International Committee of Medical Journal Editors (www.icmje.org). The manuscript should be written in grammatically and stylistically correct language. Abbreviations should be avoided. If their use is necessary, they should be explained at the first time mentioned. The technical data should conform to the SI system. The manuscript, excluding the references, tables, figures and figure legends, must not exceed 5000 words, and the number of figures and tables is limited to 8. Organize the text so that it includes: Introduction, Materials and methods, Results and Discussion. Exceptionally, the results and discussion can be combined in a single section. Start each section on a new page, and number each page consecutively with Arabic numerals.

The Title page should include a concise and informative title, followed by the full name(s) of the author(s); the institutional affiliation of each author; the name and address of the corresponding author (including telephone, fax and E-mail), and an abbreviated title (not exceeding 60 characters). This should be followed by the abstract page, summarizing in less than 250 words the reasons for the study, experimental approach, the major findings (with specific data if possible), and the principal conclusions, and providing 3-6 key words for indexing purposes. Structured abstracts are preferred. Slovene authors are requested to provide title and the abstract in Slovene language in a separate file. The text of the research article should then proceed as follows:

Introduction should summarize the rationale for the study or observation, citing only the essential references and stating the aim of the study.

Materials and methods should provide enough information to enable experiments to be repeated. New methods should be described in details.

Results should be presented clearly and concisely without repeating the data in the figures and tables. Emphasis should be on clear and precise presentation of results and their significance in relation to the aim of the investigation.

Discussion should explain the results rather than simply repeating them and interpret their significance and draw conclusions. It should discuss the results of the study in the light of previously published work.

Charts, Illustrations, Images and Tables

Charts, Illustrations, Images and Tables must be numbered and referred to in the text, with the appropriate location indicated. Charts, Illustrations and Images, provided electronically, should be of appropriate quality for good reproduction. Illustrations and charts must be vector image, created in CMYK color space, preferred font "Century Gothic", and saved as .AI, .EPS or .PDF format. Color charts, illustrations and Images are encouraged, and are published without additional charge. Image size must be 2.000 pixels on the longer side and saved as .JPG (maximum quality) format. In Images, mask the identities of the patients. Tables should be typed double-spaced, with a descriptive title and, if appropriate, units of numerical measurements included in the column heading. The files with the figures and tables can be uploaded as separate files.

References

References must be numbered in the order in which they appear in the text and their corresponding numbers quoted in the text. Authors are responsible for the accuracy of their references. References to the Abstracts and Letters to the Editor must be identified as such. Citation of papers in preparation or submitted for publication, unpublished observations, and personal communications should not be included in the reference list. If essential, such material may be incorporated in the appropriate place in the text. References follow the style of Index Medicus. All authors should be listed when their number does not exceed six; when there are seven or more authors, the first six listed are followed by "et al.". The following are some examples of references from articles, books and book chapters:

Dent RAG, Cole P. In vitro maturation of monocytes in squamous carcinoma of the lung. *Br J Cancer* 1981; **43**: 486-95.

Chapman S, Nakielny R. *A guide to radiological procedures*. London: Bailliere Tindall; 1986.

Evans R, Alexander P. Mechanisms of extracellular killing of nucleated mammalian cells by macrophages. In: Nelson DS, editor. *Immunobiology of macrophage*. New York: Academic Press; 1976. p. 45-74.

Authorization for the use of human subjects or experimental animals

When reporting experiments on human subjects, authors should state whether the procedures followed the Helsinki Declaration. Patients have the right to privacy; therefore the identifying information (patient's names, hospital unit numbers) should not be published unless it is essential. In such cases the patient's informed consent for publication is needed, and should appear as an appropriate statement in the article. Institutional approval and Clinical Trial registration number is required.

The research using animal subjects should be conducted according to the EU Directive 2010/63/EU and following the Guidelines for the welfare and use of animals in cancer research (*Br J Cancer* 2010; 102: 1555 – 77). Authors must state the committee approving the experiments, and must confirm that all experiments were performed in accordance with relevant regulations.

These statements should appear in the Materials and methods section (or for contributions without this section, within the main text or in the captions of relevant figures or tables).

Transfer of copyright agreement

For the publication of accepted articles, authors are required to send the License to Publish to the publisher on the address of the editorial office. A properly completed License to Publish, signed by the Corresponding Author on behalf of all the authors, must be provided for each submitted manuscript.

The non-commercial use of each article will be governed by the Creative Commons Attribution-NonCommercial-NoDerivs license.

Conflict of interest

When the manuscript is submitted for publication, the authors are expected to disclose any relationship that might pose real, apparent or potential conflict of interest with respect to the results reported in that manuscript. Potential conflicts of interest include not only financial relationships but also other, non-financial relationships. In the Acknowledgement section the source of funding support should be mentioned. The Editors will make effort to ensure that conflicts of interest will not compromise the evaluation process of the submitted manuscripts; potential editors and reviewers will exempt themselves from review process when such conflict of interest exists. The statement of disclosure must be in the Cover letter accompanying the manuscript or submitted on the form available on www.icmje.org/coi_disclosure.pdf

Page proofs

Page proofs will be sent by E-mail to the corresponding author. It is their responsibility to check the proofs carefully and return a list of essential corrections to the editorial office within three days of receipt. Only grammatical corrections are acceptable at that time.

Open access

Papers are published electronically as open access on www.degruyter.com/view/j/raon, also papers accepted for publication as E-ahead of print.

Vsak dan šteje

za bolnike z napredovalim karcinomom ledvičnih celic



28. september

Jesenski festival

15. december

Zimske počitnice

30. april

Družinsko srečanje

2. avgust

Začetek kuharskega tečaja

BISTVENI PODATKI IZ POVZETKA GLAVNIH ZNAČILNOSTI ZDRAVILA

SUTENT 12,5 mg, 25 mg, 37,5 mg, 50 mg trde kapsule

Sestava in oblika zdravila: Ena kapsula vsebuje 12,5 mg, 25 mg, 37,5 mg ali 50 mg sunitiniba (v obliki sunitinibijevega malata). **Indikacije:** Zdravljenje neizrežljivega in/ali metastatskega malignega gastrointestinalnega stromalnega tumorja (GIST) pri odraslih, če zdravljenje z imatinibom zaradi odpornosti ali neprenašanja ni bilo uspešno. Zdravljenje napredovalega/metastatskega karcinoma ledvičnih celic (MRCC) pri odraslih. Zdravljenje neizrežljivih ali metastatskih, dobro diferenciranih neuroendokrinih tumorjev trebušne slinavke (pNET), kadar gre za napredovanje bolezni pri odraslih (izkušnje z zdravilom Sutent kot zdravilom prve izbire so omejene). **Odmerjanje in način uporabe:** Terapijo mora uvesti zdravnik, ki ima izkušnje z uporabo zdravil za zdravljenje rakavih bolezni. **GIST in MRCC:** Priporočeni odmerek je 50 mg peroralno enkrat na dan, 4 tedne zapored; temu sledi 2-tedenski premor (Shema 4/2), tako da celotni cikel traja 6 tednov. **pNET:** Priporočeni odmerek je 37,5 mg peroralno enkrat na dan, brez načrtovanega premora. **Prilaganje odmerka:** Odmerek je mogoče prilagajati v povečanih po 12,5 mg, upoštevaje individualno varnost in prenašanje. Pri GIST in MRCC dnevni odmerek ne sme preseči 75 mg in ne sme biti manjši od 25 mg; pri pNET je največji odmerek 50 mg na dan, z možnimi prekinitvami zdravljenja. Pri sočasni uporabi z močnimi zaviralci ali induktorji CYP3A4 je treba odmerek ustrezno prilagoditi. **Pediatrična populacija:** Uporaba sunitiniba ni priporočljiva. **Starejši bolniki (≥ 65 let):** Med starejšimi in mlajšimi bolniki niso opazili pomembnih razlik v varnosti in učinkovitosti. **Okvara jeter:** Pri bolnikih z jetrno okvaro razreda A in B po Child-Pughu prilagoditev odmerka ni potrebna; pri bolnikih z okvaro razreda C sunitinib ni bil preizkušen, zato njegova uporaba ni priporočljiva. **Okvara ledvic:** Prilaganje začetnega odmerka ni potrebno, nadaljnje prilaganje odmerka naj temelji na varnosti in prenašanju pri posameznem bolniku. **Način uporabe:** Zdravilo Sutent se uporablja peroralno, bolnik ga lahko vzame s hrano ali brez nje. Če pozabi vzeti odmerek, ne sme dobiti dodatnega, temveč naj vzame običajni predpisani odmerek naslednji dan. **Kontraindikacije:** Preobčutljivost na zdravilo učinkovino ali katerokoli pomožno snov. **Posebna opozorila in previdnostni ukrepi:** **Bolezni kože in tkiv:** obarvanje kože, gangrenozna pioderma (običajno izgine po prekinitvi zdravljenja), hude kožne reakcije (multiformni eritem (EM), Stevens-Johnsonov sindrom (SJS) in toksična epidermalna nekroliza (TEN)). Če so prisotni znaki EM, SJS ali TEN, je treba zdravljenje prekiniti. **Krvavitve v prebavilih, dihalih, sečilih, možganih;** najpogostejše epistaksa; krvavitve tumorja, včasih s smrtnim izidom. Pri bolnikih, ki se so asno zdravijo z antikoagulantmi, se lahko redno spremlja celotna krvna slika (trombociti), koagulacijski faktorji (PT / INR) in opravi telesni pregled. **Bolezni prebavil:** poleg diareje, navzee/bruhanja, bolečine v trebuhu, zaprtje, dispepsije, stomatitis/bolečine v ustih in ezofagitisa tudi hudi zapleti (včasih s smrtnim izidom), vključno z gastrointestinalno perforacijo. **Hipertenzija:** pri bolnikih s hudo hipertenzijo, ki je ni mogoče urediti z zdravili, je priporočljivo začasno prenehanje zdravljenja. **Hematološke bolezni:** zmanjšanje števila nevtrofilcev, trombocitov, anemija. **Bolezni srca in ožilja:** srčno-žilni dogodki, vključno s srčnim popuščanjem, kardiomiopatijo in motnjami v delovanju miokarda, v nekaterih primerih s smrtnim izidom. Sunitinib povečuje tveganje za pojav kardiomiopatije. **Podaljšanje intervala QT:** previdna uporaba pri bolnikih z znano anamnezo podaljšanja intervala QT, tistih, ki jemljejo antiaritmike, in tistih z relevantno, že obstoječo srčno boleznijo, bradikardijo ali elektrolitskimi motnjami. **Venski in arterijski tromboembolični dogodki;** arterijski včasih s smrtnim izidom. **Dogodki na dihalih:** dispneja, plevalni izliv, pljučna embolija

ali pljučni edem; redki primeri s smrtnim izidom. **Moteno delovanje ščitnice:** bolnike je treba med zdravljenjem rutinsko spremljati glede delovanja ščitnice vsake 3 mesece. **Pankreatitis,** tudi resni primeri s smrtnim izidom. **Hepatotoksičnost,** nekateri primeri s smrtnim izidom. **Holecistitis,** vključno z akalkuloznim in emfizemskim holecistitisom. **Delovanje ledvic:** primeri zmanjšane delovanja ledvic, odpovedi ledvic in/ali akutne odpovedi ledvic, v nekaterih primerih s smrtnim izidom. **Fistula:** če nastane fistula, je treba zdravljenje s sunitinibom prekiniti. **Oteženo celjenje ran:** pri bolnikih, pri katerih naj bi bil opravljen večji kirurški poseg, je priporočljiva začasna prekinitev zdravljenja s sunitinibom. **Osteonekroza čeljustnic:** pri sočasnem ali zaporednem dajanju zdravila Sutent in intravenskih bisfosfonatov je potrebna previdnost; invazivni zobozdravstveni posegi predstavljajo dodatni dejavnik tveganja. **Preobčutljivost/angioedem. Motnje okušanja. Konvulzije:** obstajajo poročila, nekatera s smrtnim izidom, o preiskovanih s konvulzijami in radiološkimi znaki sindroma reverzibilne posteriorne levkoencefalopatije. **Sindrom lize tumorja,** v nekaterih primerih s smrtnim izidom. **Okužbe:** hude okužbe z ali brez nevtropenije (okužbe dihal, se il, kože in sepsa), vklju no z nekaterimi s smrtnim izidom; redki primeri nekrotizirajočega fasciitisa, vključno s prizadetostjo presredka, ki so bili včasih smrtni. **Hipoglikemija:** če se pojavi simptomatska hipoglikemija, je treba zdravljenje s sunitinibom začasno prekiniti. Pri sladkornih bolnikih je treba redno preverjati raven glukoze v krvi in, če je treba, prilagoditi odmerek antidiabetika. **Medsebojno delovanje z drugimi zdravili:** (Študije so izvedli le pri odraslih.) Zdravila, ki lahko zvečajo koncentracijo sunitiniba v plazmi (ketokonazol, ritonavir, itrakonazol, eritromicin, klaritromicin ali sok grenivke). Zdravila, ki lahko zmanjšajo koncentracijo sunitiniba v plazmi (deksametazon, fenitoin, karbamazepin, rifampin, fenobarbital, *Hypericum perforatum* oz. šentjanževka). **Plodnost, nosečnost in dojenje:** Zdravila Sutent ne smemo uporabljati med nosečnostjo in tudi ne pri ženskah, ki ne uporabljajo ustrezne kontracepcije, razen če možna korist odtehta možno tveganje za plod. Ženske v rodni dobi naj med zdravljenjem z zdravilom Sutent ne zanosijo. Ženske, ki jemljejo zdravilo Sutent, ne smejo dobiti. Neklinični izsledki kažejo, da lahko zdravljenje s sunitinibom poslabša plodnost samcev in samic. **Vpliv na sposobnost vožnje in upravljanja s stroji:** Sutent lahko povzroči omotico. **Neželeni učinki:** Najbolj resni neželeni učinki (nekateri s smrtnim izidom) so: odpoved ledvic, srčno popuščanje, pljučna embolija, gastrointestinalna perforacija in krvavitve (npr. v dihalih, prebavilih, tumorju, sečilih in možganih). Najpogostejši neželeni učinki (ki so se pojavili pri vsaj 20 % bolnikov v registracijskih preskušanjih) so: zmanjšan apetit, motnje okušanja, hipertenzija, utrujenost, prebavne motnje (npr. driska, slabost, stomatitis, dispepsija in bruhanje), sprememba barve kože in sindrom palmarno-plantarne eritrosidestezije. Med najbolj pogostimi neželenimi učinki so hematološke motnje (nevtropenija, trombocitopenija, anemija in levkopenija). Ostali zelo pogosti (≥ 1/10) neželeni učinki so: hipotiroidizem, nespečnost, omotica, glavobol, dispneja, epistaksa, kašelj, bolečina v trebuhu, zaprtje, obarvanje kože, izpuščaji, sprememba barve las, suha koža, bolečine v udih, artralgija, bolečine v hrbtu, vnetje sluznice, edem, pireksija. **Način in režim izdaje:** Predpisovanje in zdajja zdravila je le na recept, zdravilo pa se uporablja samo v bolnišnicah. Izjemoma se lahko uporablja pri nadaljevanju zdravljenja na domu ob odpustu iz bolnišnice in nadaljnjem zdravljenju. **Imetnik dovoljenja za promet:** Pfizer Limited, Ramsgate Road, Sandwich, Kent, CT13 9NJ, Velika Britanija. **Datum zadnje revizije besedila:** 24.07.2014. **Pred predpisovanjem se seznanite s celotnim povzetkom glavnih značilnosti zdravila.**

